

TOOTH MICROWEAR, DIET AND FEEDING IN ORNITHISCHIAN
DINOSAURS

Thesis submitted for the degree of
Doctor of Philosophy
at the University of Leicester

by

Vincent Stanley Williams BSc (Hons) M.Geol
Department of Geology
University of Leicester

September 2010

Vincent Stanley Williams

Abstract

Tooth microwear, diet and feeding in ornithischian dinosaurs

Understanding the feeding mechanisms and diet of ornithopod dinosaurs is fundamental to understanding their role in Late Cretaceous ecosystems. Current hypotheses of feeding behaviour are based on functional morphology, and testing these is problematic. Microscopic scratches, microwear, that form on teeth *in vivo* during feeding are known to record the relative movement of the tooth rows and to capture evidence of tooth-food interactions; however, their applicability to ornithischian dinosaurs has not been tested. The development of a fast non-abrasive and residue free method for the removal of resistant consolidant, along with a safe, rapid technique for replicating tooth surfaces was the first step towards assessing the suitability of quantitative tooth microwear analysis techniques for dinosaur teeth. An evaluation of appropriate statistical analysis methods followed, identifying suitably stringent tests for the analysis of variance in the multi-modal directional microwear data. Analysis of microwear orientation in *Iguana iguana* provided direct evidence for relative motion of the jaws. Microwear from the basal ornithischian *Lesothosaurus diagnosticus* revealed three distinct sets of scratches in different orientations that were comparable to those of *I. iguana*, confirming the isognathic, near-vertical, simple adduction predicted for this dinosaur. Results from the basal ornithopod *Hypsilophodon foxii* indicate a propalinal translation of the lower jaw during feeding and provide strong support for muscular cheeks, whilst those from the hadrosaurid *Edmontosaurus* indicate a near-vertical posterodorsal power stroke with a secondary propalinal action and support the presence of a pleurokinetic hinge. Analysis of a range of hadrosaurid taxa found that three differing mastication methods existed, potentially diet related. Furthermore, microwear suggests that there is no significant difference in the jaw mechanics between iguanodontians and hadrosaurids. The results demonstrate that microwear has great potential for unravelling the mystery of dinosaur feeding and identifying key stages in the evolution of jaw mechanics in ornithopods.

ACKNOWLEDGEMENTS

This project would not have been possible without the vital assistance of many people. My thesis committee were extremely generous with their time and provided all of the support that I needed without hesitation. My most profound thanks go to my main supervisor Mark Purnell who must have aged disproportionately over the course of this project particularly during the development of a new circular statistical analysis technique. His input was essential as were the contributions of my other supervisors Sarah Gabbott and Paul Barrett, and committee member Richard Aldridge. Thanks also to Rob Wilson and Rod Branson first, who patiently taught me the intricacies of two scanning electron microscopes and provided assistance in preparing my early original specimens and casts for imaging. I could not have completed this project without them. I would also like to thank Adrian Doyle and Nicholas Eastaugh for their advice on cleaning consolidant from specimens.

I could not have embarked upon this project without access to the fossil collections held in museums around the world. I owe great thanks to Sandra Chapman of the Natural History Museum; Christopher Norris, Carl Mehling and Jeanne Kelly of the American Museum of Natural History; Walter Joyce and Marilyn Fox of the Yale Peabody Museum; Matthew Lamanna and Amy Henrici of the Carnegie Museum; Matthew Carrano of the Smithsonian Institution; Derek Siveter and Paul Jeffery of the Oxford University Museum of Natural History and Martin Munt and Lorna Steel of the Dinosaur Isle Museum; for granting access to and permission to clean the dinosaur teeth. I also thank John Larkham of Coltène Whaledent for donating sufficient polyvinylsiloxane moulding compound for my entire project.

Finally and probably of most importance, thanks to my family and friends who have supported me through the tumultuous past three years and in particular to my wife who made it possible for me to begin this project, gave me reason to continue and encouraged me to finish.

CONTENTS

CHAPTER 1: INTRODUCTION	1
CHAPTER 2: Cleaning fossil tooth surfaces for microwear analysis: use of solvent gels to remove resistant consolidant.....	15
CHAPTER 3: Dental microwear in dinosaurs: a comparative analysis of polysiloxane replication	35
CHAPTER 4: Tooth replication techniques for SEM imaging and microwear analysis in dinosaurs	45
CHAPTER 5: Statistical analysis of microwear orientation data	60
CHAPTER 6: Dental microwear on Iguana teeth: implications for the reconstruction of jaw movement.....	73
CHAPTER 7: Comparative dental microwear analysis of the basal ornithischian <i>Lesothosaurus diagnosticus</i> and the squamate <i>Iguana iguana</i>	112
CHAPTER 8: Dental microwear analysis of the ornithopod dinosaur <i>Hypsilophodon foxii</i> : evidence for muscular cheeks.....	158
CHAPTER 9: Quantitative analysis of dental microwear in hadrosaurid dinosaurs and the implications for hypotheses of jaw mechanics and feeding.....	188
CHAPTER 10: Dental microwear analysis: the implications for pleurokinesis in ornithopods	214
Summary.....	283
Appendices.....	286
Bibliography	312

CHAPTER 1

INTRODUCTION

This PhD thesis demonstrates the applicability of quantitative tooth microwear analysis techniques to the teeth of herbivorous dinosaurs, and uses microwear analysis to test hypotheses of jaw mechanics and to better understand diet and feeding behaviour in ornithischians, ornithomimids and an extant analogue.

Tooth microwear analysis

As tooth moves against tooth during occlusion, microscopic marks are left on the surface of each tooth. As a tooth cuts through or crushes food, this causes microscopic marks to form on the surface of that tooth. In herbivores these marks are caused primarily by the tough lignified cuticle and hard silica particles known as phytoliths within the plants and to some extent by fine mineral grit on the surface of the plants (Baker *et al.* 1959; Walker *et al.* 1978; Teaford 1988a; Mainland 2006). This is microwear. However, the amount of wear caused by phytoliths and which can therefore be used to identify diet directly (as phytolith form and assemblage is plant specific) has been questioned by Sanson *et al.* (2007). These authors consider that grit eaten with the plant material is responsible for the majority of microwear in mammals. Their research found that silica phytoliths, from four species of grass, were softer than sheep tooth enamel. For herbivorous dinosaur research the point is academic as the bulk of the functional (occlusal) surface of dinosaur teeth consists of the softer dentine and not enamel.

The microwear left by tooth-tooth or tooth-food-tooth contact can be quantified and analysed to address questions including how tooth moved against tooth, upon what an animal fed and how that food was processed (e.g., Mills 1967; Teaforde and Byrd 1989; Semprebon *et al.* 2004; Ungar *et al.* 2007).

In studies of diet and feeding of mammals, it is possible to compare the wear patterns at the same point on the same cusp of the same tooth in different individuals (e.g., Schubert *et al.* 2006). The similarity of dentition in mammals also means that such comparisons are not restricted to a single species. Changes in diet over time and niche partitioning can be detected, and the nuances in feeding in different species of mammal can be compared. It is also possible to categorize herbivorous mammals as grazers (grass eaters), browsers (eaters of less abrasive vegetation such as leaves and twigs) or mixed feeders based on microwear texture (Solounias *et al.* 1988).

Quantitative analysis of tooth microwear is an extremely powerful tool and has been applied extensively to mammals, particularly primates in order to evaluate the role of dietary changes in hominin evolution (e.g., Gordon 1984a; Teaforde and Ungar 2000; Ungar 2004; Ungar *et al.* 2008) and ungulates to reveal how feeding has tracked past environmental change (e.g., Semprebon *et al.* 2004). Recent research on living and fossil fishes suggests that quantitative microwear has broad applicability beyond mammals (Purnell *et al.* 2006; Purnell *et al.* 2007). Microwear analysis has been applied to dinosaurs (Fiorillo 1991, 1998; Upchurch and Barrett 2000; Schubert and Ungar 2005), but this thesis contains the first quantitative analysis of tooth microwear in dinosaurs (Williams *et al.* 2009).

Why apply microwear analysis to dinosaur teeth?

Much is known about the diet and feeding habits of extant herbivores, especially herbivorous mammals, through direct observation of both wild and captive behaviour. Determining the diet of extinct fossil herbivores however, is more problematic. Fossilised stomach contents are extremely useful but rare. Coprolites are more common and their contents may indicate dietary preferences (Scott 1977; Walker *et al.* 1978), but it is difficult to associate a specific coprolite with the species of animal that made it (e.g., Chin 2007). Isotopic analysis of the carbonate component in tooth enamel (biogenic apatite) can reflect the photosynthetic pathway (C_3 or C_4) of the source of vegetation, i.e. the plant food (Koch 1998). This is useful, since most trees and shrubs use the C_3 pathway, whereas most grasses use the C_4 pathway (O'Leary 1988). However, care must be taken to ensure that diagenetic processes have not affected the isotope ratios.

Another informative method for determining both diet and feeding habits in extinct animals is to use the knowledge gained from extant relatives. Where these do not exist, extant animals that occupied a similar niche and had similar jaw mechanics and dentition may provide a good functional analogue. In addition interpretation of tooth morphology can be informative, in that tooth form can be a good general predictor of diet. However, there are problems with using tooth form alone. The same tooth form can serve more than one purpose and this can vary with specific feeding behaviour. Animals that have adapted to process fallback foods in times of resource scarcity typically have a tooth form that is partly or fully optimized for the fallback food, rather than the preferred diet (Robinson and Wilson 1998). Dental microwear analysis offers a

more reliable and quantitative method for the examination of jaw movements and deduction of dietary habit.

Ornithischian and ornithopod dinosaurs

Of the various groups of dinosaurs, ornithopods show the highest degree of adaptation to herbivory, characterized by a transverse grinding style of mastication that is unique to this group of dinosaurs (Norman 1984; Weishampel 1984; Norman and Weishampel 1985). They have one of the most complete fossil records known for dinosaurs, spanning the early Jurassic and late Cretaceous, and this includes hatchlings and juveniles as well as adults. Ornithopods achieved a near-global distribution and became the dominant herbivorous vertebrates, in terms of both species-richness and abundance, in many Late Cretaceous ecosystems (Horner *et al.* 2004; Weishampel *et al.* 2004). It is likely that their success was related to the complex jaw mechanics that gave them the ability to process food more efficiently than other herbivores. In the case of hadrosaurids, food processing efficiency was comparable to that of modern ungulates (Weishampel and Norman 1989). Figure 1 illustrates the results of a cladistic analysis of ornithischian dinosaurs performed by (Serenio 1984). This shows the relationship between the taxa that make up Ornithopoda, with *Heterodontosaurus* (Heterodontosauridae) as the most basal ornithopod, and *Lesothosaurus* as the most basal known ornithischian. It is one example of a number of conflicting ornithischian phylogenies (e.g., Norman 1984; Serenio 1984; Maryanska and Osmolska 1985; Serenio 1986). Recent work by Butler *et al.* (2008) moved Heterodontosauridae from Ornithopoda to a position close to the base of Ornithischia however, these authors excluded both *Echinodon* and *Lycorhinus* from Heterodontosauridae, and their results

found four possible phylogenetic positions for Heterodontosauridae: two at basal positions within Ornithischia, one as a basal ornithopod and one as a sister group to Ornithopoda+Ceratopsia.

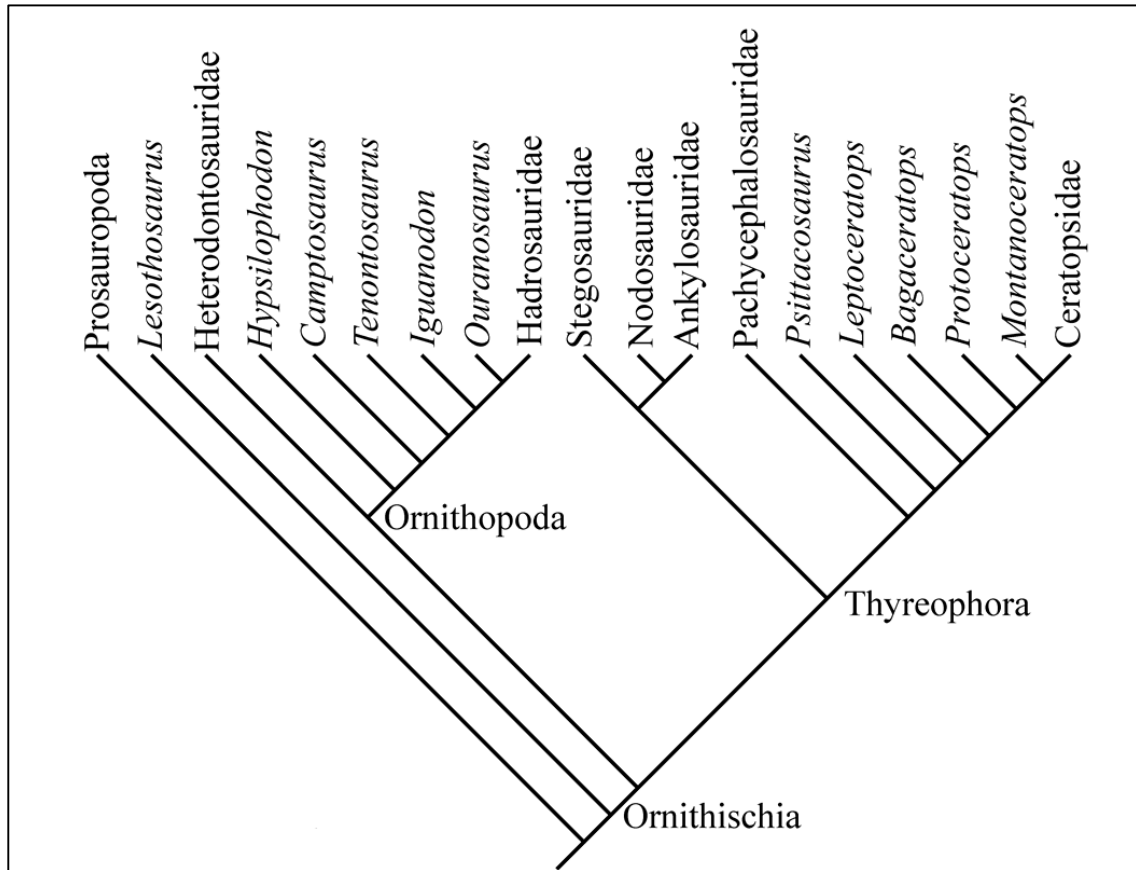


Figure 1. Ornithischian phylogeny, redrawn from Sereno (1984).

In terms of ornithischian adaptations to herbivory, primitive traits include marginal (lateral) teeth (i.e. teeth that line the outer edge of the jaws) and a jaw hinge that is level with the occlusal surface of the tooth rows. More advanced traits include inset teeth, a dentary (lower jaw) that curves ventrolaterally, and a jaw hinge lowered to a point below the occlusal surface of the tooth rows (King 1996). A jaw hinge that is level with the occlusal surface of the tooth rows will operate with a scissor action, such that the point of contact between occluding teeth will move forward from the hinge as the jaw closes. A jaw hinged below the occlusal surface of the tooth rows enables all of

the teeth to come into occlusion simultaneously. As marginal teeth cut through plant food, material lateral to the tooth rows will simply fall from the mouth. Having inset teeth retains that material in the mouth, in the space between the tooth row and the edge of the mouth (the cheek space). Figure 2 shows the changes in skull morphology from basal ornithischian (*Lesothosaurus*), through the ornithopod dinosaurs.

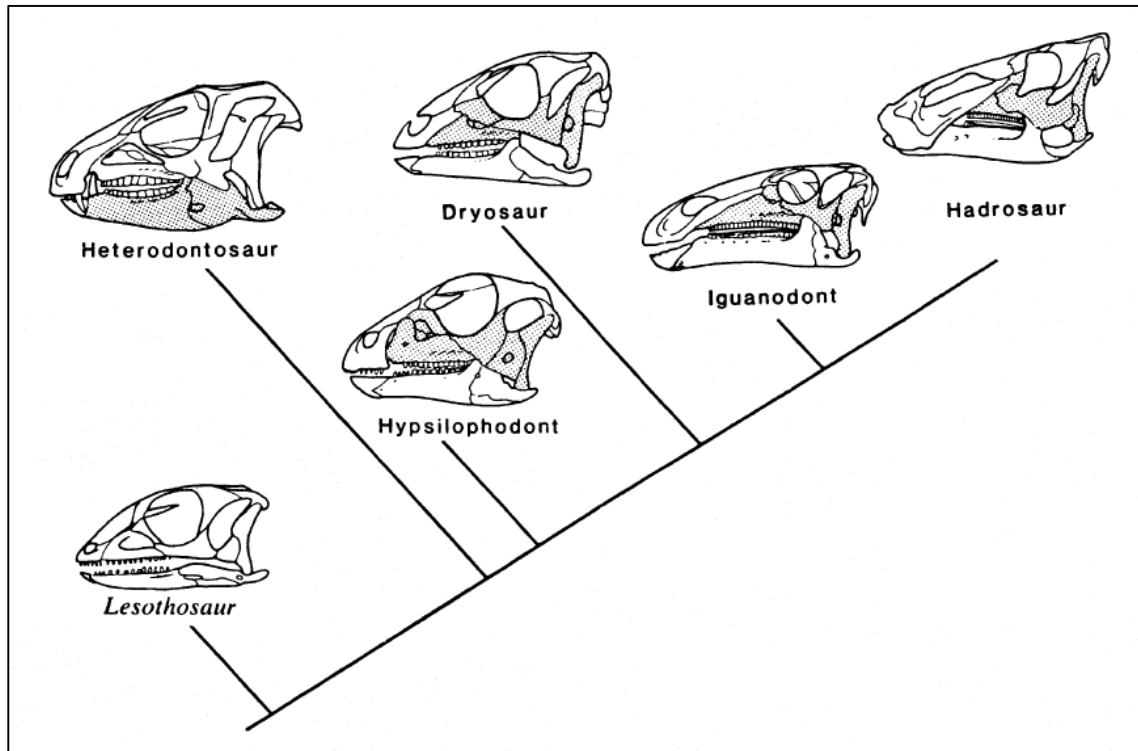


Figure 2. An ornithischian phylogeny. Modified from Norman and Weishampel (1985). Stipple indicates portion of skull able to undergo axial rotation.

Whilst the basal ornithischian *Lesothosaurus* had a partially recessed tooth row (Galton 1978; Norman and Weishampel 1991; Sereno 1991) its jaw hinge was in line with the occlusal surface of the tooth rows, giving a simple scissor action to its jaws. The teeth were thin, leaf shaped and lanceolate with many sharp denticles; they were arranged en-echelon and interlocked during occlusion, with a tooth from the upper jaw coming down between two teeth of the lower jaw and showing wear on two surfaces of the crown. *Lesothosaurus* was a small animal and in terms of size, skull morphology

and tooth form, the modern squamate *Iguana iguana* makes a very good functional analogue.

The basal ornithopod *Heterodontosaurus* had its teeth inset medially, providing cheek space, and it had a jaw hinge point that was below the occlusal surface of the tooth rows. This condition is also seen in all other ornithopods. The cheek teeth of *Heterodontosaurus* are broad and chisel shaped with flattened wear facets and they are packed more closely together than those of *Lesothosaurus*, providing a near continuous dental battery. Unlike most other ornithopods, *Heterodontosaurus* (as the name suggests) was heterodont and had canine-like teeth as well as cheek teeth. The caniniform teeth are present in both the dentary and premaxilla, close to the front of the mouth where the jaws formed a beak (Thulborn 1974). The jaw mechanics are more complex than that seen in *Lesothosaurus*. A flexural mechanism, unique to heterodontosaurids, allowed either mandible rotation or streptostylism (or a combination of both) (e.g., Hopson 1980; Weishampel 1984; Porro 2007). Mandible rotation would have produced a transverse grinding action (Figure 2), whilst streptostylism (movement of the quadrate/squamosal joint allowing the lower jaw, attached to the other end of the quadrate, to move against the skull roof; see Figure 3.4) would have produced a propalinal (fore-aft) grinding action. Due to the rarity of specimens and the lack of microwear preservation on the only specimen obtained, *Heterodontosaurus* is not included in this study.

All other ornithopods had a pleurokinetic hinge (Norman 1984) – a moveable joint within the skull that allowed flexion and expansion during feeding (Figure 3). This was formed by two lines of weakness running from the front to the back of the skull (one either side) along the sutures joining the maxilla, jugal and quadrate bones to the skull. The pleurokinetic hinge allowed the maxilla (the upper jaw carrying teeth) to

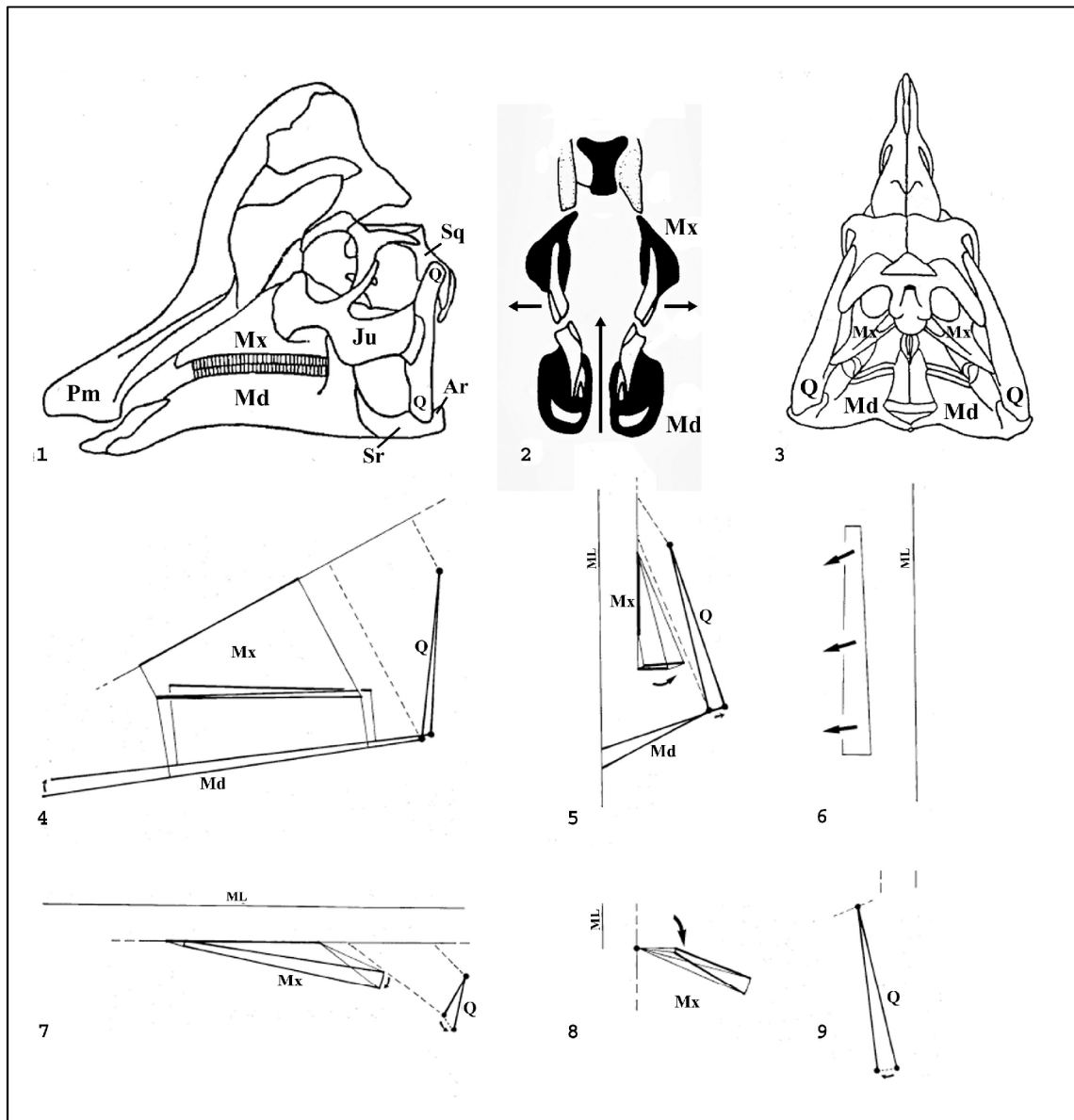


Figure 3. Skull and partial kinematic diagram of the ornithomimid dinosaur *Corythosaurus casuarius* illustrating the predicted movements of the mandible, maxilla and quadrate, after Weisampel (1984). 3.1 Skull in left lateral view showing the articulation points of the quadrate bone (with the squamosal in the cranium and the articular/surangular of the mandible) that could allow a propalinal translation of the lower jaw (fore-aft movement of the mandible against the maxilla). 3.2 Transverse section through skull showing the displacement that takes place during jaw closure; arrows show the upward movement of the lower jaws and the lateral displacement of the upper jaws. 3.3 Skull in caudal view. 3.4 Left lateral view. 3.5 Anterior view. 3.6 Occlusal view of the left dentary teeth; arrows indicate direction of relative motion of the maxillary teeth against the dentary teeth. 3.7 Dorsal view. 3.8 View along the pre-maxilla/maxilla joint. 3.9 View of the left quadrate along its plane of motion. Abbr: Ar – articular; Ju – jugal; Md – mandible; ML – midline; Mx – maxilla; Pm – pre-maxilla; Q – quadrate; Sq – squamosal; Sr – surangular.

move laterally over the dentary (the lower jaw carrying teeth) giving a transverse grinding action during feeding (Figure 3.2). However, recent research on dinosaurs in general (Holliday and Witmer 2009) and hadrosaurids in particular (Rybczynski *et al.*

2008), has questioned the degree of cranial kinesis in ornithomorphs and this has raised doubts about the role of pleurokinesis in hadrosaur jaw mechanics and feeding.

Hadrosaurids were the most derived ornithomorphs and the only dinosaurs that could “chew” in any real sense (e.g., Weishampel 1984; Sereno 1997). They had multiple rows of interlocking diamond shaped teeth in both dentary and maxilla. Combined with continuous replacement, this arrangement of teeth arguably made hadrosaurids better equipped for a herbivorous life than today’s herbivores (Figure 4).

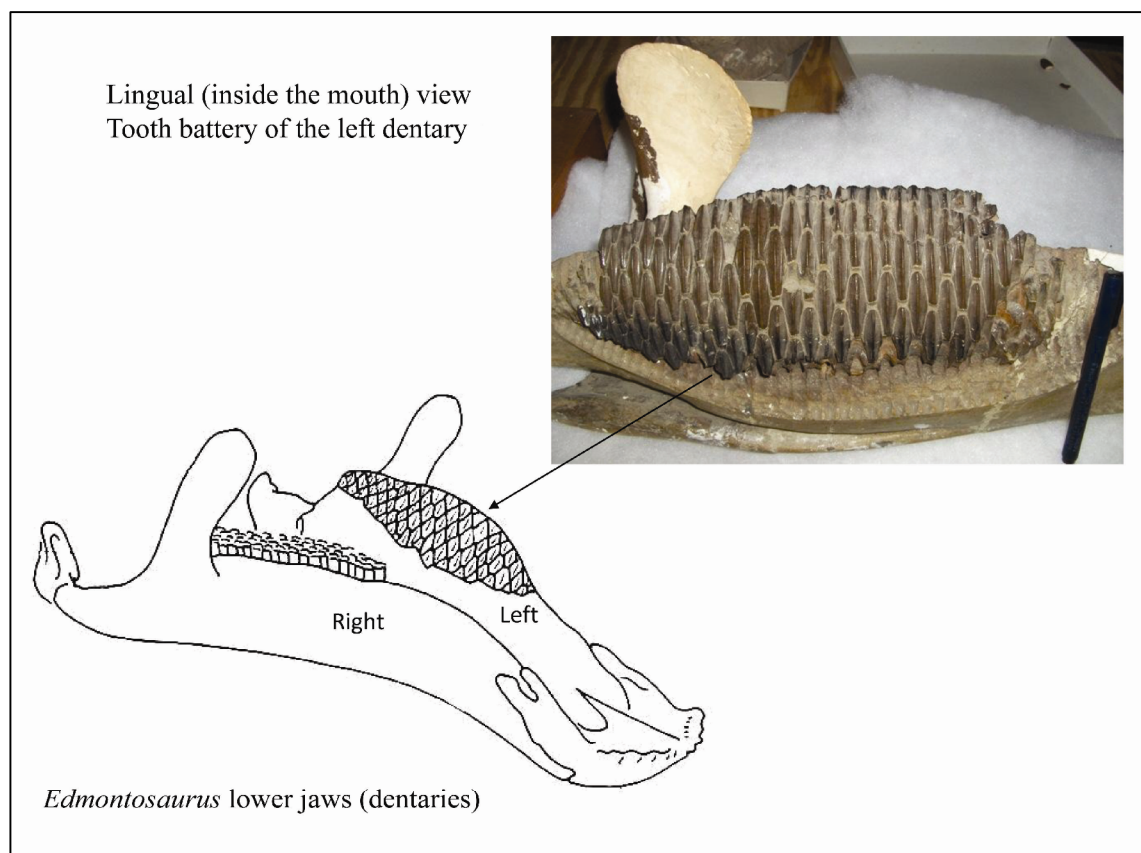


Figure 4. Lower jaws of *Edmontosaurus* SM 22102 showing the dental batteries of multiple interlocking teeth with a continuous series of replacement teeth below. SM – Smithsonian Institution, National Museum of Natural History, Washington, D.C.

The flattened wear surfaces created by occlusion are not level but angled with respect to the tooth row. The angle varies between species but in all cases the surfaces slope down and outward on the labial side of dentary teeth and the lingual side of maxillary teeth forming a sloping occlusal plane (Figure 5). These planes were not parallel as

ornithomimid jaws tend to taper, narrowing from back to front where they generally terminate with a cropping beak. The 3D orientation of these planes needs to be considered when using microwear data captured in 2D to reconstruct relative jaw movements.

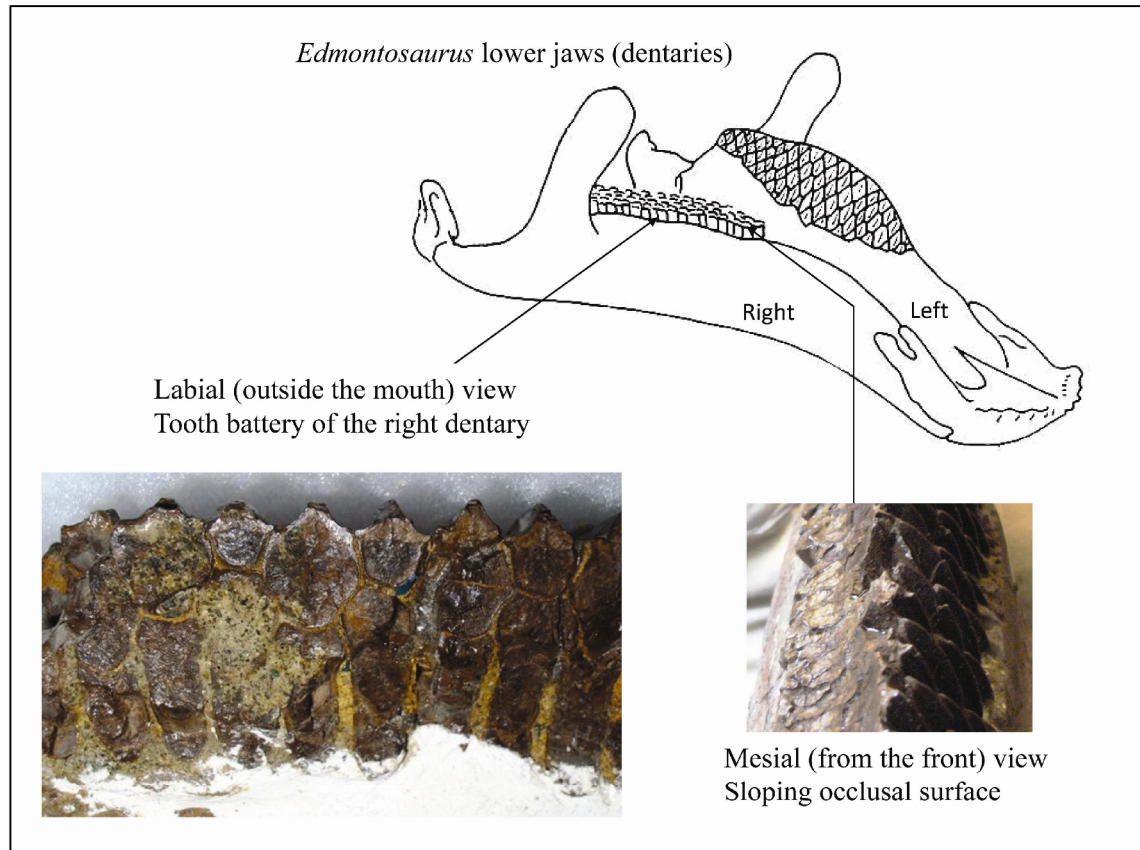


Figure 5. Lower jaws of *Edmontosaurus* SM 22102 showing a dental battery in labial occlusal view, highlighting the interlocking nature of the teeth, and in mesial view highlighting the down & outward slope of the occlusal surface. SM – Smithsonian Institute, National Museum of Natural History, Washington, D.C.

Problems with feeding models

As there are no living non-avian dinosaurs, understanding the evolution of feeding mechanisms in dinosaurs relies upon data from the fossil record and observation of extant euryptiles. Whilst various studies have been made, involving biomechanical analysis, Finite Element Analysis and 3D computer modelling (e.g., Ostrom 1961; Norman 1984; Weishampel 1984; Norman and Weishampel 1985;

Rayfield 2004; Rybczynski *et al.* 2008), the current models of feeding mechanisms in dinosaurs require the reconstruction of musculature. This is problematic in that there is no direct evidence and with the exception of the most basal of dinosaurs (those with the simplest jaw mechanics), there are no sufficiently similar extant species for comparative studies. Additionally, no fossil evidence exists to show the size and shape of the interarticular fibro-cartilages (the soft pad that sat in the hinge between the upper and lower jaws) and the limitations these would have placed on jaw motions.

Although there are extant herbivorous eurentiles, such as *Iguana iguana*, no extant eurentile can masticate plant food, which means that to model anything more than the simplest jaw mechanics the function of many muscles must be estimated. One prime example is the jaw opening musculature. In eurentiles the usual jaw opening muscle is the depressor mandibuli muscle, which connects the back of the skull to the retroarticular process (a small bump on the back of the lower jaw) (King 1996). In extant eurentiles this is a small muscle relative to the jaw closing muscles, generally too weak to do the job of jaw opening on its own and so the assistance of gravity is required if the jaw closing muscles are not contracted. There is no proxy for the jaw opening musculature that would have been required in ornithomimid dinosaurs, such as *Edmontosaurus* and *Corythosaurus casuarius*, to enable true mastication.

The current models therefore, whilst well constrained, are difficult to test.

Tooth microwear analysis techniques

In extensive mammal studies, microwear on tooth surfaces has been imaged at high magnification using a scanning electron microscope (SEM) then measured and quantified for analyses. Feature dimensions (length & width) along with orientation

data are derived from equal area samples sites (Figure 6). Data is then used for various comparative purposes e.g. for analyses of variance between individuals of the same or differing species, or as a test for hypotheses of jaw mechanics. In ornithopod dinosaurs, the orientation of microwear scratches, which relate to relative jaw motion, provide a test for the streptostyly and pleurokinesis models of jaw mechanics.

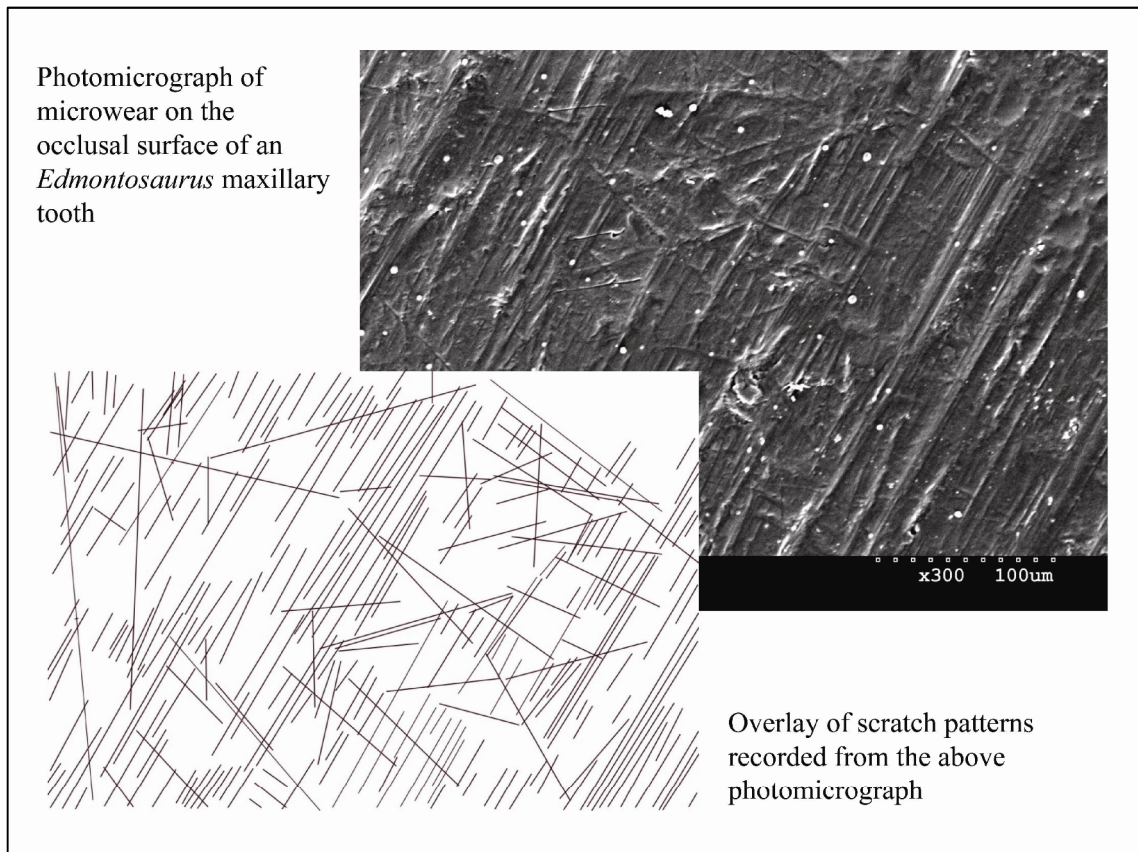


Figure 6. Microwear captured from the occlusal tooth surface of a right maxillary tooth of the hadrosaurid dinosaur *Edmontosaurus* sp. NHMUK R3638. Photomicrograph with overlay of scratch co-ordinates extracted from it. NHMUK – Natural History Museum, London.

Prior to imaging, tooth surfaces must be cleaned in order for the microwear features and textures to be accurately detected or replicated. Any surface contaminant or coating that could potentially mask microwear must be removed.

Thesis aims

The aims of this thesis are to determine:

1. If herbivorous dinosaur teeth preserve microwear.
2. If the quantitative tooth microwear analysis techniques developed for mammals, can be applied to herbivorous dinosaurs.
3. If microwear can be used to reconstruct feeding behaviour in ornithischian dinosaurs and test models of jaw mechanics.

Thesis structure

This thesis is presented as a series of scientific papers, one per chapter, some of which have been published. For clarity a common reference style has been used throughout. Individual papers have been published in or targeted toward specific journals and for this reason the layout of individual chapters has been governed by the requirements of the relevant journal. The target journal is identified in each chapter and for those published works, reprints in the published format have been included in the appendices.

Chapters 2, 3 and 4 detail the methods used for cleaning teeth and replicating microwear features through moulding and casting. In chapter 5 the statistical approaches to microwear analysis are discussed and a new technique for the analysis of multi-modal circular data is described, which allows for the testing of hypotheses of variance in tooth microwear features between sample sites. A test of tooth microwear analysis techniques as a predictor of jaw mechanics is presented in chapter 6; microwear orientation data from the extant squamate *Iguana iguana* are used to predict

jaw mechanics and the results are compared with the observed jaw mechanics of a living animal. In chapter 7, a comparative study of tooth microwear is performed using the extant squamate *Iguana iguana* as a living analogue for the basal ornithischian *Lesothosaurus diagnosticus*. A test for the presence of muscular cheeks in *Lesothosaurus diagnosticus* is also performed using data from *Hypsilophodon foxii* and *Iguana iguana*. The remaining chapters use tooth microwear analysis to test the existing models of jaw mechanics and food processing in ornithopod dinosaurs.

CHAPTER 2

Cleaning fossil tooth surfaces for microwear analysis: use of solvent gels to remove resistant consolidant

Published: *Palaeontologia Electronica* 2010, 13(3), 2T:12p

ABSTRACT

Fine-scale surface texture analysis of teeth has become increasingly useful for anthropologists and palaeontologists to infer diet and jaw mechanics in fossil animals. Here I describe a fast, non-abrasive and residue-free method for the removal of resistant consolidant from fossil teeth. The method utilises solvent gels and its use is a significant improvement over previous techniques, particularly where microwear analysis is to be performed. The method adapts techniques originally developed by art conservators for the removal of varnish from oil paintings without damaging the oil paint beneath. A combination of Carbopol (a water soluble acrylic polymer) and Ethomeen (a polyoxyethylene cocoamine detergent) allow solvents such as acetone and ethanol to be suspended in a gel for application to consolidant coated tooth surfaces. Key advantages are that dissolved consolidant is lifted away from the tooth surface into the solvent gel and a high degree of control is possible such that small discrete areas can be cleaned of consolidant. Because the solvents are held within a gel, cleaning of the tooth surface can be performed without the need for a fume hood.

INTRODUCTION

Microwear analysis requires images or 3D data to be acquired from tooth surfaces at relatively high magnification, sampling data from very small areas, typically only a few hundred micrometres across. In order for the microwear features and textures to be accurately detected or replicated it is imperative that the tooth surface be thoroughly cleaned prior to imaging or moulding. Any surface contaminant or coating that could potentially mask microwear must be removed. The cleaning process must not abrade or etch the tooth surface or leave residue that might obscure the original microwear.

Quantitative analysis of tooth microwear has been applied extensively to mammals (Walker *et al.* 1978; Gordon 1984a; Teaforde 1988a; Organ *et al.* 2005; Ungar *et al.* 2007) and is starting to be applied to dinosaurs (Williams *et al.* 2009); prior studies of dinosaur tooth microwear have been qualitative (e.g., Fiorillo 1991, 1998; Upchurch and Barrett 2000; Schubert and Ungar 2005). The cleaning methods employed by most of these researchers involve soft brushing or gentle swabbing (using cotton swabs) with either distilled water or a solvent such as acetone or ethanol. Whilst these methods work well on material that has been treated with modern consolidants such as the methacrylate co-polymer Paraloid, they have proven time consuming and laborious where more traditional consolidants such as shellac or glyptal have been used and totally ineffective where the shellac has aged.

Material from the older museum collections (19th and early 20th century), particularly dinosaur material, has often been treated with one or both of two consolidants: shellac and animal resin. As shellac ages it darkens and becomes cross-linked (bonds develop that link one polymer chain to another) making it extremely

resistant to solvents. As microwear analysis is increasingly applied to dinosaurs, more researchers are likely to encounter this problem.

Problems with brush based cleaning:

When attempting to remove consolidant from the occlusal surface of a tooth by the brushing on of a solvent and continual cleaning of the brush, or by the use of disposable swabs, the whole tooth and surrounding area tends to become soaked in a combination of the solvent and dissolved consolidant. Given that consolidants like shellac typically form a coating rather than penetrate a surface when they are originally applied, this is a backward step. The brushing process also tends to move consolidant around, smearing it over microwear and making it difficult to determine when all vestiges have been removed. This is especially problematic if SEM analysis is to be performed on moulds and casts rather than the original specimens (brush marks in remaining consolidant are a particular hazard). Use of this technique also results in a high rate of solvent evaporation requiring the use of a fume cupboard. It has also been suggested that repeated applications of solvents such as alcohol and acetone can dehydrate enamel and dentine leading to surface damage (Fernandez-Jalvo and Monfort 2008), although this is questioned by dental researchers who claim dentine in particular becomes more resistant (e.g., Nalla *et al.* 2005). This is of particular concern as the process can be time consuming and requires repeated application of brushed on solvent where the consolidant is shellac, as the older this gets the more resistant it tends to become. Figure 1 shows a tooth surface after each of two consecutive attempts to remove the consolidant coating via the brushing on of ethanol. The left hand images show the first attempt and brush strokes are clearly visible in the higher magnification images. The right hand images show the second attempt and whilst an underlying

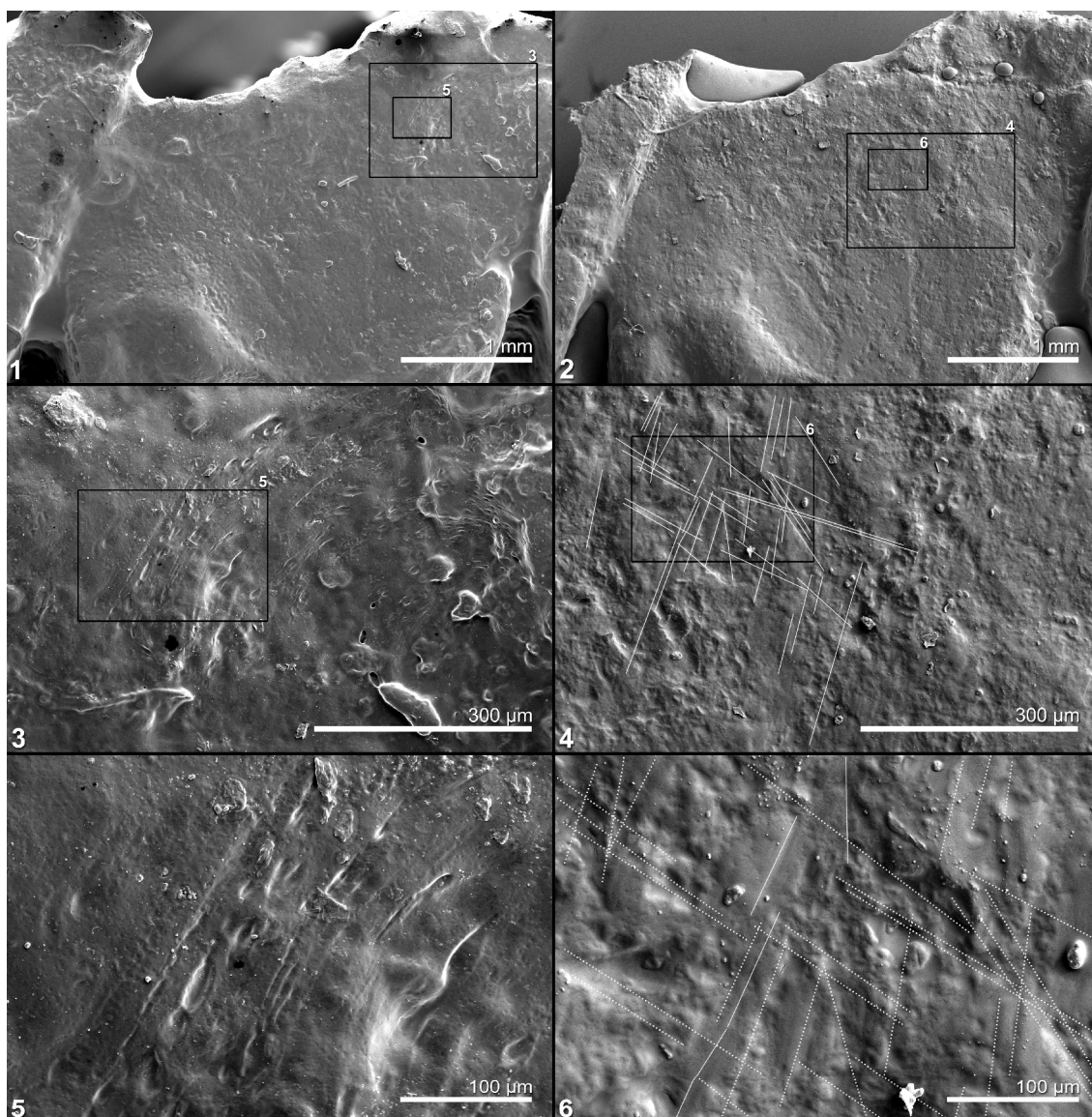


Figure 1. Occlusal surface of a *Heterodontosaurus* tooth (SEM images of casts of SAM PK-1332 right dentary tooth, 3rd from posterior) illustrating the difficulties of cleaning by brush & solvent (ethanol).

- 1.1 Cast 1 made after first attempt to remove varnish from tooth surface; boxes show areas illustrated in 1.3 & 1.5.
- 1.2 Cast 2 made after second attempt to remove varnish from tooth surface, at low magnification the tooth appears to be clean; boxes show areas illustrated in 1.4 & 1.6. Microwear patterns can be identified at this magnification.
- 1.3 Enlargement of area in box 3 of 1.1; varnish has been smeared across the tooth surface and brush marks can be seen clearly in it.
- 1.4 Enlargement of area in box 4 of 1.2; a dominant near vertical microwear pattern (part highlighted with solid white lines) is discernable but varnish still remains infilling and obscuring the pattern.
- 1.5 Enlargement of area in box 5 of 1.1 & 1.3; at higher magnification there is still no visible microwear beneath the brush marks in the varnish.
- 1.6 Enlargement of area in box 6 of 1.2 & 1.4; at higher magnification several different orientations of microwear (part highlighted with solid white lines (visible microwear) and dashed white lines (obscured microwear)) are just discernable through the obscuring varnish, highlighting the amount of varnish still remaining on the surface of a tooth that had been cleaned twice and appeared to be free of varnish at low magnification.

pervasive and dominant near vertical microwear pattern is emerging, sufficient varnish remains to in-fill and partially obscure this.

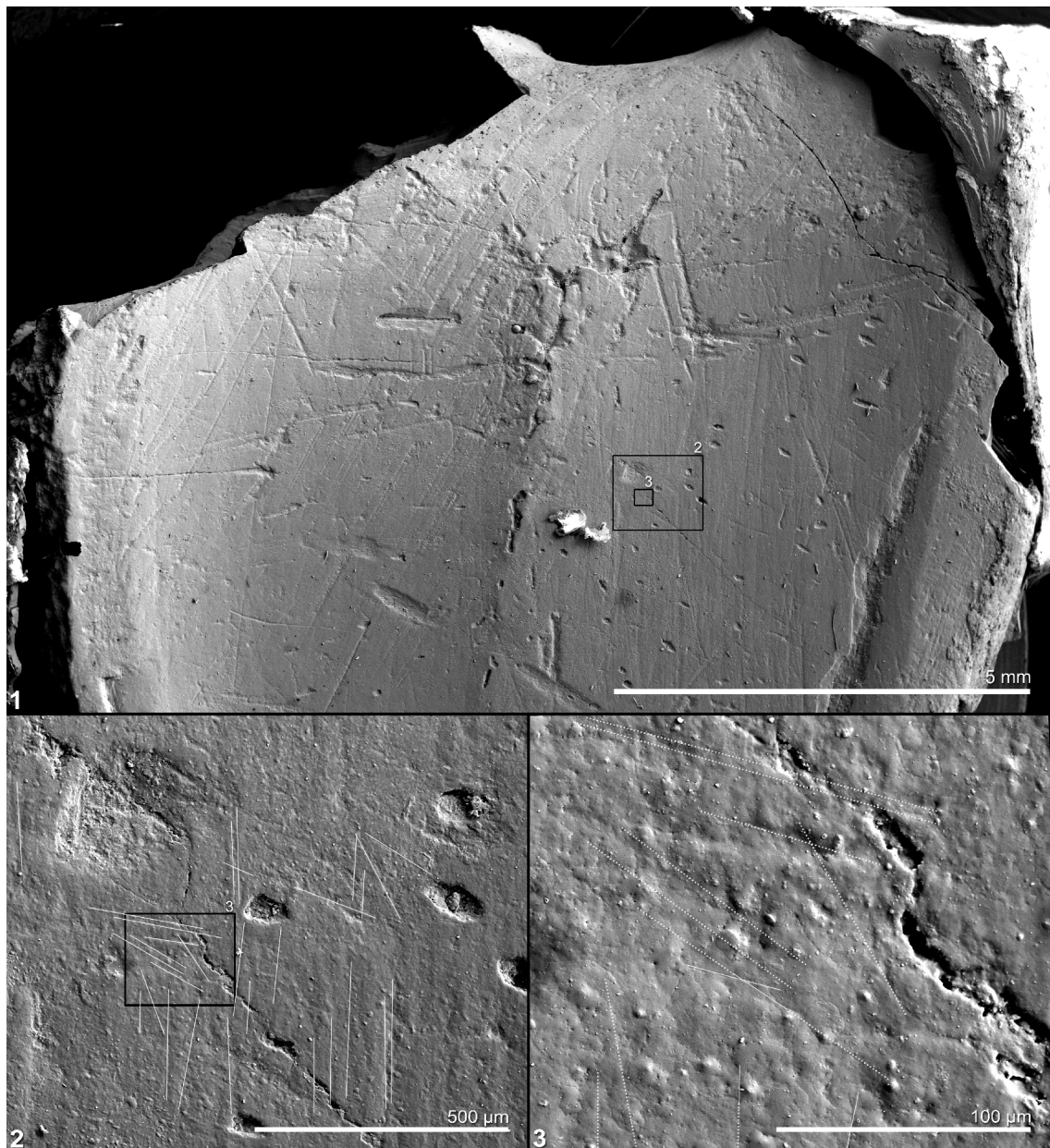


Figure 2. Occlusal surface of an isolated tooth of hadrosaurid (SEM images of cast of AMNH 21700) illustrating the difficulties of cleaning with brush & solvent (ethanol).

- 2.1 Low magnification image showing full width of tooth, at this magnification the tooth appears to be clean; boxes show areas illustrated in 2.2 & 2.3. Microwear patterns can be identified at this magnification.
- 2.2 Enlargement of area in box 2 of 2.1; at higher magnification it can be seen that the microwear (part highlighted with solid white lines) is largely obscured.
- 2.3 Enlargement of area in box 3 of 2.1 & 2.2; at higher magnification it is clear the surface is still coated in consolidants and the microwear patterns (part highlighted with solid white lines (visible microwear) and dashed white lines (obscured microwear)) are largely obscured.

Figure 2 shows a tooth surface that was cleaned whilst being viewed under a stereo-microscope (at x40 magnification giving a 5mm field of view) by brushing on ethanol until it appeared to be clear of consolidant. The higher magnification SEM images clearly show that the tooth surface is still coated in consolidant.

It is both time consuming and frustrating to complete a sequence of brush cleaning, moulding, casting and SEM imaging only to discover that a tooth surface is not clean; especially if the original tooth is in a remote museum collection and a return visit needs to be arranged. A more reliable cleaning method is needed.

Solvent gels:

Art conservators wanting to clean varnish from paintings without damaging the oil paint beneath discovered that by suspending the solvent in a gel they could limit evaporation and control both contact time and the pH. The addition of soaps and detergents to the gel allowed the dissolved varnish to be sequestered by the gel and thus easily removed from the painting (Southall 1988). They found that overpainted areas could be dealt with by the addition of xylene to the gel, causing partial dissolution and swelling of the paint layer (Wolbers *et al.* 1990). It is this solvent gel formulation, used for varnish on paintings, which has been adapted for the removal of various consolidants, including aged shellac, from dinosaur teeth.

This paper describes the cleaning method used by the authors, developed from a technique pioneered by museum conservators. This technique, for the removal of varnish from oil paintings via the application of solvent gels, is not widely known and papers describing its use are not widely available (Hedley 1980; Burnstock and White 1990; Eastaugh 1990; Wolbers *et al.* 1990; Wolbers 1992).

MATERIAL AND METHODS

Ornithopod dinosaur specimens to which the cleaning methods described herein have been applied include teeth and jaw elements from the collections of the Natural History Museum, London (**NHMUK**); the American Museum of Natural History, New York (**AMNH**); the Peabody Museum of Natural History, Yale University (**YPM**); the Smithsonian Institute National Museum of Natural History, Washington, D.C. (**SM**); the Carnegie Museum of Natural History, Pittsburgh (**CM**), the Dinosaur Isle Museum, Isle of Wight (**MIWG**) and the Oxford University Museum of Natural History, Oxford (**OUM**). All were cleaned using solvent gels, and then moulded with a vinyl polysiloxane impression medium. Epoxy resin casts were taken from the vinyl polysiloxane moulds, sputter coated with gold and imaged in a Hitachi S-3600N Scanning Electron Microscope (SEM).

Shellac, glyptal and shellac/animal resin combinations were removed from the occlusal surfaces of hundreds of teeth from one hundred and forty three specimens which consisted of individual teeth, teeth within jaw fragments and teeth within complete jaw elements by the application of solvent gels.

Fossil teeth that were cleaned by the traditional brushing on of ethanol method were also moulded, cast and imaged.

Creating the solvent gel:

Components:

200 ml ethanol (IMS)

200 ml acetone

50 ml xylene

20 ml Ethomeen C/25 (a polyoxyethylene cocoamine detergent; Akzo / Linden Chemicals)

6g Carbopol EZ2 (a water soluble acrylic acid polymer; Noveon / Linden Chemicals)

50 ml pure water (distilled or deionised)

Care should be taken to follow the manufacturer's instructions regarding safe use and storage of all of these products. Material Safety Data Sheets (MSDS) are available via the manufacturer's and distributor's web sites. Both Ethomeen and Carbopol can be obtained from Linden Chemicals (www.lindenchemicals.com), Ethomeen is a product of Akzo (www.akzonobel.com) and Carbopol is a product of Noveon (www.lubrizol.com). Ethanol, iso-propanol, acetone and xylene can be obtained from standard suppliers of laboratory chemicals.

The solvent gel should be prepared and stored in polyethylene or polypropylene bottles to prevent reaction between container and gel. Bottles with transparent sides allow progress to be monitored during preparation of the gel and those with wide opening tightly sealing lids are preferable.

The quantities listed above will produce approximately 500 ml of solvent gel; for smaller volumes reduce the component quantities on a pro-rata basis. The solvent gel can be created quickly for immediate use via a one stage method but a two stage method (see below) produces a more consistent gel, allows the pH of the gel to be

controlled and gives flexibility in the combination of solvents used. Standard laboratory procedures should be followed with reference to all relevant health and safety legislation. I recommend that the addition of ethanol, acetone and/or xylene to the solvent gel should be performed in a fume cupboard. However, once the solvents have been added to the gel, a fume cupboard is no longer required. The solvent gel can be used with standard air extraction systems or in a well ventilated area.

Mixing of the gel can be achieved using a one stage or a two stage method. For the one stage method sprinkle the Carbopol EZ2 powder onto the Ethomeen C/25 whilst stirring continuously until a uniform paste is produced. Stir in the required combination of solvents ethanol/acetone/xylene, then add the pure water gradually whilst stirring continuously. Apply a tight fitting lid to the bottle and shake the bottle vigorously.

For the two stage method, first prepare a Carbopol gel as follows: Sprinkle the Carbopol EZ2 powder onto pure water whilst stirring continuously, until a smooth, stiff ‘wallpaper paste’ like mixture forms. This Carbopol gel can be used within a few minutes if necessary (as soon as it settles and takes on a uniform consistency) but will benefit from being left to stand overnight in a sealed bottle to allow the Carbopol to fully disperse. Next, pour the Ethomeen EZ2 into the Carbopol gel and stir until a smooth, colourless and transparent Carbopol/Ethomeen gel forms. The bottle lid can be screwed tight and the bottle shaken vigorously to aid mixing at this stage. The introduction of Ethomeen should neutralize the acidity of the Carbopol. Testing with pH paper strips should show a pH between 7 and 8. If this is not the case, adding more Ethomeen will increase the pH and adding more Carbopol gel will reduce the pH. Next mix the required combination of solvents ethanol/acetone/xylene in a second bottle and then cut in the Carbopol/Ethomeen gel gradually. If the gel becomes cloudy or a sticky white residue begins to form then water will need to be added to the gel to

allow the solvents to be fully absorbed. Adding the above solvents should result in Solvent gel with a pH of around 8.5.

The advantage of using the two stage method of production is that stock Carbopol/Ethomeen gel can be made up as a first stage and then later small samples of this can be cut into various combinations of solvents for testing on unknown consolidants.

Variations in composition:

Various formulations of the gel can be made by substituting one solvent for another. The above formula, which adds a small quantity of xylene to a 50:50 solution of acetone and ethanol, acts to break the cross-links in aged shellac and enable it to be dissolved. It is effective on glyptal as it takes the guess-work out of which solvent was used (in the formulation of the glyptal) and it will also work on young shellac (although not as effectively as ethanol alone) and so can be used as a universal formula. An alternative formulation substituting additional ethanol for the acetone and xylene (i.e., 450 ml of ethanol) is more effective on shellac that has not developed cross-links. Typically this is shellac that is less than two years old but, depending upon the additives used in the shellac, it may still dissolve readily in ethanol after many years. It is worth testing a small area to assess how first to treat shellac.

When solvents are added to the Carbopol/Ethomeen gel, the pH can be tested and if it is too acidic Ethomeen can be added to reduce the acidity. Whilst slight acidity of the solvent gel is not critical for use on the highly resistant enamel and dentine surfaces of teeth, this ability to control pH has great importance for the wider application of solvent gels to less resistant surfaces such as bone.

It is worth noting that linseed oil may be a component in shellac and whilst I did not encounter a consolidant of this composition, in such instances the acetone/ethanol combination would not be as effective. Tests carried out on oleo-resinous varnish by Burnstock & White (1990) had greater success with iso-propanol.

Application of the solvent gel:

Loose dirt should be brushed from the surface being cleaned and a thick layer (>8 mm) of solvent gel applied. A layer of stretch plastic wrap should be wrapped over the solvent gel and the teeth/jaw to hold the gel in place. This has a number of positive effects. The plastic wrap provides gentle pressure, keeping the gel in contact with the consolidant surface, it prevents the gel from spreading to adjacent surfaces, and it reduces the amount of solvent evaporation from the gel. I found that a 17 μ m thick, commercial, food quality, polyethylene stretch film plastic wrap, with cling/tack on one side, worked well but thicker versions of the domestic ‘cling film’ (UK) or SaranTM Wrap (US) should be equally suitable.

Over a period of 15 to 20 minutes the consolidant will soften, dissolve and be drawn into the gel. Typically, the dissolved consolidant (particularly shellac) discolours the gel, and, as both plastic wrap and gel are transparent, the process can be monitored. One application of gel is usually enough but if the consolidant has been applied in multiple layers it may be necessary to repeat the process. The plastic wrap can be used to scoop the gel from the tooth surface and both plastic wrap and gel can be discarded (subject to the relevant local regulations on the disposal of hazardous waste). With shellac, a very thin blistered film typically remains and this should be ‘teased’ away from the tooth surface. A wooden spatula, wooden dental stick or latex block (to avoid

introducing scratches) will work well for this purpose. Any remaining solvent gel can be brushed from the tooth surface with a little ethanol or water and a fine soft brush.

The Carbopol EZ2 gel allows a solvent or combination of solvents to be held in suspension, preventing immediate evaporation and allowing their action to be concentrated at a specific point and over a significant period of time. Being an amine with detergent properties Ethomeen C/25 serves two purposes when mixed with a Carbopol EZ2 gel. The slight alkalinity of the amine neutralizes the acidity of the gel and the detergent properties enable the gel to sequester material dissolved by the suspended solvents. This latter quality is of key importance in that the dissolved consolidant is taken away from the tooth surface and locked into the gel. As a layer of shellac dissolves into the gel it thins and eventually reaches the point where it will distort and blister, lifting away from the tooth surface cleanly. This virtually eliminates instances of remaining consolidant and the consequent need to re-clean and re-mould/cast.

Solvent gels do need to be stored, handled and disposed of as hazardous chemicals but no more so than their solvent components. The lower rate of evaporation from gels makes them considerably more pleasant to work with. Carbopol/Ethomeen gel is not hazardous until solvents are added and so it can be made up in bulk and stored for extended periods of time. Small volumes for immediate use can be measured out as needed and the solvents added moments before use. Alternatively, solvent gel can be made up from scratch within an hour and potentially within a few minutes.

RESULTS AND DISCUSSION

Figures 1 and 2 show casts taken from teeth that were cleaned by the traditional method of brushing on ethanol. These casts appear to be free of consolidant at low magnification but at higher magnifications the microwear is clearly being obscured by smeared consolidant.

Figures 3 and 4 compare the quality of microwear obtained from tooth surfaces that have been cleaned via the application of solvent gel to that from adjacent uncleaned areas. It can be seen from these images that the use of solvent gel leaves little or no remaining consolidant. The ability of solvent gels to lift consolidant cleanly rather than dissolve it and allow it to in-fill microwear can be seen in Figure 5. Here I show a selection of teeth that were marginal to areas cleaned with solvent gel, such that only part of the tooth surface has been cleaned. In each case there is no smearing or blurring, the edge of the consolidant coating is sharp and well defined. All of these casts showed large areas of tooth surface that were either completely free of consolidant or that had only small, discrete patches of consolidant within them.

A combination of acetone, ethanol and xylene make a good universal solvent gel and holding the pH down to a value around 8.5 slows the action of the solvent gel causing the shellac to swell and blister and this has proven more effective at removing thick coatings of shellac. More alkaline solvent gels tend to act more rapidly, penetrate the shellac and remove it unevenly.

A note of caution on the removal of shellac: Conservators are aware that removing any consolidant from a fossil may cause damage and in the case of aged shellac that damage can be significant. This is due to the tendency of shellac to shrink over time, exerting pressure on the fossil. In some cases, if this pressure is removed the

fossil can fracture and disintegrate (Davidson and Alderson 2009). For microwear analysis there is no alternative to removing the consolidant, but by using solvent gels the area of removal can be restricted to very small parts of the tooth minimizing the risk. None of the hundreds of teeth to which the solvent gel cleaning method has been applied showed any evidence of resulting damage.

Solvent gels concentrate the action of the solvent on the specific part of the surface being cleaned and in doing so reduce the diffusion of the solvent into the surrounding area. Where a tooth or jaw has been reconstructed by gluing several parts together, use of a solvent gel will enable cleaning of a portion of the tooth without compromising the reconstruction.

By retaining the solvent within the gel the volume of evaporate is greatly reduced, conserving the solvent and allowing cleaning to be performed with simple air extraction rather than a fume cupboard (subject to all relevant health and safety legislation, especially where xylene is used within a solvent gel) leading to a more comfortable working environment.

Solvent gels remove consolidant more cleanly, more reliably, in considerably less time and in a more comfortable working environment than the brushing on of solvent method. Specific areas of interest can be cleaned without any adverse effects on adjacent areas and the flexibility in formulation allows various consolidants to be tackled. This coupled with the ability to control pH (and thus the level of aggression) allows the possibility of its wider application to less resistant consolidant coated surfaces.

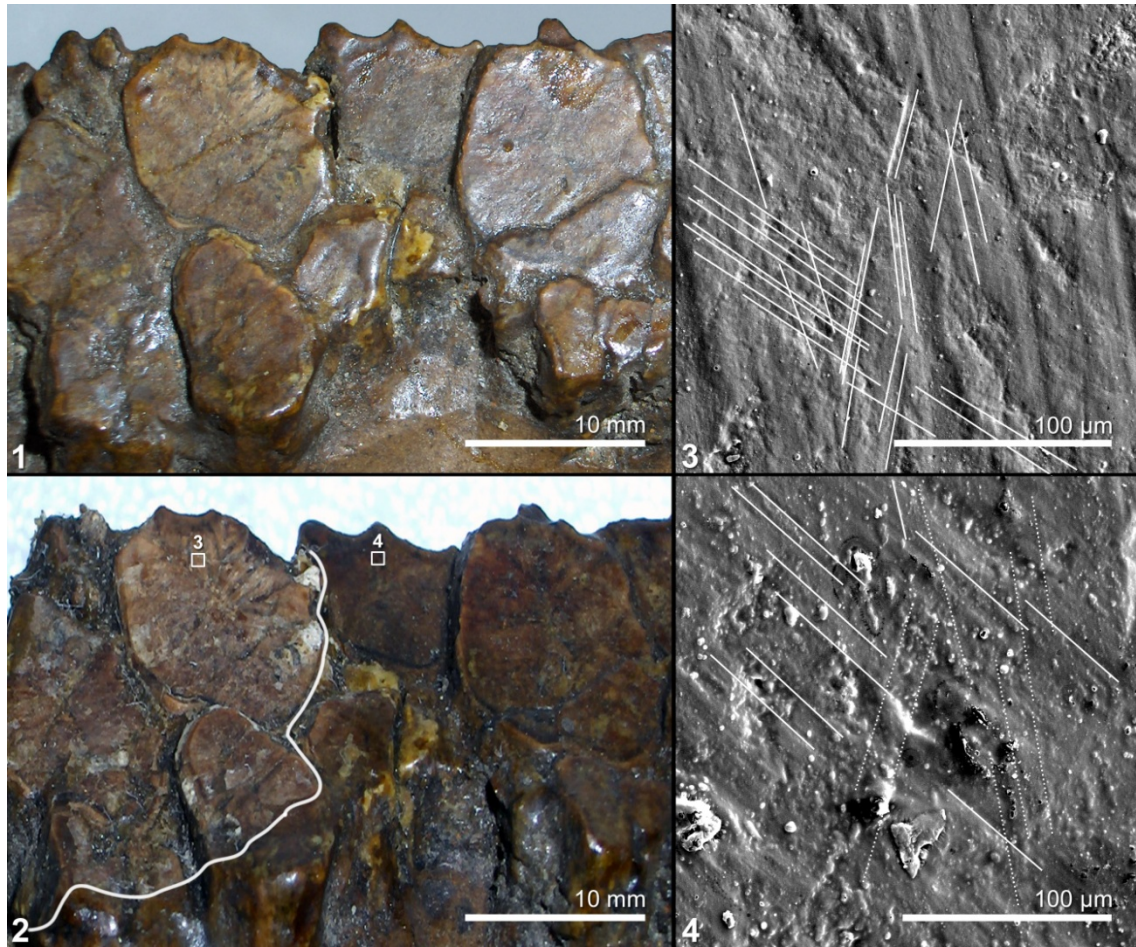


Figure 3. Occlusal surface of left dentary teeth of *Corythosaurus casuarius* (AMNH 3971), illustrating the results of cleaning with solvent gel.

- 3.1 Photograph of mesial fragment of left dentary prior to cleaning.
- 3.2 Post cleaning, shellac removed from teeth on the left by application of solvent gel; boxes show areas illustrated in 3.3 & 3.4. Broad white line drawn on to highlight the sharp boundary of the area from which shellac has been removed.
- 3.3 SEM micrograph of cast of central portion of a cleaned tooth (area in box 3 of 3.2); multiple microwear orientations (part highlighted with solid white lines) are visible with no remnant of varnish.
- 3.4 SEM micrograph of cast of central portion of an un-cleaned tooth (area in box 4 of 3.2); microwear (part highlighted with solid white lines) is discernable but is largely obscured by varnish; in particular the near vertical microwear (part highlighted with dashed white lines), which is visible in 3.3, is barely noticeable here.

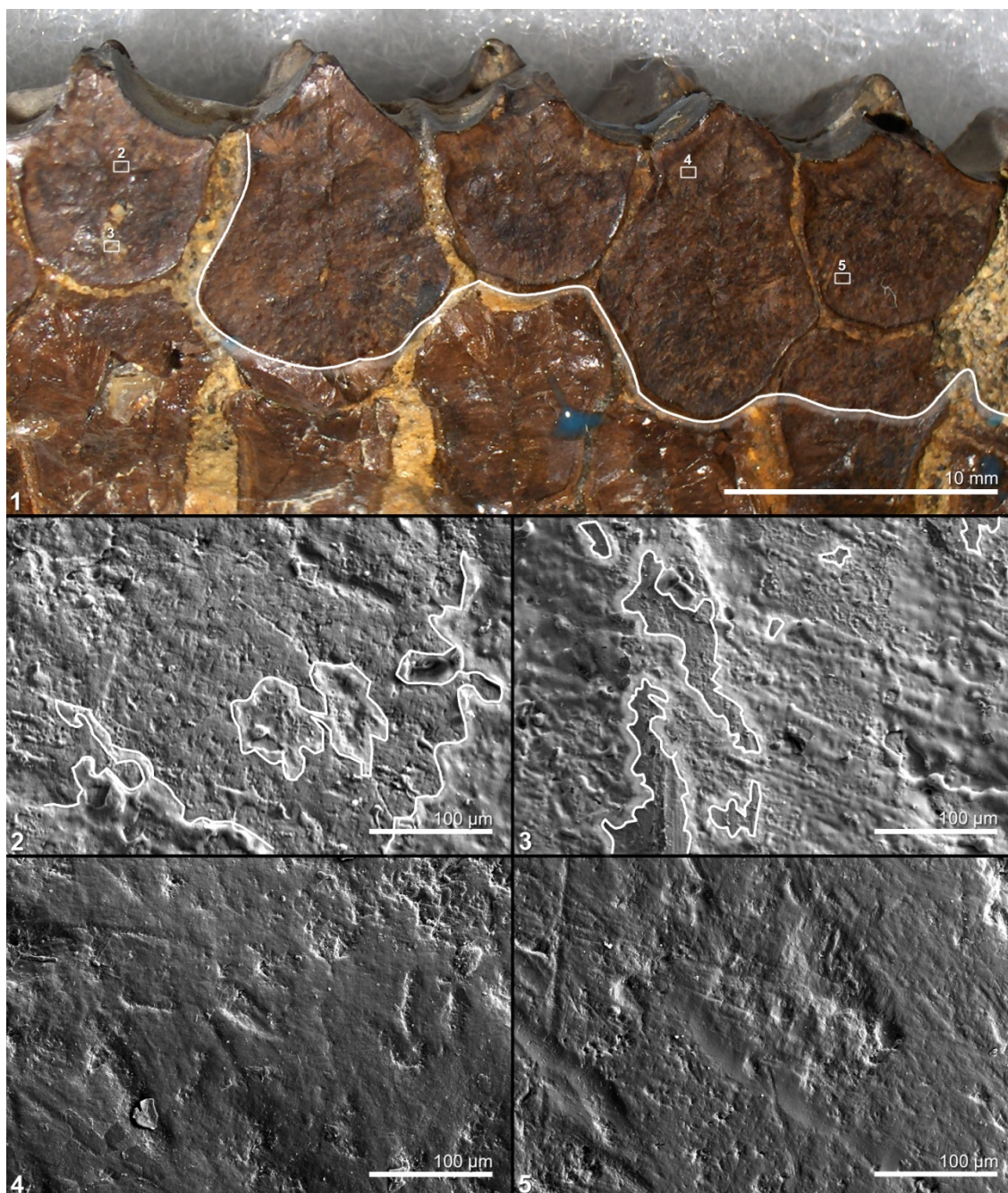


Figure 4. Occlusal surface of left dentary teeth of *Edmontosaurus* (SM 22102), illustrating the results of cleaning with solvent gel.

- 4.1 Photograph of distal section of a left dentary. White line drawn on to highlight the sharp boundary of the area from which shellac has been removed. The teeth on the top row and to the right have been cleaned by application of solvent gel. The teeth on the left and along the bottom row were not cleaned and remain coated in shellac. Boxes show areas of tooth illustrated in 4.2 to 4.5.
- 4.2 SEM micrograph of cast of site on un-cleaned tooth (area in box 2 of 4.1); microwear is obscured by shellac. White lines drawn around areas of shellac, with shading in the shellac.
- 4.3 SEM micrograph of cast of site on un-cleaned tooth (area in box 3 of 4.1); microwear is obscured by shellac. White lines drawn around areas of shellac, with shading in the shellac.
- 4.4 SEM micrograph of cast of site on cleaned tooth (area in box 4 of 4.1); showing microwear with no remnant of shellac.
- 4.5 SEM micrograph of cast of site on cleaned tooth (area in box 5 of 4.1); showing microwear with no remnant of shellac. (Note: the broad shallow grooves are typical of tool marks left by a vibro-tool during preparation of a fossil.)

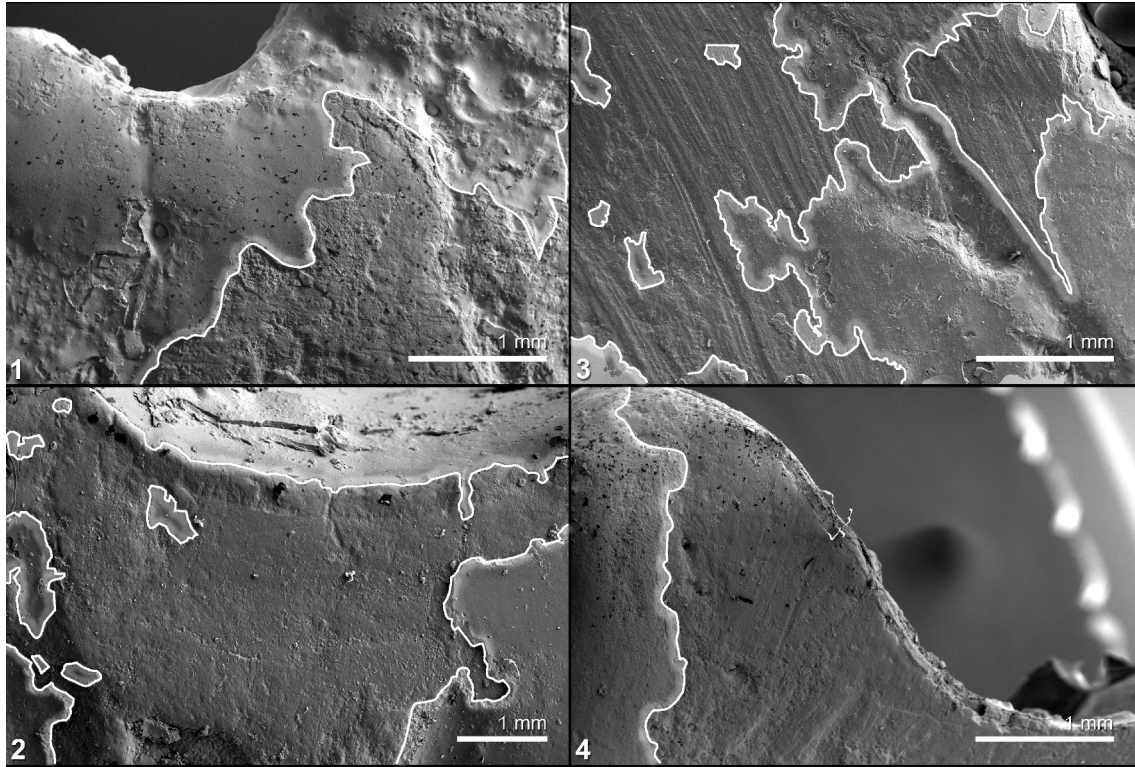


Figure 5. Occlusal surfaces of hadrosaurid teeth (SEM images of casts) illustrating the results of cleaning with solvent gel. These teeth were marginal to areas that were cleaned by the application of solvent gel prior to moulding and casting and show the clear boundary between the consolidant layer and clean tooth surface. White lines drawn around areas of shellac, with shading in the shellac.

5.1 *Edmontosaurus* AMNH 5879 right maxilla tooth, right hand side of tooth has been cleaned.

5.2 Hadrosaurid AMNH 5896 maxilla tooth, left hand side of tooth has been cleaned; vestiges of consolidant remain on the left hand side in depressions.

5.3 *Hadrosaurus notabilis* SM 5465 left dentary tooth, left hand side of tooth has been cleaned.

5.4 Hadrosaurid AMNH 6387 right maxilla tooth, right hand side of tooth has been cleaned

ACKNOWLEDGEMENTS

This paper has benefited from discussions with Mark Purnell of The University of Leicester, Nicholas Eastaugh of The Pigmentum Project and the comments of the anonymous reviewers. I am grateful to Paul Barrett & Sandra Chapman, Natural History Museum; Christopher Norris, Carl Mehling & Jeanne Kelly, American Museum of Natural History; Walter Joyce & Marilyn Fox, Yale Peabody Museum; Matthew Lamanna & Amy Henrici, Carnegie Museum; Matthew Carrano, Smithsonian Institution; Derek Siveter & Paul Jeffery, Oxford University Museum of Natural History and Martin Munt & Lorna Steel, Dinosaur Isle Museum; for granting access to and permission to clean the dinosaur teeth. John Larkham of Coltène Whaledent is thanked for donating polyvinylsiloxane moulding compound.

APPENDIX

Components and Suppliers:

Carbopol was originally manufactured by B F Goodrich (now Noveon). It was available in several formulations (e.g., 934, 940, 950 and 954) and it is these that are discussed by painting conservators (Southall 1988; Wolbers *et al.* 1990). EZ2 is a newer but comparable formulation of Carbopol and is more readily available today than the older versions. It is supplied as a white powder and when mixed with pure water forms a clear, slightly acidic, viscous gel. The water must be pure otherwise any minerals present (particularly calcium) will react with the Carbopol and precipitate out. The manufacturers claim that the EZ formulations disperse more quickly and this certainly appears to be the case (EZ2 can be used within minutes of mixing whereas 954 took over an hour to achieve a uniform consistency). Carbopol 954 based solvent gels were used within the Palaeontology Conservation Unit at the Natural History Museum, London and Carbopol EZ2 based solvent gels were used on specimens at all other sites.

Ethomeen is manufactured by Akzo. There are two forms suitable for use in solvent gels (C/12 and C/25) with C/25 being recommended for use with the more polar solvents (Wolbers *et al.* 1990). Ethomeen is an ochre coloured viscous liquid and is slightly alkaline. Both forms are available from Linden Chemicals.

CHAPTER 3

Dental microwear in dinosaurs: a comparative analysis of polysiloxane replication

Published: *Dental Practice*, March 2006, 44:3

Every time a tooth comes into contact with food or with another tooth it is damaged. Abrasive particles cause microscopic scratching and pitting, and while this may seem undesirable from the point of view of the tooth's owner, it is good news for palaeontologists because the 'microwear' that accumulates on the tooth surface provides a record of what has been eaten and the range of tooth movements involved. This is true of humans and any other animals with teeth, both extant and fossil, and studies of living mammals with controlled or known diets have established the relationship between feeding and microwear sufficiently well for the microwear footprint on fossil teeth to be used to interpret diet.

This is an extremely powerful tool with which to analyse feeding in extinct animals and has been applied extensively to fossil hominoids in order to evaluate the role of dietary changes in human evolution (Teaford and Ungar 2000). It has also been applied to extinct mammals and has revealed in surprising detail how feeding in mammals has tracked past environmental change (Solounias and Hayek 1993; Semprebon *et al.* 2004). But can the same technique be applied to dinosaurs?

We are attempting to find out by conducting the first systematic study of dinosaur microwear. Our main aims are to understand how diet and feeding changed during the evolution of a major group of herbivorous dinosaurs, and assess whether dietary changes were related to known changes in the environment and vegetation. For example, we know from the fossil record that between 150 and 60 million years ago, the gymnosperm conifer forests which had dominated the global flora for more than 100 million years were replaced by angiosperm flowering plants. It seems quite likely that such a major change in food supply would have had significant effect on herbivorous dinosaurs and their evolution. More surprisingly, it has also been suggest

that the grazing activities of dinosaurs may have been an important factor in causing this change in vegetation.

Before we can evaluate what the microwear footprint of dinosaurs can tell us, however, we need to understand two things. Firstly, we need to see what microwear in dinosaur teeth looks like, because dinosaur teeth are very different to those of mammals. Mammals replace their teeth just once, so adult teeth are retained in the mouth for a long time over which microwear can accumulate. Dinosaurs, on the other hand, shed worn teeth and continued to grow replacements throughout their life. To further complicate matters, dinosaur jaw articulation is very different to that of mammals and they did not bite or chew their food in the same way. In fact the jaws of most dinosaurs, including all of the earliest forms, could only move up and down, meaning that their tooth surfaces could not slide across each other like those of mammals do, making chewing impossible.

Secondly, we cannot conduct the experiments required to establish the relationship between food type and microwear in dinosaurs because most of them are extinct and those that survive (birds) have no teeth. The nearest extant relatives with teeth are reptiles, so we need to investigate microwear and feeding in living reptiles. Our dinosaur study will focus on ornithopods, a large group of herbivorous dinosaurs including well-known characters like *Iguanodon*. They make an ideal group to investigate because they are known from strata of earliest Jurassic through to latest Cretaceous age, an interval of 140 million years, with their continuous evolutionary history spanning most of the time that dinosaurs existed.

The earliest ornithopods had no ability to masticate food as their jaws occluded in the vertical plane only, slicing and shredding vegetation in a manner similar to that of living iguanas. Later ornithopods, however, evolved two different but highly successful

mechanisms for masticating food. The most advanced forms evolved a hinge in the top of their skulls that allowed the upper jaws to slide laterally over the lower jaws and grind plant material between them, in essence allowing them to chew.

To carry out our research we need to examine teeth under high magnifications in a scanning electron microscope (SEM), but ornithomimid specimens are distributed in various museums and private collections around the world, and most are either too large to fit in a SEM or unavailable for loan. Consequently we need to obtain casts of teeth, and this requires a moulding material that will replicate tooth microwear with high fidelity and, crucially, leave fragile dinosaur material undamaged. This is a tough challenge because after millions of years, dinosaur teeth tend to be rather brittle and cracked, and are usually held together with a cross between glue and varnish known as a consolidant.



Fig 1a - *Lambeosaurus lambei* YPM 3222 skull, from the Upper Cretaceous Oldman Formation of Alberta, Canada. YPM – Yale Peabody Museum.

The varnish-like sheen can be seen on **Fig 1a**, a skull of the ornithomimid dinosaur *Lambeosaurus lambei* that is coated in consolidant. Obviously this has to be removed from the tooth surface to get at the microwear, so what starts out as an already fragile fossil suddenly becomes very fragile indeed. Similar studies on fossil mammal teeth have used room temperature vulcanizing (RTV) silicone rubbers, but these are unsuitable for a number of reasons. The silicon fluid they contain tends to penetrate and stain the surface of fossils, and many have a high tear strength, meaning that unless a release agent is used, parts of the fossil can be pulled away as the mould is removed – and this is not good. In addition most RTV silicone rubbers have long cure times, and while this may be acceptable for use on fossils it is unworkable where live reptiles, an important part of our study, are concerned.

Polysiloxane impression mediums have none of these drawbacks and look to be ideal for our purposes. Their low tear strength in particular means that they are likely to give-way before a fossil tooth gets pulled apart. The only aspect of using polysiloxanes about which we were uncertain was the fidelity with which they can replicate microwear. The scratches and pits we are interested in are measured in microns (thousandths of a millimetre), and the replicated surface must pick up every feature or the statistical analysis of the microwear patterns will be fatally flawed. In order to evaluate whether polysiloxanes were up to the job, we performed a comparative test of a number of polysiloxane dental impression mediums, including Aquasil, Reprosil, GC Examix, GC Exafast, Coltene President Jet & Coltene Speedex.

After removal of any consolidant, tooth surfaces were cleaned with a fine, soft brush. Impression medium was mixed according to the manufacturer's instructions; small quantities (less than 30 ml) were generally used, but this varied according to the size of the specimen being moulded.

After moulding the occlusal tooth surfaces (**Fig 1b**), casts were prepared using low viscosity Araldite 20/20 epoxy resin. These were then mounted for SEM and sputter coated with gold (**Fig. 1c**).

Fig 1b - Speedex Light moulds of isolated teeth from the ornithomimid dinosaur *Hypsilophodon foxii* (MIWG 6362), from the Wessex Formation, Isle of Wight. MIWG –Dinosaur Isle Museum, Isle of Wight.



Due to the fragile nature of dinosaur teeth, the initial testing was performed on hyena teeth progressing to dinosaur teeth only when the moulding process was proven safe.



Fig 1c - Araldite 20/20 cast of a tooth from the ornithomimid dinosaur *Hypsilophodon foxii*, made from a Speedex Light mould, then mounted on a SEM stub and sputter coated with gold.

Results

The results of comparative testing showed that the condensation polymerizing polysiloxanes gave the best performance, and out of these the best was Coltene/Whaledent's Speedex Light, which produced near perfect replication of the dental microwear once the casts were splutter coated in gold.

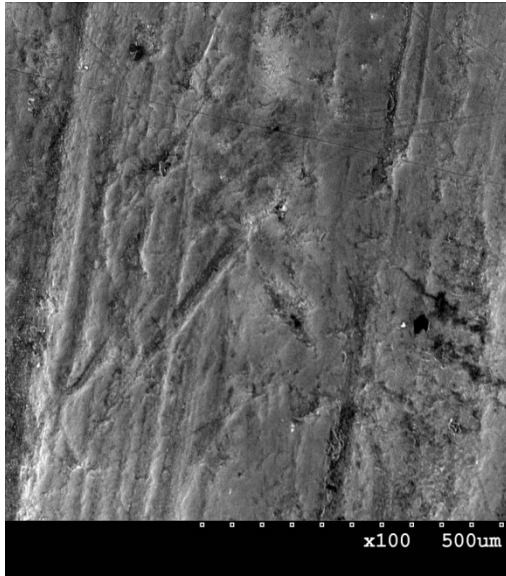


Fig 2a – SEM Image of a Hyena canine tooth.

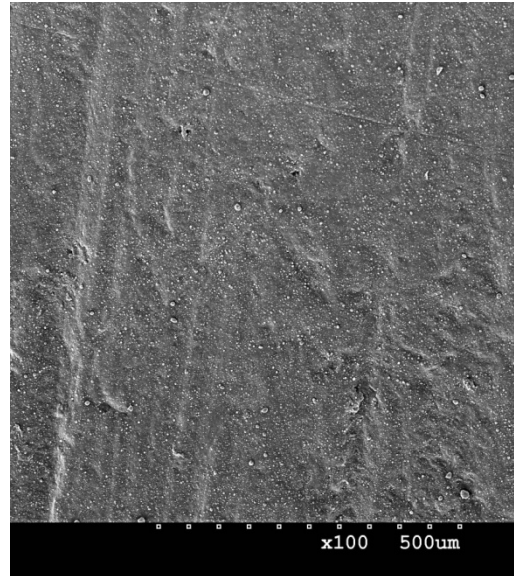


Fig 2b – SEM Image of a cast made from a GC Exafast mould.

Fig 2 compares microwear on a fossil hyena tooth (**Fig 2a**) to that replicated on casts made from a GC Exafast mould (**Fig 2b**) and a Speedex Light mould (**Fig 2c**). (GC Exafast was the next best performing medium after Speedex Light).

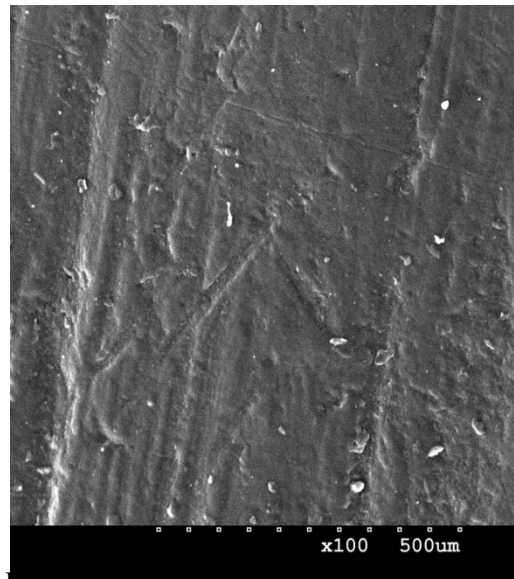


Fig 2c – SEM Image of a cast made from a Speedex Light mould.

Fig 3a - SEM image of microwear on a *Hypsilophodon foxii* tooth. MIWG.6362.

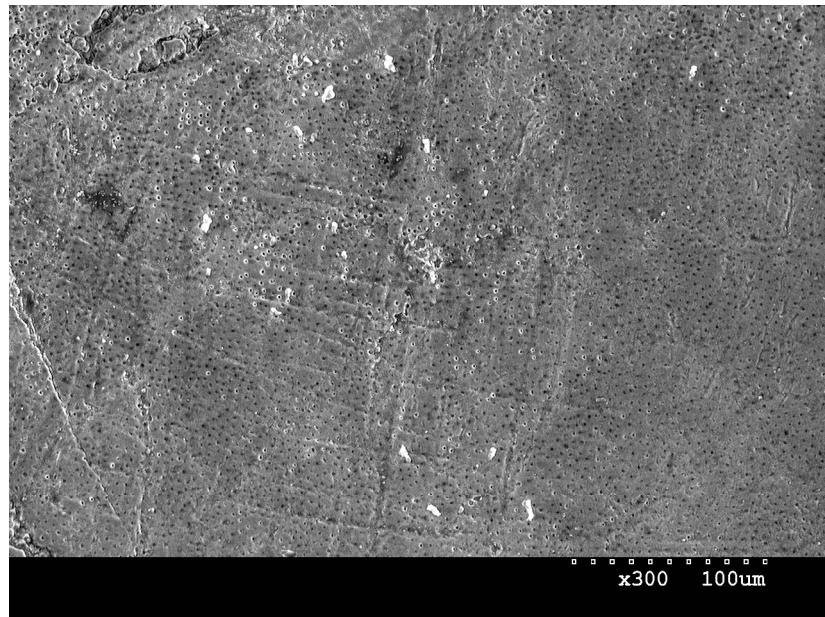


Fig 3b - SEM image of microwear on a cast made from a Speedex Light mould.

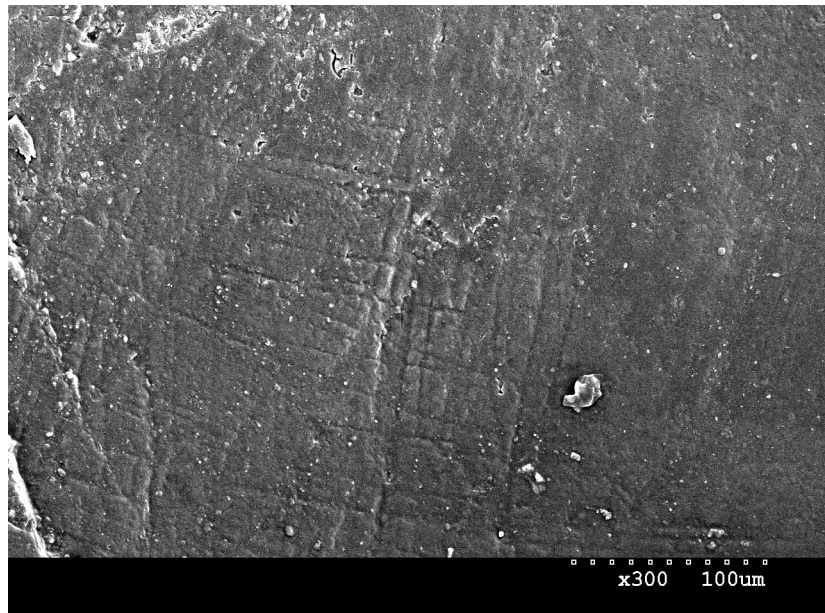


Fig 3c - Microwear highlighted



Fig 3 compares microware, at a much higher magnification, on an ornithopod dinosaur (*Hypsilophodont foxii*) tooth (**Fig 3a**) to that replicated on a cast made from Speedex Light (**Fig 3b**), the microwear in which we are interested is highlighted in **Fig 3c**. Here the cast gives better definition than the original tooth; this is typical and relates to the coating in gold which cannot be applied to the original tooth.

Multiple casts were taken from the same Speedex Light mould with no appreciable difference in the quality of the casts and there was no significant shrinkage of the moulds over three months.

Summary

Care needs to be taken when de-moulding as the polysiloxanes, whilst reasonably elastic, will tear if more than gentle ‘teasing’ is attempted. Immediately after de-moulding, the polysiloxanes are susceptible to condensation and the moulds must be dried thoroughly before casting. Many of the polysiloxanes require mixing guns and whilst these were very easy to use, the ability to be hand mixed proved to be a great advantage as it allowed the working time to be varied.

Due to the low viscosity of the polysiloxanes, it was necessary to create a ‘dam’ around some specimens to prevent overflow from the area to be moulded. No damage was caused to any of our specimens by Speedex Light or GC Exafast.

Our results demonstrate that Speedex Light can replicate tooth microware at magnifications in excess of 300 times and this is more than sufficient for our research needs. Using this medium our research will progress to form a systematic investigation of tooth microwear in ornithopod dinosaurs, building on previous microwear work. Our studies will have clear implications for understanding the diet and the evolution of feeding mechanisms in dinosaurs and present day reptiles.

Acknowledgements

We thank Martin Munt and Lorna Steel (Dinosaur Isle Museum, Isle of Wight) for loan of the *Hypsilophodont foxii* specimens and Walter Joyce (Yale Peabody Museum) for access to the *Lambeosaurus lambei* specimen. We also thank Coltene/Whaledent and GC for supplying samples of their polysiloxane impression mediums for inclusion in our comparative testing.

CHAPTER 4

Tooth replication techniques for SEM imaging and microwear analysis in dinosaurs

Written in the format for the journal *Palaeontologia Electronica*, but intended for internal department use rather than publication.

ABSTRACT

To obtain the best results from scanning electron microscope (SEM) photomicrography, the subject material usually needs to be coated (metalized) and the SEM operated in full vacuum. Whilst the metallization process can be reversible, few museum conservators are willing to risk damage to dinosaur material from either the coating process or the vacuum. Although uncoated material can be imaged in partial vacuum, the resultant images are rarely as good and the SEM chamber is will only accommodate the smaller dinosaur jaw elements. The alternative is to mould and cast the original and SEM image the coated mould or cast. For any moulding and casting technique to be suitable for use in dental microwear analyses it must replicate tooth microwear with a high degree of fidelity. The technique must also be acceptable to museum curators and conservators or access to specimens could be denied. Traditional room temperature vulcanising (RTV) rubbers have a long cure time and require a releasing agent to prevent damage to the fossil. I describe here a safe and rapid technique for replicating dinosaur tooth surfaces that is acceptable to museum curators. The resultant casts can produce micrographs that can be shown to be comparable with those of coated original teeth imaged in full vacuum and superior to those of uncoated original teeth imaged in partial vacuum.

INTRODUCTION

Due to their high fossilization potential, teeth tend to be more abundant in the fossil record than the jaw bones and other component parts of fossil animals. Their rarity however, can still be a cause of concern to museum curators and conservators. For Scanning Electron Microscopy (SEM) research, the desire to coat (metalize) material and subject it to full vacuum for imaging adds to the conservators concerns and whilst original uncoated material can be imaged in partial vacuum in a SEM equipped with an environmental chamber, the results are rarely as good. More problematic are complete jaws and large jaw fragments which are too big for the SEM's environmental chamber. Even when a jaw element is small enough to fit in an environmental chamber it can be difficult to manipulate and achieve the correct orientation to the beam. As a consequence, coated tooth casts tend to be the main source for SEM research (Galbany *et al.* 2004).

The use of tooth casts has additional advantages in that casts are reproducible and can therefore be cut and mounted in any orientation for imaging, and otherwise inaccessible parts of jaw elements can be moulded and replicated. For any moulding and casting technique to be suitable for use in dental microwear analyses it must replicate tooth microwear with a high degree of fidelity. The technique must also be acceptable to museum curators and conservators or access to specimens could be denied. Coated casts imaged in full vacuum should produce micrographs that can be shown to be comparable with those of coated original teeth imaged in full vacuum and superior to those of uncoated original teeth imaged in partial vacuum.

This paper describes the moulding and casting method used by the author for the replication of ornithopod dinosaur teeth, specifically for quantitative microwear analysis at x300 magnification.

Moulding & Casting Techniques

Room temperature vulcanizing silicone rubber (RTV) impression mediums, traditionally used for moulding fossils (Waters and Savage 1971; Chaney and Goodwin 1989) are capable of reproducing detail at the sub-micrometer level for SEM imaging purposes (Rose 1983). There are a number of advantages to these mediums, including low shrinkage and good shelf life stability, and they have been used successfully for tooth microwear analysis (Purnell 2003). The disadvantages are long cure times, relatively high tear strengths, the need to use a release agent on some fossils to prevent damage whilst de-moulding, and staining of the fossil surface by silicon fluid ingress. For these reasons, RTV mediums were deemed unsuitable for a project that involved the replication of large numbers of museum specimens of dinosaur teeth from different museums on a limited time scale.

Polysiloxane dental impression materials have been used extensively in tooth microwear analysis research on mammal teeth (Gordon 1984a; Grine 1986; Ungar 1996; Galbany *et al.* 2004), in particular the President Jet (Coltene\Whaledent) line which is available in various viscosities. These impression mediums have a rapid cure time, do not need a releasing agent and have relatively low tear strengths. This latter point is critical for the moulding of dinosaur material since it is often brittle, cracked and less robust than mammal material. One disadvantage is that most of these products are auto-mixed via an applicator gun and so the working time is limited and significant amounts of the mixed medium are wasted in the disposable mixing nozzles.

Following a comparative study of polysiloxane impression mediums and original fossils (Williams *et al.* 2006) the hand mixed medium Speedex Light

(Coltene\Whaledent) was selected, this gave near perfect replication of tooth microwear and allowed a degree of control over working time and tear strength.

Casting was performed with Araldite 2020 (Hunstman), a casting medium with a high fidelity to RTV moulds and a track record in tooth microwear analysis (Chaney 1989; Purnell 2003). Araldite 2020 is a two part, room temperature curing, low viscosity adhesive specifically designed for bonding glass but also suitable for clear castings. The resin and hardener mix produces a water-white epoxy resin that flows easily into the micrometer scale detail of the Speedex Light moulds replicating the tooth microwear. It has proven to be compatible with Speedex Light, allowing several casts to be made from a mould with no appreciable reduction in quality.

MATERIALS

Ornithopod dinosaur specimens from the collections of the Natural History Museum, London (**NHMUK**); the American Museum of Natural History, New York (**AMNH**); the Peabody Museum of Natural History, Yale University (**YPM**); the Smithsonian Institution National Museum of Natural History, Washington, D.C. (**SM**); the Carnegie Museum of Natural History, Pittsburgh (**CM**); the Dinosaur Isle Museum, Isle of Wight (**MIWG**) and the Oxford University Museum of Natural History, Oxford (**OUM**) were cleaned using solvent gels (Williams and Doyle 2010) and moulded with Speedex Light (Coltene\Whaledent).

The cleaned occlusal surfaces of hundreds of teeth from one hundred and forty three specimens which consisted of individual teeth, teeth within jaw fragments and teeth within complete jaw elements were moulded a minimum of three times each. The first moulds were discarded and epoxy resin casts from the second and third moulds were sputter coated in gold and SEM imaged.

METHOD

Dinosaur teeth tend to be rather brittle and cracked, and it is not unusual to find them glued together from multiple pieces or to find teeth glued in place within jaw fragments. Typically consolidants such as shellac, glyptal or paraloid coat the occlusal surfaces. Prior to moulding, the surface of the specimen should be cleaned of consolidant (Williams and Doyle 2010). Voids or cracks where impression medium might penetrate and cause damage during de-moulding should be temporarily filled to a point slightly below the surface. Areas where the tooth or bone is fragile and there is danger of loose material being removed when de-moulding, particularly along the base of the tooth rows, should be given temporary protection. A water soluble wax such as polyethylene glycol (PEG) is ideal for this. Good results have been obtained with PEG 1500 (Fisher Scientific).

Preparation:

Remove consolidant from the occlusal surfaces to be moulded and orient the teeth or jaw element such that the occlusal surface is level and use a soft brush to remove any loose dirt.

To infill holes/cracks or protect fragile areas, melt flakes of PEG in a container and apply it to the tooth with a fine (00 or 0) brush. PEG can be melted by floating the container in hot water or placing the container in a microwave at full power for two or three minutes. It will harden when cool and can be removed after the moulding process is complete by brushing on warm water into which it will dissolve.

For the best possible results, build a dam around the area to be moulded using stretch plastic wrap (cling film/Saran Wrap) and Plasticine or modelling clay (Figure 1).



Figure 1. Preparing to mould a portion of *Edmontosaurus* NHMUK R4929 left maxilla. The bone surrounding the teeth to be moulded has been covered with stretch plastic wrap onto which plasticine has been applied to create a dam wall. The stretch plastic wrap is folded back to cover the plasticine wall, to protect the bone from staining due to the oil in the plasticine and to prevent a reaction with the Speedex light

The plastic wrap should be applied first, between the fossil and the Plasticine to prevent oil within the Plasticine staining the fossil. Plastic wrap should also be used inside the walls of the dam to prevent contamination of the impression medium by the Plasticine. The dam wall should be at least 2 to 3 mm higher than the surface to be moulded and its base should be a similar distance below the tooth surface (more if off-occlusal microwear is required).

Moulding:

Make up a small volume of impression medium by squeezing out a strand of Speedex Light base and a strand of Universal Activator onto a glass plate. The thin green strand of Universal Activator should be one third to one half the length of the

thick blue strand of Speedex Light base. The volume required will vary according to the size of the specimen being moulded, but any more than 30 ml will be difficult to apply successfully within the working time available. Scoop the thin green strand of activator up onto a spatula and spread evenly over the thicker blue strand of base material and then mix the two components thoroughly for ten to fifteen seconds until a uniform colour is achieved. When thoroughly mixed, a thin initial coating of Speedex Light can be applied to the specimen. The best results are achieved by trickling a small quantity of the Speedex Light onto the surface of the specimen from a spatula positioned around 1 cm above the specimen and allowing the impression medium to flow into the fine surface features and form a thin coating. Air can be trapped forming bubbles in the mould if this stage is rushed or the Speedex Light is applied too thickly. Re-load the spatula and repeat the application at several points on the tooth surface. Aim to use up the Speedex Light within two to three minutes of mixing.



Figure 2. Moulding a portion of *Edmontosaurus* NHMUK R4929 left dentary. The blue Speedex light impression medium has been poured over the teeth into a prepared plasticine and stretch plastic wrap dam and left to cure

Make up a larger volume of impression medium by squeezing out equal strand lengths of Speedex Light base and Universal Activator onto a glass plate and mixing thoroughly as before. Apply this on top of the initial thin coating before it has cured (whilst the initial thin coating is still tacky) to surround and cover the tooth surface (Figure 2). Aim to use up this mix of Speedex Light within one minute of mixing.

By varying the relative proportion of activator to base, the viscosity and working time can be controlled. A normal mix uses equal strand lengths of activator and base and has an effective working time of approximately 45 seconds (assuming 15 seconds of mixing). It can continue to be worked after this time (e.g. to build up a mould), but its viscosity will be too high to flow into any fine surface features. The full cure time from first base/activator contact of a normal mix is 120 to 150 seconds. Less activator will produce a lower viscosity mix that will take longer to cure and will produce a mould with lower tear strength. One third of the recommended amount of activator will produce a mix that can take up to thirty minutes to cure and has an effective working time (i.e. will reliably replicate microwear features throughout this time) of five to six minutes.

If it is not practical to build a dam around the surface to be moulded, an alternative method that has proven successful uses a normal to slightly more viscous mix of Speedex Light. This is applied directly to a flat, level tooth surface in a spiral action, in a similar fashion to the icing of an ice-cream cone. The Speedex Light must be used within a few seconds of mixing in order to flow into and replicate microwear. The cone of Speedex Light will tend to collapse under gravity as it cures and this pushes trapped air to the circumference.

Cured Speedex Light can be simply peeled from the glass mixing plate. The plate can also be cleaned with soap and water; additionally Speedex Light will dissolve in acetone.

If a lower viscosity mix has been used, de-moulding should not be attempted within one hour of mixing. Care needs to be taken when de-moulding as Speedex Light, whilst reasonably elastic, will tear if more than gentle 'teasing' is attempted.

Immediately after de-moulding, polysiloxanes are susceptible to condensation and the



Figure 3. Speedex light mould. This is the first one taken and contains detritus from the tooth surface. These first moulds were discarded.

moulds must be dried thoroughly before casting is attempted. The first mould of a surface will tend to pick up any loose material from the fossil surface along with residues of cleaning solvents and swabs

that may have been missed. Experience suggests that this first mould should be discarded (Figure 3).

Speedex Light base and its Universal Activator are human dental impression mediums and if used as directed by the manufacturer there are no known hazards. PEG 1500 however, is a mild irritant. Care should be taken to follow the manufacturer's instructions regarding safe use and storage of all of these products. Material Safety Data Sheets (MSDS) are available via the manufacturer's web sites. Speedex Light is a product of Coltene\Whaledent (www.coltenewhaledent.biz) and PEG 1500 is a product of Fisher-Scientific (www.fisher.co.uk, www.fishersci.com).

Casting:

The casting technique used here is based upon the method described by Purnell (2003) and is suitable for use with either the Araldite 2020 hand mix working pack (as detailed below) or the auto-mix gun.

Make up a small batch of Araldite 2020 according to the manufacturer's instructions for weight measurement (e.g. 100:30 by weight of resin 2020/A to hardener 2020/B). There is a clear colour difference between the resin and the darker hardener which will initially sit on top of the resin forming a separate layer. Stir the two together until the liquid is a uniform water-white, this may take several minutes. As air bubbles will inevitably be formed, allow the mixed liquid to stand for a few minutes for these to dissipate.

If the moulding process did not produce moulds with a continuous intrinsic wall around their outer edges, a small batch of Speedex Light or the more viscous Speedex Putty should be mixed up and pressed around the outside of the moulds to make them liquid tight.

To limit the formation of air bubbles add the mixed Araldite 2020 drop by drop to the wall of each mould at the highest point, allowing it to flow slowly over the surface of the mould until the mould is filled.

When mixed in small batches (< 30 ml) Araldite 2020 has a working time of approximately 45 minutes and a cure time of 20 hours at 15°C (48 hours for full hardness). The cure time decreases with rising ambient temperature (16 hours at 23°C, 3 hours at 40°C) and increases with falling ambient temperature (24 hours at 10°C) and the time to achieve full hardness varies likewise. In addition, because the reaction between resin and hardener is endothermic, mixing larger batches will also reduce both working time and cure time. It can be handled as soon as it is no longer tacky.



Care needs to be taken when de-moulding as the Speedex Light moulds, whilst reasonably elastic, will tear if more than gentle 'teasing' is attempted (Figure 4).

Figure 4. Transparent Araldite 2020 cast. This will be sputter coated in gold before imaging in the SEM.

Araldite 2020 has toxic components and is an irritant. Any spillage should be cleaned up immediately with disposable paper towels as although cured residue will dissolve in acetone it can be extremely difficult to remove. Care should be taken to follow the manufacturer's instructions regarding safe use and storage of this product. The MSDS is available from the manufacturer's web site (www.araldite.com). The MSDS for Speedex Putty base is available from (www.coltenewhaledent.biz).

SEM Imaging of teeth and casts:

A comparison of tooth microwear from an original dinosaur tooth (*hypsilophodont foxii*) and a cast replicated from that tooth using the procedure described in this paper shows the high fidelity of the replication technique (Figure 5). For image capture, the orientation of the occlusal surface of the teeth was standardized, with the long axis of the tooth row and the flat occlusal surfaces of the teeth perpendicular to the electron beam. SEM images were captured at a magnification of 300, providing a sampling site field of view of 417 x 312 μm , comparable with that commonly used in analysis of occlusal microwear in mammals (Grine *et al.* 2002; Scott *et al.* 2005). The microwear features in which I am interested are highlighted (Figure 5.3) and it can be seen that the cast (Figure 5.2) gives better definition than the original

tooth (Figure 5.1). This is typical and relates to the sputter coating in gold that was given to the cast which cannot be applied to the original tooth.

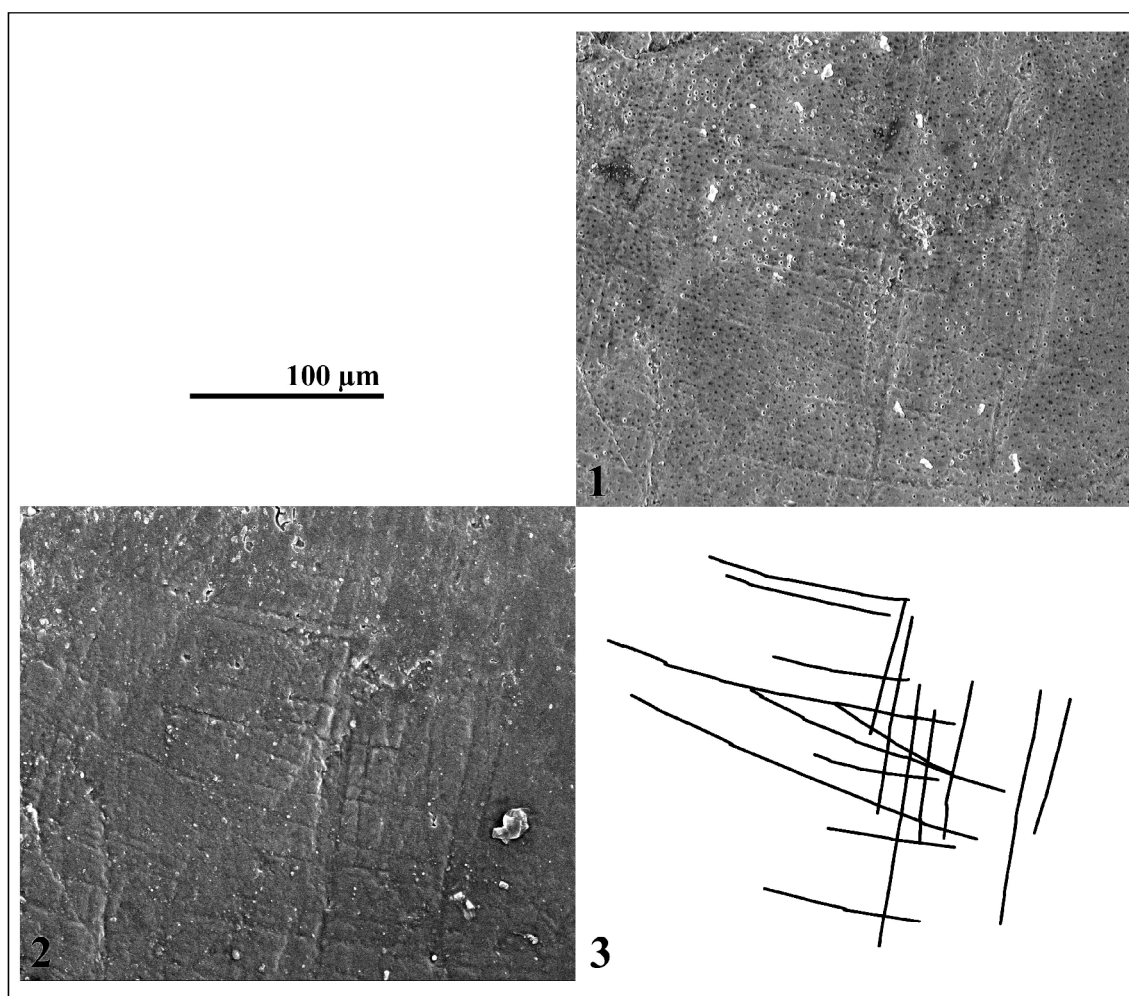


Figure 5. SEM image of microwear on a tooth from the ornithomimid dinosaur *Hypsilophodon foxii*. MIWG 6362. 5.1 SEM image of original tooth. 5.2 SEM image of an Araldite 20/20 coated cast. 5.3 Sample of the replicated microwear.

RESULTS AND DISCUSSION

The results demonstrate that Speedex Light can replicate tooth microwear to a standard that is comparable to that of uncoated original teeth at magnifications in excess of 300 times. The added flexibility of hand mixing means that the tear strength of the polysiloxane moulding medium can be sacrificed to protect the fossil. The low tear strength generated by using reduced amounts of activator result in a mould that is likely to give-way before a fossil tooth is pulled apart allowing moulding of less robust fossils and safe moulding in confined spaces. Multiple casts can be taken from the same Speedex Light mould with no appreciable difference in the quality of the casts. This allows multiple casts to be made and then cut and mounted in various orientations such that otherwise inaccessible parts can be imaged. Additional casts can be made as and when needed during an extended research period as no significant shrinkage or deterioration of the moulds occurred over nine months.

The casting and moulding techniques and the materials described in this paper were cleared and authorised for use by the museum curators and collection managers listed.

ACKNOWLEDGEMENTS

This paper has benefited from discussions with Adrian Doyle of the Natural History Museum, Palaeontology Conservation Unit, London and Mark Purnell of the University of Leicester. I am grateful to Paul Barrett & Sandra Chapman, Natural History Museum, London; Christopher Norris, Carl Mehling & Jeanne Kelly, American Museum of Natural History; Walter Joyce & Marilyn Fox, Yale Peabody Museum; Matthew Lamanna & Amy Henrici, Carnegie Museum; Matthew Carrano, Smithsonian Institution; Derek Siveter & Paul Jeffery, Oxford University Museum of Natural History and Martin Munt & Lorna Steel, Dinosaur Isle Museum; for granting access to and permission to clean the dinosaur teeth. John Larkham of Coltène Whaledent is thanked for donating polyvinylsiloxane moulding compound.

CHAPTER 5

Statistical analysis of microwear orientation data

Targeted for the journal *Biometrika*

SUMMARY

This paper considers the problem of testing for variance in multimodal directional data obtained from tooth microwear analysis. Circular statistical methods traditionally used for this purpose such as the parametric Watson-Williams F test and the non-parametric Mardia-Watson-Wheeler test, and linear tests such as Wilcoxon/Mann-Whitney U test have proven susceptible to both Type I and Type II errors. Here I describe a less error-prone yet appropriately stringent statistical test for the analysis of microwear orientation data.

1. INTRODUCTION

Microwear refers to the microscopic polished, scratched or pitted textures produced *in vivo* by the actions of abrasives in or on food and by the compressive and shearing forces that act on teeth during feeding (Walker *et al.* 1978; Teaford 1988a). The variation in microwear texture with respect to size, shape, density and orientation of the features is a function of the force and direction of jaw motion but it is also influenced by the physical properties of the food being processed. The orientation of scratches within these textures have been used to predict the direction of movement of teeth (e.g., Teaford and Byrd 1989; Goswami *et al.* 2005; Schubert *et al.* 2006), but only at the most rudimentary level, using rose diagrams and orientation concentration (r). What is needed is an accurate, reliable test to determine if microwear features show consistent preferred directions (that relate to jaw movement) in an individual animal and if those directions are common to all individuals within a species, or between species.

Any variable that indicates direction is by definition a circular variable, since the beginning and end of the scale is the same. Circular scales have no true zero and any designation of high or low is purely arbitrary (e.g., a direction of 359 degrees is closer to 5 degrees than 10 degrees is, because 0 and 360 degrees are the same direction). The linear statistical analysis techniques familiar to most people do not work with circular variables because they assume the data is linear. One example would be the calculation of an arithmetic mean of directions; the average of 5 degrees, 10 degrees and 354 degrees (which are all Northerly directions) would be 123 degrees (a South-East direction) and this is clearly incorrect. The field of circular statistics was developed to address just such problems; it is not new, nor is its application to biological and geological science (Batschelet 1978; Fisher 1993; Zar 1999). A few authors have

acknowledged that, strictly speaking, standard tests based on properties of linear distributions are not applicable to directional data (e.g., Gordon 1984a; Teafor and Byrd 1989), but I am unaware of any analysis that has applied directional statistical tests to microwear data. Rather, non-parametric linear statistical tests have been applied, either with or without explicit justification (Gordon 1984a; Teafor and Byrd 1989; Charles *et al.* 2007).

Existing analysis techniques for directional data, such as the Watson-Williams F test, tend to assume that samples come from a population conforming to a von Mises (circular normal) distribution and that the population dispersions are the same in each sample (Zar 1999). Whilst these may yet prove to be applicable to mammal teeth, in herbivorous dinosaurs, unlike mammals, the major proportion of the food processing occlusal surface of a tooth is dentine rather than enamel (Norman and Weishampel 1985) with enamel forming only a thin layer on one side of a tooth. As these teeth occlude during feeding a self sharpening action occurs with enamel cutting the softer dentine. A result of this is that microwear abundance is not consistent across the surface of a tooth. Different successive jaw motions tend to overprint existing microwear. When microwear is sampled at different sites the feature counts, distribution and dispersion can vary markedly and the less dominant jaw motions can be poorly represented. Visually the microwear scratches align into discrete groups that appear to be consistent across the surface of a tooth and from tooth to tooth. In order to confirm this quantitatively through statistical analysis it was necessary to develop a new methodology.

This paper highlights the problems and describes the circular statistical methods that can be used to analyse tooth microwear scratch orientation data from the teeth of herbivorous dinosaurs.

2. CIRCULAR STATISTICS

A circular datum can be treated as a point on a circle of unit radius, or a unit vector (i.e. a direction from the origin of the circle) in the plane (Fisher 1993).

Microwear features are typically measured as a series of X/Y co-ordinates on the occlusal surface of a tooth, to capture the start and end of the long and short axis of each feature (Ungar 1995). From this data, the orientation of the feature can be calculated as the number of degrees from a notional zero direction (i.e. a point on a circle). Being a circle there is no true zero and any designation of high or low values is purely arbitrary.

The simplest way to present microwear data is to plot the raw data as points on a circle, i.e. a circular plot, and the visual effect can be improved by using either a circular histogram or rose diagram, especially if the frequencies of the data are too large for a circular plot. These show the distribution of the data, the degree of symmetry or asymmetry and identify any modes and antimodes. With microwear data, the direction in which a scratch was generated can be difficult to identify (Gordon 1984b) and it is common practice to treat the data as axial such that the diagrams are half circles (e.g., Fiorillo 1998; Goswami *et al.* 2005; Charles *et al.* 2007).

To determine if there is a preferred orientation statistically, each raw data point can be treated as a unit vector and then the mean vector (μ) and mean vector length (r) calculated. These equate to an average direction (or mean angle) and a measure of the consistency of this average direction respectively. The mean vector length (r) is a measure of concentration; it varies inversely with the dispersion of circular data and is referred to by different authors variously as angular dispersion, orientation concentration and the degree of parallelism. It has no units and varies from $r = 1$, where

all features are parallel to each other and thus concentrated around the mean direction, to $r = 0$, where the features are so randomly dispersed about the circle that a mean direction cannot be described (Note: this does not necessarily indicate a uniform distribution), see Fig 1.

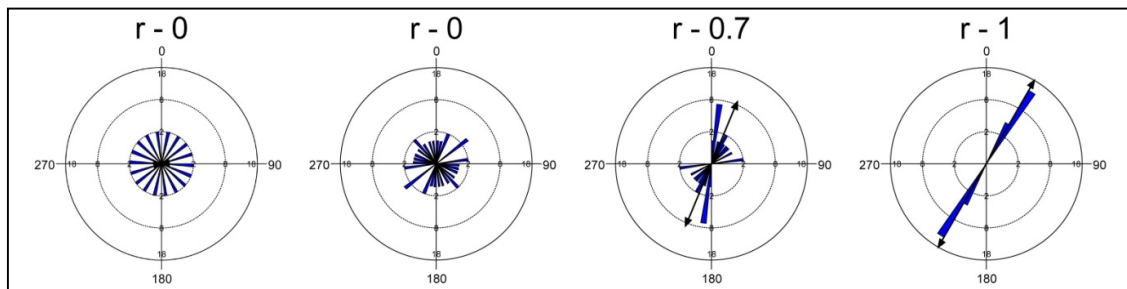


Fig 1. Example of various values of mean vector length (r), from left to right: $r = 0$ uniform distribution no preferred orientation; $r = 0$ non-uniform distribution no preferred orientation; $r = 0.7$ data spread around a preferred orientation; $r = 1$ data tightly clustered around a preferred orientation.

This is, of course, only meaningful for unimodal frequency distributions. Specific tests for multimodal frequency distributions have yet to be developed for circular statistics. For bimodal and multimodal data sets (that are typical of tooth microwear as jaws can open, close and move relative to each other in various planes) the modes must be identified and the data broken up and treated as two or more overlapping unimodal distributions (Batschelet 1978). This can be achieved by treating the multimodal circular distribution as a linear combination of unimodal distributions; the antimodes can be identified, roughly, from circular histograms and discriminant function analyses performed to accurately divide the distributions.

Where there is no preferred orientation and the features are distributed evenly around the circle then the distribution is uniform. There are various tests for uniformity and non-uniformity that can establish the significance of the mean angle, such as the Rayleigh Uniformity test, Rao Spacing test and the Fisher V test. Rayleigh's Uniformity test is based on the mean vector length (r) and simply calculates a Z value equal to nr^2 (where n is the number of features) and the probability (p) of the null hypothesis that

the data are uniformly distributed. Rao's Spacing test examines the spacing between adjacent points on the circle to see if they are roughly equal and again calculates the probability of the null hypothesis that the data are uniformly distributed. Fisher's V test is a variant of the Rayleigh Uniformity test but uses a pre-defined expected mean angle to test the alternative hypothesis that the data are a non-uniform distribution with a specified mean angle.

Having identified preferred orientations through tests of uniformity, further analysis is required to test hypotheses that these preferred orientations relate to jaw movements. For this it is necessary to perform an analysis of variance on multiple samples. Performing a series of two sample tests (i.e. pairwise testing all possible pairs of samples) must be discounted since the probability of committing a Type I error will approach certainty as the number of samples increases (Zar 1999) and so a multi-sample test is needed. A number of parametric and non-parametric tests exist that can be used to establish if sample microwear orientations belong to the same population or vary significantly and thus belong to different populations; each have their strengths, weaknesses and prerequisites. Some assume the data has a von Mises distribution, some that the concentration and dispersion are equal between samples.

Parametric tests are considered more powerful than non-parametric tests (Fisher 1993; Mardia and Jupp 2000) and have been used successfully in orientation studies (e.g., Burda *et al.* 2009). The parametric multi-sample Watson-Williams F test (Fisher 1993) compares the mean vectors from independent samples to that of the pooled data to determine if mean angles differ significantly. It does however make assumptions about the form of the sample distributions; specifically that they are von Mises and that their concentrations are similar and large. Because dinosaur microwear orientation data tends to be multimodal (relating to a number of discrete jaw motions) with overlapping

modes, it is difficult to identify the tails of each individual distribution and the act of dividing the data into unimodal distributions invariably leads to a loss of information. This coupled with the issue of overprinting by successive jaw motions often leads to the unimodal distributions being skewed and leptokurtic where the samples are not large (central limits theorem comes into effect on larger samples forcing a von Mises distribution (Davis 2002)). The common lack of a von Mises distribution and unequal concentrations between samples makes a Watson-Williams F test unsuitable for dinosaur microwear orientation data and indeed it has proven to be susceptible to Type I errors (Williams *et al.* 2009).

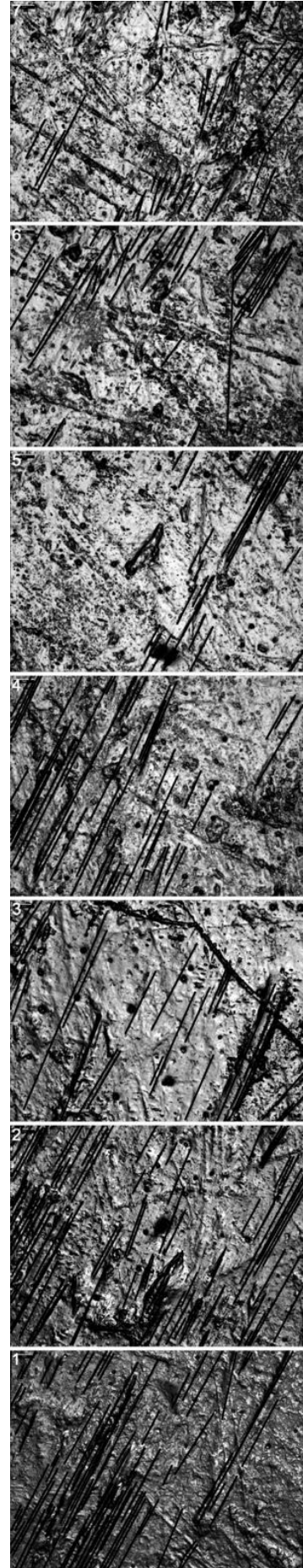
Of the non-parametric tests the Mardia-Watson-Wheeler test (Fisher 1993) and Wilcoxon/Mann-Whitney U test (Zar 1999) have been used in tooth microwear studies (e.g., Gordon 1984a; Teaforde and Byrd 1989; Charles *et al.* 2007) even though the latter is essentially a linear test. These pool the data, ranking the orientations by increasing angles. They then compare the distributions by rank rather than orientation to determine if the distributions are the same or differ significantly. Both of these test types have problems with tied data (i.e. where a number of orientations are identical) and an adjustment must be made to break the ties such that each datum receives a random different rank otherwise the standard deviations will be overestimated in the calculation. It is the loss of information by dealing with ranks that cause these non-parametric tests to be considered less powerful than parametric tests. The popularity of such tests however, is due to their reputed ability to work with data that is not normally distributed and with samples of unequal size (Zar 1999). When performed on dinosaur microwear orientation data, both tests have proven to be susceptible to Type I errors (Williams *et al.* 2009). In part this is likely to relate to the large amount of tied data due to the high degree of parallelism. However, the ability to handle unequal sample sizes, particularly

within the Wilcoxon test, has also been questioned (e.g., Hsiung *et al.* 1994); with small (but reasonable) sample sizes, population means are underestimated, and mean differences among populations can be overestimated as a result of unequal sample sizes thus invalidating the tests.

The non-parametric Watson U^2 test is the analogue on the circle of the Mann-Whitney test on the line (Mardia and Jupp 2000). Whilst tied data must be broken and a random assignment of rank is required, this test compares data using mean square deviations rather than the maximum deviation and the high degree of parallelism within the data set does not appear to affect the result of the test. A further advantage is that this test can be performed on multimodal data. It does however appear to be prone to Type II errors where the sample sizes are small and Type I errors where sample dispersions differ.

Ideally we want to measure the variation of individual values about a population mean and the variation of population means about an overall mean to determine if the variation is significant. What is needed is a test less prone to Type I and Type II errors that can compare the mean vectors from independent samples to the population mean. If the variability within the sample populations is small relative to the variation between their respective means then the population means are different. A second order mean of means (Batschelet 1978; Zar 1999) provides an accurate way to estimate the population mean and can establish if there is a significant directionality in the data (Hotelling 1931; Zar 1999). By calculating the confidence limits for the second order mean of means a measure of the precision of the estimated population mean can be obtained (Batschelet 1981; Zar 1999). The means from independent samples can then be compared to the estimated population mean without making assumptions about the form of the sample distributions.

Fig. 2. Transect from apex (site 1) to base (site 7) across the functional surface of an *Edmontosaurus* tooth from posterior, right maxilla specimen NHMUK R3638. Microwear features are marked. Field of view is 285 μm wide. NHMUK – Natural History Museum, London



3. ANALYSIS OF MICROWEAR ORIENTATION DATA

A unimodal subset of scratch orientation data was sampled from 7 sites along a straight line transect from tip to base of a single herbivorous dinosaur tooth (Fig. 2). The scratches are straight and the data exhibit a consistently high degree of parallelism (angular dispersal, R) and the Rayleigh, Rao and Fisher (V) uniformity tests show the pooled data for the 7 sites to be non-uniformly distributed, with a significant mean orientation (Table 1).

Two alternative interpretations of these data are possible: either the samples are drawn from a single population of scratches that are straight, strongly parallel, and occur over the whole length of the transect (i.e. orientation is the same across the surface of the tooth), or the samples are drawn from multiple populations of scratches that differ slightly in orientation, but within which scratches are straight and parallel. For the purposes of this study, with controlled sampling across the transect, it is quite clear that the first of these two hypotheses is the correct one; yet three tests reject it (type 1 error): a non-parametric Wilcoxon test shows significant differences between the 7 samples ($P < 0.05$), as does the Watson-Williams F test ($P < 0.05$), and the Watson's U^2 test finds significant differences in all but three of its pairwise comparisons (Table 1). Even when sites 1 to 4, which are close together and clearly the most similar, are compared, both the Watson's U^2 test and the Wilcoxon test find significant differences between all of the sites except 1 and 2, and the Watson-Williams F test finds that site 4 differs significantly from sites 1 and 2. The results of this analysis indicate that when testing for differences in microwear scratch orientation between sample sites, the Wilcoxon, Watson-Williams F and Watson's U^2 tests are susceptible

to type 1 errors. Taken at face value, the results of these tests would lead us to reject the hypothesis that scratch orientations for the 7 sites are drawn from the same population (i.e., the tests wrongly indicate that their means differ), when in fact they are drawn from the same population and, in the context of this analysis, the means are not significantly different.

A second order mean of means calculation (Zar 1999) performed on the mean angle (μ) and angular dispersion (R) from each of the 7 samples yields a grand mean (ϑ ; a sample estimate of the population mean) and its associated confidence interval (a measure of the precision of the sample estimate) and a test of the significance of the grand mean shows that the population from which the grand mean was calculated has a mean direction ($P < 0.05$). This second order mean of means test yields correct results (i.e., the means from each of the 7 sample sites fall within the 99% confidence interval for the grand mean; see Table 1). This provides a less error-prone yet appropriately stringent statistical test for the analysis of microwear orientation data. My analysis does not support the view advocated in previous analyses of microwear orientation data (Gordon 1984a; Teaforde and Byrd 1989; Charles *et al.* 2007) that axial data (i.e., distributed through 0-180°) can be treated as linear data and subjected to linear statistical tests. This approach would have led us to wrongly reject the hypothesis that mean orientation does not differ between sites and previous analyses of this type may have made similar errors.

Table 1. Sample microwear orientation data for 7 sites along a straight transect of a tooth.

Data for transect across tooth 2 (7 sites): means (μ) by site, mean of means, and 99% confidence interval							
Site	1	2	3	4	5	6	7
Angular dispersal, R	0.995	0.995	0.975	0.996	0.998	0.977	0.970
Mean vector, μ	62.235	62.598	62.548	64.423	61.704	59.375	66.056
Rayleigh, Z	73.292	81.101	23.753	49.626	26.911	40.096	31.965
Rayleigh, p	< 0.0001	< 0.0001	< 0.0001	< 0.0001	< 0.0001	< 0.0001	< 0.0001
Rao Spacing, U	324.548	326.521	300.76	324.02	331.319	297.47	295.883
Rao Spacing, p	< 0.01	< 0.01	< 0.01	< 0.01	< 0.01	< 0.01	< 0.01
Fisher V, V (expected μ 62.702)	0.995	0.995	0.975	0.996	0.998	0.975	0.968
Fisher V, p	< 0.0001	< 0.0001	< 0.0001	< 0.0001	< 0.0001	< 0.0001	< 0.0001
Wilcoxon/Kruskal-Wallis, Score Sum	11733	13044	4869.5	11656	3909.5	3161.5	7571.5
Wilcoxon/Kruskal-Wallis, Score Mean	158.554	159.073	194.78	233.12	144.796	75.274	222.691
1-way test, ChiSquare approximation 77.2591, df 6, prob > ChiSq < 0.0001							
Watson's U^2	1	----	< 0.5	< 0.001	< 0.001	< 0.001	< 0.001
Site numbers horizontal & verical	2	0.102	----	< 0.001	< 0.001	< 0.5	< 0.001
U^2 scores (lower half) and	3	0.733	0.628	----	< 0.001	< 0.001	< 0.5
probabilities (upper half)	4	0.686	0.981	0.421	----	< 0.001	< 0.001
	5	0.057	0.107	0.653	0.557	----	< 0.001
	6	1.194	1.256	0.628	1.431	0.842	----
	7	0.559	0.503	0.093	0.454	0.536	0.785
Watson-William F-Test (pairwise)	1	----	0.443	0.743	< 0.0001	0.36	< 0.0001
Site numbers horizontal & verical	2	0.595	----	0.958	< 0.0001	0.146	< 0.0001
F scores (lower half) and	3	0.108	0.003	----	0.08	0.523	0.053
probabilities (upper half)	4	19.546	12.831	3.151	----	< 0.0001	< 0.0001
	5	0.844	2.14	0.415	25.51	----	0.062
	6	11.454	15.032	2.888	27.56	3.612	----
	7	15.6	13.526	3.67	2.187	9.484	18.761
Wilcoxon/Kruskal-Wallis Test (Rank Sums)							
1-way test, ChiSquare approximation 77.251, df 6, prob > ChiSq < 0.0001							
Watson-Williams F Test (multisample), F = 9.273, df 6, P < 0.0001							
Mean of means, θ = 62.702, significance F = 18009.06, 99% confidence interval 58.28 - 67.16							

CHAPTER 6

Dental microwear on Iguana teeth: implications for the reconstruction of jaw movement

Targeted for the journal *Proceedings of the National Academy of Sciences of the United States of America*

Abstract

Dental microwear analysis uses the microscopic scratches and pits on the surface of teeth to deduce dietary habit and offers a fresh approach to the reconstruction of jaw movements during feeding in extinct animals, particularly where the absence of tooth wear facets hampers the reconstruction via functional morphology. Most dental microwear studies have been carried out on mammals, with comparative analyses of microwear patterns between fossil and modern living counterparts. Here I show that analysis of tooth microwear orientation provides direct evidence for the relative motion of jaws in the extant squamate *Iguana iguana* demonstrating that dental microwear studies have an application beyond mammals. Due to the similarities in tooth and skull morphology between *I. iguana* and early ornithischian dinosaurs, *I. iguana* provides a suitable extant model for feeding in these early herbivores.

1. Introduction

Dental microwear analysis is now widely used in palaeodietary reconstruction, with the interpretation of microwear patterning in fossil mammals, based on comparison with modern animals/mammals with known diets. Evidence of dietary habit and the mastication process can be deduced from the microscopic scratches and pits on the surface of teeth (e.g., Walker *et al.* 1978; Teaforde and Byrd 1989; Semprebon *et al.* 2004; Ungar *et al.* 2007) and the orientation of these scratches and pits reflect the dominant direction of jaw movements (e.g., Butler 1952; Mills 1967; Charles *et al.* 2007). That microwear analysis has a broad applicability beyond mammals has been shown by research on both fossil fishes (Purnell *et al.* 2006; Purnell *et al.* 2007) and dinosaurs (e.g., Fiorillo 1991, 1998; Upchurch and Barrett 2000; Williams *et al.* 2009).

The squamate *Iguana iguana* is an important extant model for feeding in early herbivores. It has an akinetic skull, lacks cheek space and shares a similar jaw and tooth morphology with the basal anodont *Suminia getmanovi* (Rybczynski and Reisz 2001) and both *Lesothosaurus* (basal ornithischia) and prosauropod dinosaurs (Norman and Weishampel 1985; Barrett 2000). Here I evaluate the validity of microwear analysis on *I. iguana* in determining the dominant direction of jaw movements and thus its potential for use in comparative studies with extinct early herbivores.

1.1 *Iguana* dentition and mastication

Iguana iguana has a complete marginal dentition of lanceolate and coarsely denticulate teeth that are labiolingually compressed and have widened cylindrical bases. From the base each tooth expands into a crown forming a thin, vertically curving blade with a convex labial surface and a concave lingual surface that expands in the mesial

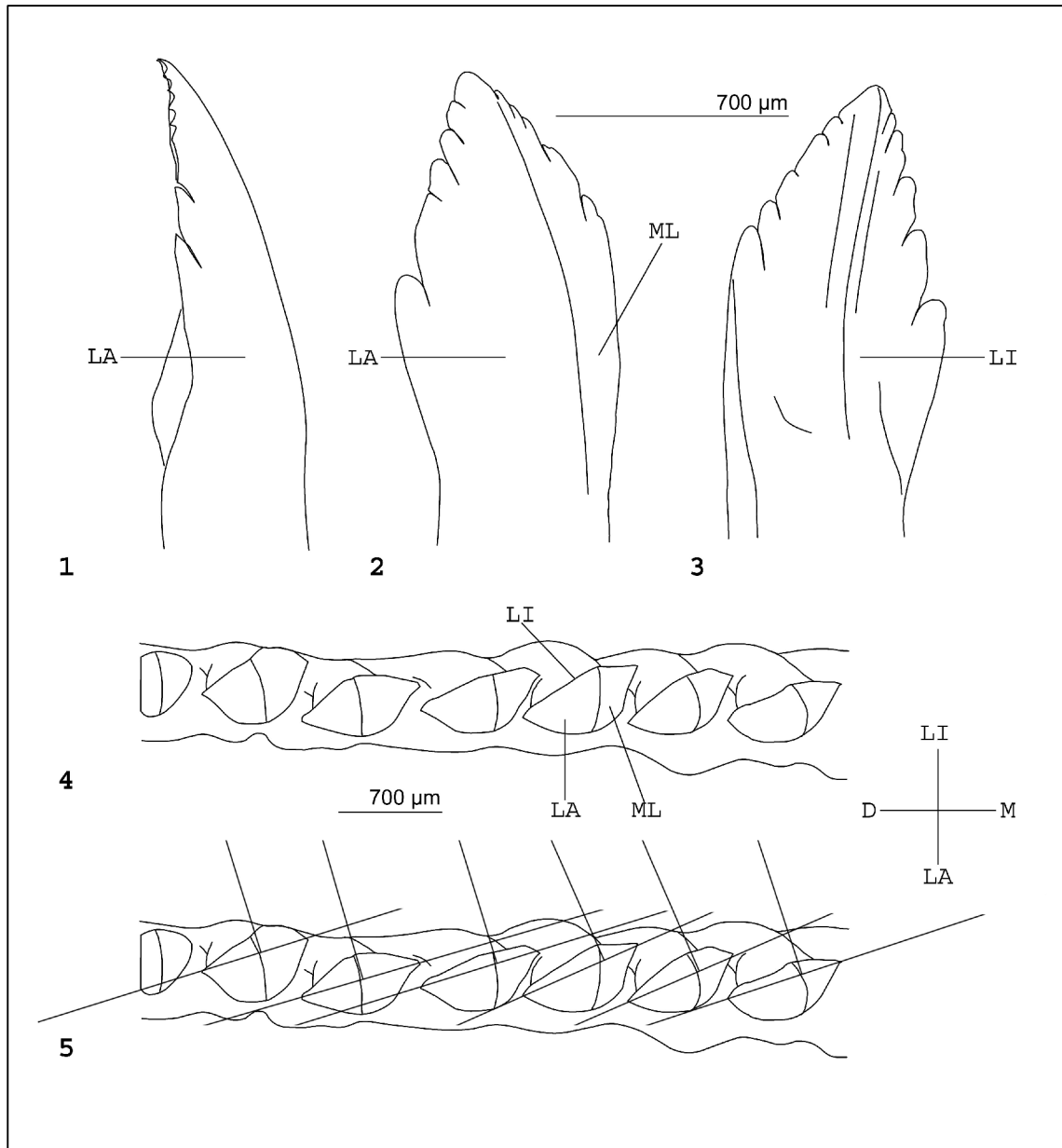


Figure 1. Cheek teeth of *Iguana iguana* Right dentary. 1.1 Distal view showing the labial surface at an oblique angle – lingual is to the left. 1.2 Labial view – mesial is to the right. 1.3 Lingual view – mesial is to the left. 1.4 Apical view – lingual (LI) is up, mesial (M) is to the right, distal (D) is to the left and labial (LA) is down; one tooth is labelled to identify the three distinct tooth faces: Mesiolabial (ML), Labial (LA) and Lingual (LI). 1.5 Apical view with perpendicular symbols showing variation in orientation of the lingual faces (modified from Throckmorton, 1976).

(anterior) and distal (posterior) directions, with the tip of the crown pointing slightly distal. The labial surface has both a lateral and mesial facing component and for clarity the lateral facing component will henceforth be referred to as the labial face and the mesial facing component as the mesiolabial face. Figure 1 shows a right dentary tooth viewed from the back of the jaw along the tooth row, and viewed from positions

perpendicular to the long axis of the tooth row, from outside the mouth (lateral to the tooth row) and inside the mouth (medial to the tooth row), illustrating the labiolingual compression and mesiodistal (anteroposterior) expansion. A portion of the right dentary viewed from above (apical) is also shown, from which it can be seen that the teeth are oriented *en echelon* such that the mesial and distal denticulate margins of the teeth are angled obliquely relative to the long axis of the tooth row, with the mesial edge of each tooth medial (further inside the mouth) to the tooth preceding it, and the distal edge lateral (further outside the mouth) to the tooth behind it. This mesiodistal elongation of the compressed teeth leaves only a small gap between teeth so that together they form a near continuous shearing edge (Throckmorton 1976; King 1996). As the animal feeds, each tooth from the upper jaw comes down between, but not in contact with, two teeth of the lower jaw in a simple, shearing, scissor action. Figure 2 shows the teeth in lateral and apical view. As the jaws close the lingual face of a maxillary tooth shears past the mesiolabial face of a dentary tooth, whilst simultaneously the mesiolabial face of that same maxillary tooth shears past the lingual face of the next dentary tooth along the row. The labial face of dentary teeth and the labial face of maxillary teeth do not interact with any other tooth face in the shearing process; they pierce and shred plant material but no plant material can be trapped between them and another tooth face.

Throckmorton (1976) observed the cropping behaviour of *Iguana iguana* via frame by frame analysis of slow motion film and determined that the multiple sharp cusps which form the denticulate tooth margins hold the plant material in place whilst it is sheared (preventing it being pushed forward in the mouth), cutting and perforating it into small pieces. These observations together with the lack of wear facets on the teeth suggested that oral processing involved a tooth-food-tooth shearing action rather than tooth-tooth occlusion (Throckmorton 1976). The same conclusion was reached by King

(1996) who further observed that there was little mastication involved in the feeding process. Both Throckmorton (1976) and King (1996) noted that *I. iguana* uses whole head movement in the cropping process, employing a vigorous jerk to separate material not released by the initial bite. No lateral movement of the lower jaw, streptostylic movement of the quadrate or any cranial kinesis was observed during feeding, just the elevation and depression of the lower jaw around the mandibular joint (with a mean gape of 30.8° and a maximum gape of 48°).

1.2 Predicted microwear patterns

When an iguana is feeding, the shearing surfaces can be identified along with the relative jaw motion and so the likely form and position of tooth microwear can be predicted. This is possible because the orientation of scratches is related to the direction of jaw movement and the compressive forces involved (Teaford and Byrd 1989). Vertical adduction of the style described by King (1996) and Throckmorton (1976) should produce dominant scratch orientations near 90° to the tooth row long axis and although it was stated that food did not move forward in the mouth, being trapped and held in place by the tooth denticles, a shearing scissor action jaw could still be expected to produce some, albeit micron scale, anterior movement of the food resulting in minor more oblique scratch orientations. This is because as a scissor action jaw closes the point of shearing has to move forward. As successive teeth come together or shear past each other, they apply a force to any food in the mouth and because the upper and lower tooth rows are not parallel (they converge at the hinge) that force will act to push food forward. Examination of film footage on a millimetre scale may not identify such micron scale movement.

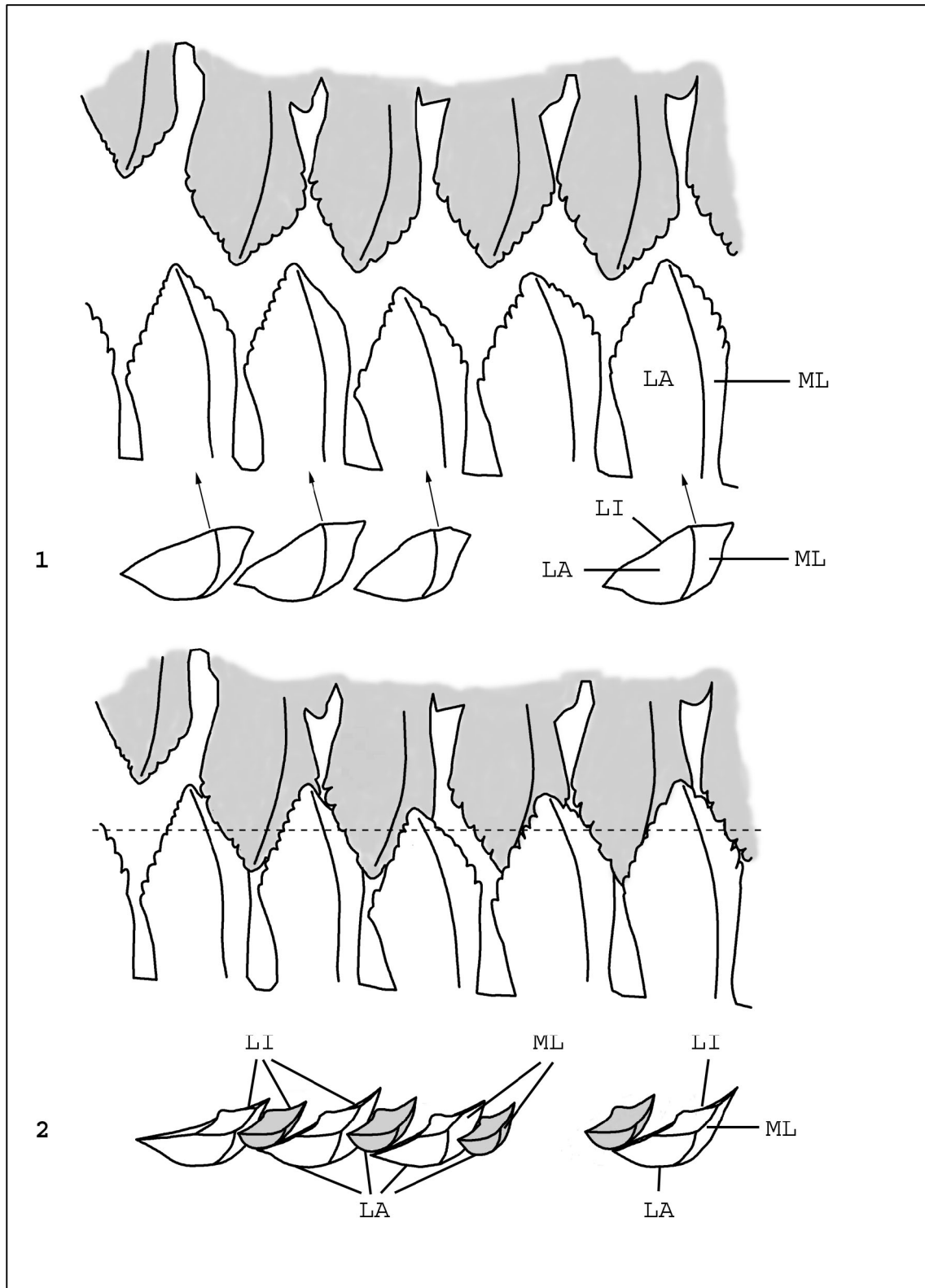


Figure 2. Opposing tooth surfaces of *Iguana iguana* Right dentary & maxilla. 2.1 Labial view showing maxillary teeth (shaded) approaching dentary teeth during jaw closure, mesial is to the right; below: apical view of dentary teeth, one tooth is labelled to identify the three distinct tooth faces: Mesiolabial (ML), Labial (LA) and Lingual (LI), mesial is to the right, medial is up. 2.2 Labial view showing maxillary teeth (shaded) shearing past but not contacting dentary teeth with jaws closed, mesial is to the right, dashed line shows position of cross-section; below: apical view of cross section through dentary and maxillary (shaded) teeth with jaws closed; shearing takes place between dentary ML and maxillary LI, and between maxillary ML and dentary LI, mesial is to the right, medial is up.

It should be noted that the physical properties of the food will influence any such forward movement. It is also a distinct possibility that microwear patterns will vary systematically with distance from the jaw hinge as the compressive forces change (highest at the hinge), although the short length of the jaws in *Iguana iguana* will diminish this effect. However, the fact that neither the orientation of the teeth nor the spacing between them is uniform, may act against any systematic variation effect (Figure 1.5). If the attitudes of opposing tooth faces differ then the shearing and compression forces between them will also differ from that of other pairs of opposing tooth faces.

As a consequence of the *en echelon* arrangement of teeth, there are two sets of active surfaces where microwear should be concentrated: the lingual surfaces of maxillary teeth act against the mesiolabial surfaces of dentary teeth and the mesiolabial surfaces of maxillary teeth act against the lingual surfaces of dentary teeth. The nature of the opposing tooth surfaces also suggests that microwear should be reduced on the mesial portion of the lingual faces and the distal portion of the labial faces of both dentary and maxillary teeth since no tooth-food-tooth contact can occur here. The microwear pattern should differ from the pattern found on the tooth surfaces that are interactively opposed during feeding. The observed vigorous whole head movement may be expected to produce more variable oblique scratch orientations, particularly on the opposing tooth faces (mesiolabial and lingual) between which plant material is trapped. The lack of a kinetic skull and no observed anteroposterior macro movement of the lower jaw relative to the upper jaw should rule out any propalinal (horizontal) microwear.

Being marginal (i.e. lining the outside of jaw) the teeth leave no inset for cheek space. Food falls from the mouth, rather than being retained between the tooth row and

lips as it is in mammals. This should restrict microwear generated by regular contact with food items on the labial tooth surfaces (which in a mammal would be the non-occlusal microwear; generated during mastication by food items held inside the mouth, against the labial side of cheek teeth by muscular cheeks). In mammals this would be tooth-food-cheek microwear.

By comparing the microwear patterns on the corresponding faces of the upper and lower teeth and correlating one with the other, reconstruction of the movement of the upper teeth across the lower teeth should be possible. My aim is to establish if tooth microwear is preserved in *Iguana iguana*, and to determine if that microwear exhibits a relationship with jaw mechanics and feeding. Here, I test the null hypotheses that microwear does not have a uniform distribution (i.e. that it shows a preferred orientation), that microwear does not differ between sample sites within a tooth, that microwear does not differ between teeth within a jaw element, that microwear does not differ between teeth of different jaw elements and that microwear does not differ between opposing and non-opposing tooth faces, within an individual.

2. Material and Methods

Dentary and maxillary teeth from a Recent, preserved, wild caught, specimen of *I. iguana* (S. T. Turvey, private collection, held at Zoological Society of London) were repeatedly washed with deionised water, dried, sputter coated with gold and examined with a Scanning Electron Microscope (Hitachi S-3600N SEM). In mammals, microwear patterns develop on wear facets and at specific points that relate to the places where teeth are abraded by food or occlusion with other teeth (Teaford 1988b). In dinosaurs, the length, width and frequency of microwear features have been found to be consistent within the occlusal surface of sauropod teeth (Fiorillo 1991, 1998) and orientation has been found to occur consistently within the occlusal surface of hadrosaur teeth

(Williams *et al.* 2009). Because of the differences between iguana teeth and those of mammals and dinosaurs it was not obvious which sites should be used for microwear acquisition or at what magnification. Dentaries and maxillae were inserted into the SEM chamber and oriented with the long axis of the tooth row as a reference frame and then rotated about the long axis of the tooth such that the surface being imaged was perpendicular to the electron beam. The *en echelon* arrangement made imaging of the mesiolabial faces difficult, restricting available sample sites. Gaps in the tooth rows were exploited to overcome this problem and one right dentary tooth was deliberately extracted to generate a gap. Exploratory photomicrographs were taken at magnifications of x1000, providing a field of view of 125 x 85 μm , and x300, providing a sampling site field of view of 417 x 312 μm , comparable with that commonly used in analysis of occlusal microwear in mammals (Grine *et al.* 2002; Scott *et al.* 2005). A magnification of x300 was found to represent the best compromise between surface area covered and clarity of dental microwear. SEM settings were standardized at: accelerating voltage, 15kV; working distance, 20 mm; automatic contrast and brightness. Standardization is important for comparability of datasets (Gordon 1988). In determining a sampling strategy a qualitative survey was performed to identify how microwear was distributed. Microwear from sites on the crown, centre and base of teeth along a vertical median line, and sites mesial and distal to these was compared. Figure 3 shows a representative distribution of microwear across the mesiolabial and lingual faces of a right dentary tooth and a maximized distribution across the labial face (beyond the curved overlapping area between the labial and mesiolabial faces, microwear is sparse on labial faces). On the lingual and mesiolabial faces, sample sites slightly mesial of centre (large shaded circles), appeared suitably representative and were standardized upon for the purposes of this study.

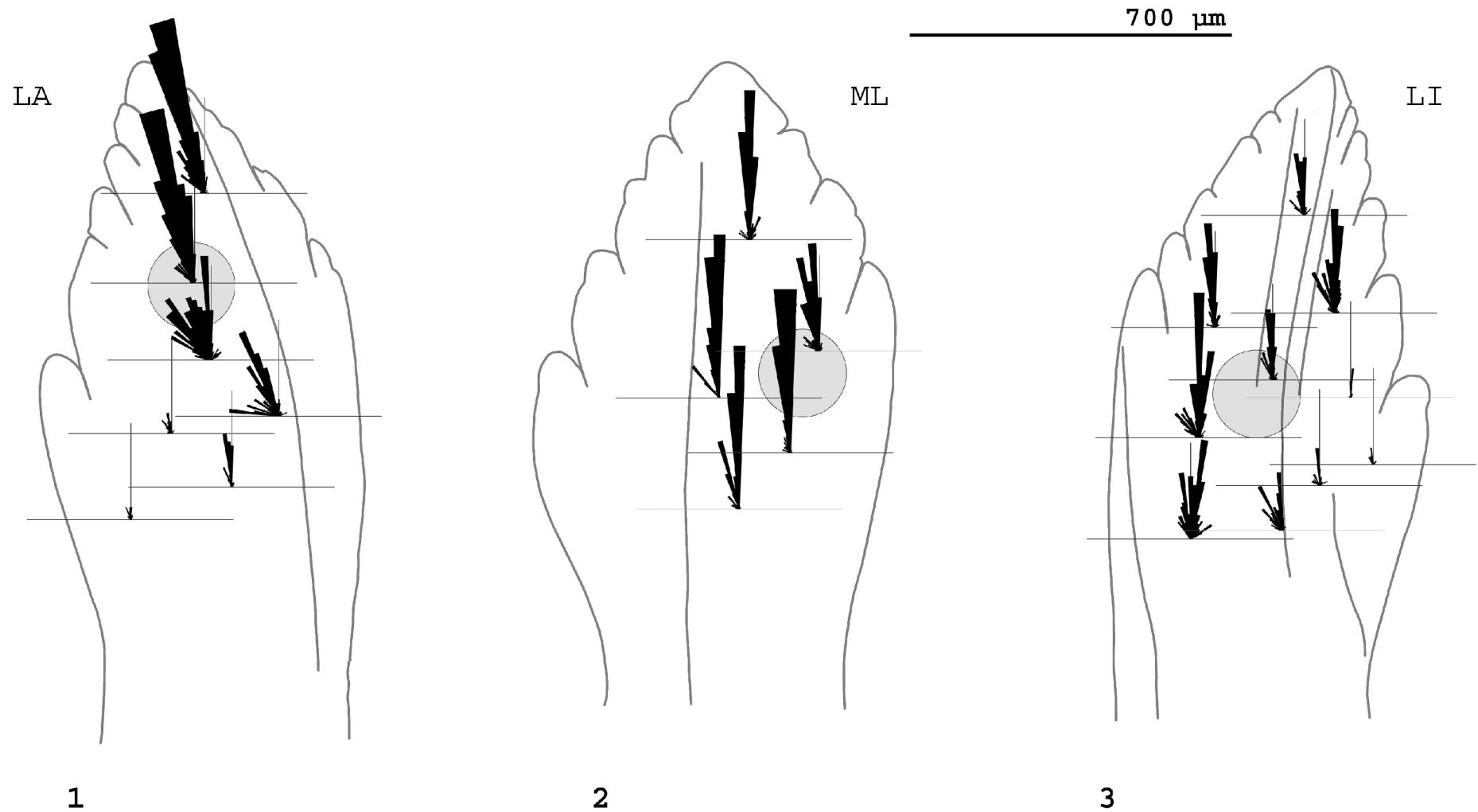


Figure 3. Microwear distribution on the tooth surfaces of *Iguana iguana*; rose diagrams show frequency as the radius of the wedge using 4° bins, vertical axis N=25. 3.1 Labial view of a right dentary tooth showing a maximized distribution (*made from highest feature count sites*), mesial is to the right. 3.2 Mesiolabial view of a right dentary tooth showing a representative distribution, mesial is to the right. 3.3 Lingual view of a right dentary tooth showing a representative distribution, mesial is to the left. Shaded circles show areas chosen for standardized sampling.

A less constrained, more crown-ward and distal site (centred in or near the shaded circled area) was chosen for the labial face in order to maximize the microwear present.

All thirty three teeth present on the left and right dentaries and the right maxilla were examined. Damaged teeth (those with unusually large gouges, cracks or pieces broken off that were suspected to be the result of post-mortem activity) were excluded. Part erupted teeth (and their counterparts in the opposing jaw element) were found to have zero microwear features and were also excluded as uninformative. A total of 4199 microwear features were captured and analysed, from 42 sites on 17 teeth. Of the 42 sites, 28 occur on lower dentition and 14 on upper dentition with 16 sites on lingual surfaces, 13 on labial and 13 on mesiolabial. Sites were chosen such that microwear was captured from multiple sites on the shearing and non-shearing faces of both the crown and neck from three teeth, and from standardized sites on multiple teeth. Labial sites were selected to maximize available microwear as it was considered that the collection of orientation data justified any introduced bias in feature count. Three labial sites were smooth and free of microwear and have been included to allow a balanced analysis of scratch density/count. The digital SEM photomicrographs were downsampled to 900 pixels wide by 675 pixels high using Adobe Photoshop 7. As pits (features of roughly equal length and width) were rare to absent and this study is concerned particularly with microwear orientation, only scratches (elongate features) were considered. All microwear scratches within each photomicrograph were measured and recorded using the custom software package Microware 4.02 (Ungar 2001); x,y co-ordinates were extracted from the resulting overlay files and entered into a database which used simple trigonometric functions to calculate the length, width and long axis orientation of each feature/scratch. Scratch orientation data were suitably transformed to allow direct comparison to the labial face of the right dentary teeth. When looking at

the labial face of a right dentary tooth, mesial will be to the right but on a left dentary tooth mesial will be to the left, in order to compare microwear patterns one set of data will need to be transformed – to achieve the equivalent of flipping the photomicrograph image horizontally before measuring the scratches. Measurement and recording took place on a Dell Latitude D505 computer running Windows XP Professional (Microsoft), with a 15-inch active matrix TFT display set at a screen resolution of 1024 x 768 pixels, resulting in an onscreen magnification of approximately x630 for SEM photomicrographs taken at x300.

Analyses of variance (ANOVA) for linear data, and mean of mean angle confidence interval (CI) tests for circular data were conducted on scratch count (N), orientation, angular dispersion (i.e. the degree of parallelism as measured by R), length and width to determine if significant differences occur between separate sites within a single tooth, between teeth within a jaw element, between teeth of different jaw elements and between tooth faces. Correlations between microwear variables and distance from jaw hinge were also tested. Classes of orientation and their boundaries were established by rose diagram (to 1° resolution if necessary) and tested by discriminant function analysis (DFA) for an acceptable error rate (typically < 2%). Scratch length data were not normally distributed (Shapiro-Wilk W; $P < 0.01$) and were therefore log-transformed before statistical analysis. Statistical analyses were carried out using the dedicated software packages Oriana 3.31 (Kovach Computing Services) for orientation data and JMP 8.0.2 (SAS Institute Inc) for both linear data and DFA.

3. Results

Of the 33 teeth examined, seven were damaged, three partially erupted and six had no microwear at all. Tooth five of the right dentary had very little microwear on its mesiolabial face (only one site with seven scratches) and it was noted that there was a gap in both the dentary tooth row adjacent to this tooth anteriorly, and in the opposing maxilla tooth row. Visual inspection of photomicrographs revealed that *Iguana iguana* teeth do preserve microwear, and that scratches dominate (Figure 4). Pits were rare and were therefore excluded from the analyses. Dentary and maxillary teeth show dominant near vertical and minor sub horizontal microwear patterns on all three tooth faces, although the distal third of lingual faces and the distal half of labial faces, beyond the denticles, are largely smooth and free from microwear. In addition the labial faces of both dentary and maxillary teeth tend to have very patchy microwear.

Scratches are not random in orientation, appearing to fall into a small number of classes, within which scratches are predominantly straight and subparallel, but with an orientation that differs from that of other classes. To test the hypothesis that discrete classes of scratches exist, microwear data (4,199 scratches from 42 sites on 17 teeth) were partitioned into three subsets (classes 1-3) based on visual assessment of scratch orientation. The micrographs in combination with detailed rose diagrams (compiled using both radius of the wedge and area of the wedge to show frequency, and with varying bin sizes down to 1°; see Figure 5.3) were used to identify class boundaries. Discriminant function analysis (DFA) performed on scratch orientation provides strong confirmation that the microwear data falls into three distinct classes – 94% of scratches classified by visual inspection were correctly assigned by DFA.

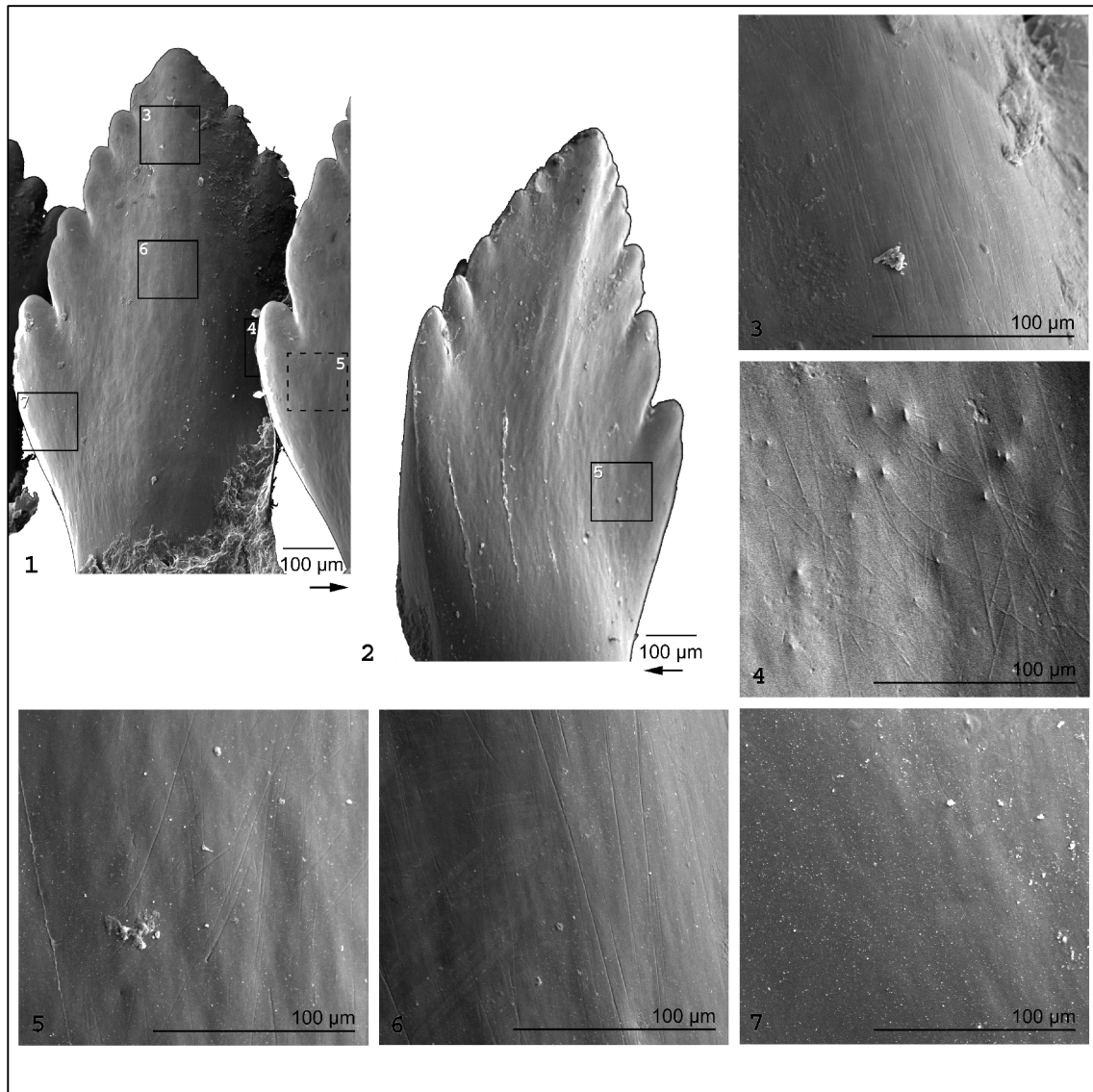


Figure 4. Microwear patterns of *Iguana iguana* Right dentary teeth. 4.1 Labial view of tooth 6, with inset boxes showing locations for (4.3 to 4.7); partial labial view of tooth 7, with dashed inset box showing location for (4.5) on hidden lingual face; arrow points to mesial. 4.2 Lingual view of tooth 7, with inset box showing location for (4.5); arrow points to mesial. 4.3 Crown-ward, distal edge of mesiolabial face. 4.4 Centre of mesiolabial face. 4.5 Distal side of lingual face (mesial is to the left). 4.6 Distal edge of mesiolabial face. 4.7 Distal side of labial face, no microwear.

When DFA was performed using scratch orientation, length and width as covariates, only 0.7% of the scratches assigned a class by scratch orientation alone were identified as misclassified, further supporting the existence of three distinct classes. Rather than conduct subsequent statistical testing on these imperfectly classified data, the DFA results were used to reassign the incorrectly assigned scratches to their correct class (leading to 100% correct discrimination; see Table 1 for summary); all three classes were not present on all sites. Figure 5.1 and 5.2 show rose diagrams of the three classes

with their mean orientations and 99% confidence intervals (the rose diagrams have 4° bins and their Y axes are scaled to $N = 500$). In Figure 5.1 frequency is shown by the area of the wedge to illustrate the distribution of the minor classes (1 and 3) and in Figure 5.2 frequency is shown by the radius of the wedge, this illustrates the dominance of class 2 microwear. Figure 5.3 shows the central portion of a rose diagram (with 1° bins, the Y axis scaled to $N = 75$ and frequency shown by the radius of the wedge). Whilst there are no clear gaps in the distribution, the positions of the class boundaries can be identified and the two boundaries chosen are marked. A potential third boundary (marked with a question mark (?)) had a sufficiently low N to discount it as a separate class.

Table 1. Summary statistics from unclassified microwear data (42 sites on 17 teeth), and partitioned into three classes based on scratch orientation.

Subgroup	Unclassified	Class 1	Class 2	Class 3
No. of observations	4199	287	2895	1017
Angular dispersion, R	0.66	0.78	0.93	0.87
Mean orientation (mean vector, μ)	104.89°	44.07°	97.85°	141.12°
95% confidence interval for μ	$\pm 0.80^\circ$	$\pm 2.30^\circ$	$\pm 0.40^\circ$	$\pm 0.92^\circ$
99% confidence interval for μ	$\pm 1.06^\circ$	$\pm 3.02^\circ$	$\pm 0.52^\circ$	$\pm 1.21^\circ$
Mean scratch length, μm	40.97	28.95	43.78	36.38
Mean log scratch length, μm	3.55	3.17	3.62	3.45
Mean scratch width, μm	0.5	0.42	0.47	0.58

Analysis of the data revealed significant differences ($P < 0.05$) in N , angular dispersion (R), length and width between classes (Table 2). Pairwise comparisons (Tukey-Kramer honestly significant difference (HSD) for linear variables, Watson-Williams F for axial variables) indicate that the three classes differ significantly from each other in all cases except for classes 1 and 3 for N and R. Summary statistics for each site are given in Table S1, and for each site by class in Tables S2, S3 and S4.

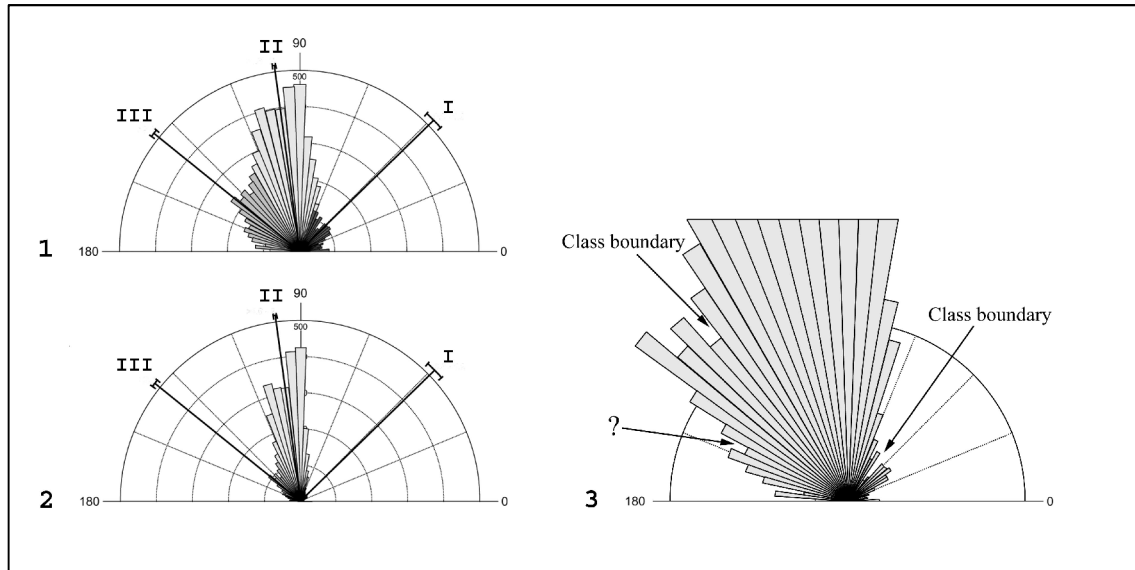


Figure 5. Rose diagrams of microwear scratch orientations (4199 features from 42 sites on 17 teeth). 5.1 Rose diagram showing frequency as area of wedge. 5.2 Rose diagram showing frequency as radius of wedge; data partitioned into 3 orientation classes (I,II & III). Black lines running from the centre of the rose diagram to the outer edge, with arcs extending to either side show the mean orientation and 99% confidence interval for each class, bins = 4°, Y axis scale - scratch count (N) = 500. 5.3 Central portion of rose diagram showing frequency as radius of wedge, bins = 1°, Y axis scale – scratch count (N) = 75. Chosen class boundaries are marked; query (?) = discounted class boundary.

Table 2. Results of null hypothesis testing for differences in microwear between classes.

	d.f.	F	P
Length does not differ between classes (one way ANOVA; log data)	2,4196	104.72	< 0.0001
Width does not differ between classes (one way ANOVA)	2,4196	27.64	< 0.0001
R does not differ between classes (one way ANOVA)	2,104	11.18	< 0.0001
N does not differ between classes (one way ANOVA)	2,104	23.61	< 0.0001

The scratches fall into a small number of tightly constrained width categories, separated by clear space. Figure 6 shows a histogram of scratch width by scratch count for the unclassified data. The majority of the 4199 scratches, 64% (N=2699), have been categorized as fine (narrow and shallow with sharp well defined edges and a width in the range 0.3 to 0.4 μm) with 22% (N=948) medium (deeper with sharp well defined edges and a consistent width of approximately 0.7 μm) and 12.5% (N=523) coarse (poorly defined edges, with variable depth and a width in the range 1.1 to 1.2 μm and

1.6 to 1.7 μm). The remaining features, 1.5% (N=59), have been defined as gouges (variable width in the range 2.2 μm to 3.75 μm). Scratch length is highly variable, however the majority, 75%, of the scratches have a length of 50 μm or less. There is no correlation between scratch width and length ($r < 0.16$, $P > 0.05$) within the unclassified data or within the subsets of data (classes 1-3).

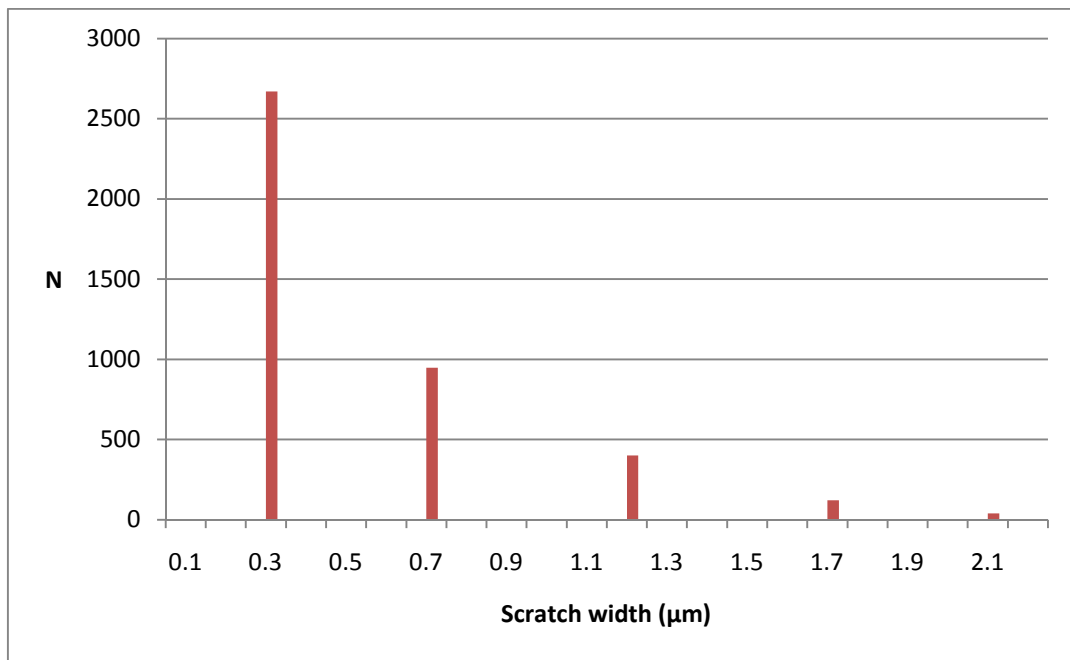


Figure 6. Variation in scratch width, unclassified microwear data (4199 features from 42 sites on 17 teeth).

Continuous and near vertical scratches, up to 1.2 mm long, were observed from crown to base on several teeth at lower magnification. These are not represented in the microwear data due to the limitations of the field of view at x300 magnification. Of the class 2 scratches, 6% (N=71) are length limited (i.e. they exceeded the upper and lower boundaries of the field of view) and this must be considered when examining the mean scratch length data. Cross scratching (oblique scratches cutting across and overprinting other scratches) was also common; although due to the relatively low scratch counts the obscuring effect of this cross scratching did not cause a problem. A few scratches, approximately 5%, exhibit a curvature within the field of view. Microwear

measurement software is not designed to cope with curved scratches. The only way to deal with these features is to score a continuous scratch as two or more scratches with changing orientation. This is not ideal, but the small number of scratches involved will have little impact on the dataset as a whole.

Analysis of the data reveals that overall, the hypothesis that data for each site are uniformly distributed can be rejected (i.e. they show a preferred orientation; Rayleigh uniformity test and Rao spacing test, $P < 0.05$; Table S1). For the unclassified data, mean orientation for each site does not differ significantly from the pooled mean (V test expected mean 104.89° , $P < 0.05$). Of the 42 sites tested there was only one exception to this result however, the number of scratches assigned to that site was only five. Analysis of the three subsets of data (classes 1-3) provides confirmation of this result and the hypothesis that data within classes for each site are uniformly distributed can be rejected (i.e., they show a preferred orientation; Rayleigh uniformity test and Rao spacing test, $P < 0.05$; Tables S2, S3 and S4). Mean orientation for each class for each site does not differ significantly from the overall class mean (all sites, all teeth; V test expected means class 1 = 44.07° , class 2 = 97.85° , class 3 = 141.12° , $P < 0.05$). Of the 95 samples tested (3 classes, 42 sites, 31 sites with $n \leq 1$), there are only seven exceptions to this result – five class 1 and two class 3. In all seven cases, the number of scratches assigned to the class that failed the tests was three or fewer.

The near vertical class 2 data exhibit a consistently high degree of parallelism (i.e. angular dispersion as measured by mean vector length (R), for pooled class 2 data $R = 0.93$ and by sample site $R > 0.91$; (Zar 1999)), and the V test shows the data to be non-uniformly distributed, with a significant mean orientation (V; expected mean = 97.85° , $V = 0.92$, $U = 70.69$, $P < 0.001$). The majority of the class 1 and class 3 data exhibit a similarly high degree of parallelism (54% (37) of the sample sites have $R >$

0.9; based on the 68 of 78 class 1 and 3 sample sites which have an $N > 0$, see Tables S2, S3 and S4). The V test shows also shows the class 1 and class 3 data to be non-uniformly distributed, with significant mean orientations although not as tightly constrained as the class 2 (V; class 1 expected mean = 44.07° , $V = 0.78$, $U = 18.72$, $P < 0.001$; class 3 expected mean = 141.12° , $V = 0.87$, $U = 39.29$, $P < 0.001$).

Subdividing a distribution of circular (orientation) data into classes will invariably lead to an increase in parallelism (R) within each class. Even with a random or uniform distribution, as the number of classes increase or the width of a specific class decreases R will approach 1. To test the hypotheses that the distribution of scratches does not differ from a random distribution, results from the analysis of a random distribution of 4199 orientations partitioned into the three classes (1-3) were compared with those of the real data. The random dataset for the classes (1-3) produced R values of 0.76, 0.82 and 0.87 respectively and V test V values of 0.77, 0.89 and 0.81 respectively. The real class 2 and class 3 data show a greater degree of parallelism and uniformity than would be expected from a random distribution of data partitioned into the three orientation classes and therefore reflect preferred orientations. For the real class 1 data, 19 of the 27 (70%) sites with $N > 1$ have $R > 0.77$, and therefore show a greater degree of parallelism than would be expected from a random distribution however, the V test results do not differ significantly from that of a random distribution. This analysis reveals that overall we can reject the hypothesis that the distribution of scratches does not differ from a random distribution.

To test the null hypothesis that microwear does not differ between sample sites within a tooth, subsets of data were generated for three individual teeth consisting of eight sites from a right maxilla tooth (six lingual and two labial), six sites from a right dentary tooth (two mesiolabial, one lingual and three labial), and six sites from a left

dentary tooth (all mesiolabial). Analysis of these within-tooth data sets reveal that microwear orientation does not differ significantly between samples sites within a tooth (Table 3).

Table 3. Analysis of variation in orientation between sites, within a tooth (8 sites from tooth 10 of the right maxilla, 6 sites from tooth 6 of the right dentary and 5 sites from tooth 6 of the left dentary). Mean of means of means (μ of μ) and confidence intervals calculated for each tooth. Figures in bold fall outside the 99% confidence interval for the mean of means.

Right Maxilla Tooth-Site	10-1	10-2	10-4	10-5	10-6	10-7	10-8	10-20
Unclassified angular dispersal, R	0.757	0.773	0.738	0.805	0.767	0.452	0.684	0.758
Mean vector, μ	79.911	82.377	90.450	95.301	105.812	101.352	99.698	113.738
Class 1 angular dispersal, R	0.697	0.633	0.925	0.816	0.947	0.906	0.789	1
Mean vector, μ	54.578	44.990	46.479	36.469	16.096	39.555	30.966	62.723
Class 2 angular dispersal, R	0.950	0.938	0.952	0.942	0.947	0.929	0.944	0.931
Mean vector, μ	86.196	84.327	92.384	96.214	102.035	94.911	97.475	102.127
Class 3 angular dispersal, R	1	0.908	0.914	0.735	0.879	0.967	0.867	0.908
Mean vector, μ	163.369	154.736	135.405	148.414	143.743	143.964	135.784	137.400
Unclassified mean of means 95.74, 99% confidence interval 75.11 – 118.12								
Class 1 mean of means 41.37, 99% confidence interval 14.01 – 68.09								
Class 2 mean of means 94.45, 99% confidence interval 82.84 – 106.06								
Class 3 mean of means 145.52, 99% confidence interval 126.91 – 163.22								
Right Dentary Tooth-Site	6-1	6-3	6-5	6-6	6-10	6-15		
Unclassified angular dispersal, R	0.669	0.882	0.875	0.728	0.783	0.840		
Mean vector, μ	117.09	107.921	109.476	114.459	89.085	94.006		
Class 1 angular dispersal, R	0.943	0.468	0.745	1	0.838	0.907		
Mean vector, μ	45.259	13.874	25.677	59.744	54.217	58.880		
Class 2 angular dispersal, R	0.940	0.970	0.968	0.965	0.979	0.956		
Mean vector, μ	102.314	104.066	104.565	103.156	90.714	94.638		
Class 3 angular dispersal, R	0.906	0.935	0.917	0.815	0.910	0.843		
Mean vector, μ	138.247	135.726	132.962	136.678	145.640	145.372		
Unclassified mean of means 104.98, 99% confidence interval 77.88 – 135.77								
Class 1 mean of means 46.48, 99% confidence interval 7.84 – 69.97								
Class 2 mean of means 99.90, 99% confidence interval 84.28 – 115.52								
Class 3 mean of means 139.04, 99% confidence interval 125.30 - 153.94								
Left Dentary Tooth-Site	6-1	6-2	6-3	6-4	6-5			
Unclassified angular dispersal, R	0.765	0.802	0.741	0.621	0.696			
Mean vector, μ	116.184	114.665	119.992	124.704	118.389			
Class 2 angular dispersal, R	0.973	0.948	0.952	0.947	0.955			
Mean vector, μ	104.683	103.310	103.245	107.559	105.302			
Class 3 angular dispersal, R	0.896	0.963	0.923	0.789	0.801			
Mean vector, μ	141.664	137.883	141.356	145.775	143.806			
Unclassified mean of means 118.50, 99% confidence interval 107.57 - 141.22								
Class 2 mean of means 104.82, 99% confidence interval 97.77 - 111.95								
Class 3 mean of means 141.90, 99% confidence interval 132.89 - 159.54								

Mean of mean angles and their 99% confidence intervals (Zar 1999) were calculated for each within-tooth data set (for the unclassified microwear data, the dominant near vertical class 2 microwear and the more oblique class 1 and 3 microwear). Mean orientation for each site falls within the confidence interval of the mean of mean angles calculated for its within-tooth data set (for the unclassified microwear data and when partitioned by class). There was only one exception to this result; one class 3 site from tooth 10 of the right maxilla had an orientation that fell outside the confidence interval for its class mean of means. The number of scratches assigned to this site was only one.

However, whilst the hypothesis that microwear orientation differs between sample sites within a tooth can be rejected, the hypothesis that microwear differs between sample sites within a tooth cannot be rejected as significant differences ($P < 0.5$) in both scratch length and scratch width exist in each within-tooth data set (Table S5).

There were only five exceptions to this result; of the 24 within-tooth subsets (length & width, three teeth, unclassified and by classes 1 to 3) scratch length was not significantly different in two class 1 and one class 3 subsets and scratch width was not significantly different in two class 1 subsets. Tukey-Kramer HSD results reveal that there is a pattern to these differences in scratch length and width as the sites which do not differ significantly from each other tend to form groupings based on the vertical position of the site within the tooth face (crown, centre and base). For unclassified data and subsets of data by class (1 to 3) scratch length does not differ significantly between sites within the crown of a tooth, the centre of a tooth or the base of a tooth. There are only three exceptions to this result; site 20 from tooth 10 of the right maxilla differs significantly from the other centre sites and all other lingual sites for the unclassified

data and for the class 2 data, and from one of the other centre sites for the class 3 data.

A similar but less consistent trend exists for scratch width (see Table S6 for unclassified data and Tables S7, S8 and S9 for subsets by class).

The results of within-tooth analysis revealed a significant difference in microwear between tooth faces that required further investigation. Figure 7 illustrates the scratch orientations for the pooled, unclassified data (7.1), by tooth face: mesiolabial, lingual and labial (7.2 to 7.4) and by jaw element: left dentary, right dentary, right maxilla (7.5 to 7.7). Microwear distributions on the three faces appear to be different.

To test the hypothesis that scratch patterns differ between faces, microwear data from 13 mesiolabial, 16 lingual and 13 labial sites on 17 teeth (4,199 scratches) were compared (see Table 4 for summary). Analysis shows no significant difference in angular dispersion (i.e. the degree of parallelism as measured by R) or scratch length between faces however there are significant differences ($P < 0.05$) in scratch count (N), scratch width and orientation (Table 5). Mesiolabial and labial faces differ significantly in scratch count and all three faces differ significantly in scratch width (see Table S6 for means). Pairwise comparisons (Watson-Williams F) of scratch orientation indicate that the lingual face differs significantly from the labial and mesiolabial faces; this was taken into consideration for the between-teeth analysis.

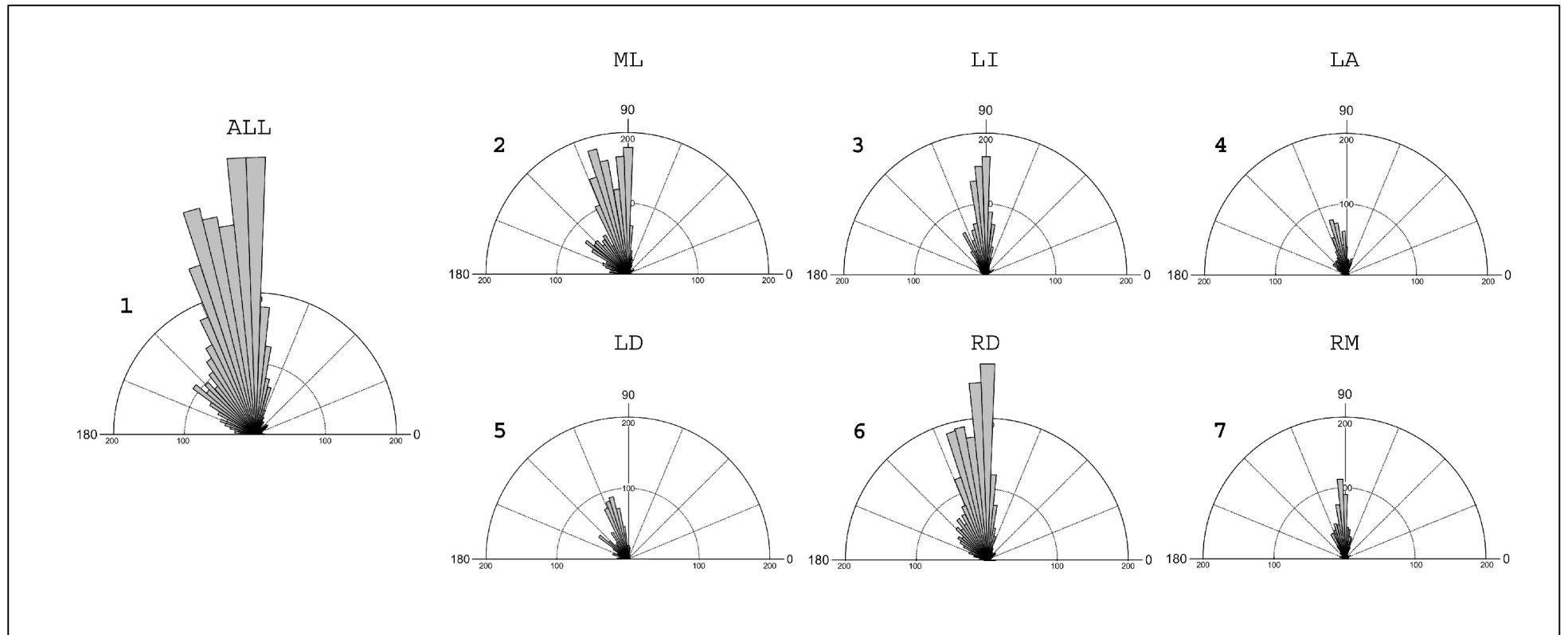


Figure 7. Rose diagrams of microwear scratch orientations, pooled, unclassified microwear data (4199 features from 42 sites on 17 teeth). 7.1 All sites. 7.2 Mesiolabial sites. 7.3 Lingual sites. 7.4 Labial sites. 7.5 Left dentary sites. 7.6 Right dentary sites. 7.7 Right maxilla sites. Frequency is shown by the radius of the wedge, inner circles measure hundreds, 4° bins.

Table 4. Summary statistics from pooled, unclassified microwear data (42 sites on 17 teeth) partitioned by tooth face, mesiolabial (ML), lingual (LI) and labial (LA).

Subgroup	ML	LI	LA
No. of observations (N)	2004	1447	748
Mean (N)	154.15	90.44	57.54
Angular dispersion, R	0.65	0.71	0.67
Mean orientation (mean vector, μ)	110.97°	96.60°	106.12°
95% confidence interval for μ	$\pm 1.19^\circ$	$\pm 1.21^\circ$	$\pm 1.84^\circ$
99% confidence interval for μ	$\pm 1.57^\circ$	$\pm 1.60^\circ$	$\pm 2.41^\circ$
Mean scratch length, μm	41.2	40.65	41
Mean log scratch length, μm	3.56	3.53	3.53
Mean scratch width, μm	0.58	0.36	0.51

Table 5. Results of null hypothesis testing for differences in microwear between mesiolabial (ML), lingual (LI) and labial (LA) tooth faces, (collected from 42 sites on 17 teeth).

	d.f.	F	P
Orientation does not differ between faces (Watson Williams F)	2,4196	133.43	< 0.0001
Length does not differ between faces (one way ANOVA; log data)	2,4196	1.7	0.1822
Width does not differ between faces (one way ANOVA)	2,4196	119.49	< 0.0001
R does not differ between faces (one way ANOVA)	2,36	0.37	0.6911
N does not differ between faces (one way ANOVA)	2,39	4.47	0.0179

To test the null hypothesis that microwear does not differ between teeth within a jaw element, data were partitioned between left and right jaw elements and mean of mean angles and their 99% confidence intervals were calculated for the unclassified data and each class of data (all sites from right dentary or left dentary data). Analysis of these between-tooth datasets reveals that there are significant differences in microwear orientation between teeth of the same jaw element even when comparing data from the same sample position and tooth face (Table S10). Of the 88 samples tested (unclassified data, three classes, 24 sites, eight sites with $n = 0$) 26 mean orientations fall outside the

calculated 99% confidence intervals – ten unclassified, three class 1, eight class 2 and five class 3 – only 12 of which can be attributed to the low number of scratches ($n < 10$) assigned to the sample.

Recalculating mean of mean angles and their 99% confidence intervals based on further partitioning of the data by tooth face, by restricting the data sets to one site per tooth and by separating right dentary and right maxilla, does not significantly alter the above results. I cannot therefore reject the hypothesis that microwear differs between teeth within a jaw element. The variation between teeth is not systematic; orientation does not vary significantly with distance from the jaw hinge and there is no correlation between distance from the jaw hinge and R, N, scratch length or width ($P \gg 0.05$) with the exception of a weak but significant correlation (circular-linear: $r = 0.08$, $P = 0.03$) of class 2 orientations from labial face sample sites within the right dentary (which steepen, approaching 90° with increasing distance from the jaw hinge).

To determine if microwear orientations differed between opposing and non-opposing tooth faces, data were partitioned into eight subsets based on jaw element and tooth face for null hypothesis testing (112 pairwise comparisons; eight subsets, unclassified data and classes 1-3). Table S11 shows the results for 20 of the 112 pairwise comparisons (Watson-Williams F) where orientation for either the unclassified or class 1-3 data does not differ significantly; the 92 pairwise comparisons of opposing and non-opposing tooth faces that are not listed differed significantly ($P < 0.05$). Of the 110 comparisons of non-opposing tooth face data only ten showed no significant difference; left and right dentary labial for unclassified, class 1 and class 2 data, left dentary labial and mesiolabial all data, right dentary and right maxilla labial class 1 data, and right maxilla labial and mesiolabial for unclassified and class 2 data.

Therefore the hypothesis that microwear orientation differs between non-opposing tooth faces cannot be rejected.

For the opposing tooth faces, there is no significant difference between the subsets for the right dentary mesiolabial and the right maxilla lingual faces when data is partitioned by class although the unclassified data does differ significantly. Conversely there is no significant difference between the subsets for the right dentary lingual and the right maxilla mesiolabial faces for the unclassified data but the class 2 data does have a small ($P = 0.007$) significant difference. However the low scratch count ($N=26$) for the right maxilla mesiolabial sites tempers this result. Given the microwear patterns on opposing maxilla and dentary tooth faces are related (i.e. they belong to the same population) the hypothesis that microwear orientation differs between opposing tooth faces cannot be rejected. However, variation does exist within these subsets. A between tooth analysis of one pair of opposing tooth faces from the right dentary mesiolabial and right maxilla lingual subset, (1940 scratches, 15 sites, eight teeth; see Tables S2, S3 and S4), reveals that eight of the 15 class 2 mean orientations fall outside the calculated 99% confidence intervals for the combined subsets (mean of means 96.63° , $CI \pm 4.6^\circ$) and a pairwise (Watson-Williams F) comparisons of sites show significant differences ($P < 0.05$) confirming these CI results.

4. Discussion

Given that the teeth of *Iguana iguana* do not come into contact with each other, it is a significant finding that microwear is affected by gaps in the tooth row and that the opposing tooth faces from maxilla and dentary have microwear orientations that do not differ significantly (i.e. statistically they belong to the same population). That the teeth

are not uniform in terms of spacing or the orientation of their shearing faces (Figure 1.5) will undoubtedly have contributed to the between tooth variation found in microwear orientation; both because successive opposing maxilla and dentary teeth are not interacting with a consistent orientation and spacing, and because the data acquisition employed a standardization of surface orientation that involved rotation to bring the surface perpendicular to the electron beam. Inconsistencies are apparent in the microwear, particularly in N, with samples sites that are at or near the boundary between labial and mesiolabial faces. This coupled with the fact that opposing faces can differ from non-opposing faces and each other, suggests that some marginal mesiolabial sites may be acting as labial sites and vice versa as the attitude of the opposing shearing faces change within a tooth and along the tooth row. The significant non-systematic variation in microwear orientation between teeth within the same jaw element means that a single tooth is not representative of an individual animal however this does not prevent tooth microwear data from being useful in inferring relative jaw motion in *Iguana iguana*.

How does the pattern of microwear in *I. iguana* fit the predictions? In terms of predicted vs. actual microwear the data correctly identified a predominantly dorsoventral cropping action with a signal strong enough to dominate the tri-modal pooled data. The dominant mode (class 2) gave a mean orientation of 97.85° (0° being anterior, 180° posterior along the long axis of the jaw). This mean orientation calculated from the combined data (all sites, Table 2) is highly significant given the tight 95% confidence intervals (CI) of $\pm 0.4^\circ$. How many sites are necessary to be representative of an individual? Reducing the number of sample sites from 42 to 17 (one site per tooth) gives a mean of 97.38° (95% CI $\pm 0.7^\circ$) and a further reduction to six sample sites (two per jaw element) gives a mean of 97.40° (95% CI $\pm 1.05^\circ$). This suggests that

as few as six sample sites could be sufficiently representative of an individual for comparative purposes. Further research will be needed to determine any within-species variation given the limited conclusions that can be drawn from a single individual.

No significant horizontal microwear was found, supporting the prediction of no propalinal jaw motion. The sub-horizontal microwear patterns have mean orientations that are at similar inclinations (i.e. class 1: 44° , class 3: 141° or 39° from the horizontal) but differ significantly from each other in terms of scratch length and width and it seems unlikely that both are purely related to the vigorous jerking motion of the head described by Throckmorton (1976). It is possible that the patterns are related to variation in the material properties, in particular hardness, of the food being processed as it has been suggested that this could affect microwear orientation (Grine 1986; Goswami *et al.* 2005) in addition to relative jaw motion. The difference in scratch width between the opposing tooth faces, with the mesiolabial faces having a mean scratch width 60% greater than that of the lingual faces also suggests a mechanical difference in the tooth surface (Table 4).

The lack of microwear on the non-opposing (labial) tooth surfaces, relative to the opposing (mesiolabial and lingual), supports the observations of Throckmorton (1976) and King (1996) with relation to the cropping action and lack of mastication and meets the predictions for an animal without cheeks.

Whilst DFA on scratch width and orientation identify one dominant mode in the dorsoventral plane (class 2), it is possible that increasing the dataset through analysis of multiple individuals may determine a second mode (Figure 5.1 suggests a mode at 90° and another at 104°). Throckmorton (1976) noted that as well as the elevation and depression of the lower jaw *Iguana iguana* had a second cropping action, that of

elevation of the upper jaw (movement of the whole head whilst the lower jaw remained stationary) and even though no streptostylic movement was observed, the potential for up to 14° of anteroposterior movement was found in the quadrate. It is therefore possible that the 7.85° departure from the vertical in class 2 data could relate to minor posterodorsal retraction of the lower jaw and or forward movement of food in the mouth during jaw closure (a 1.2 mm long scratch with a 7.85° departure from the vertical only requires a 160 micron long axis movement). If the class 2 mode can be further divided, then a between-tooth analysis of variation can be re-visited and it still may be the case that a single tooth could be used to infer the direction of jaw motion.

Iguana iguana has potential for comparative studies with early herbivores that possess similar simple jaw mechanics, particularly those where degrees of cranial kinesis, streptostylism or the presence of muscular cheeks are suspected to have been utilized during feeding; all features which *I. Iguana* lacks.

Acknowledgements

I wish to thank Samuel Turvey, Zoological Society of London and Carl Mehling & Jeanne Kelly, American Museum of Natural History for granting access to *Iguana iguana* specimens and giving permission to clean the tooth surfaces.

Supporting Information

Table S1. Microwear summary statistics, unclassified data

Element	Tooth	Site	Face	Angular disp.		Rayleigh		Rao	Orientation		(μm)	(μm)
				n	r	Z	p	U	p	μ	length	width
L.Dentary	1	1	LA	53	0.571	17.309	<< 0.001	207.911	< 0.01	115.650	38.4	0.6
	6	1	ML	133	0.765	77.757	<< 0.001	224.002	< 0.01	116.184	41.4	0.7
	6	2	ML	93	0.802	59.855	<< 0.001	241.515	< 0.01	114.665	43.6	0.5
	6	3	ML	103	0.741	56.573	<< 0.001	209.191	< 0.01	119.992	44.4	0.8
	6	4	ML	162	0.621	62.426	<< 0.001	205.907	< 0.01	124.704	51.4	0.8
	6	5	ML	135	0.696	65.419	<< 0.001	211.797	< 0.01	118.389	56.7	1.0
	9	1	ML	169	0.684	79.056	<< 0.001	205.066	< 0.01	121.804	47.2	1.0
R.Dentary	1	1	LI	179	0.713	90.886	<< 0.001	199.631	< 0.01	86.065	31.9	0.3
	1	2	ML	224	0.753	126.847	<< 0.001	247.151	< 0.01	88.256	41.0	0.3
	3	1	LI	17	0.882	13.221	<< 0.001	272.775	< 0.01	92.637	42.2	0.3
	3	2	LA	0								
	5	1	LA	0								
	5	3	LA	7	0.916	5.873	<< 0.001	235.579	< 0.01	107.225	77.4	0.4
	5	6	ML	7	0.692	3.352	0.029	161.904	< 0.05	99.786	37.8	1.0
	6	1	LA	245	0.669	109.805	<< 0.001	201.257	< 0.01	117.090	33.4	0.5
	6	3	LA	240	0.882	186.759	<< 0.001	258.129	< 0.01	107.921	45.3	0.3
	6	5	ML	243	0.875	185.978	<< 0.001	255.337	< 0.01	109.476	41.4	0.3
	6	6	LA	34	0.728	18.017	<< 0.001	213.960	< 0.01	114.459	29.1	0.4
	6	10	ML	132	0.783	80.842	<< 0.001	240.425	< 0.01	89.085	42.6	0.3
	6	15	LI	104	0.840	73.411	<< 0.001	242.613	< 0.01	94.006	34.8	0.3
	7	1	LI	43	0.886	33.742	<< 0.001	256.883	< 0.01	91.554	32.9	0.2
	7	2	LA	0								
	10	1	LI	155	0.788	96.284	<< 0.001	223.440	< 0.01	97.194	35.9	0.3
	10	2	LI	180	0.673	81.418	<< 0.001	212.516	< 0.01	98.546	47.1	0.3
	12	4	ML	149	0.765	87.231	<< 0.001	224.198	< 0.01	105.294	36.5	0.5
	12	8	ML	428	0.556	132.282	<< 0.001	187.259	< 0.01	120.617	30.2	0.5
	13	1	LI	12	0.977	11.458	<< 0.001	288.704	< 0.01	85.489	41.7	0.2
	R.Maxilla	13	3	LA	6	0.711	3.033	0.041	152.976	< 0.05	127.408	32.7
3		1	LA	6	0.832	4.155	0.009	193.614	< 0.05	76.721	30.4	0.2
5		1	LI	163	0.605	59.721	<< 0.001	214.624	< 0.01	92.209	38.1	0.3
7		1	ML	26	0.847	18.662	<< 0.001	244.362	< 0.01	86.587	38.8	0.3
9		1	LA	5	0.439	0.965	0.402	119.255	< 0.05	65.240	33.0	1.0
9		20	LI	54	0.924	46.087	<< 0.001	261.736	< 0.01	103.828	37.2	0.9
10		1	LA	54	0.757	30.985	<< 0.001	229.412	< 0.01	79.911	52.6	0.9
10		2	LA	98	0.773	58.576	<< 0.001	237.414	< 0.01	82.377	47.5	0.9
10		4	LI	57	0.738	31.048	<< 0.001	225.089	< 0.01	90.450	44.9	0.3
10		5	LI	83	0.805	53.750	<< 0.001	238.245	< 0.01	95.301	48.3	0.3
10		6	LI	90	0.767	52.897	<< 0.001	227.849	< 0.01	105.812	38.6	0.3
10		7	LI	35	0.452	7.161	<< 0.001	200.565	< 0.01	101.352	35.4	0.3
10		8	LI	139	0.684	65.059	<< 0.001	223.642	< 0.01	99.698	42.0	0.3
10		20	LI	97	0.758	55.760	<< 0.001	215.315	< 0.01	113.738	61.8	1.0
11		1	LI	39	0.767	22.940	<< 0.001	245.758	< 0.01	91.433	37.6	0.3

Table S2. Microwear summary statistics, class 1 data

Class 1				Angular disp.		Rayleigh		Rao		Orientation		(μm)	(μm)
Element	Tooth	Site	Face	n	r	Z	p	U	p	μ	length	width	
L.Dentary	1	1	LA	6	0.809	3.930	0.012	199.440	< 0.05	40.003	27.6	0.3	
	6	1	ML	1	1	1				37.569	15.3	0.2	
	6	2	ML	0									
	6	3	ML	0									
	6	4	ML	7	0.781	4.260	0.009	214.380	< 0.01	47.478	51.8	0.6	
	6	5	ML	2	0.538	0.579	0.626			35.948	88.7	0.7	
R.Dentary	9	1	ML	6	0.740	3.280	0.030	204.680	< 0.05	54.976	41.9	0.8	
	1	1	LI	40	0.880	30.970	<< 0.001	261.460	< 0.01	50.476	24.8	0.3	
	1	2	ML	28	0.821	18.890	<< 0.001	223.200	< 0.01	32.795	25.2	0.3	
	3	1	LI	1	1					32.471	24.1	0.2	
	3	2	LA	0									
	5	1	LA	0									
	5	3	LA	0									
	5	6	ML	1	1					64.799	17.6	0.7	
	6	1	LA	13	0.943	11.57	<< 0.001	277.620	< 0.01	45.259	23.2	0.5	
	6	3	LA	3	0.468	0.658	0.560			13.874	18.1	0.2	
	6	5	ML	2	0.745	1.111	0.383			25.677	17.4	0.2	
	6	6	LA	1	1					59.744	19.5	0.2	
	6	10	ML	18	0.838	12.646	<< 0.001	236.208	< 0.01	54.217	19.0	0.3	
	6	15	LI	8	0.907	6.580	<< 0.001	236.370	< 0.01	58.880	17.8	0.3	
	7	1	LI	4	0.904	3.260	0.026	201.940	< 0.05	50.688	21.9	0.2	
	7	2	LA	0									
	10	1	LI	8	0.754	4.540	0.006	200.630	< 0.01	54.503	29.0	0.2	
	10	2	LI	8	0.794	5.040	0.003	182.560	< 0.05	40.317	25.8	0.3	
	12	4	ML	3	0.921	2.540	0.067			59.068	22.1	0.7	
	12	8	ML	24	0.768	14.160	<< 0.001	220.830	< 0.01	39.336	19.7	0.6	
	13	1	LI	1	1					65.480	29.2	0.2	
	13	3	LA	0									
R.Maxilla	3	1	LA	2	0.980	1.920	0.152			55.644	26.2	0.2	
	5	1	LI	25	0.923	21.280	<< 0.001	253.200	< 0.01	33.700	24.2	0.3	
	7	1	ML	1	1					53.973	19.0	0.2	
	9	1	LA	3	0.981	2.880	0.040			62.331	30.0	1.0	
	9	20	LI	0									
	10	1	LA	15	0.697	7.280	<< 0.001	236.830	< 0.01	54.578	63.3	0.9	
	10	2	LA	12	0.633	4.800	0.006	229.560	< 0.01	44.990	44.8	1.0	
	10	4	LI	8	0.925	6.844	<< 0.001	234.798	< 0.01	46.479	34.8	0.3	
	10	5	LI	6	0.816	3.999	0.011	203.169	< 0.05	36.469	36.3	0.3	
	10	6	LI	4	0.947	3.587	0.015	217.873	< 0.05	16.096	36.7	0.2	
	10	7	LI	6	0.906	4.925	0.002	227.936	< 0.01	39.555	25.2	0.2	
	10	8	LI	15	0.789	9.330	<< 0.001	203.950	< 0.01	30.966	26.7	0.3	
	10	20	LI	1	1					62.723	33.4	0.7	
	11	1	LI	4	0.931	3.460	0.019	213.320	< 0.05	54.424	32.5	0.2	

Table S3. Microwear summary statistics, class 2 data

Class 2				Angular disp.		Rayleigh		Rao		Orientation		(μm)	(μm)
Element	Tooth	Site	Face	n	r	Z	p	U	p	μ		length	width
L.Dentary	1	1	LA	31	0.969	29.130	<< 0.001	285.790	< 0.01	104.677		48.0	0.7
	6	1	ML	85	0.973	80.421	<< 0.001	291.781	< 0.01	104.683		44.5	0.8
	6	2	ML	61	0.948	54.865	<< 0.001	279.586	< 0.01	103.310		47.3	0.5
	6	3	ML	56	0.952	50.786	<< 0.001	278.899	< 0.01	103.245		45.6	0.8
	6	4	ML	75	0.947	67.240	<< 0.001	285.080	< 0.01	107.559		53.3	0.8
	6	5	ML	79	0.955	72.005	<< 0.001	285.314	< 0.01	105.302		55.3	1.0
	9	1	ML	83	0.933	72.240	<< 0.001	274.280	< 0.01	105.224		52.3	1.0
R.Dentary	1	1	LI	128	0.911	106.180	<< 0.001	264.530	< 0.01	91.659		34.8	0.3
	1	2	ML	186	0.981	179.030	<< 0.001	300.770	< 0.01	90.468		43.9	0.4
	3	1	LI	16	0.970	15.050	<< 0.001	292.620	< 0.01	94.231		43.4	0.3
	3	2	LA	0									
	5	1	LA	0									
	5	3	LA	7	0.916	5.870	<< 0.001	235.570	< 0.01	107.225		77.4	0.4
	5	6	ML	4	0.957	3.660	0.013	225.480	< 0.01	93.199		50.3	0.6
	6	1	LA	125	0.940	110.500	<< 0.001	283.220	< 0.01	102.314		36.0	0.5
	6	3	LA	203	0.970	191.049	<< 0.001	295.039	< 0.01	104.066		47.7	0.3
	6	5	ML	193	0.968	180.685	<< 0.001	290.168	< 0.01	104.565		44.0	0.3
	6	6	LA	19	0.965	17.705	<< 0.001	285.947	< 0.01	103.156		34.5	0.3
	6	10	ML	104	0.979	99.669	<< 0.001	297.117	< 0.01	90.714		48.4	0.3
	6	15	LI	90	0.956	82.290	<< 0.001	277.850	< 0.01	94.638		36.6	0.3
	7	1	LI	39	0.968	36.520	<< 0.001	287.550	< 0.01	94.273		34.0	0.2
	7	2	LA	0									
	10	1	LI	127	0.915	106.430	<< 0.001	264.403	< 0.01	94.371		37.8	0.3
	10	2	LI	130	0.930	112.540	<< 0.001	270.970	< 0.01	91.165		52.0	0.3
	12	4	ML	115	0.960	105.930	<< 0.001	288.080	< 0.01	98.938		39.2	0.5
	12	8	ML	197	0.939	173.770	<< 0.001	275.630	< 0.01	98.467		31.6	0.5
	13	1	LI	11	0.998	10.950	<< 0.001	315.970	< 0.01	87.167		42.9	0.2
	13	3	LA	1	1					86.309		43.1	0.2
R.Maxilla	3	1	LA	4	0.944	3.560	0.016	218.300	< 0.05	86.913		32.5	0.2
	5	1	LI	121	0.951	109.400	<< 0.001	281.840	< 0.01	94.450		41.3	0.3
	7	1	ML	24	0.924	20.460	<< 0.001	270.900	< 0.01	86.685		40.0	0.3
	9	1	LA	1	1					110.772		43.1	0.7
	9	20	LI	50	0.938	44.000	<< 0.001	273.020	< 0.01	102.269		38.1	0.9
	10	1	LA	38	0.950	34.320	<< 0.001	283.680	< 0.01	86.196		48.8	0.9
	10	2	LA	82	0.938	72.140	<< 0.001	279.930	< 0.01	84.327		48.4	0.9
	10	4	LI	44	0.952	39.882	<< 0.001	280.718	< 0.01	92.384		48.4	0.3
	10	5	LI	74	0.942	65.685	<< 0.001	275.539	< 0.01	96.214		49.9	0.3
	10	6	LI	75	0.947	67.291	<< 0.001	282.075	< 0.01	102.035		40.7	0.3
	10	7	LI	20	0.929	17.266	<< 0.001	281.121	< 0.01	94.911		41.4	0.3
	10	8	LI	105	0.944	93.470	<< 0.001	276.470	< 0.01	97.475		42.1	0.3
	10	20	LI	61	0.931	52.894	<< 0.001	277.493	< 0.01	102.127		70.9	1.0
	11	1	LI	31	0.973	29.350	<< 0.001	298.100	< 0.01	91.863		37.8	0.3

Table S4. Microwear summary statistics, class 3 data

Class 3				Angular disp.		Rayleigh		Rao	Orientation		(μm)	(μm)
Element	Tooth	Site	Face	n	r	Z	p	U	p	μ	length	width
L.Dentary	1	1	LA	16	0.945	14.280	<< 0.001	257.420	< 0.01	147.550	23.9	0.5
	6	1	ML	47	0.896	37.695	<< 0.001	263.387	< 0.01	141.664	36.3	0.6
	6	2	ML	32	0.963	29.692	<< 0.001	289.960	< 0.01	137.883	36.5	0.5
	6	3	ML	47	0.923	40.027	<< 0.001	260.282	< 0.01	141.356	42.9	0.7
	6	4	ML	80	0.789	49.830	<< 0.001	255.450	< 0.01	145.775	49.7	0.9
	6	5	ML	54	0.801	34.672	<< 0.001	245.498	< 0.01	143.806	57.5	1.1
	9	1	ML	80	0.882	62.170	<< 0.001	257.620	< 0.01	141.929	42.3	1.0
R.Dentary	1	1	LI	11	0.986	10.690	<< 0.001	291.100	< 0.01	126.218	24.2	0.2
	1	2	ML	10	0.903	8.150	<< 0.001	242.090	< 0.01	150.696	30.4	0.3
	3	1	LI	0								
	3	2	LA	0								
	5	1	LA	0								
	5	3	LA	0								
	5	6	ML	2	0.985	1.940	0.148			133.235	22.9	1.9
	6	1	LA	107	0.906	87.750	<< 0.001	262.540	< 0.01	138.247	31.6	0.4
	6	3	LA	34	0.935	29.706	<< 0.001	267.486	< 0.01	135.726	33.4	0.3
	6	5	ML	48	0.917	40.372	<< 0.001	272.979	< 0.01	132.962	31.7	0.3
	6	6	LA	14	0.815	9.309	<< 0.001	233.000	< 0.01	136.678	22.3	0.5
	6	10	ML	10	0.910	8.276	<< 0.001	245.415	< 0.01	145.640	24.6	0.3
	6	15	LI	6	0.843	4.260	0.008	216.630	< 0.01	145.372	31.5	0.2
	7	1	LI	0								
	7	2	LA	0								
	10	1	LI	20	0.922	17.000	<< 0.001	271.170	< 0.01	132.731	26.6	0.3
	10	2	LI	42	0.885	32.870	<< 0.001	250.610	< 0.01	138.177	36.1	0.3
	12	4	ML	31	0.897	24.940	<< 0.001	255.900	< 0.01	143.583	27.8	0.5
	12	8	ML	207	0.882	160.950	<< 0.001	254.770	< 0.01	144.409	30.1	0.5
13	1	LI	0									
13	3	LA	5	0.849	3.600	0.018	200.970	< 0.05	134.153	30.7	0.3	
R.Maxilla	3	1	LA	0								
	5	1	LI	17	0.755	9.680	<< 0.001	244.790	< 0.01	150.047	36.0	0.3
	7	1	ML	1	1					148.449	31.0	0.2
	9	1	LA	1	1					177.510	32.0	1.2
	9	20	LI	4	0.994	3.950	0.008	254.310	< 0.01	123.793	25.7	0.9
	10	1	LA	1	1					163.369	37.1	0.7
	10	2	LA	4	0.908	3.300	0.025	206.680	< 0.05	154.736	36.6	0.9
	10	4	LI	5	0.914	4.174	0.007	220.821	< 0.01	135.405	30.1	0.3
	10	5	LI	3	0.735	1.622	0.211			148.414	32.7	0.2
	10	6	LI	11	0.879	8.496	<< 0.001	237.273	< 0.01	143.743	25.0	0.3
	10	7	LI	9	0.967	8.413	<< 0.001	280.441	< 0.01	143.964	29.0	0.3
	10	8	LI	19	0.867	14.270	<< 0.001	264.790	< 0.01	135.784	53.6	0.4
	10	20	LI	35	0.908	28.882	<< 0.001	260.837	< 0.01	137.400	46.8	1.0
	11	1	LI	4	0.845	2.850	0.047	190.510	< 0.01	147.537	41.1	0.2

Table S5. Results of null hypothesis testing for differences in microwear (scratch length and width) between sites, within a tooth (8 sites from tooth 10 of the right maxilla, 6 sites from tooth 6 of the right dentary and 5 sites from tooth 6 of the left dentary).

	Unclassified			Class 1			Class 2			Class 3		
Length does not differ between sites	d.f.	F	P	d.f.	F	P	d.f.	F	P	d.f.	F	P
Left dentary tooth 6	4,621	7.953	< 0.0001	2,7	2.608	0.1425	4,351	3.309	0.0111	4,255	5.438	0.0003
Right dentary tooth 6	5,992	9.459	< 0.0001	5,39	0.766	0.5797	5,728	5.334	< 0.0001	5,213	1.550	0.1758
Right maxilla tooth 10 (one way ANOVA; log data)	7,645	8.973	< 0.0001	7,59	3.173	0.0065	7,491	8.288	< 0.0001	7,79	2.890	0.0097

	Unclassified			Class 1			Class 2			Class 3		
Width does not differ between sites	d.f.	F	P	d.f.	F	P	d.f.	F	P	d.f.	F	P
Left dentary tooth 6	4,621	16.268	< 0.0001	2,7	0.294	0.7544	4,351	8.328	< 0.0001	4,255	10.070	< 0.0001
Right dentary tooth 6	5,992	17.299	< 0.0001	5,39	1.243	0.3078	5,728	15.186	< 0.0001	5,213	2.572	0.0277
Right maxilla tooth 10 (one way ANOVA)	7,645	92.658	< 0.0001	7,59	10.330	< 0.0001	7,491	69.902	< 0.0001	7,79	10.656	< 0.0001

Table S6, Within tooth analysis of scratch length and width (Tukey-Kramer HSD). Within tooth sites not connected by the same letter are significantly different.

Unclassified				Position on face		Scratch Length (μm)		Scratch Width (μm)		n	r
Element	Tooth	Site	Face	vrt	hrz	Connection	LogMean	Connection	Mean		
L. Dentary	6	1	ML	crow n	posterior	C	3.599	B	0.737	133	0.765
	6	2	ML	crow n	posterior	B C	3.691	C	0.521	93	0.802
	6	3	ML	crow n	posterior	B C	3.653	B	0.762	103	0.741
	6	4	ML	centre	posterior	A B	3.807	B	0.835	162	0.621
	6	5	ML	centre	posterior	A	3.904	A	1.048	135	0.696
R. Dentary	6	1	LA	centre	anteroir	B	3.354	A	0.455	245	0.669
	6	3	LA	crow n	anteroir	A	3.627	B	0.313	240	0.882
	6	5	ML	crow n	posterior	A	3.607	B	0.268	243	0.875
	6	6	LA	base	posterior	B	3.249	A B	0.368	34	0.728
	6	10	ML	centre	centre	A B	3.485	B	0.274	132	0.783
	6	15	LI	centre	anteroir	B	3.387	B	0.272	104	0.840
R. Maxilla	10	1	LA	crow n	centre	A B	3.859	A	0.875	54	0.757
	10	2	LA	crow n	centre	B C	3.716	A	0.912	98	0.773
	10	4	LI	centre	posterior	B C	3.680	B	0.280	57	0.738
	10	5	LI	crow n	centre	B C	3.705	B	0.287	83	0.805
	10	6	LI	centre	anterior	C	3.496	B	0.309	90	0.767
	10	7	LI	base	posterior	C	3.448	B	0.271	35	0.452
	10	8	LI	base	centre	C	3.572	B	0.345	139	0.684
	10	20	LI	centre	centre	A	3.991	A	0.962	97	0.758

Table S7. Within tooth analysis of class 1 scratch length and width, (Tukey-Kramer HSD). Within tooth sites not connected by the same letter are significantly different.

Class 1				Position on face		Scratch Length (μm)		Scratch Width (μm)		n	r
Element	Tooth	Site	Face	vrt	hrz	Connection	LogMean	Connection	Mean		
L. Dentary	6	1	ML	crow n	anterior	A	2.727	A	0.232	1	1
	6	2	ML	crow n	centre					0	
	6	3	ML	crow n	posterior					0	
	6	4	ML	centre	anteroir	A	3.868	A	0.629	7	0.781
	6	5	ML	centre	centre	A	4.239	A	0.695	2	0.538
R. Dentary	6	1	LA	centre	anteroir	A	3.088	A	0.481	13	0.943
	6	3	LA	crow n	anteroir	A	2.753	A	0.232	3	0.468
	6	5	ML	crow n	posterior	A	2.786	A	0.232	2	0.745
	6	6	LA	base	posterior	A	2.968	A	0.232	1	1
	6	10	ML	centre	centre	A	2.843	A	0.283	18	0.838
	6	15	LI	centre	anteroir	A	2.691	A	0.290	8	0.907
R. Maxilla	10	1	LA	crow n	centre	A	3.994	A	0.880	15	0.697
	10	2	LA	crow n	centre	A B	3.628	A	1.042	12	0.633
	10	4	LI	centre	posterior	A B	3.511	B	0.347	8	0.925
	10	5	LI	crow n	centre	A B	3.468	B	0.309	6	0.816
	10	6	LI	centre	anterior	A B	3.461	B	0.232	4	0.947
	10	7	LI	base	posterior	B	3.190	B	0.232	6	0.906
	10	8	LI	base	centre	B	3.193	B	0.324	15	0.789
	10	20	LI	centre	centre	A B	3.507	A B	0.695	1	1

Table S8. Within tooth analysis of class 2 scratch length and width (Tukey-Kramer HSD). Within tooth sites not connected by the same letter are significantly different.

Class 2				Position on face		Scratch Length (μm)		Scratch Width (μm)		n	r
Element	Tooth	Site	Face	vert	hrz	Connection	LogMean	Connection	Mean		
L. Dentary	6	1	ML	crown	anterior	B	3.667	B	0.793	85	0.973
	6	2	ML	crown	centre	A B	3.772	C	0.528	61	0.948
	6	3	ML	crown	posterior	B	3.662	A B	0.844	56	0.952
	6	4	ML	centre	anteroir	A B	3.842	A B	0.818	75	0.947
	6	5	ML	centre	centre	A	3.900	A	1.023	79	0.955
R. Dentary	6	1	LA	centre	anteroir	B	3.448	A	0.476	125	0.940
	6	3	LA	crown	anteroir	A	3.689	B	0.318	203	0.970
	6	5	ML	crown	posterior	A	3.668	B	0.270	193	0.968
	6	6	LA	base	posterior	A B	3.428	B	0.305	19	0.965
	6	10	ML	centre	centre	A B	3.634	B	0.267	104	0.979
	6	15	LI	centre	anteroir	B	3.445	B	0.273	90	0.956
R. Maxilla	10	1	LA	crown	centre	B	3.812	A	0.878	38	0.950
	10	2	LA	crown	centre	B	3.736	A	0.893	82	0.938
	10	4	LI	centre	posterior	B	3.751	B	0.263	44	0.952
	10	5	LI	crown	centre	B	3.738	B	0.288	74	0.942
	10	6	LI	centre	anterior	B	3.547	B	0.312	75	0.947
	10	7	LI	base	posterior	B	3.616	B	0.255	20	0.929
	10	8	LI	base	centre	B	3.587	B	0.346	105	0.944
	10	20	LI	centre	centre	A	4.150	A	0.961	61	0.931

Table S9. Within tooth analysis of class 3 scratch length and width (Tukey-Kramer HSD). Within tooth sites not connected by the same letter are significantly different.

Class 3				Position on face		Scratch Length (μm)		Scratch Width (μm)		n	r
Element	Tooth	Site	Face	vert	hrz	Connection	LogMean	Connection	Mean		
L. Dentary	6	1	ML	crown	anterior	C	3.493	B C	0.646	47	0.896
	6	2	ML	crown	centre	B C	3.537	C	0.507	32	0.963
	6	3	ML	crown	posterior	A B C	3.643	B C	0.665	47	0.923
	6	4	ML	centre	anteroir	A B	3.769	A B	0.869	80	0.789
	6	5	ML	centre	centre	A	3.898	A	1.098	54	0.801
R. Dentary	6	1	LA	centre	anteroir	A	3.277	A B	0.463	107	0.906
	6	3	LA	crown	anteroir	A	3.333	A	0.426	34	0.935
	6	5	ML	crown	posterior	A	3.393	A B	0.324	48	0.917
	6	6	LA	base	posterior	A	3.026	A B	0.286	14	0.815
	6	10	ML	centre	centre	A	3.092	B	0.261	10	0.910
	6	15	LI	centre	anteroir	A	3.437	A B	0.232	6	0.843
R. Maxilla	10	1	LA	crown	centre	A B	3.613	A B	0.695	1	1
	10	2	LA	crown	centre	A B	3.565	A B	0.927	4	0.908
	10	4	LI	centre	posterior	A B	3.324	B	0.324	5	0.914
	10	5	LI	crown	centre	A B	3.367	B	0.232	3	0.735
	10	6	LI	centre	anterior	B	3.156	B	0.316	11	0.879
	10	7	LI	base	posterior	A B	3.248	B	0.335	9	0.967
	10	8	LI	base	centre	A	3.791	B	0.354	19	0.867
	10	20	LI	centre	centre	A	3.728	A	0.973	35	0.908

Table S10. Analysis of variation in orientation between teeth, using standardized site positions for each tooth face (24 sites from 17 teeth, 1 site per tooth face). Data for lingual (LI), labial (LA) & mesiolabial (ML) faces of left dentary (LD), right dentary (RD) and right maxilla (RM) transformed to allow direct comparison with right dentary labial face. Mean of means (μ of μ) and confidence intervals calculated from all RD or LD sites, pooled and by class. Mean orientation values in bold fall outside the 99% confidence intervals

Right Dentary							Right Maxilla			
Tooth-Site	1-1	3-1	6-15	7-1	10-2	13-1	5-1	9-20	10-6	11-01
Face	LI	LI	LI	LI	LI	LI	LI	LI	LI	LI
Unclassified n	179	17	104	43	180	12	163	54	90	39
μ	86.065	92.637	94.006	91.554	98.546	85.489	92.209	103.828	105.812	91.433
Class 1 n	40	1	8	4	8	1	25	0	4	4
μ	50.476	32.471	58.88	50.688	40.317	65.48	33.7		16.096	54.424
Class 2 n	128	16	90	39	130	11	121	50	75	31
μ	91.659	94.231	94.638	94.273	91.165	87.167	94.45	102.269	102.035	91.863
Class 3 n	11	0	6	0	42	0	17	4	11	4
μ	126.218		145.372		138.177		150.047	123.793	143.743	147.537

Right Dentary								Right Maxilla			
Tooth-Site	1-2	5-3	5-6	6-1	6-10	12-4	13-3	3-1	7-1	9-1	10-1
Face	ML	LA	ML	LA	ML	ML	LA	LA	ML	LA	LA
Unclassified n	224	7	7	245	132	149	6	6	26	5	54
μ	88.256	107.225	99.786	117.090	89.085	105.294	127.408	76.721	86.587	65.240	79.911
Class 1 n	28	0	1	13	18	3	0	2	1	3	15
μ	32.795		64.799	45.259	54.217	59.068		55.644	53.973	62.331	54.578
Class 2 n	186	7	4	125	104	115	1	4	24	1	38
μ	90.468	107.225	93.199	102.314	90.714	98.938	86.309	86.913	86.685	110.772	86.196
Class 3 n	10	0	2	107	10	31	5	0	1	1	1
μ	150.696		133.235	138.247	145.64	143.583	134.153		148.449	177.51	163.369

Left Dentary			Right dentary & maxilla			
Tooth-Site	1-1	6-1	9-1			
Face	LA	ML	ML			
Unclassified n	53	133	169	Unclassified mean of means 101.02, 99% confidence interval 91.22 - 111.99		
μ	115.650	116.184	121.804	Class 1 mean of means 48.43, 99% confidence interval 34.54 - 59.86		
Class 1 n	6	1	6	Class 2 mean of means 95.87, 99% confidence interval 90.55 - 101.30		
μ	40.003	37.569	54.976	Class 3 mean of means 138.26, 99% confidence interval 131.39 - 145.51		
Class 2 n	31	85	83	Left dentary		
μ	104.677	104.683	105.224	Unclassified mean of means 118.66, 99% confidence interval 111.69 - 127.30		
Class 3 n	16	47	80	Class 1 mean of means 43.17, 99% confidence interval 25.99 - 64.42		
μ	147.55	141.664	141.929	Class 2 mean of means 104.85, 99% confidence interval 101.78 - 107.95		
				Class 3 mean of means 142.76, 99% confidence interval 136.03 - 150.38		

CHAPTER 7

Comparative dental microwear analysis of the basal ornithischian *Lesothosaurus diagnosticus* and the squamate *Iguana iguana*

Targeted for the journal *Palaaios*

ABSTRACT

Dental microwear analysis uses the microscopic scratches and pits on the surface of teeth to deduce dietary habit and offers a fresh approach to the reconstruction of jaw movements during feeding in extinct animals, particularly where the absence of tooth wear facets hampers the reconstruction via functional morphology. Most dental microwear studies have been carried out on mammals, with comparative analyses of microwear patterns between fossil and modern living counterparts. Whilst the presence of tooth wear facets can aid in reconstruction of jaw movements during feeding, their absence does not affect the ability to discern repetitive jaw motion from tooth microwear patterns. Here I show that analysis of tooth microwear orientation provides direct evidence for the relative motion of jaws during feeding in the basal ornithischian dinosaur *Lesothosaurus diagnosticus*. Statistical testing demonstrates that the teeth of *L. diagnosticus* preserve 3 distinct sets of scratches in different orientations that are comparable to those of the modern squamate *Iguana iguana*. In terms of jaw mechanics, these data indicate the isognathic near-vertical simple adduction predicted for this animal. The analyses support the assertion that muscular cheeks were not present in *L. diagnosticus*.

INTRODUCTION

Lesothosaurus diagnosticus is one of the earliest and least derived of the ornithischian dinosaurs (Serenó 1991). Initially associated with *Fabrosaurus*, its affinities have a history of controversy (e.g., Thulborn 1971a; Galton 1972; Thulborn 1974; Galton 1978). Similarities in skull morphology led to *Lesothosaurus* and *Fabrosaurus* being grouped with the ornithopod dinosaur *Hypsilophodon*, and the precladistic view was that together they gave rise to all other ornithischian groups. Cladistic analyses however, have shown that there is no family Fabrosauridae or Hypsilophodontidae (Gauthier 1986; Sereno 1986, 1997; Butler *et al.* 2008). Whilst the exact phylogenetic position of *L. diagnosticus* within basal ornithischians is still a matter of debate, it is representative of the earliest stages of adaptation to herbivory in ornithischians (Serenó 1997; Norman *et al.* 2004), predating the advanced jaw mechanics of the ornithopod dinosaurs.

Previous studies of basal ornithischians such as *Lesothosaurus* (e.g., Thulborn 1971b; Weishampel 1984) suggested that they relied solely on simple adduction of the lower jaws to produce vertical or near vertical tooth-tooth shearing motion between bilaterally occluding maxillary and dentary teeth. With *L. diagnosticus* wear facets are not present on all specimens (Galton 1978) however, Norman *et al.* (2004) found near vertical wear facets developed on the lingual side of maxillary teeth and the labial side of dentary teeth in some specimens, supporting the argument for tooth-tooth occlusion. The possibility that *L. diagnosticus* had rudimentary cheeks was suggested by Galton (1978) and is supported by the fact that the posterior two thirds of the dentary tooth row is inset (Paul 1984; Sereno 1991). This coupled with an akinetic skull make *L. diagnosticus* an important subject for study and one that could provide an insight into key innovations in ornithopod feeding.

Ornithopod evolution

Ornithopod dinosaurs became the dominant herbivorous vertebrates in many Late Cretaceous ecosystems (Horner *et al.* 2004; Weishampel *et al.* 2004). From simple origins in the Triassic, their jaw systems diversified and increasingly complex jaw mechanics developed. Kinematic analyses of the skulls and jaws of ornithopod dinosaurs show that all but the most basal could chew, by mobilizing either cranial or mandibular segments to generate a transverse grinding power stroke (Norman 1984; Weishampel 1984; Norman and Weishampel 1985). Galton (1973) suggested that an important reason for the success of ornithopods was the development of cheeks and postulated that most ornithischians had cheeks and a small subterminal mouth, citing *Hypsilophodon foxii* as an example. Coupled with inset tooth rows and self sharpening teeth, cheeks would have enabled ornithischians to process more resistant plant material and retain it inside the mouth during chewing. Norman and Weishampel (1985) contested Galton's view, proposing that the evolution of cheeks was a sequel to the development of the pleurokinetic hinge (moveable joints within the skull that allow flexion and expansion during feeding) and the consequent transverse grinding stroke. These authors considered basal ornithischians such as *Lesothosaurus* to represent the functional prototype for the more advanced ornithopods with the transverse grinding stroke. A recent analysis of the evidence for cranial kinesis in dinosaurs concluded that it was unlikely that anything more than very slight movements at sutural junctures would be possible (Holliday and Witmer 2009), the inference being that this would serve to dissipate mechanical stresses and strains rather than facilitate a transverse power stroke during feeding. Three dimensional animation modelling of the hadrosaurid *Edmontosaurus* (Rybczynski *et al.* 2008) also questioned the pleurokinesis model proposed by Norman and Weishampel, suggesting that extensive secondary

(intracranial) movements beyond the pleurokinetic hinge would be required. However, quantitative microwear analysis (an examination of the microscopic scratches on teeth generated during feeding) has shown evidence for a transverse power stroke in *Edmontosaurus* and provides strong evidence for the presence of a pleurokinetic hinge (Williams *et al.* 2009).

Dental microwear analysis

Dental microwear analysis is now widely used in palaeodietary reconstruction, with the interpretation of microwear patterns in fossil mammals based on comparison with modern animals/mammals with known diets. Whilst the presence of tooth wear facets can aid a reconstruction of jaw movements during feeding, their absence does not affect the ability to discern repetitive jaw motion from tooth microwear patterns. Evidence of dietary habit and the mastication process can be deduced from the microscopic scratches and pits on the surface of teeth (e.g., Walker *et al.* 1978; Teaford and Byrd 1989; Semprebon *et al.* 2004; Ungar *et al.* 2007) and the orientation of the scratches reflect the dominant direction of jaw movements (e.g., Butler 1952; Mills 1967; Teaford and Byrd 1989; Charles *et al.* 2007). That microwear analysis has a broad applicability beyond mammals has been shown by research on both fossil fishes (Purnell *et al.* 2006; Purnell *et al.* 2007) and dinosaurs (e.g., Fiorillo 1991, 1998; Upchurch and Barrett 2000; Williams *et al.* 2009).

Since no present-day reptile can chew (a typical cycle of jaw movement involves an opening stroke, a closing stroke and ingestion (e.g., Throckmorton 1976; King 1996)), no extant species has a sufficiently similar skull morphology to act as a convincing functional analogue for the more advanced ornithomimids. However, this is not the case for more primitive ornithomimids; the squamate *Iguana iguana* provides a suitable extant model for feeding in these early herbivores. It has an akinetic skull, lacks

cheek space and shares a similar jaw and tooth morphology with the basal anomodont *Suminia getmanovi* (Rybczynski and Reisz 2001), basal ornithischians such as *Lesothosaurus* and prosauropod dinosaurs (Norman and Weishampel 1985; Barrett 2000). The teeth of *I. iguana* preserve microwear (see Chapter 6) and those microwear patterns support the observed predominantly dorsoventral cropping action described by Throckmorton (1976) in *I. iguana*.

Here the dental microwear of *Lesothosaurus diagnosticus* and the squamate *Iguana iguana* is compared to test Thulborn's (1971b) and Weishampel's (1984) hypotheses of feeding in primitive ornithischians, and to test the hypothesis that *L. diagnosticus* had muscular cheeks.

Dentition and mastication

In labial view the teeth of both *L. diagnosticus* and *I. iguana* are diamond shaped, with denticles on the mesial (anterior) and distal (posterior) sides of the crown (Figure 1), whilst in dorsoventral view the teeth are labiolingually compressed and mesiodistally expanded to form a single narrow row. Tooth emplacement is *en echelon* such that the mesial edge of one tooth is labially overlapped by the distal edge of the next anterior tooth, producing an imbricate pattern when viewed dorsoventrally (Figure 2). Tooth positions in the upper and lower tooth rows are staggered.

Differences in dentition are minor; in *I. iguana* the teeth curve, with the tip of the crown pointing slightly distal and the tooth rows of both maxilla and dentary are marginal, whilst in *L. diagnosticus* the teeth are symmetrical in labial view and

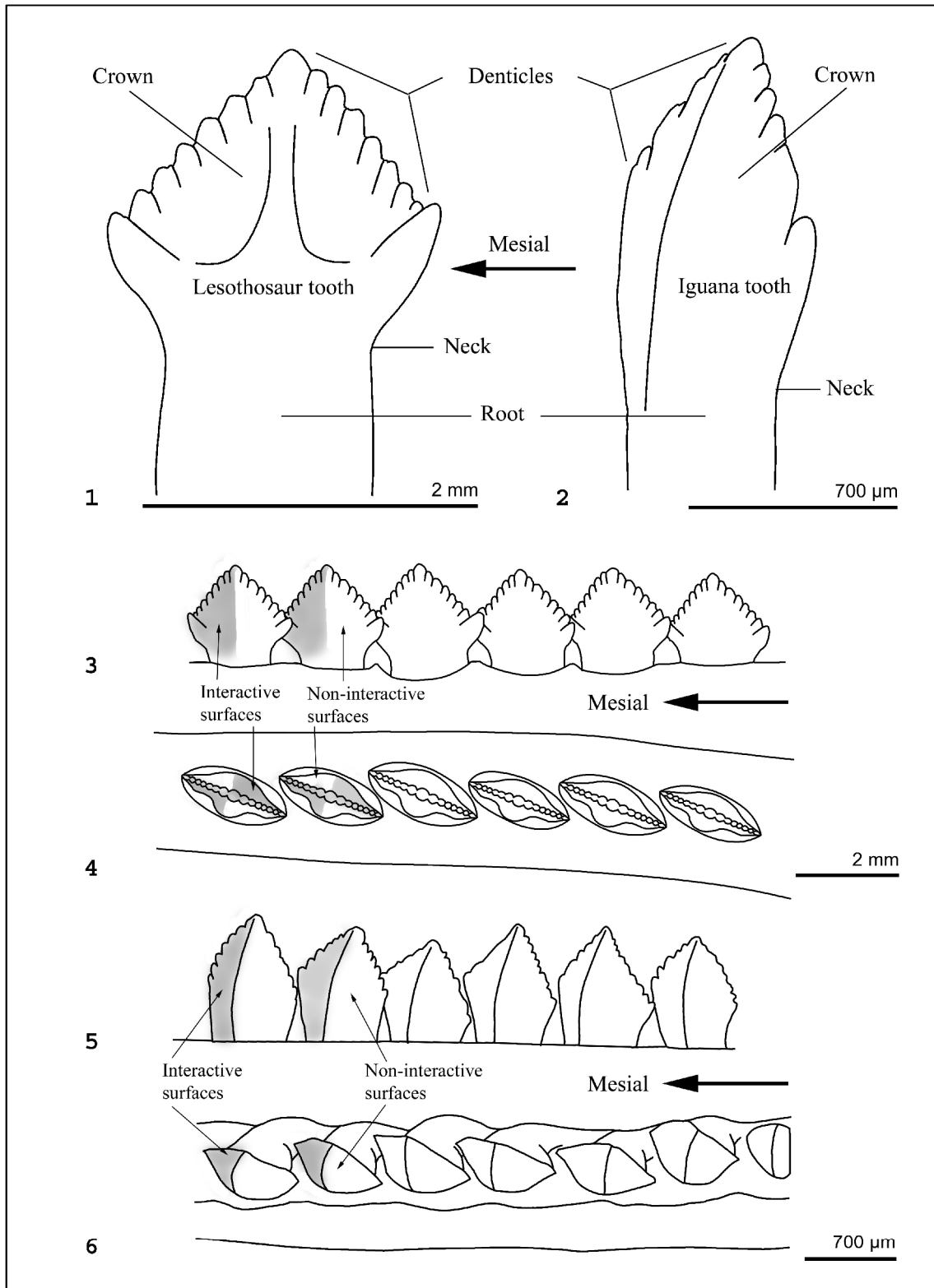


Figure 1. Left dentary cheek teeth of *Lesothosaurus diagnosticus* and *Iguana iguana* in labial view and apical view. 1.1 *L. diagnosticus*, mesial (anterior) is to the left. 1.2 *I. iguana*, mesial (anterior) is to the left. 1.3 *L. diagnosticus*, labial view showing each tooth in the row being overlapped by the distal edge of the next anterior tooth. 1.4 *L. diagnosticus*, apical view showing the *en echelon* emplacement of teeth within the jaw, mesial (anterior) is to the left, medial is up. 1.5 *I. iguana*, labial view showing each tooth in the row being overlapped by the distal edge of the next anterior tooth. 1.6 *I. iguana*, apical view showing the *en echelon* emplacement of teeth within the jaw, mesial (anterior) is to the left, medial is up. Interactive surfaces - where food is trapped between opposing teeth - is shown by shading. Note the teeth of *I. iguana* are less symmetrical, more curved (both in the medial and distal direction) and vary more in orientation along the tooth row than those of *L. diagnosticus*.

although the teeth of the maxilla and the anterior third of the dentary are marginal, those of the posterior two thirds of the dentary are inset, leaving some cheek space (i.e. a gap between the outer edge of the tooth row and the outer edge of the dentary where food could be held between tooth and cheek if the animal possessed cheeks).

During feeding the teeth of *Iguana iguana* shear past, but do not come into contact with each other (Throckmorton 1976) and this observation is supported by the lack of wear facets on the teeth, suggesting that oral processing relies on a tooth-food-tooth shearing action rather than tooth-tooth occlusion. With *Lesothosaurus diagnosticus* near vertical wear facets have been noted on the lingual side of maxillary teeth and the labial side of dentary teeth in some specimens (Norman *et al.* 2004) suggesting tooth-tooth occlusion, however wear facets are not present on all specimens (Galton 1978) and are absent on the specimen used in this study (Figure 2), suggesting a tooth-food-tooth shearing action. The teeth of *I. iguana* slice and shred vegetation rather than grind or chew it and material labial to the tooth row simply falls from the mouth as the jaws close, since there are no cheeks to retain it. In *Hypsilophodon foxii* well developed, flattened, wear facets exist on the occluding surfaces of the upper and lower cheek teeth between which food was ground. Muscular cheeks would have aided this grinding process by retaining food within the mouth. If *L. diagnosticus* lacked muscular cheeks and its jaw mechanics are comparable to those of *I. iguana*, then microwear pattern development should be similar in the two animals and different to that seen in *H. foxii*.

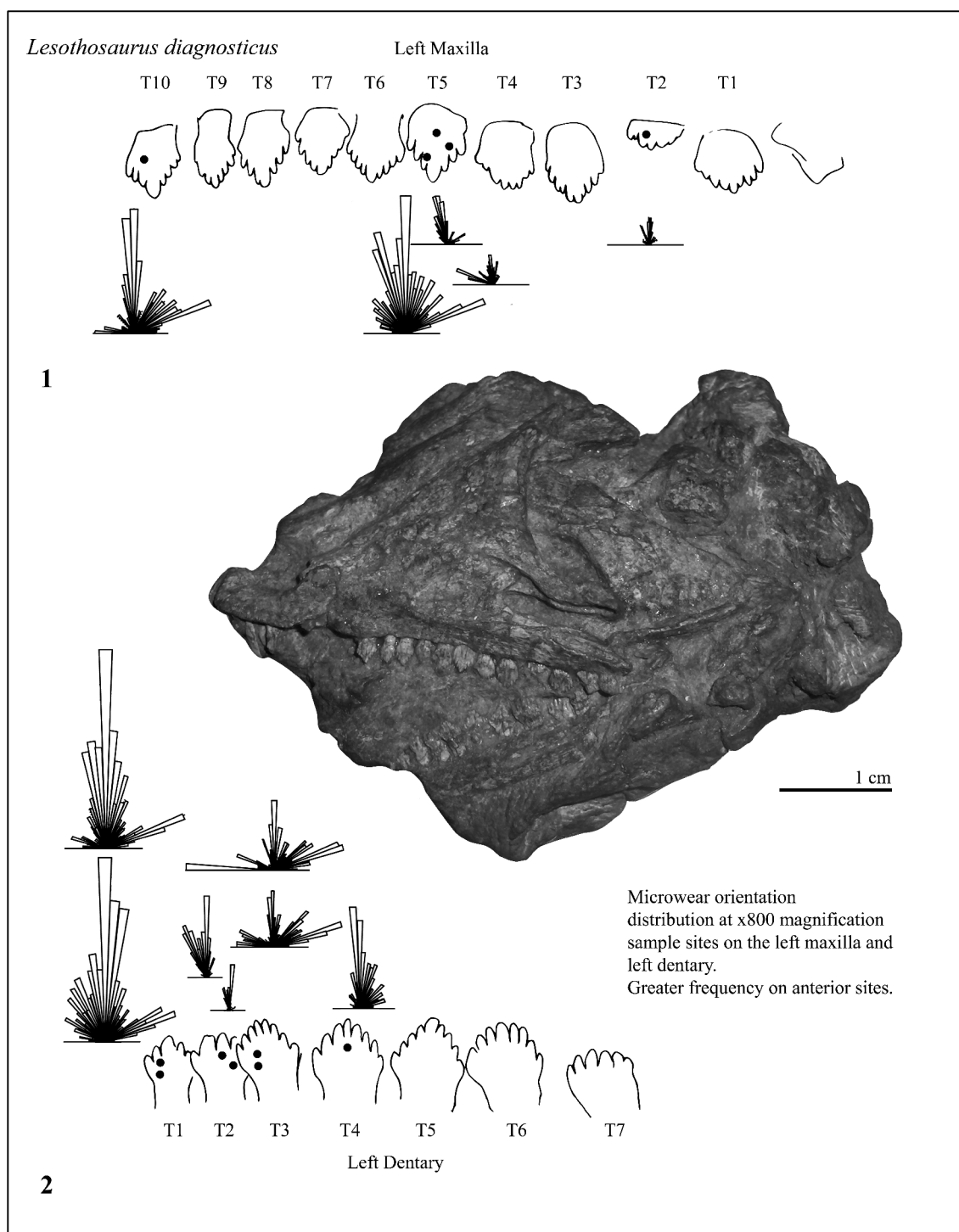


Figure 2. *Lesothosaurus diagnosticus* NHMUK R11956. Photograph - labial view of specimen; note the lack of wear facets. Sketch outlines - labial view of left maxillary and left dentary teeth with x800 magnification sample sites marked (black circles) and rose diagrams of microwear scratch orientations; frequency shown by the radius of the wedge, bin size 4°, scale relative to left dentary T4 (max N = 50). 2.1 Left maxilla. 2.2 Left dentary. Frequency greater on the interactive (mesial) tooth faces. NHMUK - The Natural History Museum, London.

Predicted microwear patterns

In *Iguana iguana*, microwear is concentrated on the active shearing surfaces (the lingual surface and the mesial (anterior) facing portion of the labial surface of opposing teeth, between which food is sliced and shredded, see Figure 1) and much reduced on the marginal labial (non-interactive) surfaces. In *Hypsilophodon foxii*, whilst microwear is heavily concentrated on the flattened occlusal surfaces (labial on the dentary and lingual on the maxillary teeth) it is also well developed on the off-occlusal labial surfaces of both dentary and maxillary teeth (which are comparable to the marginal labial surface of *I. iguana* teeth) where food held between muscular cheeks and teeth has abraded the teeth.

Simple vertical adduction, with bilateral occlusion of the style described by Throckmorton (1976) in *I. iguana* and predicted by Thulborn (1971b) and Weishampel (1984) for primitive ornithischians like *Lesothosaurus diagnosticus* should produce dominant scratch orientations near 90° to the tooth row long axis. Minor more oblique scratch orientations are also likely as although the tooth denticles should act to hold food in place whilst it is sheared, a shearing scissor action jaw would still be expected to produce some, albeit micron scale, anterior movement. This is because as a scissor action jaw closes, the point of shearing has to move forward. As successive teeth come together or shear past each other, they apply a force to any food in the mouth and because the upper and lower tooth rows are not parallel (they converge at the hinge) that force will act to push food forward. The scissor action will also cause compressive forces to change along the tooth row (highest at the hinge) and occlusion may be better constrained closer to the hinge. For both of these reasons it is a distinct possibility that microwear patterns will vary systematically with distance from the jaw hinge, although the effects will be limited in animals with short jaws. Bilateral occlusion should

produce comparable microwear orientations between left and right jaw elements however orientation can also change if one jaw rotates relative to the other. The observed vigorous whole head movement (Throckmorton 1976) of *I. iguana*, used to tear plant material from the host plant when the shearing action of jaw closure does not completely detach the food, might be expected to produce more variable oblique scratch orientations and a similar feeding technique may have been employed by *L. diagnosticus*. The lack of muscular cheeks should restrict microwear generated by regular contact with food items on the labial tooth surfaces whereas the presence of muscular cheeks should concentrate microwear on these same surfaces and introduce more random orientations as food is moved around between cheeks and teeth.

By comparing the microwear patterns on the corresponding non-interactive or off-occlusal labial tooth faces reconstruction of the movement of the upper teeth in cheek space should be possible. My aim is to establish if tooth microwear is preserved on these tooth surfaces in *L. diagnosticus*, and to determine if that microwear exhibits a relationship with jaw mechanics and feeding. Here I test the null hypotheses that microwear does not have a uniform distribution (i.e. that it shows a preferred orientation), that microwear does not differ between teeth within a jaw element, that microwear does not differ between teeth of different jaw elements, within an individual, that microwear does not differ between *L. diagnosticus* and *I. iguana*, and that microwear does not differ between *L. diagnosticus* and *Hypsilophodon foxii*.

ABBREVIATIONS

Institutional – **NHMUK**, The Natural History Museum, London; **MIWG**, Dinosaur Isle Museum, Isle of Wight.

METHODS

Dentary and maxillary teeth from *Lesothosaurus diagnosticus* NHMUK R11956 (Jurassic, Lesotho, Southern Africa), a Recent, preserved, wild caught specimen of *Iguana iguana* (S. T. Turvey, private collection, held at Zoological Society London), and *H. foxii* specimens MIWG 6362 and 6273 (Lower Cretaceous, Isle of Wight) were examined using a Scanning Electron Microscope (Hitachi S-3600N SEM). Prior to imaging *L. diagnosticus* NHMUK R11956 was cleaned, to remove consolidant, by the Palaeontology Conservation Unit of the Natural History Museum, London, and was imaged uncoated. The teeth of *I. iguana* were repeatedly washed with deionised water, dried and imaged both uncoated and after sputter coating with gold. The teeth of *H. foxii* specimens MIWG 6362 and 6273 were cleaned with solvent gel (see Chapter 2) and imaged uncoated. The specimens were inserted into the SEM chamber and oriented with the long axis of the tooth row as a reference frame and then rotated about the long axis of the tooth such that the surface being imaged was perpendicular to the electron beam. Exploratory photomicrographs were taken at magnifications of x300, x800 and x1000, providing fields of view of 417 x 312 μm , 156 x 116 μm and 125 x 85 μm respectively, comparable with that commonly used in analysis of occlusal microwear in mammals (Grine *et al.* 2002; Scott *et al.* 2005). In mammals, microwear patterns develop on wear facets and at specific points that relate to the places where teeth are abraded by food or occlusion with other teeth (Teaford 1988b) making sampling strategies relatively simple to formulate. In dinosaurs, there have been too few microwear studies to establish which sites should be used for microwear acquisition or at what magnification. A study of hadrosaur teeth (Williams *et al.* 2009) found microwear to occur consistently across the whole occlusal surface of teeth, and sauropod studies (Fiorillo 1991, 1998) found the length, width and frequency of

microwear features to be consistent within the occlusal surface. It is my experience that a similar situation occurs with iguana teeth. Due to the absence of wear facets on the teeth of *Lesothosaurus diagnosticus* and the nature of the specimen, potential sample sites were sufficiently limited in availability and extent (only the labial faces were available for imaging and exposed enamel was patchy) that the only practical option in terms of a sampling strategy was to image all available microwear. For comparative purposes, to test for the presence or absence of muscular cheeks in *L. diagnosticus*, sample sites on the labial (non-interactive) surface of *Iguana iguana* teeth were chosen such that they matched the same physical position as the sample sites on the non-interactive (posterior) portion of *L. diagnosticus* teeth. A magnification of x800 for *L. diagnosticus* was chosen to represent the best compromise between surface area covered, clarity of dental microwear and the size of available enamel areas containing microwear, and was chosen for the analyses of variance in *L. diagnosticus*, however some sample sites were also imaged at x1000 magnification for direct comparison with *I. iguana* as a magnification of x1000 appeared to produce more reliable results for the non-interactive portion of the labial surfaces of *I. iguana* teeth (where microwear occurrence is reduced relative to the active surfaces, see Figure 1). To facilitate a general comparison of labial microwear patterns to test for the presence or absence of muscular cheeks, labial sample sites that were off the occlusal surface and in the centre of the tooth face were chosen for *Hypsilophodon foxii* and imaged at x800 magnification.

For uncoated specimens the SEM was operated in a partial vacuum (20Pa) using the environmental secondary electron detector (ESED); SEM settings were standardized at: accelerating voltage, 10kV; working distance, 23 mm; and automatic contrast and brightness. For coated specimens the SEM was operated in full vacuum using the

secondary electron detector (SE); SEM settings were standardized at: accelerating voltage, 15kV; working distance 20 mm; and automatic contrast and brightness.

Standardisation is important for comparability of datasets (Gordon 1988).

All 21 teeth present on the left maxilla and dentary of *Lesothosaurus diagnosticus* were examined. Damaged teeth (those with unusually large gouges, cracks or pieces broken off that were suspected to be the result of post-mortem activity) were excluded. A total of 4628 microwear features were captured and analysed from 16 sites on seven teeth (11 sites from the lower dentition and five from the upper dentition). Of the 16 sites, data for four (1055 features) were captured from x1000 magnification images and data for 12 (3573 features) from x800 magnification images (consisting of 7 sites (2852 features) from interactive tooth surfaces and 5 sites (721 features) from non-interactive tooth surfaces). For comparative purposes a further 902 microwear features were captured from four sites on three *Iguana iguana* teeth, all from x1000 magnification images, and 1707 microwear features were captured from two sites on two *Hypsilophodon foxii* teeth, both from x800 magnification images. The digital SEM photomicrographs were downsampled to 900 pixels wide by 675 pixels high using Adobe Photoshop 7. As pits (features of roughly equal length and width) were rare to absent and this study is concerned particularly with relative jaw motion, and therefore microwear orientation, only scratches (elongate features) were considered. All microwear scratches within each photomicrograph were measured and recorded using the custom software package Microware 4.02 (Ungar 2001), which produced overlay files of x, y co-ordinates that were processed in a database using simple trigonometric functions to calculate the length, width and long axis orientation of each feature/scratch. Where the number of scratches per image exceeded 1000, more than one overlay file was used to cover the entire image (Microware 4.02 has a limitation of 1000 features

per overlay file). The grid lines option in Microware 4.02 was used to ensure the same feature was not measured twice. Scratch orientation data were suitably transformed for comparison to the labial face of the left dentary teeth; e.g. when looking at the labial face of a left dentary tooth, mesial will be to the left but on a right dentary tooth mesial will be to the right, in order to compare microwear patterns one set of data will need to be transformed – to achieve the equivalent of flipping the photomicrograph image horizontally before measuring the scratches. Measurement and recording took place on a Dell Latitude D505 computer running Windows XP Professional (Microsoft), with a 15-inch active matrix TFT display set at a screen resolution of 1024 x 768 pixels, resulting in an onscreen magnification of approximately x630 for SEM photomicrographs taken at x300, x1670 onscreen for those taken at x800 and x2080 onscreen for those taken at x1000.

Analyses of variance (ANOVA) for linear data and mean of mean angle confidence interval (CI) tests for circular data were conducted on scratch count (N), orientation, angular dispersion (i.e. the degree of parallelism as measured by R), length and width to determine if significant differences occur between teeth within a jaw element and between teeth of different jaw elements. Correlations between microwear variables and distance from jaw hinge were also performed. Scratch length data were not normally distributed (Shapiro-Wilk W; $P < 0.01$) and were therefore log-transformed before statistical analysis. Statistical analyses were carried out using the dedicated software packages Oriana 3.31 (Kovach Computing Services) for orientation data and JMP 8.0.2 (SAS Institute Inc) for both linear data and the discriminant function analyses (DFA) of orientation data.

RESULTS

Lesothosaurus diagnosticus

Of the 21 *Lesothosaurus diagnosticus* teeth examined, four were damaged, one was partially erupted but not yet emergent and five had no microwear at all. Of the 11 remaining teeth, seven, including a part erupted tooth, contained small patches of exposed enamel with sufficient microwear to fill the SEM field of view at x800 magnification. No single tooth had full coverage of exposed enamel or sufficient available sites to allow a within-tooth analysis of microwear. Visual inspection of photomicrographs revealed that *L. diagnosticus* teeth do preserve microwear, and that scratches dominate (Figure 3). Pits were rare, only 31 were recorded from five sites on three teeth and were therefore excluded from the analyses. Dentary and maxillary teeth show dominant near vertical and minor low angle oblique microwear patterns at all sample sites. Scratch length is highly variable as the extent of individual scratches was difficult to determine due to cross scratching (oblique scratches cutting across and overprinting other scratches). All scratches had widths of less than 2.6 microns and the majority (81%) were 1 micron or less in width. There is no correlation between scratch length and width (linear-linear correlation; $r < 0.1$, $P > 0.05$). Some scratches, approximately 3%, exhibit a curvature within the field of view. Microwear measurement software is not designed to cope with curved scratches. The only way to deal with these features is to score a continuous scratch as two or more scratches with changing orientation. This is not ideal, but the small number of scratches involved will have little impact on the dataset as a whole.

Scratches are not random in orientation, appearing to fall into a small number of classes within which scratches are predominantly straight and subparallel, but with an

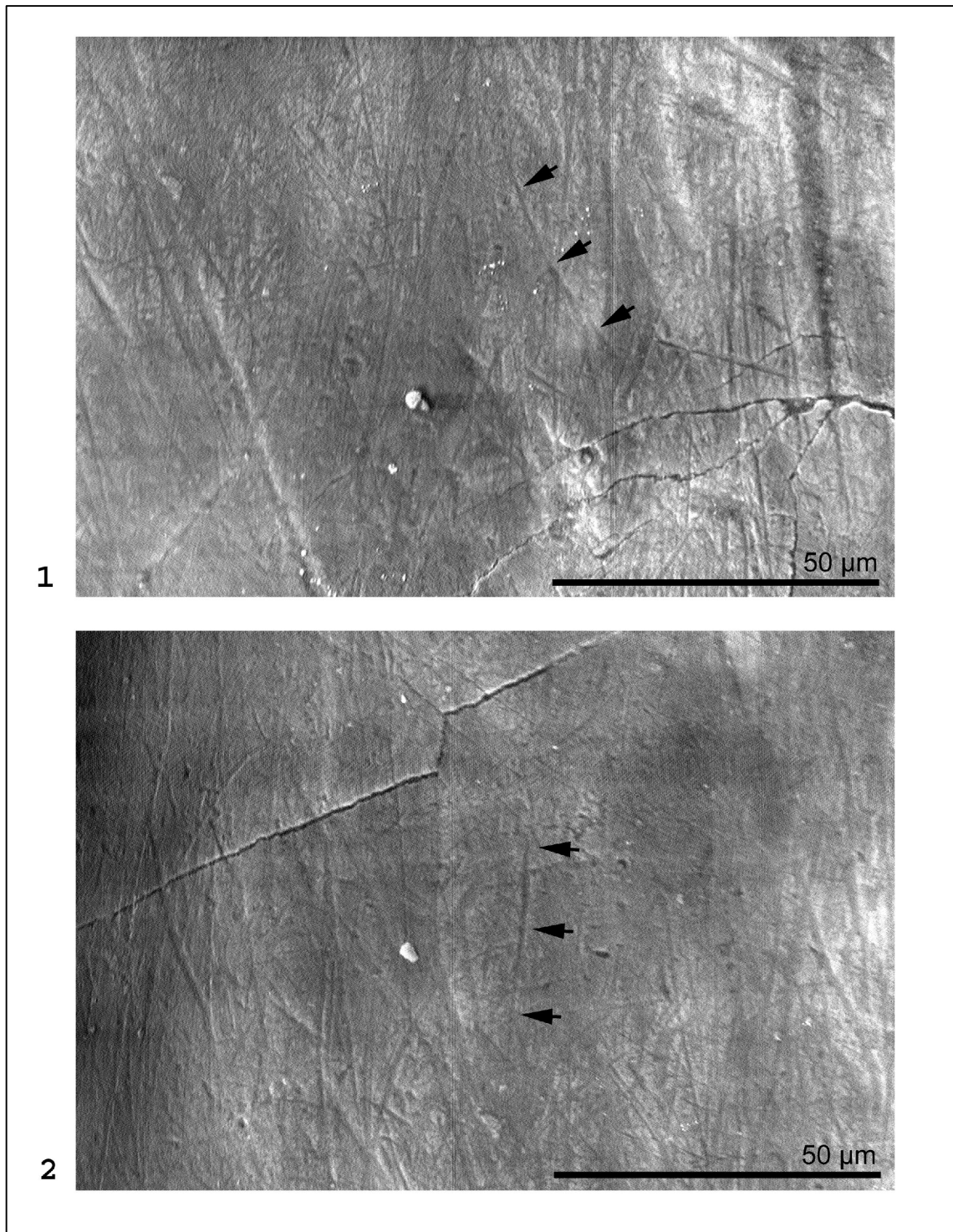


Figure 3. Labial surface of *Lesothosaurus diagnosticus* NHMUK R11956 left dentary tooth 1, showing microwear distribution at two vertically adjacent sample sites. Both sites, which are slightly mesial of the tooth centre, show a combination of coarse and fine microwear scratches, heavily overprinted, in various orientations but with a dominant near vertical mode. 4.1 Arrows highlight the curved nature of some of the scratches. 4.2 Arrows highlight the symmetrical nature (broadening in the middle and tapering at each end) of some of the near vertical scratches. Mesial is to the left and crownward is up. SEM ESED mode images (see Methods).

orientation that differs from that of other classes. To test the hypothesis that discrete classes of scratches exist, raw microwear data (4628 scratches from 16 sites on seven teeth) were partitioned into three subsets (classes 1-3), one major dominant near vertical class and two minor low angle oblique classes, based on visual assessment of scratch orientation via detailed rose diagrams (Figure 4). Discriminant function analysis provides strong confirmation that the microwear data falls into three distinct classes – 98.4% of scratches classified by visual inspection were correctly assigned by DFA.

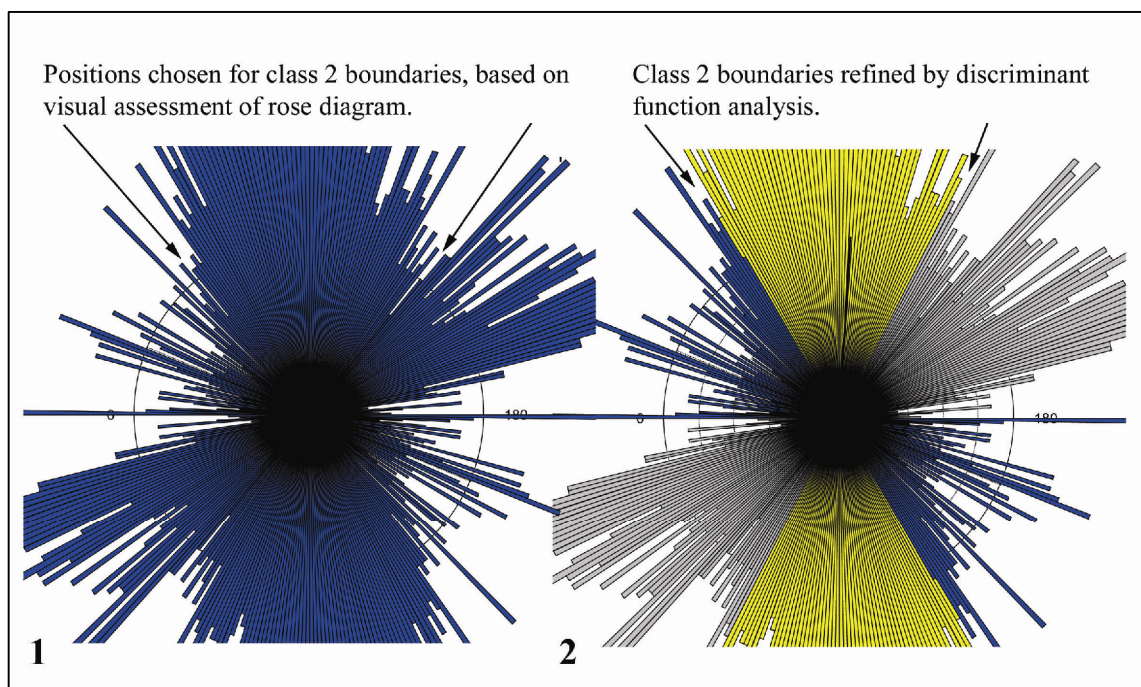


Figure 4. Detailed rose diagram used to identify class boundaries; frequency shown as radius of the wedge, 1° bins, scale N = 15. 4.1 Potential class boundaries identified by gaps in the distribution. 4.2 Refined boundaries established by discriminant function analysis (DFA) with incorrectly assigned scratches (< 2%) re-assigned.

When the data was separated by magnification (3573 scratches at x800 and 1055 scratches at x1000) and DFA was performed using scratch orientation, length and width as covariates, no scratches assigned a class by scratch orientation alone were identified as misclassified from the x800 data and only 0.47% were identified as misclassified from the x1000 data, further supporting the existence of three distinct classes. Rather than conduct subsequent statistical testing on these imperfectly classified data, the DFA

results were used to reassign the incorrectly assigned scratches to their correct class (leading to 100% correct discrimination; see Tables 1 and 2 for summary); all three classes were not present on all sites.

Table 1. *Lesothosaurus diagnosticus* - summary statistics from unclassified microwear data (12 sites on 7 teeth imaged at x800 magnification) and data partitioned into three classes based on scratch orientation.

Subgroup	Unclassified	Class 1	Class 2	Class 3
No. Of observations	3573	654	1875	1044
Angular dispersion, R	0.292	0.815	0.894	0.849
Mean orientation (mean vector, μ)	96°	29.82°	87.89°	147.71°
95% confidence interval for μ	$\pm 2.22^\circ$	$\pm 1.39^\circ$	$\pm 0.61^\circ$	$\pm 0.99^\circ$
99% confidence interval for μ	$\pm 2.92^\circ$	$\pm 1.83^\circ$	$\pm 0.80^\circ$	$\pm 1.30^\circ$
Mean scratch length, μm	16.17	13.97	17.39	15.55
Mean log scratch length, μm	2.78	2.64	2.86	2.74
Mean scratch width, μm	0.28	0.29	0.28	0.28

Table 2. *Lesothosaurus diagnosticus* - summary statistics from unclassified microwear Data (4 sites on 2 teeth imaged at x1000 magnification) and data partitioned into three classes based on scratch orientation.

Subgroup	Unclassified	Class 1	Class 2	Class 3
No. Of observations	1055	128	692	235
Angular dispersion, R	0.512	0.89	0.904	0.885
Mean orientation (mean vector, μ)	89°	45.19°	85.52°	146.13°
95% confidence interval for μ	$\pm 2.21^\circ$	$\pm 2.39^\circ$	$\pm 0.95^\circ$	$\pm 1.81^\circ$
99% confidence interval for μ	$\pm 2.91^\circ$	$\pm 3.14^\circ$	$\pm 1.25^\circ$	$\pm 2.37^\circ$
Mean scratch length, μm	12.97	11.00	13.84	11.48
Mean log scratch length, μm	2.56	2.40	2.63	2.44
Mean scratch width, μm	0.17	0.15	0.16	0.19

Figure 5.1 shows rose diagrams of the three classes produced from the combined x800 and x1000 datasets, with their mean orientations and 99% confidence intervals.

Frequency (scratch count (N) in 4° bins) is shown by the area of the wedge and by the radius of the wedge. Both types of rose diagram are shown as a dominant mode tends to obscure minor modes when radius of the wedge is used, and the dominance of a mode is understated when area of the wedge is used. When the two datasets (x800 and x1000) are separated and rose diagrams produced from each are compared (Figure 5.2 and 5.3), the distributions are largely consistent with the exception of a significant difference in

the class 1 mean orientation. Analysis of these datasets revealed significant differences ($P < 0.05$) in N and length between classes (Table 3).

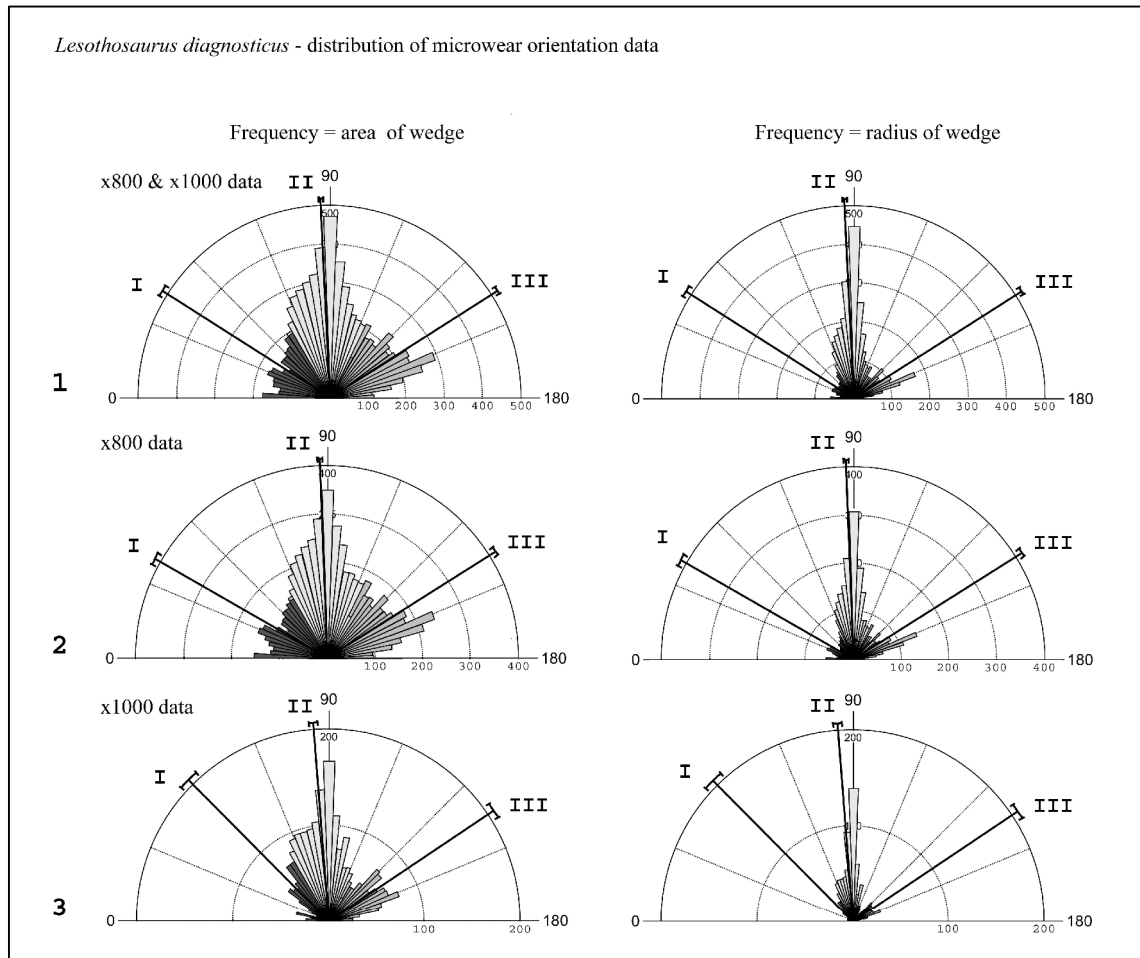


Figure 5. Rose diagrams of microwear scratch orientations partitioned into 3 orientation classes (I, II & III). Black lines running from the centre of the rose diagram to the outer edge, with arcs extending to either side show the mean orientation and 99% confidence interval for each class. Inner circles measure $N = 100$, compiled with 4° bins, frequency shown as area of the wedge (left) and radius of the wedge (right). 5.1 Combined dataset (4628 features from 16 sites on 7 teeth from x800 and x1000 magnification images). 5.2 x800 dataset (3573 features from 12 sites on 7 from x800 magnification images). 5.3 x1000 dataset (1055 features from 4 sites on 2 teeth from x1000 magnification images).

Pairwise comparisons (Tukey-Kramer honestly significant difference (HSD)) indicate that the three classes differ significantly from each other in all cases except for classes 1 and 3 for N and length. I was unable to reject the null hypothesis that angular dispersal (i.e. the degree of parallelism of scratches as measured by R, mean vector length) and width does not vary between classes. Summary statistics for each site are given in Table S1, and for each site by class in Tables S2, S3 and S4.

Analysis of the unclassified data reveals that overall, the hypothesis that data for each site are uniformly distributed can be rejected (i.e. they show a preferred orientation; Rayleigh uniformity test and Rao spacing test, $P < 0.05$; Table S1). Mean orientation for each site does not differ significantly from the pooled mean (V test expected mean 93.62° , $P < 0.05$; Table S1). Analysis of the three subsets of data (classes 1-3) provides confirmation of this result and the hypothesis that data within classes for each site are uniformly distributed can be rejected (i.e., they show a preferred orientation; Rayleigh uniformity test and Rao spacing test, $P < 0.05$; Tables S2, S3 and S4). Mean orientation for each class for each site does not differ significantly from the overall class mean (all sites, all teeth; V test expected means class 1 = 29.82° , class 2 = 87.89° , class 3 = 147.71° , $P < 0.05$; Table S2, S3 and S4). Of the 46 samples tested (3 classes, 16 sites, 2 sites with $n \leq 1$), there was only 1 exception to this result; 1 class 3 sample site failed the Rayleigh uniformity test, however the number of scratches assigned to this site was only 2.

The near vertical class 2 data exhibit a consistently high degree of parallelism (i.e. angular dispersion as measured by mean vector length (R), for pooled data $R = 0.89$ and by sample site $R > 0.88$; (Zar 1999)), and the V test shows the data to be non-uniformly distributed, with a significant mean orientation (V; expected mean = 87.89° ; $U = 64.2$; $P < 0.001$). The majority of the class 1 and 3 data exhibit a similarly high degree of parallelism (58% (18) of the sample sites have $R > 0.87$ and 97% (30) have $R > 0.8$; based on 31 of 32 class 1 and 3 sample sites which have an $N > 0$, see Tables S2, S3 and S4).

Subdividing a distribution of circular (orientation) data into classes will invariably lead to an increase in parallelism (R) within each class. Even with a random or uniform distribution, as the number of classes increase or the width of a specific class

decreases R will approach 1. To test the hypotheses that the distribution of scratches does not differ from a random distribution, results from the analysis of a random distribution of 4628 orientations partitioned into the three classes (1-3) were compared with those of the real data. The random unclassified data produced an R value of 0.02 signifying a uniform distribution. The random data partition by class (1-3) produced R values of 0.82, 0.83 and 0.81 respectively. The real data show a greater degree of parallelism than would be expected from a random distribution of data partitioned into the three orientation classes and therefore reflect preferred orientations. This analysis reveals that overall we can reject the hypothesis that the distribution of scratches does not differ from a random distribution.

Table 3. *Lesothosaurus diagnosticus* - results of null hypothesis testing for differences in microwear between classes.

	x800 d.f.	F	P	x1000 d.f.	F	P
Length does not differ between classes (one way ANOVA; log data)	2,3570	42.32	< 0.0001	2,1052	30.03	< 0.0001
Width does not differ between classes (one way ANOVA)	2,3570	1.07	0.341	2,1052	3.08	0.046
R does not differ between classes (one way ANOVA)	2,32	1.26	0.295	2,9	0.04	0.953
N does not differ between classes (one way ANOVA)	2,32	4.56	0.018	2,9	5.47	0.027

To test the null hypothesis that microwear does not differ between teeth within a jaw element in *Lesothosaurus diagnosticus*, subsets of data were generated for the left dentary and left maxilla from the x800 magnification dataset. Analysis of these jaw element datasets reveal that microwear orientation does not differ significantly between samples sites within a jaw element (Table 4). Mean of mean angles and their 99% confidence intervals (Zar 1999) were calculated for each dataset (for the unclassified microwear data, the dominant near vertical class 2 microwear and the more oblique class 1 and 3 microwear). Mean orientation for each site falls within the confidence

interval of the mean of mean angles calculated for its specific dataset (for the unclassified microwear data and when partitioned by class). There was only one exception to this result; one pooled data site from tooth 3 of the left dentary had an orientation that fell outside the confidence interval for its mean of means.

However, whilst the hypothesis that microwear orientation differs between teeth within a jaw element can be rejected, I cannot reject the hypothesis that microwear differs between teeth within a jaw element as significant differences ($P < 0.5$) in N (Table S5), and both scratch length and scratch width exist in each dataset (Table S6). N varies between the interactive and non-interactive portions of the tooth face, with a greater density on the interactive portion. Only one site from the interactive portion of a tooth had a scratch count (N) lower than that of a site from the non-interactive portion of a tooth, and this was from the partially erupted tooth 2 in the left maxilla.

With the exception of N, variation between sample sites is not systematic. Orientation does not vary significantly with distance from the jaw hinge and there is no correlation between distance from the jaw hinge and R, N, scratch length or width (circular-linear and linear-linear correlations, $P \gg 0.05$).

To test the null hypothesis that microwear does not differ between opposing jaw elements, the left dentary and left maxilla x800 magnification subsets of data were compared (for the unclassified microwear data and for each class 1-3), revealing significant differences in orientation (Watson-Williams F, $P < 0.05$; Table 5) in all cases with the single exception of the class 1 data. Significant differences in orientation between individual sites within the upper and lower dentition were also revealed (Table 6). Mean of mean angles and their 99% confidence intervals were calculated for the combined left dentary and left maxilla x800 magnification datasets (for the unclassified microwear data and for each class 1-3); a combined dataset was used since precise

Table 4. *Lesothosaurus diagnosticus* - analysis of variation in orientation between sites within the left dentary (7 sites from 4 teeth) and left maxilla (5 sites from 3 teeth). Mean of means (μ of μ) and confidence intervals calculated for the unclassified data and each orientation class (1-3) for each jaw element. Figures shown in bold fall outside the 99% confidence interval (differ significantly).

Left Dentary Tooth-Site	1-2	1-3	2-1	2-3	3-1	3-2	4-1
Unclassified angular dispersal, R	0.328	0.396	0.790	0.862	0.227	0.258	0.545
Mean vector, μ	89.489	97.284	79.647	87.529	148.767	147.251	102.350
Class 1 angular dispersal, R	0.845	0.829	0.939		0.892	0.873	0.854
Mean vector, μ	36.519	29.144	51.489		18.827	14.396	42.610
Class 2 angular dispersal, R	0.893	0.905	0.884	0.925	0.912	0.893	0.913
Mean vector, μ	89.035	89.604	81.359	86.600	90.912	90.053	92.885
Class 3 angular dispersal, R	0.866	0.848	0.933	0.999	0.858	0.856	0.849
Mean vector, μ	147.809	148.541	131.442	153.835	151.679	151.974	143.407
Unclassified mean of means 97.16, 99% confidence interval 75.79 – 147.46							
Class 1 mean of means 32.32, 99% confidence interval 3.95 – 66.66							
Class 2 mean of means 88.65, 99% confidence interval 80.67 – 96.35							
Class 3 mean of means 146.95, 99% confidence interval 129.91 – 163.39							

Left Maxilla Tooth-Site	2-1	5-1	5-2	5-4	10-1
Unclassified angular dispersal, R	0.592	0.340	0.543	0.477	0.277
Mean vector, μ	94.679	90.944	76.073	55.165	116.518
Class 1 angular dispersal, R	0.987	0.871	0.931	0.881	0.782
Mean vector, μ	33.832	35.070	46.245	28.003	22.644
Class 2 angular dispersal, R	0.900	0.880	0.906	0.918	0.932
Mean vector, μ	91.103	86.964	78.390	81.307	87.920
Class 3 angular dispersal, R	0.917	0.870	0.910	0.802	0.838
Mean vector, μ	136.165	143.869	154.264	125.870	146.489
Unclassified mean of means 83.85, 99% confidence interval 35.99 – 157.46					
Class 1 mean of means 33.54, 99% confidence interval 5.57 – 61.67					
Class 2 mean of means 85.12, 99% confidence interval 65.09 – 105.45					
Class 3 mean of means 141.61, 99% confidence interval 99.64 – 175.62					

Table 5. *Lesothosaurus diagnosticus* - results of null hypothesis testing for differences in Microwear orientation between opposing jaw elements. Pairwise comparisons, where data does not differ significantly (by one or more of unclassified data and classes 1 – 3), are listed. Significant differences ($P < 0.05$) are shown in bold.

Orientation does not differ between left dentary and left maxilla	df2	F	P	Mean μ
Unclassified	1,3571	15.620	< 0.001	96.00
Class 1	1,652	3.176	0.075	29.83
Class 2	1,1873	22.189	< 0.001	87.89
Class 3	1,1042	12.943	< 0.001	147.71
(Watson-Williams F)				

occlusion should produce the same microwear orientation on opposing tooth surfaces.

Of the 47 samples tested (unclassified data, three classes, 12 sites, one site in one class with N = 0), 11 mean orientations fall outside the calculated 99% confidence intervals –

three unclassified, two class 1, four class 2 and two class 3 – only two of which can be attributed to the low number of scratches ($n < 10$) assigned to the sample. Recalculating mean of mean angles and their 99% confidence intervals based on further partitioning of the data by restricting the data sets to one site per tooth, or to an upper or lower jaw element, does not significantly alter the above results. Whilst there are significant differences in microwear orientation between opposing jaw elements, 80% of the mean orientations fall within the 99% confidence intervals of the mean of means suggesting a high level of interaction between the teeth of opposing jaw elements.

Table 6. *Lesothosaurus diagnosticus* - analysis of variation in orientation between sites (12 sites from 7 teeth). Mean of means (μ of μ) and confidence intervals calculated for the unclassified data and each orientation class (1-3). Figures shown in bold fall outside the 99% confidence interval (differ significantly).

Left Dentary Tooth-Site	1-2	1-3	2-1	2-3	3-1	3-2	4-1
Unclassified angular dispersal, R	0.328	0.396	0.790	0.862	0.227	0.258	0.545
Mean vector, μ	89.489	97.284	79.647	87.529	148.767	147.251	102.350
Class 1 angular dispersal, R	0.845	0.829	0.939		0.892	0.873	0.854
Mean vector, μ	36.519	29.144	51.489		18.827	14.396	42.610
Class 2 angular dispersal, R	0.893	0.905	0.884	0.925	0.912	0.893	0.913
Mean vector, μ	89.035	89.604	81.359	86.600	90.912	90.053	92.885
Class 3 angular dispersal, R	0.866	0.848	0.933	0.999	0.858	0.856	0.849
Mean vector, μ	147.809	148.541	131.442	153.835	151.679	151.974	143.407

Left Maxilla Tooth-Site	2-1	5-1	5-2	5-4	10-1
Unclassified angular dispersal, R	0.592	0.340	0.543	0.477	0.277
Mean vector, μ	94.679	90.944	76.073	55.165	116.518
Class 1 angular dispersal, R	0.987	0.871	0.931	0.881	0.782
Mean vector, μ	33.832	35.070	46.245	28.003	22.644
Class 2 angular dispersal, R	0.900	0.880	0.906	0.918	0.932
Mean vector, μ	91.103	86.964	78.390	81.307	87.920
Class 3 angular dispersal, R	0.917	0.870	0.910	0.802	0.838
Mean vector, μ	136.165	143.869	154.264	125.870	146.489

Unclassified mean of means 91.85, 99% confidence interval 73.5 – 129.59

Class 1 mean of means 32.88, 99% confidence interval 17.78 – 47.08

Class 2 mean of means 87.18, 99% confidence interval 81.84 – 92.48

Class 3 mean of means 144.76, 99% confidence interval 133.86 – 155.06

Iguana iguana

Visual inspection of the photomicrographs revealed that *I. iguana* teeth do preserve microwear, and that scratches dominate (Figure 7). Pits were not observed. Dominant near vertical and minor sub horizontal microwear patterns were found at all sample sites. Scratch length is highly variable however the majority (93%) of the scratches had a length of 30 μm or less. All scratches had widths of less than 2 microns and the majority (98%) were less than 1 micron in width. There is no correlation between scratch length and width (linear-linear correlation; $r = 0.33$, $P > 0.05$). Some, approximately 4%, exhibit a curvature within the field of view. Continuous and near vertical scratches, up to 1.2 mm, were observed from crown to base on several teeth at lower magnification and these are not represented in the data analysed here due to a combination of the curvature of the scratches and the limitations of the field of view at x1000 magnification.

Scratches are not random in orientation, appearing to fall into a small number of classes, within which scratches are predominantly straight and subparallel, but with an orientation that differs from that of other classes. Previous research (see Chapter 6) on the teeth of this *I. iguana* (4,199 microwear scratches from 42 sites on 17 teeth; data captured from x300 magnification images), identified three discrete orientation classes based on an initial visual assessment of scratch orientation using detailed rose diagrams, and was supported by DFA. In this study, the microwear data (902 scratches from four sites on three teeth, captured from x1000 magnification images) were partitioned into three subsets (classes 1-3) based on the class boundaries from my previous research.

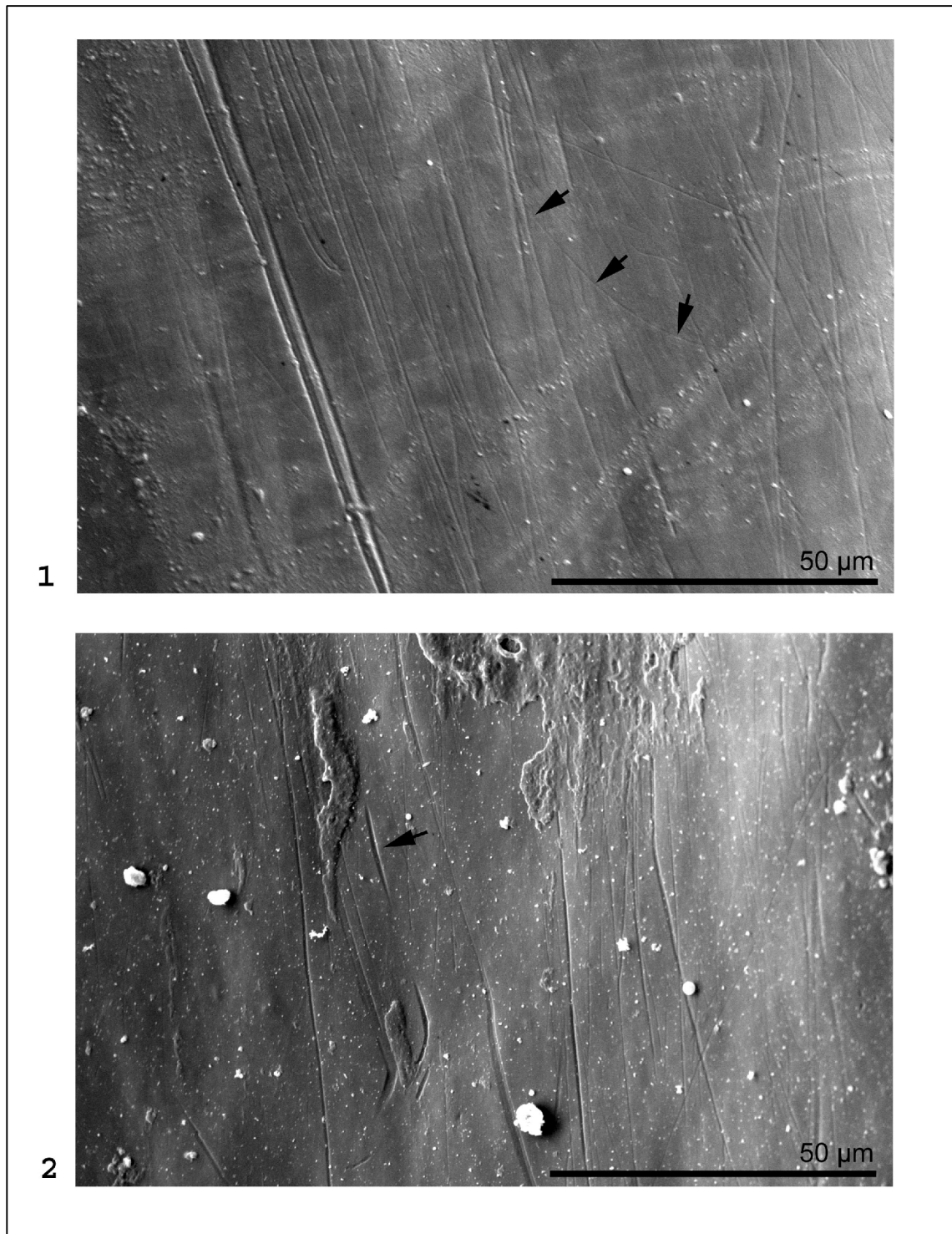


Figure 7. Labial surface of *Iguana iguana* right dentary tooth 6, showing microwear distribution at two sample sites. Both sites show a combination of coarse and fine microwear scratches in various orientations but with a dominant near vertical mode. 7.1 Sample site slightly crownward of centre; arrows highlight the curved nature of some of the scratches. 7.2 Sample site slightly below and mesial of centre; arrow highlights the symmetrical nature (broadening in the middle and tapering at each end) of some of the near vertical scratches. Mesial is to the left and crownward is up (*Images have been flipped horizontally for comparative purposes*). SEM SE mode images (see Methods)

Table 7. *Iguana iguana* - summary statistics from unclassified microwear data (4 sites on 3 teeth imaged at x1000 magnification) partitioned into three classes based on scratch orientation.

Subgroup	Unclassified	Class 1	Class 2	Class 3
No. Of observations	902	377	496	29
Angular dispersion, R	0.671	0.917	0.951	0.738
Mean orientation (mean vector, μ)	62.03°	37.51°	78.23°	140.55°
95% confidence interval for μ	$\pm 1.68^\circ$	$\pm 1.20^\circ$	$\pm 0.79^\circ$	$\pm 8.06^\circ$
99% confidence interval for μ	$\pm 2.21^\circ$	$\pm 1.58^\circ$	$\pm 1.05^\circ$	$\pm 10.59^\circ$
Mean scratch length, μm	12.97	9.71	15.77	7.44
Mean log scratch length, μm	2.56	2.27	2.76	2.01
Mean scratch width, μm	0.21	0.17	0.23	0.16

When DFA was performed on this x1000 magnification dataset using scratch orientation, length and width as covariates, only four (0.44%) of the scratches were identified as misclassified, supporting the existence of three distinct classes (see Table 7 for summary).

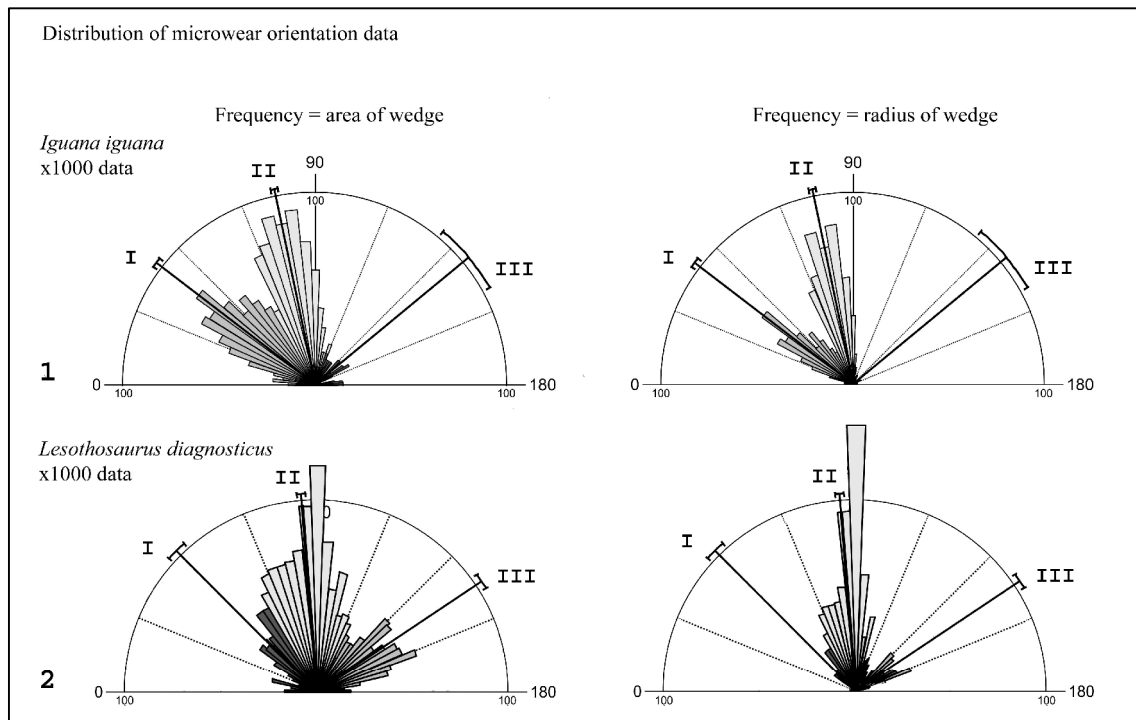


Figure 8. Rose diagrams of microwear scratch orientations captured from x1000 magnification images, comparing *Iguana iguana* and *Lesothosaurus diagnosticus*. Data partitioned into 3 orientation classes (I, II & III). Black lines running from the centre of the rose diagram to the outer edge, with arcs extending to either side show the mean orientation and 99% confidence interval for each class. Scale N=100, compiled with 4° bins, frequency shown as area of wedge (left) and radius of wedge (right). 8.1 *I. iguana* (902 features from 4 sites on 3 teeth). 8.2 *L. diagnosticus* (1055 features from 4 sites on 2 teeth).

Figure 8 compares the three orientation classes of *Iguana iguana* and *Lesothosaurus diagnosticus*, showing rose diagrams of the three classes produced from the x1000 magnification dataset, with their mean orientations and 99% confidence intervals. Two types of rose diagram are used (showing frequency by radius and by area of wedge) to better illustrate the minor modes. Analysis of this dataset revealed significant differences ($P < 0.05$) in N, angular dispersion (R), length and width between classes (Table 8). Pairwise comparisons (Tukey-Kramer honestly significant difference (HSD)) indicate that the class 2 microwear differs from classes 1 and 3 in all cases except for N and R with class 1 (see Table 8). Summary statistics for each site are given in Table S7.

Table 8. *Iguana iguana* - results of null hypothesis testing for differences in microwear between classes.

	d.f.	F	P
Length does not differ between classes (one way ANOVA; log data)	2,899	66.29	< 0.0001
Width does not differ between classes (one way ANOVA)	2,899	14.59	< 0.0001
R does not differ between classes (one way ANOVA)	2,9	20.99	< 0.0001
N does not differ between classes (one way ANOVA)	2,9	4.29	< 0.0001

Means comparisons Tukey-Kramer HSD (levels not connected by the same letter differ significantly)	Class 1	Class 2	Class 3
Length (log data): Means	2.1	2.5	1.8
levels	B	A	B
Width: Means	0.17	0.23	0.16
levels	B	A	B
R: Means	0.92	0.95	0.73
levels	A	A	B
N: Means	94	124	7
levels	A	A	B
	B		B

Analysis of the unclassified data reveals that overall, the hypothesis that data for each site are uniformly distributed can be rejected (i.e. they show a preferred orientation; Rayleigh uniformity test and Rao spacing test, $P < 0.05$; Table S7). Mean orientation for each site does not differ significantly from the pooled mean (V test expected mean 62.03° , $P < 0.05$). Analysis of the three subsets of data (classes 1-3) provides confirmation of this result and the hypothesis that data within classes for each site are uniformly distributed can be rejected (i.e., they show a preferred orientation; Rayleigh uniformity test and Rao spacing test, $P < 0.05$; Tables S2, S3 and S4). Mean orientation for each class for each site does not differ significantly from the overall class mean (all sites, all teeth; V test expected means class 1 = 37.51° , class 2 = 78.23° , class 3 = 140.55° , $P < 0.05$). Of the 12 samples tested (3 classes, 4 sites), there are only two exceptions to this result – two class 3. In both cases, the number of scratches assigned to the class that failed the tests was three or fewer.

The near vertical class 2 data exhibit a consistently high degree of parallelism (i.e. angular dispersion as measured by mean vector length (R), for pooled data $R = 0.95$ and by sample site $R > 0.92$; (Zar 1999)), and the V test shows the data to be non-uniformly distributed, with a significant mean orientation (V; expected mean = 78.23° ; $U = 29.95$; $P < 0.001$). The class 3 sample sites exhibit a similarly high degree of parallelism, all have $R > 0.9$. The class 1 sample sites are less well constrained with $0.81 < R < 0.63$ however N is 16 or less in all cases (Table S7). The degree of parallelism shown by the class 1 and class 3 data is comparable to that of my previous research on the teeth of this *Iguana iguana* specimen (see Chapter 6) where it was established that the R values were higher than could be obtained from a random distribution of orientation data.

My previous research on the teeth of this *Iguana iguana* specimen (see Chapter 6), also established that microwear differed significantly between teeth of the same jaw element. The variation between teeth is not systematic; orientation does not vary significantly with distance from the jaw hinge and there is no correlation between distance from the jaw hinge and R, N, scratch length or width (circular-linear and linear-linear correlations, $P \gg 0.05$). In this study significant differences ($P < 0.05$) in both scratch length and width exist between samples sites (Table S8).

To determine if the same three orientation classes exist in both *Iguana iguana* and *Lesothosaurus diagnosticus* mean of mean angles and their 99% confidence intervals were calculated for each class (1-3) for the combined left dentary and right dentary x1000 magnification datasets of *I. iguana* (902 scratches from four sites on three teeth) and *L. diagnosticus* (1055 scratches from four sites on two teeth). Of the 24 samples tested (three classes, eight sites), no mean orientations fall outside the calculated 99% confidence intervals (Table S9). Therefore the hypothesis that microwear orientation differs between *I. iguana* and *L. diagnosticus* by class can be rejected.

Tests for variation in scratch length, width and angular dispersion (R) between *I. iguana* and *L. diagnosticus* by class do however show significant differences (one-way ANOVA - log data for length; $P < 0.05$) in all cases with the exception of class 1 and class 2 data for length and class 1 data for R. It is a comparison of scratch count (N) that is of importance here however, on these non-interactive tooth surfaces where microwear is generated by tooth-food or tooth-food-cheek action only. Whilst the differences are statistically significant, N from multiple equal area sample sites, is very similar between *I. iguana* teeth and *L. diagnosticus* teeth, in the unclassified data and by class (1-3), (see Tables S1 to S4 and Table S7).

Hypsilophodon foxii

Visual inspection of the photomicrographs revealed that *H. foxii* teeth do preserve microwear on their off-occlusal labial faces, and that scratches dominate (Figure 9). Pits were observed but were not measured for this study. Two dominant (one near vertical and one oblique) along with two minor low angle oblique microwear patterns were found at both sample sites. Scratch length varies up to 90 μm however the majority (92%) of the scratches had a length of 30 μm or less. All scratches had widths of less than 2 microns and the majority (97%) were less than 1 micron in width. There is no correlation between scratch length and width (linear-linear correlation; $r = 0.1$, $P > 0.05$). Some scratches, approximately 3%, exhibit a curvature within the field of view.

The scratches are not random in orientation (Rayleigh uniformity test and Rao spacing test, $P < 0.05$; Table S10) and appear to fall into a small number of classes, within which scratches are predominantly straight and subparallel, but attempts to assign orientation classes based on visual assessment of detailed rose diagrams were not supported by DFA. Since this study is concerned with a comparison of feature density between the off-occlusal tooth surfaces of *H. foxii* and the non-interactive tooth surfaces of *Lesothosaurus diagnosticus*, additional sampling of *H. foxii* to establish class boundaries from a larger dataset was not attempted.

Analysis of the unclassified data revealed a near vertical mean orientation of 81.91° with a poor degree of parallelism (i.e. angular dispersion as measured by mean vector length R ; $R = 0.33$; (Zar 1999)).

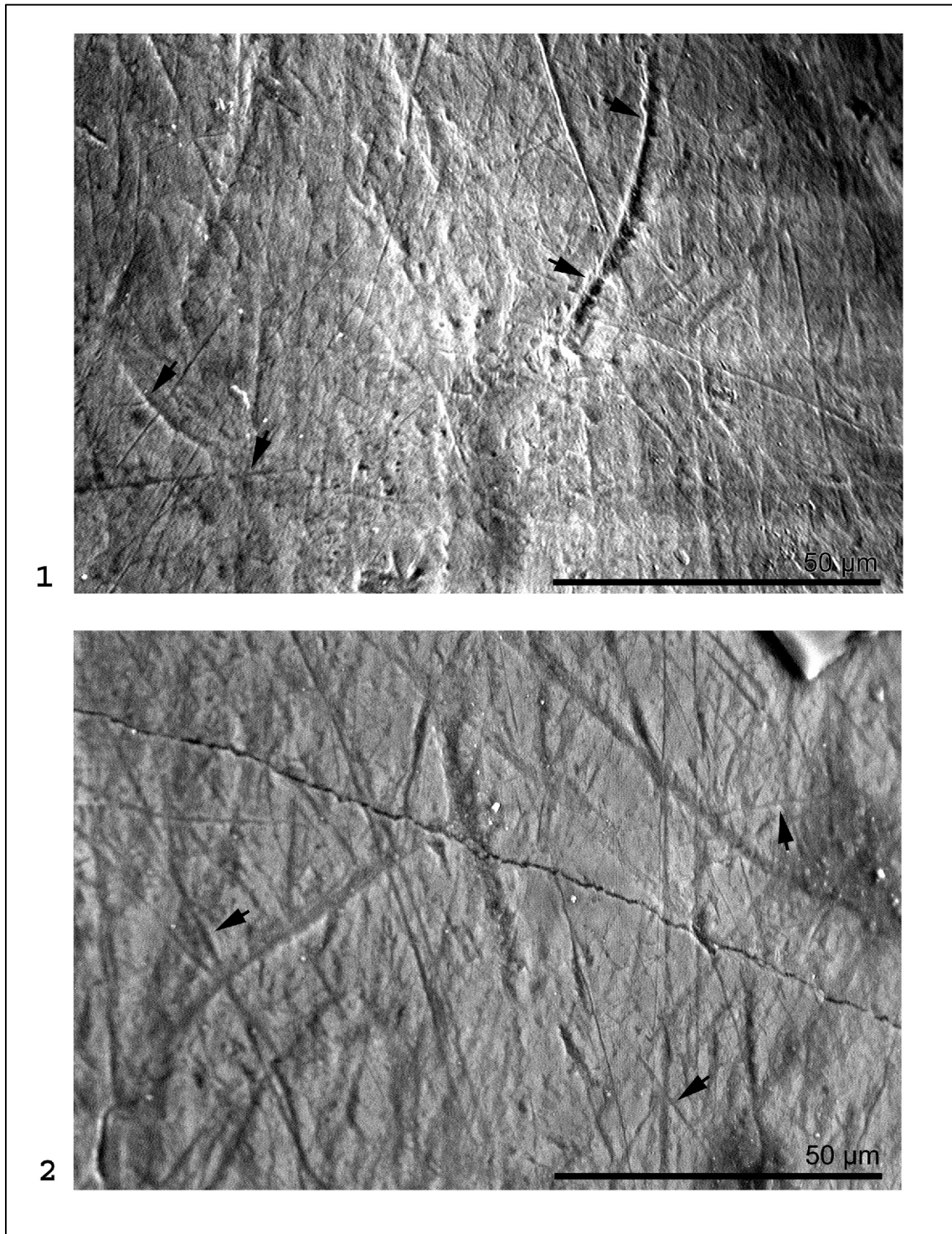


Figure 9. Off-occlusal labial surfaces of *H. foxii* MIWG 6362 cheek teeth, showing microwear distribution at two sample sites. Both sites show a combination of coarse and fine microwear scratches in various orientations with multiple modes. 9.1 Right maxilla tooth 2, sample site mesial and crownward; arrows highlight the curved nature of some of the scratches. 9.2 Left maxilla tooth 1, sample site central and crownward; arrows highlight the symmetrical nature (broadening in the middle and tapering at each end) of some of the near vertical scratches. Mesial is to the right and crownward is up (The right maxilla image has been flipped horizontally for comparative purposes). SEM ESED mode images (see Methods).

Figure 10 compares the microwear distribution of *Hypsilophodon foxii* and *Lesothosaurus diagnosticus*, showing rose diagrams of the scratch orientation produced from the off-occlusal or non-interactive tooth surfaces from the x800 magnification datasets. Scratch density is significantly higher in *H. foxii*.

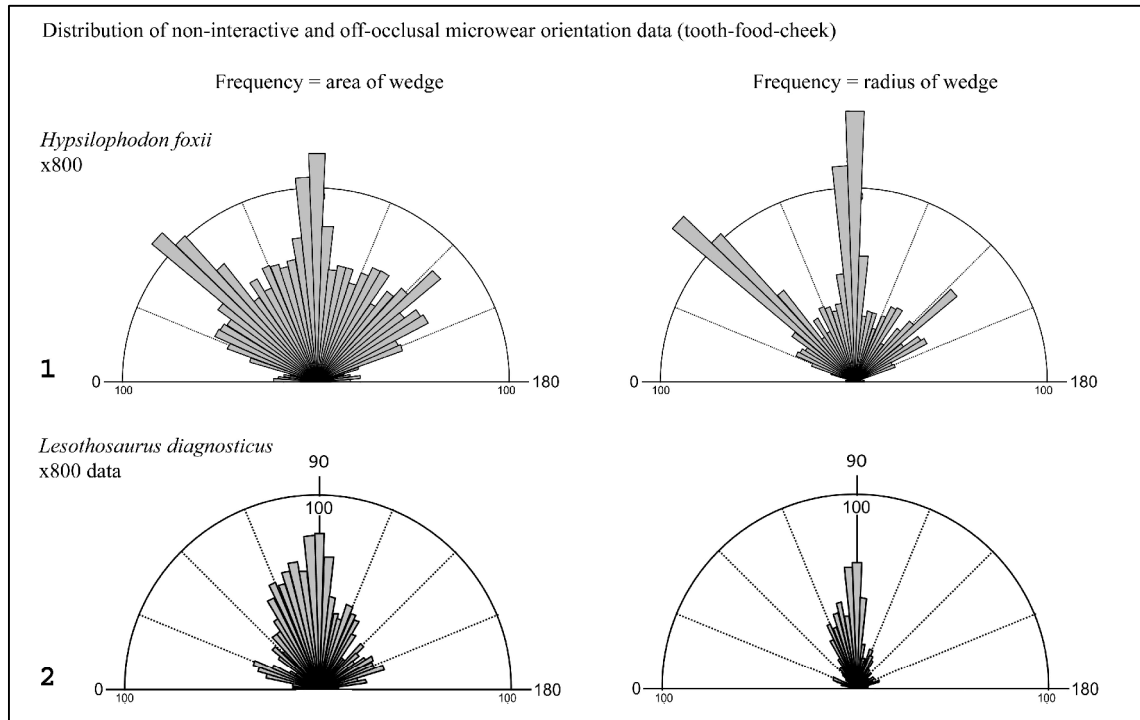


Figure 10. Rose diagrams of microwear scratch orientations comparing data captured from x800 magnification images of the off-occlusal or non-interactive tooth surfaces from *Hypsilophodon foxii* (1707 features from 2 sites on 2 teeth) and *Lesothosaurus diagnosticus* (721 features from 5 sites on 3 teeth). Scale N = 100, compiled with 4° bins, frequency shown as area of the wedge (left) and radius of the wedge (right). 10.1 *Hypsilophodon foxii* data. 10.2 *Lesothosaurus diagnosticus* data.

SUMMARY AND DISCUSSION

The microwear data for *Lesothosaurus diagnosticus* identified a predominantly dorsoventral jaw action with a signal strong enough to dominate the tri-modal pooled data. The dominant mode (class 2) gave a mean orientation of 87.89° (0° being anterior, 180° posterior along the long axis of the jaw). This mean orientation calculated from the x800 magnification raw data (Table 1) is highly significant given the tight 95% confidence intervals (CI) of $\pm 0.61^\circ$ and supports the vertical or near vertical shearing motion predicted by Thulborn (1971b) and Weishampel (1984). Whilst curvature in the microwear was observed no significant horizontal microwear was found, suggesting that *L. diagnosticus* did not employ a propalinal jaw action during feeding.

Three discrete classes of microwear exist on the teeth of *L. diagnosticus* that are largely consistent with those found on the teeth of *Iguana iguana*. The two low angle oblique microwear patterns have mean orientations that are at similar inclinations (i.e. class 1: 29.82°, class 3: 147.71° or 32.29° from the horizontal) and share scratch width and length characteristics.

Whilst scratch length and width differ between the two animals, the jaw mechanics and feeding process of *L. diagnosticus* and *I. iguana*, which produced the microwear distributions, are sufficiently similar that the class mean orientations are comparable and the mean orientations from a combined dataset of *L. diagnosticus* and *I. iguana* sample sites (Table S9) do not differ significantly from each other. A significant non-systematic variation in microwear orientation between teeth within the same individual animal is evident in both *L. diagnosticus* and *I. iguana*. It is possible that these differences are related to the lack of contact between teeth during feeding. The teeth of *I. guana* do not come into contact with each other and this may have been the case with *Lesothosaurus diagnosticus* (or it may have merely had imprecise occlusion).

However this does not prevent tooth microwear data from being useful in inferring relative jaw motion in these animals.

In both *L. diagnosticus* and *Hypsilophodon foxii*, microwear is very heavily overprinted; scratches in differing orientations cut through and partly obscure pre-existing scratches (see Figure 4 and Figure 9). This overprinting does not occur in *Iguana iguana*. There are also similarities between the rose diagrams of microwear distribution (Figure 10). However, comparison of scratch density between the non-interactive tooth surfaces of *Iguana iguana* and *Lesothosaurus diagnosticus* (x1000 magnification data) revealed no significant difference in N, from equal area sample sites. In contrast a comparison of scratch density between the off-occlusal and non-interactive tooth surfaces of *H. foxii* and *L. diagnosticus* (x800 magnification data) revealed a significantly higher scratch density in *H. foxii*. In view of these results and observations I consider the microwear present on the teeth of *L. diagnosticus* is consistent with the predictions of Thulborn (1971b) and Weishampel (1984) for a primitive ornithischian that lacked muscular cheeks.

ACKNOWLEDGEMENTS

I am grateful to Paul Barrett & Sandra Chapman, Natural History Museum (London); Samuel Turvey, Zoological Society of London and Martin Munt & Lorna Steel, Dinosaur Isle Museum; for granting access to and permission to clean the dinosaur and iguana teeth. I thank Adrian Doyle and the Palaeontology Conservation Unit at the Natural History Museum (London) for advice regarding cleaning consolidant from fossil teeth. John Larkham of Coltène Whaledent is thanked for donating polyvinylsiloxane moulding compound.

Supporting information

Table S1. *Lesothosaurus diagnosticus* - microwear summary statistics, unclassified data

Element	Tooth	Site	Angular disp.		Rayleigh	p	Rao		Rayleigh (expected mean 93.62°)			Orientation	(μ m)	(μ m)
			n	r	Z		U	p	V	u	p	μ	length	width
L. Dentary x800	1	2	630	0.328	67.786	<< 0.001	162.571	< 0.01	0.327	11.613	<< 0.001	89.489	16.6	0.3
	1	3	556	0.396	87.027	<< 0.001	171.254	< 0.01	0.395	13.166	<< 0.001	97.284	14.4	0.4
	2	1	171	0.790	106.849	<< 0.001	231.114	< 0.01	0.767	14.186	<< 0.001	79.647	18.4	0.1
	2	3	51	0.862	37.860	<< 0.001	269.808	< 0.01	0.857	8.653	<< 0.001	87.529	28.6	0.2
	3	1	310	0.227	15.909	<< 0.001	156.002	< 0.01	0.129	3.224	<< 0.001	148.767	17.9	0.4
	3	2	325	0.258	21.700	<< 0.001	164.908	< 0.01	0.153	3.907	<< 0.001	147.251	17.5	0.3
	4	1	254	0.545	75.376	<< 0.001	186.678	< 0.01	0.538	12.136	<< 0.001	102.350	22.2	0.1
	2	1	64	0.592	22.428	<< 0.001	189.815	< 0.01	0.592	6.696	<< 0.001	94.679	17.6	0.2
	5	1	545	0.340	63.011	<< 0.001	162.021	< 0.01	0.340	11.214	<< 0.001	90.944	13.5	0.3
	5	2	128	0.543	37.792	<< 0.001	199.030	< 0.01	0.518	8.289	<< 0.001	76.073	17.8	0.2
L. Maxilla x800	5	4	117	0.477	26.628	<< 0.001	185.715	< 0.01	0.374	5.715	<< 0.001	55.165	16.0	0.1
	10	1	422	0.277	32.424	<< 0.001	166.031	< 0.01	0.255	7.418	<< 0.001	116.518	12.4	0.2
	2	2	288	0.669	129.019	<< 0.001	204.071	< 0.01	0.655	15.731	<< 0.001	81.945	13.4	0.2
	2	4	294	0.617	111.842	<< 0.001	211.676	< 0.01	0.598	14.490	<< 0.001	79.276	11.9	0.1
	2	5	52	0.794	32.778	<< 0.001	229.379	< 0.01	0.780	7.953	<< 0.001	82.818	11.9	0.1
L. Dentary x1000	4	2	421	0.436	79.970	<< 0.001	176.636	< 0.01	0.421	12.213	<< 0.001	108.667	13.6	0.2

Table S2. *Lesothosaurus diagnosticus* - microwear summary statistics, class 1 data

Class 1			Angular disp.		Rayleigh	Rao		Rayleigh (expected mean 29.82°)			Orientation	(μm)	(μm)	
Element	Tooth	Site	n	r	Z	p	U	p	V	u	p	μ	length	width
L. Dentary x800	1	2	141	0.845	100.588	<< 0.001	245.848	< 0.01	0.839	14.087	<< 0.001	36.519	13.7	0.3
	1	3	74	0.829	50.901	<< 0.001	246.696	< 0.01	0.829	10.089	<< 0.001	29.144	12.5	0.4
	2	1	19	0.939	16.768	<< 0.001	273.594	< 0.01	0.873	5.382	<< 0.001	51.489	13.9	0.1
	2	3	0											
	3	1	75	0.892	59.676	<< 0.001	256.000	< 0.01	0.876	10.724	<< 0.001	18.827	17.1	0.4
	3	2	72	0.873	54.844	<< 0.001	260.685	< 0.01	0.841	10.096	<< 0.001	14.396	16.2	0.4
	4	1	20	0.854	14.575	<< 0.001	256.534	< 0.01	0.832	5.265	<< 0.001	42.610	15.1	0.1
L. Maxilla x800	2	1	7	0.987	6.826	<< 0.001	282.601	< 0.01	0.985	3.686	<< 0.001	33.832	16.8	0.3
	5	1	107	0.871	81.265	<< 0.001	251.070	< 0.01	0.868	12.695	<< 0.001	35.070	11.8	0.3
	5	2	18	0.931	15.586	<< 0.001	271.891	< 0.01	0.893	5.355	<< 0.001	46.245	14.5	0.1
	5	4	58	0.881	45.012	<< 0.001	248.765	< 0.01	0.881	9.483	<< 0.001	28.003	14.5	0.1
	10	1	63	0.782	38.494	<< 0.001	256.288	< 0.01	0.776	8.706	<< 0.001	22.644	12.6	0.3
L. Dentary x1000	2	2	36	0.925	30.775	<< 0.001	287.455	< 0.01	0.867	7.356	<< 0.001	50.174	11.5	0.1
	2	4	45	0.957	41.202	<< 0.001	296.616	< 0.01	0.905	8.582	<< 0.001	48.843	9.9	0.1
	2	5	9	0.912	7.492	<< 0.001	241.439	< 0.01	0.870	3.691	<< 0.001	47.348	8.9	0.1
	4	2	38	0.854	27.727	<< 0.001	245.254	< 0.01	0.851	7.422	<< 0.001	34.499	12.3	0.2

Table S3. *Lesothosaurus diagnosticus* - microwear summary statistics, class 2 data

Class 2			Angular disp.		Rayleigh	Rao		Rayleigh (expected mean 87.89°)			Orientation	(μm)	(μm)	
Element	Tooth	Site	n	r	Z	p	U	p	V	u	p	μ	length	width
L. Dentary x800	1	2	335	0.893	267.258	<< 0.001	257.642	< 0.01	0.893	23.115	<< 0.001	89.035	17.8	0.4
	1	3	334	0.905	273.629	<< 0.001	255.964	< 0.01	0.905	23.383	<< 0.001	89.604	15.2	0.4
	2	1	144	0.884	112.453	<< 0.001	264.644	< 0.01	0.878	14.900	<< 0.001	81.359	19.3	0.1
	2	3	49	0.925	41.912	<< 0.001	282.096	< 0.01	0.925	9.153	<< 0.001	86.600	28.6	0.2
	3	1	95	0.912	79.000	<< 0.001	250.726	< 0.01	0.911	12.552	<< 0.001	90.912	18.5	0.4
	3	2	103	0.893	82.081	<< 0.001	264.536	< 0.01	0.892	12.803	<< 0.001	90.053	17.8	0.3
	4	1	160	0.913	133.311	<< 0.001	262.344	< 0.01	0.909	16.267	<< 0.001	92.885	23.8	0.1
L. Maxilla x800	2	1	45	0.900	36.427	<< 0.001	253.495	< 0.01	0.898	8.522	<< 0.001	91.103	18.1	0.1
	5	1	292	0.880	226.260	<< 0.001	252.497	< 0.01	0.880	21.270	<< 0.001	86.964	14.2	0.3
	5	2	88	0.906	72.154	<< 0.001	270.514	< 0.01	0.893	11.848	<< 0.001	78.390	19.0	0.2
	5	4	53	0.918	44.705	<< 0.001	266.446	< 0.01	0.912	9.393	<< 0.001	81.307	18.5	0.1
	10	1	177	0.932	153.748	<< 0.001	263.453	< 0.01	0.932	17.536	<< 0.001	87.920	12.4	0.2
L. Dentary x1000	2	2	215	0.911	178.436	<< 0.001	259.949	< 0.01	0.907	18.803	<< 0.001	82.367	14.4	0.2
	2	4	205	0.929	177.002	<< 0.001	276.907	< 0.01	0.922	18.674	<< 0.001	80.870	12.7	0.2
	2	5	42	0.934	36.663	<< 0.001	268.152	< 0.01	0.934	8.563	<< 0.001	87.780	12.5	0.1
	4	2	230	0.911	191.031	<< 0.001	260.076	< 0.01	0.909	19.488	<< 0.001	92.336	14.6	0.2

Table S4. *Lesothosaurus diagnosticus* - microwear summary statistics, class 3 data

Class 3			Angular disp.		Rayleigh	Rao			Rayleigh (expected mean 147.71°)			Orientation	(μm)	(μm)
Element	Tooth	Site	n	r	Z	p	U	p	V	u	p	μ	length	width
L. Dentary x800	1	2	154	0.866	115.591	<< 0.001	259.390	< 0.01	0.866	15.205	<< 0.001	147.809	16.8	0.3
	1	3	148	0.848	106.375	<< 0.001	249.753	< 0.01	0.848	14.584	<< 0.001	148.541	13.4	0.3
	2	1	8	0.933	6.960	<< 0.001	253.364	< 0.01	0.895	3.582	<< 0.001	131.442	13.4	0.1
	2	3	2	0.999	1.994	0.14			0.993	1.986	0.019	153.835	30.7	0.1
	3	1	140	0.858	103.175	<< 0.001	252.819	< 0.01	0.856	14.330	<< 0.001	151.679	17.9	0.4
	3	2	150	0.856	109.910	<< 0.001	246.590	< 0.01	0.854	14.785	<< 0.001	151.974	18.1	0.3
	4	1	74	0.849	53.356	<< 0.001	253.995	< 0.01	0.847	10.301	<< 0.001	143.407	20.7	0.1
	4	2	150	0.856	109.910	<< 0.001	246.590	< 0.01	0.854	14.785	<< 0.001	151.974	18.1	0.3
L. Maxilla x800	2	1	12	0.917	10.092	<< 0.001	251.340	< 0.01	0.898	4.402	<< 0.001	136.165	16.1	0.1
	5	1	146	0.870	110.539	<< 0.001	258.782	< 0.01	0.868	14.835	<< 0.001	143.869	13.1	0.3
	5	2	22	0.910	18.200	<< 0.001	250.698	< 0.01	0.904	5.994	<< 0.001	154.264	15.8	0.3
	5	4	6	0.802	3.855	0.014	230.268	< 0.01	0.744	2.577	0.003	125.870	8.6	0.1
	10	1	182	0.838	127.837	<< 0.001	246.983	< 0.01	0.838	15.986	<< 0.001	146.489	12.4	0.2
L. Dentary x1000	2	2	37	0.874	28.248	<< 0.001	258.468	< 0.01	0.872	7.499	<< 0.001	143.768	9.4	0.1
	2	4	44	0.915	36.809	<< 0.001	254.801	< 0.01	0.915	8.580	<< 0.001	148.187	10.0	0.1
	2	5	1	1	1	0.512			0.949	1.341	0.116	129.245	12.8	0.1
	4	2	153	0.880	118.580	<< 0.001	249.838	< 0.01	0.880	15.395	<< 0.001	146.214	12.4	0.2

Table S5. *Lesothosaurus diagnosticus* – comparison of feature density N between sites from interactive and non-interactive tooth surfaces, with results of analysis of variance.

Element	Interactive sites (mesial portion of the tooth face)							Non- interactive sites (distal portion of the tooth face)				
	Left dentary				Left maxilla			Left dentary			Left maxilla	
Tooth - site	T1-2	T1-3	T3-1	T3-2	T2-1	T5-1	T10-1	T2-1	T2-3	T4-1	T5-2	T5-4
N	630	556	310	325	64	545	422	171	51	254	128	117

	d.f.	F	P
Onew ay Anova	1,10	8.167	0.017
	means		
Interactive	407		
Non-interactive	144		

Table S6. *Lesothosaurus diagnosticus* - results of null hypothesis testing for differences in microwear (scratch length and width) between sites within the left dentary (7 sites from 4 teeth) and left maxilla (5 sites from 3 teeth).

		Unclassified			Class 1			Class 2			Class 3		
Length does not differ between sites		d.f.	F	P	d.f.	F	P	d.f.	F	P	d.f.	F	P
Left dentary		6,2290	40.020	< 0.0001	5,395	5.387	< 0.0001	6,1213	27.380	< 0.0001	6,669	11.247	< 0.0001
Left maxilla		4,1271	24.187	< 0.0001	4,248	5.379	0.0004	4,650	17.523	< 0.0001	4,363	4.750	0.001
(one way ANOVA; log data)													
Width does not differ between sites		d.f.	F	P	d.f.	F	P	d.f.	F	P	d.f.	F	P
Left dentary		6,2290	54.860	< 0.0001	5,395	8.207	< 0.0001	6,1213	47.584	< 0.0001	6,669	8.198	< 0.0001
Left maxilla		4,1271	42.213	< 0.0001	4,248	15.097	< 0.0001	4,650	28.813	< 0.0001	4,363	4.144	0.0027
(one way ANOVA)													

Table S7. *Iguana iguana* - microwear summary statistics, unclassified data and by orientation class (1-3)

Unclassified			Angular disp.		Rayleigh		Rao		Rayleigh (expected mean 62.03°)			Orientation	(μm)	(μm)
Element	Tooth	Site	n	r	Z	p	U	p	V	u	p	μ	length	w idth
R. Dentary	6	4	404	0.730	215.015	<< 0.001	224.753	< 0.01	0.728	20.689	<< 0.001	58.114	13.4	0.2
	6	9	111	0.678	51.018	<< 0.001	224.215	< 0.01	0.677	10.091	<< 0.001	59.414	13.5	0.3
	12	7	251	0.730	133.680	<< 0.001	228.480	< 0.01	0.723	16.202	<< 0.001	69.788	14.0	0.2
	13	2	136	0.455	28.139	<< 0.001	186.480	< 0.01	0.455	7.501	<< 0.001	61.169	9.4	0.2
Class 1			Angular disp.		Rayleigh		Rao		Rayleigh (expected mean 37.51°)			Orientation	(μm)	(μm)
Element	Tooth	Site	n	r	Z	p	U	p	V	u	p	μ	length	w idth
R. Dentary	6	4	176	0.907	144.671	<< 0.001	262.482	< 0.01	0.906	16.996	<< 0.001	35.214	8.9	0.2
	6	9	60	0.919	50.710	<< 0.001	268.236	< 0.01	0.918	10.057	<< 0.001	40.479	12.6	0.2
	12	7	80	0.953	72.604	<< 0.001	280.986	< 0.01	0.950	12.019	<< 0.001	41.663	10.4	0.2
	13	2	61	0.927	52.395	<< 0.001	264.319	< 0.01	0.926	10.231	<< 0.001	35.555	8.5	0.2
Class 2			Angular disp.		Rayleigh		Rao		Rayleigh (expected mean 78.23°)			Orientation	(μm)	(μm)
Element	Tooth	Site	n	r	Z	p	U	p	V	u	p	μ	length	w idth
R. Dentary	6	4	225	0.967	210.338	<< 0.001	293.552	< 0.01	0.964	20.452	<< 0.001	73.906	17.1	0.3
	6	9	49	0.951	44.274	<< 0.001	283.846	< 0.01	0.949	9.391	<< 0.001	81.888	14.9	0.3
	12	7	163	0.969	153.119	<< 0.001	291.455	< 0.01	0.968	17.481	<< 0.001	80.892	16.0	0.2
	13	2	59	0.924	50.385	<< 0.001	275.311	< 0.01	0.918	9.975	<< 0.001	84.680	10.9	0.2
Class 3			Angular disp.		Rayleigh		Rao		Rayleigh (expected mean 140.55°)			Orientation	(μm)	(μm)
Element	Tooth	Site	n	r	Z	p	U	p	V	u	p	μ	length	w idth
R. Dentary	6	4	3	0.631	1.194	0.333			0.631	1.545	0.064	141.120	7.6	0.1
	6	9	2	0.789	1.244	0.335			0.777	1.554	0.065	130.772	6.2	0.1
	12	7	8	0.818	5.350	0.002	217.080	< 0.01	0.817	3.269	<< 0.001	142.811	8.3	0.2
	13	2	16	0.719	8.266	<< 0.001	238.271	< 0.01	0.719	4.066	<< 0.001	140.493	7.1	0.2

Table S8. *Iguana iguana* - results of null hypothesis testing for differences in microwear (scratch length and width) between sites within the right dentary (4 sites from 3 teeth).

	Unclassified			Class 1			Class 2			Class 3		
	d.f.	F	P	d.f.	F	P	d.f.	F	P	d.f.	F	P
Length does not differ between sites (one way ANOVA; log data)	3,898	12.867	< 0.0001	3,373	8.412	< 0.001	3,492	8.702	< 0.0001	3,25	0.683	0.5711
Width does not differ between sites (one way ANOVA)	3,898	3.802	0.01	3,373	2.275	0.0794	3,492	4.011	0.0077	3,25	2.136	0.1209

Table S9. *Iguana iguana* and *Lesothosaurus diagnosticus* - analysis of variation in orientation between sites (*I. iguana*: 4 sites from 3 teeth; *L. diagnosticus*: 4 sites from 2 teeth). Mean of means (μ of μ) and confidence intervals calculated for all sites for each orientation class (1-3). No site falls outside the 99% confidence interval (differs significantly).

Tooth-Site	I. iguana right dentary				L. diagnosticus left dentary			
	6-4	6-9	12-7	13-2	2-2	2-4	2-5	4-2
Class 1 angular dispersal, R	0.907	0.919	0.953	0.927	0.925	0.957	0.912	0.854
Mean vector, μ	35.214	40.479	41.663	35.555	50.174	48.843	47.348	34.499
Class 2 angular dispersal, R	0.967	0.951	0.969	0.924	0.911	0.929	0.934	0.911
Mean vector, μ	73.906	81.888	80.892	84.680	82.367	80.870	87.780	92.336
Class 3 angular dispersal, R	0.631	0.789	0.818	0.719	0.874	0.915	1.000	0.880
Mean vector, μ	141.120	130.772	142.811	140.493	143.768	148.187	129.245	146.214

Class 1 mean of means 41.82, 99% confidence interval 30.19 – 52.76

Class 2 mean of means 83.00, 99% confidence interval 73.68 – 92.91

Class 3 mean of means 140.24, 99% confidence interval 126.99 – 154.18

Table S10. *Hypsilophodon foxii*. Microwear summary statistics, pooled data

Element	Tooth	Site	Angular disp.		Rayleigh		Rao		Rayleigh (expected mean 81.91°)			Orientation	(μm)	(μm)
			n	r	Z	p	U	p	V	u	p	μ	length	width
L. Maxilla	1	2	431	0.483	100.436	<< 0.001	178.404	< 0.01	0.479	14.074	<< 0.001	75.141	13.4	0.2
R. Maxilla	2	3	1276	0.292	108.776	<< 0.001	170.129	< 0.01	0.291	14.718	<< 0.001	85.679	13.5	0.3

CHAPTER 8

Dental microwear analysis of the ornithomimid dinosaur *Hypsilophodon foxii*: evidence for muscular cheeks

Targeted for the journal *Paleobiology*

Abstract - Understanding the feeding mechanisms and diet of extinct animals is fundamental to understanding their palaeobiology and the ecosystem in which they lived. Tooth microwear analysis uses the microscopic scratches and pits on the surface of teeth to deduce dietary habit and offers a fresh approach to the reconstruction of jaw movements during feeding in extinct animals. Most studies have been carried out on mammals, with comparative analyses of microwear patterns between fossil and modern living counterparts. Where no close living functional analogue exists, reconstruction of jaw movements during feeding have relied upon biomechanical analysis of the skulls. Here I show that analysis of tooth microwear orientation provides direct evidence for the relative motion of jaws during feeding in the primitive ornithopod dinosaur *Hypsilophodon foxii* and is a powerful tool for testing hypotheses of jaw mechanics. Statistical testing demonstrates that the teeth of *H. foxii* preserve three distinct sets of scratches in different orientations on both the occlusal surfaces and the off-occlusal labial surfaces. In terms of jaw mechanics, these data indicate a propalinal (anteroposterior) translation of the lower jaw during feeding, and support the assertion that muscular cheeks were present in *H. foxii*.

Introduction

The dentary and maxillary teeth of ornithischian dinosaurs are inset medially in almost all taxa leaving a holding or “cheek” space for food (Sereno 1997). It has been argued that virtually all ornithischians, with the exception of the most basal such as *Lesothosaurus*, possessed cheeks (Galton 1978). However this is not known for certain and is currently the subject of much debate. The skull morphology of early, basal ornithischians suggests that they relied solely on simple adduction of the lower jaws to produce vertical or near vertical tooth-tooth shearing motion between bilaterally occluding maxillary and dentary teeth (e.g., Thulborn 1971b; Weishampel 1984). True mastication (the ability to chew) developed in the more derived ornithomimids; kinematic analyses of their skulls and jaws indicate that all but the most basal could chew by mobilizing either cranial or mandibular segments to generate a transverse grinding power stroke (Norman 1984; Weishampel 1984; Norman and Weishampel 1985). The precise ways in which ornithomimids chewed their food however, has not been settled.

Galton (1973) suggested that an important reason for the success of ornithomimids was the development of cheeks and he postulated that most ornithischians had cheeks and a small subterminal mouth, citing the restored *Hypsilophodon foxii* as an example. Norman and Weishampel (1985) proposed that the evolution of cheeks occurred subsequent to the development of the pleurokinetic hinge ((Norman 1984) moveable joints within the skull that allow flexion and expansion during feeding) and attributed the success of ornithomimids to the consequent transverse grinding stroke. A recent theoretical analysis of the evidence for cranial kinesis in dinosaurs concluded that it was unlikely that anything more than very slight movements at sutural junctures would be possible (Holliday and Witmer 2009), the inference being that this would serve to dissipate mechanical stresses and strains rather than facilitate a transverse power stroke

during feeding. Three dimensional animation modelling of the hadrosaurid *Edmontosaurus* (Rybczynski *et al.* 2008) also questioned the pleurokinetic model proposed by Norman and Weishampel, suggesting that extensive secondary (intracranial) movements beyond the pleurokinetic hinge would be a consequence. However, quantitative microwear analysis (an examination of the microscopic scratches on teeth generated during feeding) has shown evidence for a transverse power stroke in *Edmontosaurus* and provides strong evidence for the presence of a pleurokinetic hinge in hadrosaurids (Williams *et al.* 2009).

Dental microwear analysis is now widely used in palaeodietary reconstruction, with dietary interpretations of microwear in fossil mammals based on comparison with extant/living mammals with known diets. Evidence of dietary habit and the mastication process can be deduced from the microscopic scratches and pits on the surface of teeth (e.g., Walker *et al.* 1978; Teaforde and Byrd 1989; Semprebon *et al.* 2004; Ungar *et al.* 2007). The functional aspects of chewing can be inferred from changes in the orientation and dimensions of scratches and pits, which change as the relative motion of the upper and lower jaws change or as the compression/shear force between them changes. The orientation of these scratches and pits reflect the dominant direction of jaw movements (Butler 1952; Mills 1967; Teaforde and Byrd 1989). That microwear analysis has a broad applicability beyond mammals has been shown by research on both fossil fishes (Purnell *et al.* 2006; Purnell *et al.* 2007) and dinosaurs (e.g., Fiorillo 1991, 1998; Upchurch and Barrett 2000; Williams *et al.* 2009).

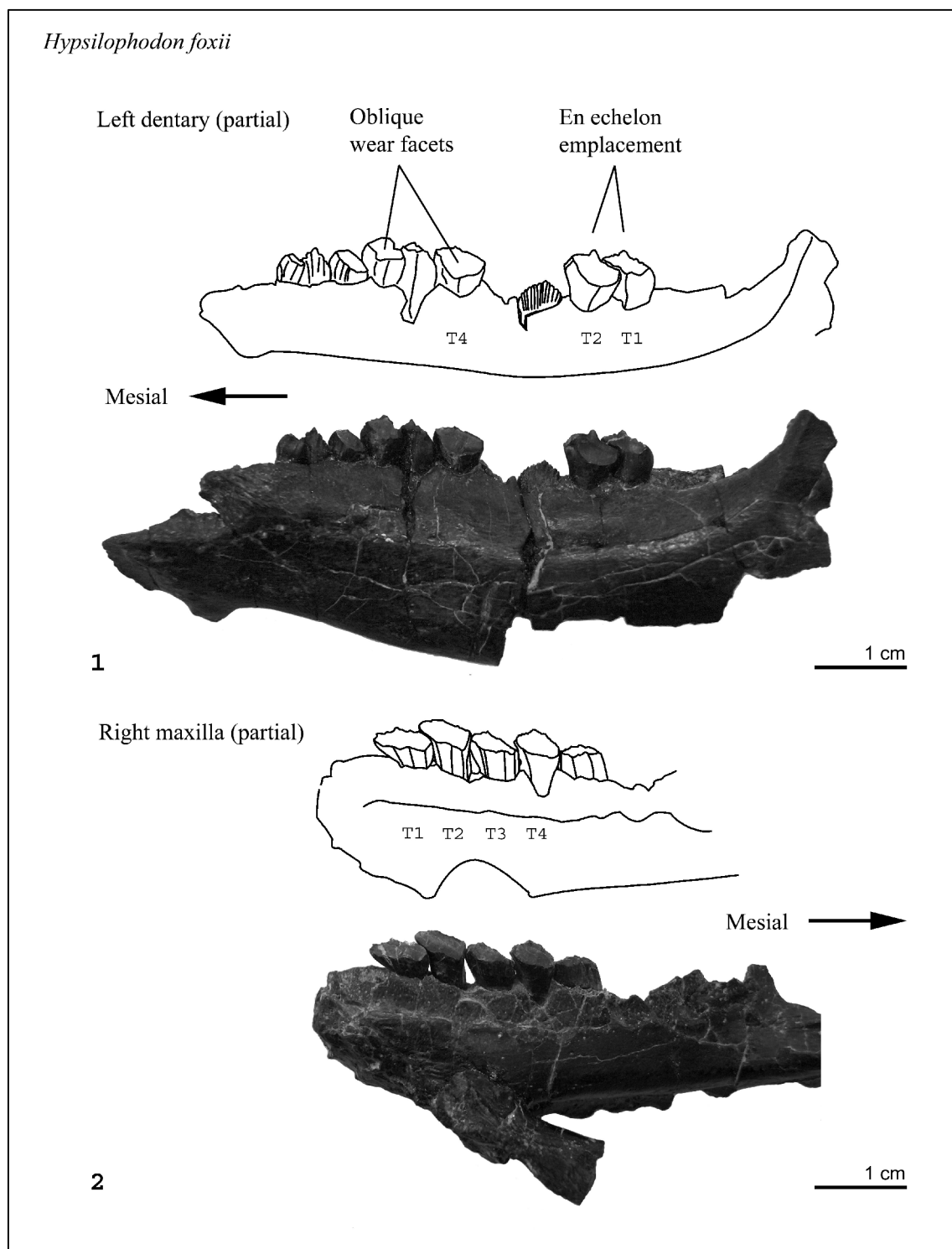


Figure 1. Cheek teeth of *Hypsilophodon foxii* MIWG 6362. 1.1 Partial left dentary in labial view showing the inset tooth row, obliquely inclined occlusal surfaces and *en echelon* emplacement of the teeth; a newly erupted tooth anterior of T4 is just beginning to develop an occlusal wear facet; anterior (mesial) is to the left. 1.2 Partial right maxilla in lingual view exposing the occlusal surfaces— anterior is to the right.

Hypsilophodon foxii

The teeth of *H. foxii* are leaf-shaped with labiolingually compressed and expanded crowns that have finely serrated edges. The crowns are heavily enamelled on one side only (labial on maxillary and lingual on dentary teeth) and show substantial wear with obliquely inclined planar wear facets (forming the occlusal plane) developed on the labial face of dentary teeth and the lingual face of maxillary teeth. Tooth emplacement is *en echelon* such that the mesial edge of one tooth is labially overlapped by the distal edge of the next anterior tooth, producing an imbricate pattern when viewed dorsoventrally, and tooth positions in the upper and lower tooth rows are staggered such that one tooth of the upper jaw shears past two teeth of the lower jaw (see Figure 1).

Analysis of dental microwear patterns on the teeth of *H. foxii*, both on the occlusal plane and on the labial surfaces, off the occlusal plane (between the cheeks and teeth), provides a test of current hypotheses on feeding in *H. foxii*. Simple vertical adduction of the style predicted by Thulborn (1971b) and Weishampel (1984) for primitive ornithischians like *Lesothosaurus* should produce dominant scratch orientations near 90° to the tooth row long axis and bilateral occlusion should produce matching (when suitably transformed – see materials and methods) microwear patterns on left and right jaw elements. Minor more oblique orientations are also possible as microwear patterns can vary as the compressive forces change along the length of the jaw, although this effect will be limited in animals with short jaws. A propalinal (anteroposterior) translation of the lower jaw would produce dominant scratch orientations near the horizontal whilst a transverse (labiolingual) translation of the upper jaw relative to the lower jaw would produce dominant scratch orientations near the vertical (inclined in 3D at the same angle as the occlusal surface); both would

require cranial kinesis. Norman and Weishampel (1984; 1985) predicted transverse with minor propalinal translation for hypsilophodonts (Figure 2). If *Hypsilophodon foxii* lacked muscular cheeks, microwear generated by regular contact with food items on the off-occlusal labial tooth surfaces would be restricted, whereas the presence of muscular cheeks would act to concentrate microwear on those same surfaces. It is also possible that more random orientations could be produced between tooth and cheek because food can be moved around by the tongue during repetitive chewing. In mammals the tongue has developed the capacity to throw food sideways onto the teeth as well as backwards for swallowing (Lucas 2004) and it has been shown to direct food, twisting and contracting, during both the closing and power strokes (Herring 1993).

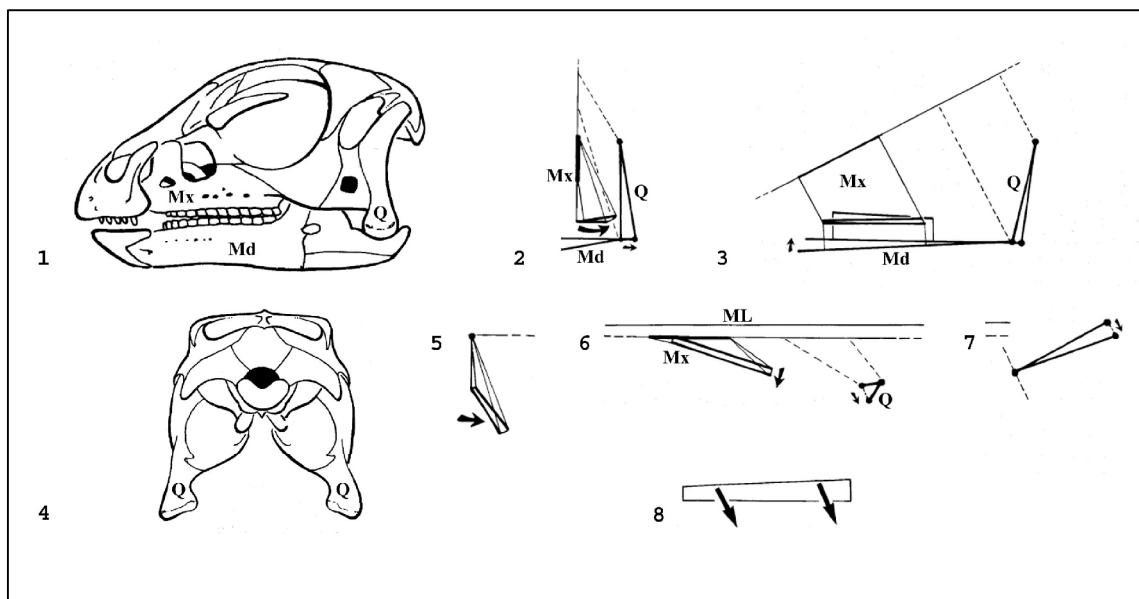


Figure 2. Predicted streptostyly mechanism for *Hypsilophodon foxii* (Weishampel 1984), illustrating movement of the maxilla, mandible and quadrate. 2.1 Skull in left lateral view. 2.2 Frontal view. 2.3. Left lateral view. 2.4 Skull in caudal view. 2.5 View along the maxilla-premaxilla teeth. 2.6 Dorsal view. 2.7 View of the left quadrate along its plane of motion. 2.8 Occlusal view of the left dentary dentition. Arrows indicate the direction of movement of the maxillary teeth against the dentary teeth. Md – mandible; ML – midline; Mx – maxilla; Q – quadrate.

Here I examine whether dental microwear analyses support the presence of muscular cheeks in *Hypsilophodon foxii* and test the hypotheses for rotation and translation of the jaws during feeding.

Material and Methods

The teeth studied are from the ornithomimid dinosaur *Hypsilophodon foxii* (2 individuals) that were collected from the Wessex Formation (Lower Cretaceous, Barremian) of the Isle of Wight and are held at the Museum of Isle of Wight Geology (MIWG). The specimens MIWG.6363 (right dentary complete, left dentary incomplete, right maxilla incomplete and isolated right maxilla tooth) and MIWG.6273 (isolated right dentary tooth - recovered from a collection of iguanodont teeth) were cleaned with solvent gel (see Chapter 2) and imaged uncoated. Imaging for the microwear analysis was performed using a scanning electron microscope (Hitachi S-3600N SEM), operated in a partial vacuum (20Pa) using the environmental secondary electron detector (ESED); SEM settings were standardized at: accelerating voltage, 10kV; working distance, 23 mm; automatic contrast and brightness. Standardisation is important for comparability of datasets (Gordon 1988). The specimens were inserted into the SEM chamber and oriented with the long axis of the tooth row as a reference frame and then rotated about the long axis of the tooth such that the surface being imaged was perpendicular to the electron beam. Photomicrographs were captured at a magnification of x300 providing a field of view of 417 x 312 μm . In mammals, microwear patterns develop on wear facets on homologous cusps and at specific points that relate to the places where teeth are abraded by food or by occlusion with other teeth (Teaford 1988b) making sampling strategies relatively simple to formulate. In dinosaurs, there have been too few microwear studies to establish which sites should be used for microwear acquisition or at what magnification. For diet related quantitative microwear research in mammals a magnification of x500 is the standard choice (e.g., Teaford 1988a). As this study relates to jaw motion, magnification was not as important as the field of view and a magnification of x300 was chosen to maximize the latter without

compromising detail. Previous work on hadrosaur teeth (Williams *et al.* 2009) found microwear pattern development to occur consistently across the whole occlusal surface, and sauropod studies (Fiorillo 1991, 1998) found the length, width and frequency of microwear features to be consistent within the occlusal surface. In this study of *H. foxii* exploratory micrographs, examined qualitatively, suggested that a central site was representative of the occlusal surface; so central sites were sampled as standard. Where this portion of the tooth surface was damaged, a slightly more anterior or posterior site was selected. For off-occlusal labial microwear, dentary teeth were excluded because the development of the downward sloping occlusal planes (at approx 62°) limits the available surface area. The use of maxillary teeth for off-occlusal labial microwear introduces a potential source of variation as the labial surface of maxillary teeth is enamel whereas the labial surface of dentary teeth (and the bulk of the occlusal plane cut into them) is dentine. For this reason I do not make statistical comparisons of scratch length and width between occlusal and off-occlusal labial surfaces. As the off-occlusal surfaces appeared inconsistent, with patchy microwear, a selection of sites across the occlusal surface were chosen that were parallel to the long axis of the tooth row, and sufficiently distant from the ridges on the tooth face to be unaffected by curvature. All available teeth were examined; damaged teeth (those with unusually large gouges, cracks or pieces broken off that were suspected to be the result of post-mortem processes) were excluded, as were part erupted teeth which were found to have zero microwear features. A total of 6253 microwear features were captured and analysed from 21 sites on 10 teeth (11 sites from the lower and 10 from the upper dentition; 2 teeth from the right dentary, 3 from the left dentary and 5 from the right maxilla). The digital SEM photomicrographs were downsampled to 900 pixels wide by 675 pixels high using Adobe Photoshop 7. As pits (features of roughly equal length and

width) were rare to absent and this study is concerned particularly with relative jaw motion and therefore microwear orientation, only scratches (elongate features) were considered. All microwear scratches within each photomicrograph were measured and recorded using the custom software package Microware 4.02 (Ungar 2001). This produces overlay files of x,y co-ordinates; these were processed in a database using simple trigonometric functions to calculate the length, width and long axis orientation of each feature/scratch. Where the number of scratches per image exceeded 1000, more than one overlay file was used to cover the entire image (Microware 4.02 has a limitation of 1000 features per overlay file). The grid lines option in Microware 4.02 was used to ensure the same feature was not measured twice. Scratch orientation data were suitably transformed for comparison to the labial face of the left dentary teeth; e.g. when looking at the labial face of a left dentary tooth, mesial will be to the left but on a right dentary tooth mesial will be to the right, in order to compare microwear patterns one set of data will need to be transformed – to achieve the equivalent of flipping the photomicrograph image horizontally before measuring the scratches. Measurement and recording took place on a Dell Latitude D505 computer running Windows XP Professional (Microsoft), with a 15-inch active matrix TFT display set at a screen resolution of 1024 x 768 pixels, resulting in an onscreen magnification of approximately x630 for SEM photomicrographs taken at x300.

Analyses of variance (ANOVA) for linear data and mean of mean angle confidence interval (CI) tests for circular data were conducted on scratch count (N), orientation, angular dispersion (i.e. the degree of parallelism as measured by R), length and width to determine if significant differences occur between sites within a tooth, between teeth within a jaw element and between teeth of different jaw elements. Scratch length data were not normally distributed (Shapiro-Wilk W; $P < 0.01$) and were

therefore log-transformed before statistical analysis. Fiorillo (1998) assessed dominant directions of wear via rose diagram plots, and interpreted these as reflecting directions of jaw movements. This approach was used here to identify dominant modes that could be used to infer relative jaw motion and to assess the distribution of dominant scratch orientations among taxa. Boundaries for these modes (classes of orientation) were identified visually (via 1° resolution rose diagram if necessary) and tested by discriminant function analysis (DFA) for an acceptable error rate (typically < 2%). Statistical analyses were carried out using the dedicated software packages Oriana 3.31 (Kovach Computing Services) for orientation data and JMP 8.0.2 (SAS Institute Inc) for both linear data and DFA.

Results

Visual inspection of photomicrographs revealed that *Hypsilophodon foxii* teeth do preserve microwear, and that scratches dominate. Pits were rare and were therefore excluded from the analyses. Dentary and maxillary teeth show dominant oblique and near vertical microwear patterns on the occlusal surface and more varied patterns on the off-occlusal labial surface. Figure 3 shows examples of the microwear imaged on the occlusal surface of a left dentary tooth and the off-occlusal labial surface of a right maxillary tooth of *Hypsilophodon foxii* MIWG 6362.

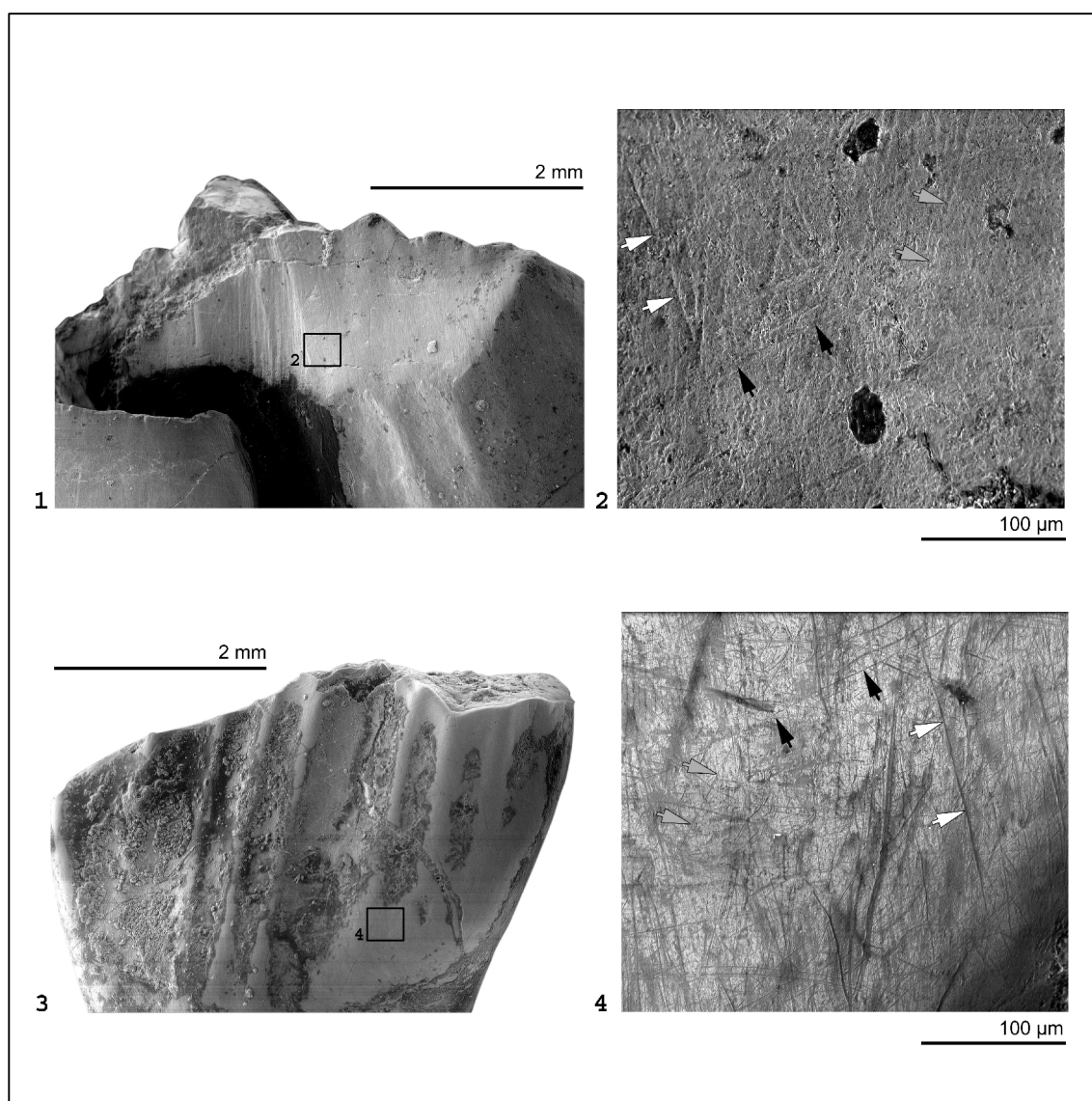


Figure 3. Microwear distribution on the tooth surfaces of *Hypsilophodon foxii* MIWG 6362. 2.1 Labial view of a left dentary tooth showing the occlusal surface, with inset box showing location for (2.2); mesial is to the left. 2.2 Occlusal surface microwear; mesial is to the left. 2.3 Labial view of a right maxillary tooth, with inset box showing location for (2.4); mesial is to the left. 2.4 Off-occlusal surface labial microwear; mesial is to the left. Arrows (2.2 and 2.4) show comparable scratch orientations between occlusal and off-occlusal surfaces.

Scratches on the occlusal surfaces are not random in orientation, appearing to fall into a small number of classes, within which scratches are predominantly straight and subparallel, but with an orientation that differs from that of other classes. To test the hypothesis that discrete classes of scratches exist, occlusal microwear data (2976 scratches from 14 sites on eight teeth) were partitioned into three subsets (classes 1-3, two dominant classes one oblique and one near vertical, and one minor low angle oblique class), based on visual assessment of scratch orientation from detailed rose

diagrams. Discriminant function analysis (DFA) provides strong confirmation that the microwear data falls into 3 distinct classes – 98.6% of scratches classified by visual inspection were correctly assigned by DFA. Rather than conduct subsequent statistical testing on these imperfectly classified data, the DFA results were used to reassign the incorrectly assigned scratches to their correct class (leading to 100% correct discrimination; see Table 1 for summary). Analysis of this dataset revealed significant differences ($P < 0.05$) in scratch count (N), angular dispersion (i.e., the degree of parallelism of scratches as measured by R, mean vector length), length and width between classes (Table 2).

Table 1. Summary statistics for microwear data from occlusal surfaces (14 sites on 8 teeth) unclassified and partitioned into three classes based on scratch orientation.

Subgroup	Occlusal			
	Unclassified	Class 1	Class 2	Class 3
No. Of observations	2976	1508	1087	381
Angular dispersion, R	0.416	0.915	0.892	0.822
Mean orientation (mean vector, μ)	49.71°	32.61°	82.92°	150.30°
95% confidence interval for μ	$\pm 1.67^\circ$	$\pm 0.61^\circ$	$\pm 0.81^\circ$	$\pm 1.78^\circ$
99% confidence interval for μ	$\pm 2.19^\circ$	$\pm 0.80^\circ$	$\pm 1.07^\circ$	$\pm 2.34^\circ$
Mean scratch length, μm	56.02	45.8	73.56	46.42
Mean log scratch length, μm	4.02	3.82	4.29	3.83
Mean scratch width, μm	0.46	0.42	0.55	0.35

Table 2. Results of null hypothesis testing for differences in occlusal surface microwear between classes.

Occlusal	d.f.	F	P
Length does not differ between classes (one way ANOVA; log data)	2,2973	186.78	< 0.0001
Width does not differ between classes (one way ANOVA)	2,2973	35.75	< 0.0001
R does not differ between classes (one way ANOVA)	2,38	5.87	0.006
N does not differ between classes (one way ANOVA)	2,38	5.87	0.006

Pairwise comparisons (Tukey-Kramer honestly significant difference) indicate that N, and scratch width differ between all classes, and R and length differ between classes 1

and 3. Scratches on the off-occlusal surfaces (labial right maxilla) appear more random by orientation, particularly when scoring the micrographs. However, rose diagrams of the pooled off-occlusal data (all sites) suggest that the same three orientation classes identified within the occlusal dataset also exist within the off-occlusal data (Figure 4).

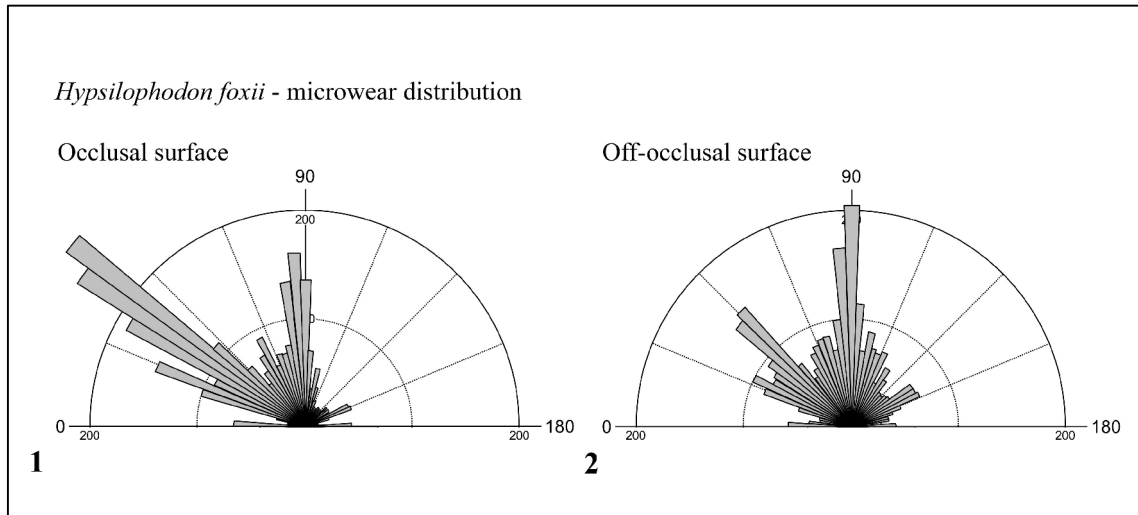


Figure 4. Rose diagrams of microwear scratch orientations, data have been transformed for comparison to the left dentary labial face (see Material and Methods for details on transforming data). Frequency is shown by the radius of the wedge, scale N=200, inner circles measure hundreds, bin size 4°. 3.1 Occlusal surface data (2976 features from 14 sites on 8 teeth). 3.2 Off-occlusal surface labial data (3276 features from 7 sites on 5 teeth).

To test the hypothesis that discrete classes of scratches exist, raw microwear data (3276 scratches from seven sites on five teeth) were partitioned into three subsets based on the class boundaries previously identified for the occlusal dataset. DFA provides strong confirmation that the off-occlusal microwear data falls into the same three distinct classes – 98.1% of scratches classified by the occlusal dataset class boundaries were correctly assigned by DFA (see Table 3 for summary).

Table 3. Summary statistics for microwear data from off-occlusal surfaces (7 sites on 5 teeth) unclassified and partitioned into three classes based on scratch orientation.

Subgroup	Off-occlusal			
	Unclassified	Class 1	Class 2	Class 3
No. Of observations	3276	825	1401	1050
Angular dispersion, R	0.226	0.865	0.866	0.845
Mean orientation (mean vector, μ)	71.676°	31.96°	90.27°	145.09°
95% confidence interval for μ	$\pm 3.03^\circ$	$\pm 1.04^\circ$	$\pm 0.80^\circ$	$\pm 1.00^\circ$
99% confidence interval for μ	$\pm 3.98^\circ$	$\pm 1.37^\circ$	$\pm 1.05^\circ$	$\pm 1.31^\circ$
Mean scratch length, μm	43.13	38.66	50.36	37.00
Mean log scratch length, μm	3.76	3.65	3.91	3.61
Mean scratch width, μm	0.38	0.34	0.44	0.32

Analysis of this dataset revealed significant differences ($P < 0.05$) in length and width between classes (Table 4). I was unable to reject the null hypotheses that angular dispersal (R) and scratch count (N) do not vary between classes in off-occlusal data. Pairwise comparisons (Tukey-Kramer honestly significant difference) indicate that class 2 differs from classes 1 and 3 for length and width, but class 1 does not differ from class 3.

Table 4. Results of null hypothesis testing for differences in off-occlusal surface microwear between classes.

Off-occlusal	d.f.	F	P
Length does not differ between classes (one way ANOVA; log data)	2,3273	122.26	< 0.0001
Width does not differ between classes (one way ANOVA)	2,3273	45.05	< 0.0001
R does not differ between classes (one way ANOVA)	2,18	2.12	0.148
N does not differ between classes (one way ANOVA)	2,18	0.87	0.433

Scratch length is variable with the majority (53%) measuring between 30 and 70 μm in both the occlusal and off-occlusal datasets, and only 10% of the occlusal and 4% of the off-occlusal scratches measured in excess of 100 μm . Scratches fall into a number of discrete width categories with approximately 70% < 0.3 μm , 19% 0.3 to 0.5 μm s, 10% 1 to 3 μm and 1% > 3 μm in both datasets. There is no correlation between

scratch length and width (linear correlation (Pearson); occlusal $r < 0.37$, $P > 0.05$; off-occlusal $r < 0.29$, $P > 0.05$).

Analysis of the unclassified occlusal and off-occlusal datasets reveals that overall, the hypothesis that data for each site are uniformly distributed can be rejected (i.e. the data show a preferred orientation; Rayleigh uniformity test and Rao spacing test, $P < 0.05$; Appendix 1). Analysis of the three subsets of data (classes 1-3) provides confirmation of this result and the hypothesis that data within classes for each site are uniformly distributed can also be rejected (i.e., the data show a preferred orientation; Rayleigh uniformity test and Rao spacing test, $P < 0.05$; Table S1). Mean orientation for each class for each site does not differ significantly from the overall class mean (all sites, all teeth; V test expected means: Occlusal: class 1 = 32.61° , class 2 = 82.92° , class 3 = 150.30° , average $V = 0.89$, Off-occlusal: class 1 = 31.96° , class 2 = 90.27° , class 3 = 145.09° , average $V = 0.86$, $P < 0.05$; Tables 1, 2, S2, S3 & S4). Of the 62 samples tested (three classes, 21 sites, one site with $n = 0$), there were only two exceptions to this result; two class 3 occlusal sites failed the Rayleigh uniformity test, however the number of scratches assigned to both of these sites was 3 or less.

Subdividing a distribution of circular (orientation) data into classes will invariably lead to an increase in parallelism (R) within each class. Even with a random or uniform distribution, as the number of classes increase or the width of a specific class decreases R will approach 1. To test the hypotheses that the distribution of scratches does not differ from a random distribution, results from the analysis of a random distribution of 6252 orientations partitioned into the three classes (1-3) were compared with those of the real data. The random unclassified data produced an R value of 0.03 signifying a uniform distribution. The random data partitioned by class (1-3) produced R values of 0.83, 0.83 and 0.80 respectively. The real data show a greater degree of

parallelism than would be expected from a random distribution of data partitioned into the three orientation classes and therefore reflect preferred orientations. This analysis reveals that overall we can reject the hypothesis that the distribution of scratches does not differ from a random distribution.

Table 5. Results of null hypothesis testing for differences in occlusal surface microwear within a tooth (5 sites from tooth 1 of the left dentary).

Within tooth occlusal (L.dentary tooth 1)	d.f.	F	P
Orientation does not differ between sites (Watson Williams F)	4,615	1.16	0.325
Length does not differ between sites (one way ANOVA; log data)	4,615	11.44	< 0.0001
Width does not differ between sites (one way ANOVA)	4,615	23.16	< 0.0001

Within tooth analyses for five sites within tooth 1 of the left dentary reveal that microwear orientation does not differ significantly between sample sites within a tooth (Table 5). Pairwise comparisons (Watson-Williams F) indicate no significant difference in orientation between sites (a mean of means confidence interval test was not used here as 5 sites are insufficient for a reliable second order mean). Whilst the hypothesis that orientation differs between sites within a tooth can be rejected, the hypothesis that other aspects microwear differ between sites cannot be rejected. Significant differences ($P < 0.5$) exist in both scratch length and width. Pairwise comparisons (Tukey-Kramer honestly significant difference) indicate that five of the ten pairs of means differed significantly for scratch length and eight of the ten pairs of means differed significantly for scratch width. The differences included sites which are immediately adjacent to each other.

To test the null hypothesis that microwear orientation does not differ between teeth within a jaw element, subsets of data were generated for the left dentary occlusal and right maxilla off-occlusal. Analysis of these jaw element datasets reveal that microwear orientation does not differ significantly between samples sites within a jaw

element (Table S5). Mean of mean angles and their 99% confidence intervals (Zar 1999) were calculated for each within jaw dataset (for the unclassified data and by class (1-3)). Mean orientation for each site falls within the confidence interval of the mean of mean angles calculated for its specific dataset (for the unclassified data and by class (1-3)). There were only three exceptions to this result; from the left dentary, 1 unclassified site from tooth 1, one class 1 site from tooth 2, and one class 3 site from tooth 4, had orientations that fell outside the confidence interval for the mean of means. The hypothesis that orientation differs between teeth within a jaw element can therefore be rejected, however the hypothesis that other aspects of microwear differ between teeth within a jaw element cannot be rejected. Significant differences ($P < 0.05$) in both scratch length and scratch width exist in each dataset. The variation between sample sites is not systematic; orientation does not vary significantly with distance from the jaw hinge and there is no correlation between distance from the jaw hinge and R, N, scratch length or width (circular-linear and linear (Pearson) correlations, $P >> 0.05$).

To assess variation between jaw elements, subsets of the occlusal surface dataset were generated for the left dentary, right dentary and right maxilla, for the unclassified microwear data and by class (1-3). Analyses of these jaw element datasets revealed significant differences in orientation, N, R, scratch length and width ($P < 0.05$) between jaw elements in all cases. There were only six exceptions to this; for class 1 data, R does not differ between jaw elements, for class 2 data, N does not differ between jaw elements and for class 3 data neither length, width or R differ between jaw elements (Table S6). Pairwise comparisons (Tukey-Kramer honestly significant difference for linear variables, Watson-Williams F for axial variables) indicate that all elements differ in all cases for the unclassified data, however for data partitioned by class (1-3), the

right dentary and right maxilla differ from the left dentary, but not from each other, for R and N in class 1, scratch length and width in class 2, and N in class 3.

Significant differences in N exist between the occlusal and off-occlusal sites, unclassified data (Oneway ANOVA; d.f. 1,19; $F = 7.28$; $P < 0.05$; means: off-occlusal 468, occlusal 212) and for classes 2 and 3 (Oneway ANOVA; Class 2: d.f. 1,18; $F = 9.83$; $P < 0.05$; means: off-occlusal 200, occlusal 83; Class 3: d.f. 1,19; $F = 9.47$; $P < 0.05$; means: off-occlusal 150, occlusal 27). N does not differ between occlusal and off-occlusal sites for class 1 data (Oneway ANOVA; Class 1: d.f. 1,19; $F = 0.06$; $P = 0.8$; means: off-occlusal 117, occlusal 107).

To identify the directions of repetitive jaw motion during mastication, rose diagrams (stacked rose, orientation and class) of microwear distribution were prepared with mean orientations and 99% confidence intervals for the established orientation classes marked (Figure 5). As N varies between sites, the rose diagrams are not to the same scale; for clarity in comparing distributions, the rose diagrams have been automatically scaled. Whilst the orientations are preferred and the classes of orientations are consistent between sample sites, the distribution varies, particularly in terms of the dominant class. Figure 5.1 shows occlusal surface data from the left dentary sample sites with the class 2 (near vertical) mode consistently dominant. In contrast to the left dentary data, the right dentary and right maxilla occlusal data, Figure 5.2, show the class 1 (low angle oblique) mode consistently dominant and the class 2 mode greatly reduced. This disparity between left and right jaw elements is inconsistent with the bilateral occlusion model for this animal.

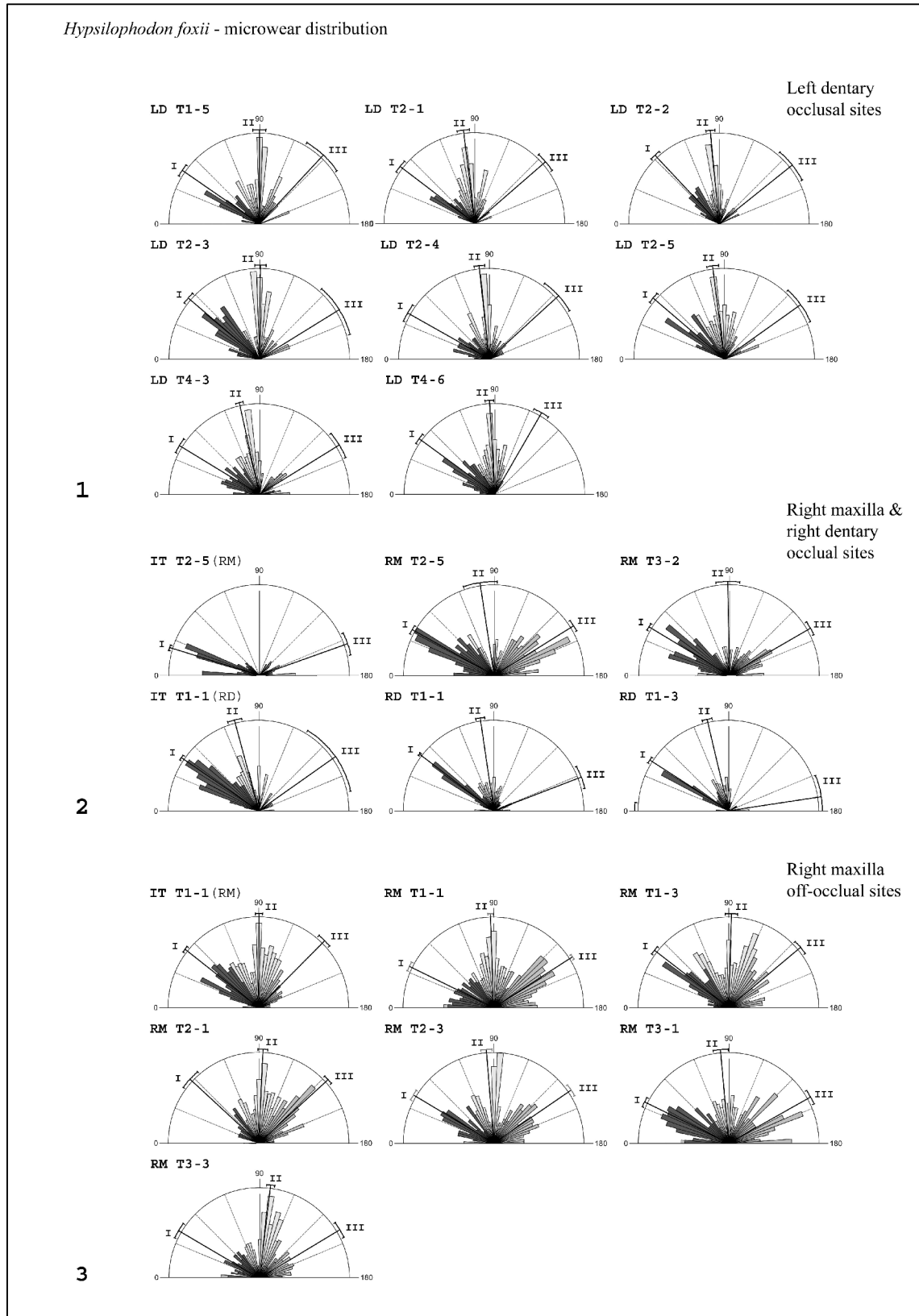


Figure 5. Rose diagrams of microwear scratch orientations partitioned into 3 orientation classes (I, II & III). Black lines running from the centre of the rose diagram to the outer edge, with arcs extending to either side show the mean orientation and 99% confidence interval for each class. 5.1 Left dentary sample sites, occlusal surfaces. 5.2 Right maxilla and right dentary sample sites, occlusal surfaces. 5.3 Right maxilla sample sites, off-occlusal surfaces. Frequency is shown by the area of wedge, individual rose diagrams automatically scaled for clarity. Bin size = 4°.

The off-occlusal data, Figure 5.3, which is all from the right maxilla shows scratches in all three orientation classes with the class 2 mode consistently dominant. Conflicting information is therefore being provided from two different surfaces of the same maxillary teeth. The off-occlusal data reflect movement of the maxillary teeth through food in the cheek space, and indicate a dominant vertical jaw motion. This vertical motion should also be reflected in the microwear on the occlusal surface of those same right maxillary teeth, but it is not. The occlusal data for the right maxilla, indicate a dominant low angle oblique jaw motion and no vertical jaw motion, and the occlusal data for the opposing right dentary, indicate that same dominant low angle oblique jaw motion and no vertical jaw motion. The only rational explanation is that the vertical movement was recorded on the occlusal surface but has been removed and overprinted by the low angle oblique movement. These data suggest a significant propalinal (anteroposterior) translation of the jaws during mastication which has overprinted the class 2 and 3 microwear on the opposing occlusal surfaces of the right maxilla and right dentary.

Summary and Discussion

Dental microwear on occlusal tooth surfaces is created by tooth-to-tooth and tooth-food-tooth contact during biting and chewing (Teaford 1988a) and microwear on non-occlusal (or off-occlusal) tooth surfaces is created by tooth-food contact (Ungar and Teaford 1996). This means that occlusal microwear can be generated by opposing teeth scratching each other directly or by abrasive particles in the food that are trapped between the teeth, whilst off-occlusal microwear must rely upon the food being abrasive and retained in the mouth during chewing. Weishampel (1984) describes the masticatory cycle as involving a closing stroke that brings the teeth into occlusion

(tooth-food-tooth or tooth-tooth contact), a power stroke where food is subdivided e.g. crushed, pulped or shredded, and an opening stroke, and it is his assertion that it is the power stroke which produces occlusal microwear.

The three orientation classes in which the microwear scratches fall exhibit a consistently high degree of parallelism (i.e. angular dispersion as measured by mean vector length (R)) and reflect three distinct jaw motions; class 1 at 32° from the long axis of the tooth row, class 2 at 83° and class 3 at 150°. I interpret class 1 scratches as being formed during the power stroke, and that most-food processing jaw motions were in this direction; scratches in this class outnumber the other classes and cut across microwear in other orientations. The removal of class 2 scratches from the occlusal surface of the right maxillary teeth (while class 2 scratches are preserved on the off-occlusal surface of the same teeth) indicate more frequent movements and higher forces.

The results demonstrate that examination of dental microwear from off-occlusal surfaces can reveal important information about relative jaw motion in dinosaurs. Quantitative microwear studies of both the occlusal and off-occlusal labial surfaces may enable us to determine more about feeding and/or diet in dinosaurs than can be derived from the occlusal surface alone due to the higher preservation potential off the occlusal surface. I interpret the presence of extensive off-occlusal microwear as a function of the presence of cheeks. In animals that do not possess muscular cheeks such as *Iguana iguana* (see chapter 6), the non-interactive labial surfaces that are the equivalent of the off-occlusal surfaces of *Hypsilophodon foxii* have little or no microwear preserved. The consistently higher scratch density off the occlusal surfaces in *H. foxii* compared to that from equal area sample sites on the occlusal surface, coupled with the preservation of class 2 and 3 microwear, provides strong support for muscular cheeks in *H. foxii*.

Whilst accepting that limited conclusions can be drawn from the jaws of an individual animal and two isolated teeth from a second individual, the results demonstrate that with appropriate statistical testing, microwear analyses of dinosaur teeth can provide robust tests of hypotheses of jaw mechanics and feeding mechanisms. By comparing the actual microwear data from the teeth of *Hypsilophodon foxii* with the patterns predicted from the published models of jaw mechanics in hypsilophodonts, it can be shown that vertical adduction alone could not cause the low angle oblique class 1 and class 3 scratch patterns that were observed and measured. The data does not preclude the pleurokinetic model (vertical adduction followed by a transverse (labiolingual) power stroke) predicted by Norman (1984), Weishampel (1984) and Norman and Weishampel (1985) but it better supports their assertion of mobilization of the quadrate-squamosal joint (a propalinal (anteroposterior) power stroke). The significant differences between microwear patterns on the left hand and right hand jaw elements within an individual suggest that the power stroke was unilateral. More hypsilophodont specimens need to be analysed to determine how microwear varies between individuals and species, and to test the hypothesis that microwear patterns differ between left and right jaw elements.

Acknowledgements

I am grateful to Martin Munt & Lorna Steel, Dinosaur Isle Museum, for granting access to and permission to clean the dinosaur teeth. I thank Adrian Doyle and the Palaeontology Conservation Unit at the Natural History Museum (London) for advice regarding cleaning consolidant from fossil teeth.

Supplementary information

Table S1. Microwear summary statistics for occlusal and off-occlusal unclassified data

Occlusal			Angular disp.		Rayleigh	p	Rao	Orientation		(μm)	(μm)
Element	Tooth	Site	n	r	Z		U	p	μ	length	width
IT (R.max.)	1	5	246	0.824	166.946	<< 0.001	260.156	< 0.01	12.069	25.7	0.3
R. Maxilla	2	5	247	0.330	26.819	<< 0.001	181.339	< 0.01	2.846	41.2	0.3
	3	2	292	0.385	43.276	<< 0.001	191.210	< 0.01	21.942	46.6	0.3
IT (R. Dent.)	1	1	226	0.725	118.657	<< 0.001	226.531	< 0.01	43.134	45.0	0.3
R. dentary	1	1	629	0.594	221.844	<< 0.001	223.574	< 0.01	49.362	42.8	0.3
	1	3	216	0.652	91.699	<< 0.001	245.007	< 0.01	47.966	64.0	0.4
L. dentary	1	5	133	0.502	33.528	<< 0.001	209.256	< 0.01	80.207	58.8	0.4
	2	1	106	0.671	47.716	<< 0.001	213.387	< 0.01	73.370	74.2	0.3
	2	2	126	0.687	59.529	<< 0.001	218.644	< 0.01	73.456	101.9	0.9
	2	3	110	0.521	29.858	<< 0.001	206.899	< 0.01	66.541	65.7	0.5
	2	4	138	0.518	37.063	<< 0.001	202.970	< 0.01	73.904	85.2	0.8
	2	5	140	0.562	44.219	<< 0.001	211.248	< 0.01	70.139	74.1	0.5
	4	3	180	0.457	37.557	<< 0.001	193.452	< 0.01	63.627	74.0	1.0
	4	6	187	0.599	67.042	<< 0.001	211.255	< 0.01	69.297	77.8	0.8
Off-occlusal			Angular disp.		Rayleigh	p	Rao	Orientation		(μm)	(μm)
Element	Tooth	Site	n	r	Z		U	p	μ	length	width
IT (R. max.)	1	1	590	0.453	120.990	<< 0.001	177.093	< 0.01	76.771	42.0	0.4
R. maxilla	1	1	1118	0.181	36.631	<< 0.001	158.699	< 0.01	126.969	38.2	0.3
	1	3	363	0.275	27.383	<< 0.001	170.482	< 0.01	88.765	54.9	0.5
	2	1	280	0.511	73.014	<< 0.001	185.880	< 0.01	108.726	49.8	0.4
	2	3	313	0.115	4.145	0.016	168.035	< 0.01	96.512	33.8	0.4
	3	3	346	0.339	39.754	<< 0.001	166.715	< 0.01	103.397	52.6	0.5
	4	1	266	0.212	11.952	<< 0.001	158.257	< 0.01	7.899	42.0	0.3

Table S2. Microwear summary statistics for class 1 occlusal and off-occlusal data

Occlusal Class 1			Angular disp.		Rayleigh	Rao			Rayleigh (expected mean 32.61°)			Orientation	(μ m)	(μ m)
Element	Tooth	Site	n	r	Z	p	U	p	V	u	p	μ	length	width
IT (R.max.)	1	5	200	0.945	178.539	<< 0.001	302.348	< 0.01	0.910	18.209	<< 0.001	17.109	25.4	0.3
R. Maxilla	2	5	115	0.913	95.896	<< 0.001	259.422	< 0.01	0.912	13.824	<< 0.001	29.205	33.9	0.3
	3	2	172	0.921	145.986	<< 0.001	272.093	< 0.01	0.921	17.800	<< 0.001	30.995	42.4	0.3
IT (R. Dent.)	1	1	160	0.952	144.939	<< 0.001	276.642	< 0.01	0.951	17.017	<< 0.001	34.431	46.0	0.3
R. dentary	1	1	363	0.972	343.081	<< 0.001	300.911	< 0.01	0.969	26.112	<< 0.001	37.167	42.9	0.3
	1	3	123	0.955	112.144	<< 0.001	312.173	< 0.01	0.955	14.976	<< 0.001	32.688	65.7	0.5
L. dentary	1	5	37	0.944	32.985	<< 0.001	278.304	< 0.01	0.944	8.117	<< 0.001	34.628	52.9	0.4
	2	1	27	0.957	24.730	<< 0.001	282.523	< 0.01	0.954	7.010	<< 0.001	37.180	65.1	0.3
	2	2	42	0.957	38.486	<< 0.001	289.140	< 0.01	0.928	8.505	<< 0.001	46.826	85.1	1.3
	2	3	52	0.927	44.723	<< 0.001	265.993	< 0.01	0.919	9.367	<< 0.001	40.528	48.4	0.6
	2	4	39	0.892	31.011	<< 0.001	251.637	< 0.01	0.890	7.863	<< 0.001	29.383	42.5	0.5
	2	5	46	0.948	41.329	<< 0.001	290.298	< 0.01	0.939	9.002	<< 0.001	40.674	60.6	0.6
	4	3	59	0.881	45.758	<< 0.001	259.660	< 0.01	0.880	9.564	<< 0.001	31.331	58.9	1.0
	4	6	73	0.920	61.742	<< 0.001	264.616	< 0.01	0.918	11.090	<< 0.001	36.249	55.3	0.6
Off-occlusal Class 1			Angular disp.		Rayleigh	Rao			Rayleigh (expected mean 31.96°)			Orientation	(μ m)	(μ m)
Element	Tooth	Site	n	r	Z	p	U	p	V	u	p	μ	length	width
IT (R. max.)	1	1	198	0.921	167.810	<< 0.001	274.876	< 0.01	0.915	18.205	<< 0.001	38.391	39.7	0.4
R. maxilla	1	1	247	0.821	166.649	<< 0.001	256.091	< 0.01	0.817	18.160	<< 0.001	26.08	35.2	0.3
	1	3	98	0.927	84.261	<< 0.001	275.432	< 0.01	0.923	12.918	<< 0.001	37.653	51.8	0.5
	2	1	27	0.898	21.767	<< 0.001	272.237	< 0.01	0.882	6.481	<< 0.001	42.771	37.3	0.4
	2	3	80	0.917	67.204	<< 0.001	267.564	< 0.01	0.916	11.591	<< 0.001	30.862	29.1	0.3
	3	3	67	0.851	48.492	<< 0.001	243.352	< 0.01	0.850	9.845	<< 0.001	30.464	38.4	0.3
	4	1	108	0.907	88.784	<< 0.001	262.276	< 0.01	0.902	13.253	<< 0.001	25.975	40.5	0.3

Table S3. Microwear summary statistics for class 2 occlusal and off-occlusal data

Occlusal Class 2			Angular disp.		Rayleigh		Rao		Rayleigh (expected mean 82.92°)			Orientation	(μ m)	(μ m)
Element	Tooth	Site	n	r	Z	p	U	p	V	u	p	μ	length	width
IT (R.max.)	1	5	0											
R. Maxilla	2	5	21	0.801	13.485	<< 0.001	255.087	< 0.01	0.801	5.192	<< 0.001	81.434	52.7	0.4
	3	2	35	0.841	24.727	<< 0.001	269.917	< 0.01	0.836	6.992	<< 0.001	89.091	48.3	0.4
IT (R. Dent.)	1	1	59	0.903	48.120	<< 0.001	281.828	< 0.01	0.894	9.716	<< 0.001	74.984	43.9	0.3
R. dentary	1	1	220	0.852	159.518	<< 0.001	265.564	< 0.01	0.851	17.857	<< 0.001	81.604	42.2	0.3
	1	3	85	0.928	73.139	<< 0.001	279.288	< 0.01	0.922	12.023	<< 0.001	76.671	64.7	0.4
L. dentary	1	5	84	0.888	66.192	<< 0.001	263.639	< 0.01	0.881	11.419	<< 0.001	89.948	64.1	0.3
	2	1	76	0.906	62.333	<< 0.001	257.316	< 0.01	0.906	11.165	<< 0.001	83.005	75.0	0.3
	2	2	77	0.945	68.725	<< 0.001	273.221	< 0.01	0.944	11.719	<< 0.001	84.585	115.1	0.8
	2	3	52	0.944	46.356	<< 0.001	272.973	< 0.01	0.936	9.545	<< 0.001	90.493	82.4	0.4
	2	4	89	0.913	74.248	<< 0.001	275.188	< 0.01	0.913	12.184	<< 0.001	83.782	108.4	0.9
	2	5	81	0.902	65.942	<< 0.001	269.869	< 0.01	0.902	11.484	<< 0.001	82.904	88.0	0.5
	4	3	96	0.952	86.939	<< 0.001	286.123	< 0.01	0.948	13.131	<< 0.001	77.676	88.3	1.2
	4	6	112	0.927	96.263	<< 0.001	269.279	< 0.01	0.925	13.844	<< 0.001	86.749	92.0	0.9
Off-occlusal Class 2			Angular disp.		Rayleigh		Rao		Rayleigh (expected mean 90.27°)			Orientation	(μ m)	(μ m)
Element	Tooth	Site	n	r	Z	p	U	p	V	u	p	μ	length	width
IT (R. max.)	1	1	328	0.854	239.322	<< 0.001	253.473	< 0.01	0.854	21.878	<< 0.001	90.198	44.5	0.5
R. maxilla	1	1	394	0.9	319.061	<< 0.001	253.071	< 0.01	0.899	25.243	<< 0.001	88.116	42.4	0.3
	1	3	171	0.797	108.736	<< 0.001	257.852	< 0.01	0.797	14.742	<< 0.001	91.685	62.3	0.6
	2	1	142	0.882	110.400	<< 0.001	256.129	< 0.01	0.881	14.849	<< 0.001	92.439	59.8	0.4
	2	3	120	0.883	93.536	<< 0.001	268.312	< 0.01	0.880	13.628	<< 0.001	85.383	41.8	0.6
	3	3	190	0.896	152.548	<< 0.001	266.443	< 0.01	0.890	17.353	<< 0.001	96.824	64.5	0.6
	4	1	56	0.89	44.329	<< 0.001	256.236	< 0.01	0.886	9.376	<< 0.001	84.975	50.5	0.3

Table S4. Microwear summary statistics for class 3 occlusal and off-occlusal data

Occlusal Class 3			Angular disp.		Rayleigh		Rao		Rayleigh (expected mean 150.30°)			Orientation	(μm)	(μm)
Element	Tooth	Site	n	r	Z	p	U	p	V	u	p	μ	length	width
IT (R.max.)	1	5	46	0.804	29.769	<< 0.001	258.807	< 0.01	0.792	7.596	<< 0.001	160.400	27.0	0.3
R. Maxilla	2	5	111	0.865	83.090	<< 0.001	244.893	< 0.01	0.864	12.881	<< 0.001	147.986	46.5	0.4
	3	2	85	0.853	61.818	<< 0.001	250.963	< 0.01	0.853	11.119	<< 0.001	149.894	54.4	0.4
IT (R. Dent.)	1	1	7	0.802	4.505	0.006	200.126	< 0.05	0.798	2.987	<< 0.001	144.737	31.2	0.2
R. dentary	1	1	46	0.801	29.549	<< 0.001	256.697	< 0.01	0.792	7.599	<< 0.001	158.990	44.2	0.3
	1	3	8	0.914	6.687	<< 0.001	248.363	< 0.01	0.853	3.412	<< 0.001	171.414	30.2	0.3
L. dentary	1	5	12	0.871	9.094	<< 0.001	260.719	< 0.01	0.831	4.072	<< 0.001	133.020	39.6	0.3
	2	1	3	0.848	2.157	0.120			0.831	2.036	0.018	138.969	135.1	0.3
	2	2	7	0.953	6.355	<< 0.001	263.378	< 0.01	0.941	3.521	<< 0.001	141.279	57.6	0.4
	2	3	6	0.918	5.056	0.002	231.429	< 0.01	0.917	3.178	0.0001	148.190	69.3	0.7
	2	4	10	0.918	8.424	<< 0.001	252.854	< 0.01	0.895	4.004	<< 0.001	137.586	45.3	0.3
	2	5	13	0.876	9.974	<< 0.001	264.445	< 0.01	0.872	4.445	<< 0.001	144.684	35.5	0.4
	4	3	25	0.841	17.689	<< 0.001	260.359	< 0.01	0.841	5.944	<< 0.001	148.275	54.4	0.3
	4	6	2	1.000	1.998	0.138			0.862	1.725	0.043	119.930	97.8	1.2
Off-occlusal Class 3			Angular disp.		Rayleigh		Rao		Rayleigh (expected mean 145.09°)			Orientation	(μm)	(μm)
Element	Tooth	Site	n	r	Z	p	U	p	V	u	p	μ	length	width
IT (R. max.)	1	1	64	0.883	49.849	<< 0.001	260.197	< 0.01	0.868	9.819	<< 0.001	134.641	36.5	0.4
R. maxilla	1	1	477	0.872	362.513	<< 0.001	254.061	< 0.01	0.871	26.906	<< 0.001	147.317	36.3	0.3
	1	3	94	0.817	62.712	<< 0.001	250.994	< 0.01	0.814	11.156	<< 0.001	140.051	44.7	0.4
	2	1	111	0.909	91.730	<< 0.001	266.382	< 0.01	0.901	13.431	<< 0.001	137.662	40.1	0.4
	2	3	113	0.851	81.873	<< 0.001	244.182	< 0.01	0.851	12.796	<< 0.001	145.587	28.6	0.3
	3	3	89	0.795	56.186	<< 0.001	242.004	< 0.01	0.793	10.577	<< 0.001	148.934	37.8	0.4
	4	1	102	0.809	66.763	<< 0.001	250.173	< 0.01	0.805	11.500	<< 0.001	150.686	38.8	0.4

Table S6. Results of null hypothesis testing for differences in microwear between jaw elements. Occlusal data (14 sites from 8 teeth).

Occlusal (L.dentary, R.dentary & R.maxilla)	Unclassified			Class 1			Class 2			Class 3		
	d.f.	F	P	d.f.	F	P	d.f.	F	P	d.f.	F	P
Orientation does not differ between elements (Watson Williams F)	2,2973	646.52	< 0.0001	2,1505	181.00	< 0.0001	2,1084	19.83	< 0.0001	2,378	16.94	< 0.0001
Length does not differ between elements (one way ANOVA; log data)	2,2973	399.13	< 0.0001	2,1505	177.65	< 0.0001	2,1084	161.20	< 0.0001	2,378	2.45	0.087
Width does not differ between elements (one way ANOVA)	2,2973	38.85	< 0.0001	2,1505	116.05	< 0.0001	2,1084	60.63	< 0.0001	2,378	1.40	0.245
R does not differ between elements (one way ANOVA)	2,38	3.34	0.045	2,11	1.98	0.184	2,10	10.80	0.003	2,11	2.39	0.136
N does not differ between elements (one way ANOVA)	2,38	4.80	0.013	2,11	10.45	0.002	2,10	3.05	0.092	2,11	17.50	0.0004

CHAPTER 9

Quantitative analysis of dental microwear in hadrosaurid dinosaurs, and the implications for hypotheses of jaw mechanics and feeding

Published: *Proceedings of the National Academy of Sciences of the United States of America* 2009, 106 (27): 11194-11199

Understanding the feeding mechanisms and diet of non-avian dinosaurs is fundamental to understanding the paleobiology of these taxa and their role in Mesozoic terrestrial ecosystems. Various methods, including biomechanical analysis and 3D computer modelling, have been employed to generate detailed functional hypotheses, but in the absence of either direct observations of dinosaur feeding behaviour, or close living functional analogues, testing these hypotheses is problematic.

Microscopic scratches that form on teeth *in vivo* during feeding are known to record the relative motion of the tooth rows to each other during feeding and to capture evidence of tooth-food interactions. Analysis of this dental microwear provides a powerful tool for testing hypotheses of jaw mechanics, diet and trophic niche, yet quantitative analysis of microwear in dinosaurs has not been attempted. Here we show that analysis of tooth microwear orientation provides direct evidence for the relative motions of jaws during feeding in hadrosaurid ornithopods, the dominant terrestrial herbivores of the Late Cretaceous. Statistical testing demonstrates that *Edmontosaurus* teeth preserve 4 distinct sets of scratches in different orientations. In terms of jaw mechanics these data indicate an isognathic, near vertical posterodorsal power stroke during feeding, near vertical jaw opening, and propalinal movements in near anterior and near posterior directions. Our analysis supports the presence of a pleurokinetic hinge, and the straightness and parallelism of scratches indicate a tightly controlled occlusion. The dominance of scratched microwear fabrics suggests that *Edmontosaurus* was a grazer rather than a browser.

Reconstructing the feeding mechanisms and details of trophic ecology of extinct animals based on functional morphology is fraught with difficulty (Lauder 1995). In vertebrates, tooth form provides only a general guide to diet: the same tooth form can serve more than one function and that function can vary with specific feeding behaviour. Further complications arise because functional optimization of tooth form can be constrained by the need to process fallback foods during times of resource scarcity (Ungar 2004) and animals with apparently specialised feeding apparatus can have generalist diets (Ferry-Graham *et al.* 2002). These problems are especially acute in groups like herbivorous non-avian dinosaurs, where most species have generalised homodont dentitions and lack close living analogues.

Among herbivorous dinosaurs, feeding of hadrosaurids has attracted particular attention. They were the dominant herbivorous vertebrates in many Late Cretaceous ecosystems, in terms of both species-richness and abundance, and achieved a near-global distribution (Horner *et al.* 2004; Weishampel *et al.* 2004). This success is frequently attributed to the complex jaw mechanisms possessed by these taxa, which would have given them a level of masticatory prowess equal to that of many extant mammals (e.g., Weishampel and Norman 1989). Current models of feeding mechanisms in hadrosaurid dinosaurs are based on analyses of functional morphology and rely on interpretations of musculature rather than direct evidence. No extant species has a sufficiently similar skull morphology to act as a convincing functional analogue, and no fossil evidence exists to show the size and shape of the interarticular fibrocartilages and the limitations these would have placed on jaw motions. Here we present the results of quantitative tooth microwear analysis of a hadrosaurian dinosaur, and demonstrate how these provide a robust test of functional hypotheses.

Previous research into hadrosaurid feeding mechanisms reached contradictory conclusions. The extensive early work of Ostrom (1961) suggested propalinal translation of the mandibles (an anteroposterior movement of the lower jaw during the power stroke). This was later questioned (Hopson 1980), and tooth wear was used to infer side to side (transverse) movements of the mandibles relative to the maxilla. Norman and Weishampel (1984; 1984; 1985; 1989) conducted kinematic and detailed functional anatomical analyses of all available hypotheses of hadrosaurid jaw mechanics and postulated a novel jaw mechanism, termed pleurokinesis. In this model isognathic vertical adduction of the lower jaws generated a transverse power stroke. This was brought about by lateral rotation of the maxillae and suspensorium relative to the skull roof, driven by contact between the dentary and maxillary teeth during occlusion. Lateral rotation of the maxillae was accommodated by a pleurokinetic hinge (between the maxilla/jugal/quadrates and the akinetic skull) and was associated with slight propalinal movements caused by abduction and retraction of the quadrates (streptostyly). However recent work involving 3D modelling of feeding kinematics in *Edmontosaurus* has suggested that pleurokinesis would generate extensive secondary (intracranial) movements beyond the pleurokinetic hinge (Rybczynski *et al.* 2008). Testing of these functional models has been difficult because of the absence of direct evidence for the mastication process in hadrosaurids.

Quantitative analysis of tooth microwear offers a hitherto unexplored route to testing feeding mechanisms in non-avian dinosaurs. Microwear refers to the microscopic polished, scratched or pitted textures produced *in vivo* by the actions of abrasives in food and by the compressive and shearing forces that act on teeth during feeding (Walker *et al.* 1978; Teaford 1988a). Quantitative analysis of tooth microwear is an extremely powerful tool and has been applied extensively to fossil primates and

hominins in order to evaluate the role of dietary changes in human evolution (Gordon 1984a; Teaford and Ungar 2000). Applied to extinct non-primate mammals, quantitative tooth microwear analysis has also provided direct evidence of tooth use, diet and feeding (Walker *et al.* 1978; Teaford and Byrd 1989; Ungar *et al.* 2007) and has revealed how feeding in ungulates has tracked past environmental change (e.g. Semprebon *et al.* 2004).

Microwear analysis is starting to be applied widely to dinosaurs (Fiorillo 1991, 1998; Upchurch and Barrett 2000; Schubert and Ungar 2005) and recent research on living and fossils fishes suggests that quantitative microwear analysis has broad applicability beyond mammals (Purnell *et al.* 2006; Purnell *et al.* 2007), but to date there has been no quantitative analysis of tooth microwear in dinosaurs. However, there are significant differences between dinosaur and mammal feeding mechanisms that make microwear analysis and interpretation more complicated. Dinosaur jaws articulate differently and lack the highly differentiated heterodont dentition of mammals. This means that, unlike mammals, comparison of functionally equivalent wear facets developed on homologous tooth cusps between different individuals and taxa is not possible. Another significant difference concerns tooth retention. In mammals, which retain their permanent dentitions until death, informative tooth wear forms over a short period relative to the functional life of the tooth. By contrast, dinosaurs, like other reptiles, shed and replaced their teeth continually, so the functional life of a tooth could be as short as a few weeks or months (Erickson 1996). Is that long enough for informative microwear patterns to develop?

This is just one of several fundamental questions that must be addressed before quantitative microwear analysis can be applied to non-avian dinosaurs. Microwear analysis by definition requires relative high magnification of tooth surfaces and

consequently samples data from small areas, only a few hundred micrometres across. Can such small areas provide data that is representative of microwear over the large functional surface of a dinosaur tooth battery? Given the lack of homologous facets, how do we sample microwear in dinosaurs?

Here we test the null hypotheses that microwear does not differ between sample sites within the occlusal surface of a tooth and that microwear does not differ between teeth along a tooth row within an individual. We show that hadrosaurid dinosaur teeth have well developed microwear signatures that allow us to conduct robust statistical testing of these hypotheses, and we demonstrate that quantitative microwear analysis can constrain details of jaw motions and provide robust tests of hypotheses of feeding mechanics in dinosaurs.

Results and Discussion

Microwear patterns. Microwear was sampled from 30 sites on the occlusal surface of 13 *Edmontosaurus* teeth (see *Material and Methods*). Visual inspection of micrographs clearly demonstrated that hadrosaur teeth do preserve microwear, confirming Weishampel's qualitative observations (Weishampel 1984), with scratched textures dominating (we use scratches throughout this paper to refer to all microwear features on a tooth; no pits were detected). Scratches are not random, appearing to fall into a small number of classes within each of which scratches are straight and subparallel, but with an orientation that differs from that of other classes.

To test the hypothesis that discrete classes of scratch exist, raw microwear data (2588 features from 20 sites on 10 teeth from the same maxilla) were partitioned into 4 subsets (classes 1 - 4) based upon visual assessment of scratch orientation.

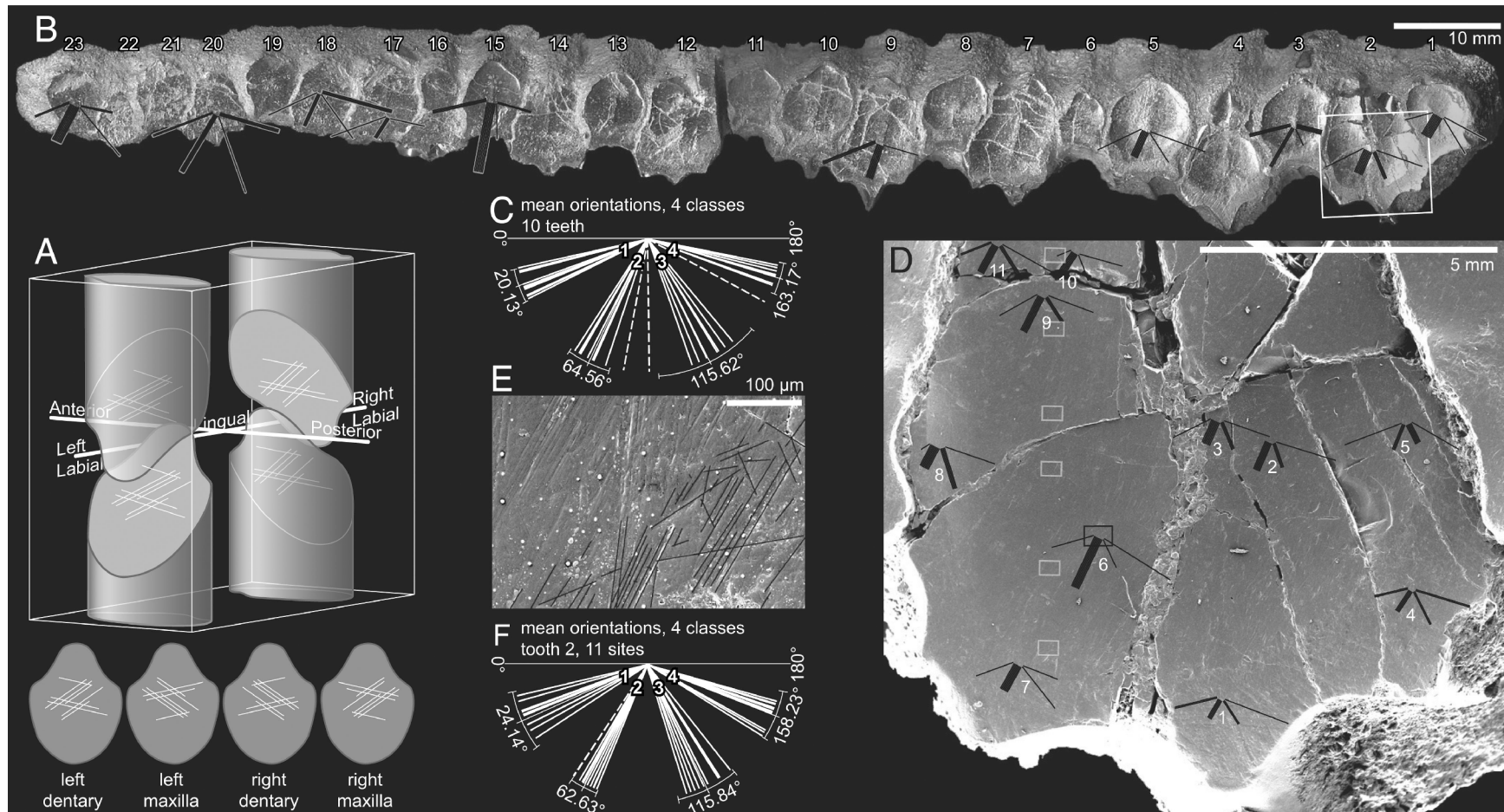


Fig. 1. Microwear in *Edmontosaurus*. (A) Orientation of functional surfaces (wear facets) on teeth, in approximate life orientation; diagrams below show these same 4 functional surfaces oriented with tips upward and viewed perpendicular to the occlusal plane. (B) Right maxilla, specimen NHMUK R3638, anterior to left. Vector plots indicate mean scratch orientation and relative length for each of the 4 classes in 10 teeth, line weight proportional to number of scratches. (C) Mean orientations for each class of scratches in each of the 10 teeth; for each class, the mean of the mean orientations with 99% confidence interval is shown. Dashed lines lie outside the confidence interval. (D) Second tooth from posterior (box in B). Vector plots indicate mean scratch orientation and relative length for each of the 4 classes in 11 sites, line weight proportional to number of scratches. Gray boxes show sites sampled for transect data (Fig. S1): 1 toward tip, 6 toward base; site 7 more basal than field of view shown. (E) One of the sampled areas (black box in D); diagonal lower right shows feature markup from Microware 4.0.2. (F) Mean orientations for each class of scratches in each of the 11 sites; for each class, the mean of the mean orientations with 99% confidence interval is also shown. Dashed lines lie outside the confidence interval.

Fig. 1 illustrates these findings for a central site from each of 10 teeth along the tooth row ('between teeth' analysis) and for 11 sites within one of those teeth ('within tooth' analysis). Discriminant function analysis (DFA) provides strong confirmation that the microwear data fall into four distinct classes – 98.3% of scratches classified by visual inspection were correctly assigned by DFA. Rather than conduct subsequent statistical testing on these imperfectly classified data, the DFA results were used to reassign the few incorrectly assigned scratches to their correct class (leading to 100% correct discrimination; see Table 1 for summary).

Table 1. Summary statistics from pooled raw microwear data (20 sites on 10 teeth on maxilla NHMUK R3638) partitioned into 4 classes based on feature orientation.

Subgroup	Class 1	Class 2	Class 3	Class 4
No. of Observations	300	1581	424	283
Angular dispersion, R	0.95	0.93	0.89	0.95
Mean orientation (mean vector, μ)	15.91°	63.29°	117.30°	164.57°
95% confidence interval for μ	$\pm 1.02^\circ$	$\pm 1.02^\circ$	$\pm 1.31^\circ$	$\pm 1.08^\circ$
99% confidence interval for μ	$\pm 1.35^\circ$	$\pm 0.55^\circ$	$\pm 1.72^\circ$	$\pm 1.42^\circ$
Mean scratch length, μm	72.33	52.85	54.75	70.85
Log mean scratch length, μm	4.04	3.74	3.74	4.02
Mean scratch width, μm	1.59	1.68	1.54	1.42

Analysis of this dataset revealed significant differences in scratch count, orientation, length and width between classes (Table 2). A test based on the mean of means (see below) also rejects the null hypothesis that scratch orientation does not differ between classes (99% and 95% confidence intervals; Table 1). We were unable to reject the null hypothesis that angular dispersal (i.e., the degree of parallelism of scratches as measured by R, mean vector length) does not vary between classes.

Pairwise comparisons (Tukey Kramer HSD for linear variables, Watson-Williams F for axial variables) indicate that, for the within tooth data, orientation differs significantly between all classes and that for length all classes differ significantly except 2 and 3 ($P < 0.05$).

Table 2. Results of null hypothesis testing for differences in microwear collected from 11 sites on 1 tooth (within-tooth; 8 dentine, 3 enamel sites, tooth 2) and from single sites on each of 9 teeth (between-tooth; all dentine) on maxilla NHMUK R3638

	Within-tooth			Between-teeth			Within-tooth, enamel			Within-tooth, dentine		
Null hypothesis	d.f.	<i>F</i>	<i>P</i>	d.f.	<i>F</i>	<i>P</i>	d.f.	<i>F</i>	<i>P</i>	d.f.	<i>F</i>	<i>P</i>
Orientation does not differ between classes (Watson Williams <i>F</i> ; W,B,WE,WD)	31,446	3794.49	0.0001	31,380	3119.81	0.0001	3,209	937.85	0.0001	31,233	2918.1	0.0001
Log Length does not differ between classes (one way ANOVA; W,B,WE,WD)	31,446	30.49	0.001	31,380	12.11	0.0001	3,209	30.89	0.0001	31,233	15.02	0.0001
R does not differ between classes (one way ANOVA)	3,39	1.644	0.194	3,34	0.83	0.485	3,8	0.39	0.76	3,27	1.56	0.22
N does not differ between classes (one way ANOVA; W,B,WE,WD)	3,39	16.48	0.0001	3,34	6.69	0.0011	3,8	6.52	0.01	3,27	23.28	0.0001
Width does not differ between classes (Kruskal Wallis one way; W,B,WD)	31,446	χ^2 19.27	0.0002	31,380	χ^2 19.54	0.0002	3,209	χ^2 7.18	0.07	31,233	χ^2 17.93	0.0005

W, B, WE, WD in parentheses, indicate for which dataset the null hypothesis is rejected ($P < 0.05$). W, within-tooth; B, between-teeth; WE, within-tooth, enamel sites; and WD, within-tooth, dentine sites.

For the between-tooth data, orientation differs significantly between all classes; length differs significantly except between classes 1 and 4, and 2 and 3 ($P < 0.05$). Variation within class for both within and between tooth datasets is illustrated in Fig. 1C and 1F.

Analysis of microwear orientation. Despite the increasing use of microwear analysis, there has been little discussion of analysis of feature orientations and statistical hypothesis testing. A few authors have acknowledged that, strictly speaking, standard tests based on properties of linear distributions are not applicable to directional data (e.g. Gordon 1984a; Teaforde and Byrd 1989), but we are unaware of any analysis that has applied directional statistical tests to microwear data. Rather, non-parametric linear statistical tests have been applied, either with or without explicit justification (Gordon 1984a; Teaforde and Byrd 1989; Charles *et al.* 2007). In order to determine how best to test our null hypotheses we applied three different tests (one based on linear distribution, two specific to axial data) to a set of class 2 scratch orientation data sampled from 7 sites along a straight line transect from tip to base of tooth 2 (Fig. 1 and Fig. S1).

Scratches are straight, and the data exhibit a consistently high degree of parallelism (i.e., angular dispersion as measured by mean vector length, R , > 0.97 (Zar 1999)) and the Rayleigh uniformity test along with the V Test show the pooled data for the 7 sites to be non-uniformly distributed, with a significant mean orientation ($V > 0.96$, $P < 0.001$). Two alternative interpretations of these data are possible: either the samples are drawn from a single population of scratches that are straight, strongly parallel and occur over the whole length of the transect (i.e., orientation is the same across the surface of the tooth), or the samples are drawn from multiple populations of scratches which differ slightly in orientation, but within which scratches are straight and

parallel. For the purposes of this study, with controlled sampling across the transect, it is quite clear that the first of these hypotheses is correct, yet two of the tests reject it (type 1 error): a non-parametric Wilcoxon test shows significant differences between the 7 samples ($P < 0.05$) as does the Watson-Williams F-test (Fisher 1993), with pairwise testing indicating significant differences ($P < 0.05$) in mean feature angle in 10 of the 21 comparisons. Even when sites 1 to 4 are compared, which are close together and clearly the most similar, the Wilcoxon test finds significant differences between all the sites except 1 and 2, and the Watson-Williams F-test finds that site 4 differs significantly from sites 1 and 2. The results of this analysis indicate that when testing for differences in microwear scratch orientation between sample sites the Wilcoxon and Watson-Williams F-test are susceptible to type 1 errors. Taken at face value, the results of these tests would lead us to reject the hypothesis that scratch orientations for the seven sites are drawn from the same population (i.e., their means differ), when in fact they are drawn from the same population and, in the context of this analysis, the means are not significantly different. The third test, utilising confidence intervals (CI) calculated for the mean of means (e.g. Grigg and Underwood 1977; Batschelet 1978), yields correct results (i.e., the means of the 7 sites all fall within the 99% CI for the mean of means; see Table 3). This provides a less error prone yet appropriately stringent statistical test, and we therefore used it for all subsequent testing of class mean orientations. Our analysis does not support the view advocated in previous analyses of microwear orientation data (Gordon 1984a; Teaford and Byrd 1989; Charles *et al.* 2007) that axial data (i.e., distributed through 0-180°) can be treated as linear data and subjected to linear statistical tests. This approach would thus have led us to wrongly reject the hypothesis that mean orientation does not differ between sites, and previous analyses of this type may have made similar errors.

Table 3. Data for transect across tooth 2 (class 2; 7 sites): means (μ) by site, mean of means, and 99% confidence interval

Site	1	2	3	4	5	6	7
Angular dispersal, R	0.995	0.995	0.975	0.996	0.998	0.977	0.97
Mean vector, μ	62.235	62.598	62.548	64.423	61.704	59.375	66.056
Mean of means 62.702, 99% confidence 58.28 - 67.16							

Analysis of the within tooth and between tooth datasets (Table S1 and Table S2) reveals that overall, we can reject the hypothesis that data within classes for each site are uniformly distributed (i.e., they show a preferred orientation; Rayleigh's Uniformity Test and Rao's Spacing Test, $P < 0.05$). Of the 77 samples tested (4 classes, 20 sites, 3 sites with $n = 0$) there are only 3 exceptions to this result: a class 1 and a class 4 sample on tooth 2, and a class 3 sample on tooth 5, but in all three cases the numbers of scratches assigned to the class that failed the test was three or fewer). Mean orientation for each class for each site does not differ significantly from the overall class mean (pooled data, all sites, all teeth; V-Test, $P < 0.05$).

For the within tooth dataset (testing class 1 data from 11 sites, class 2 data from 11 sites, and so on for each of the 4 classes), only 2 between-site differences in mean orientation are significant (99% CI test; Fig. 1 and Table S1; we note, however, that like the analysis of the transect data, application of linear statistical tests such as t tests, or nonparametric Mann-Whitney/Wilcoxon tests wrongly indicates highly significant differences ($P < 0.01$) for a large number of sites).

In the between-tooth analysis, tooth-to-tooth variation in class mean orientation is significant in only 4 of the 38 samples (99% CI test; Fig. 1 and Table S2). Orientation does not vary significantly with distance from the posterior of the jaw except for class 4, which exhibits a strong correlation (circular-linear correlation: $r = 0.72$, $P = 0.02$) (Fisher 1993; Mardia and Jupp 2000). For class 4 scratches, R exhibits a strong positive

correlation with distance from the posterior of the jaw ($r = 0.9$, $P < 0.01$); for class 2 scratches the correlation is also significant, but weaker and negative ($r = -0.65$, $P = 0.04$).

To assess variation between individuals, we analyzed teeth selected from an additional right maxilla, a left maxilla and a right dentary (with data from the left maxilla and right dentary suitably transformed; Fig. 1). This yielded comparable results to our previous analyses: scratches within classes have preferred orientations, and the mean orientation for each class from each site falls within the 99% confidence limits of the means of means calculated from both the between tooth and the within tooth datasets (Table S2).

Functional interpretation and discussion. Microwear on occlusal tooth surfaces is created by tooth-to-tooth and tooth-food-tooth contact during biting and chewing (Teaford 1988a). Thus, by comparing our actual scratch data with the patterns predicted from the published models of jaw mechanics in hadrosaurids, we can provide a robust test of the various functional hypotheses. Predicted microwear patterns are as follows: (i) Propalinal action (Ostrom 1961) would have produced dominant scratch orientations near the horizontal (anteroposterior). (ii) Vertical adduction followed by a transverse (labiolingual) power stroke and slight propalinal action (Norman and Weishampel 1985) would have produced dominant scratch orientations near 90° to the tooth row long axis (inclined in 3D at the same angle as the occlusal surface), coupled with less dominant, near horizontal scratches. (iii) Secondary movements (disarticulation of the facial bones during the power stroke) and rotation of the mandibles about their long axes during occlusion (Rybczynski *et al.* 2008) would cause scratch curvature and systematic variation in microwear scratch orientation: mandibular rotation (labio-

lingual, pivoting around the pre-dentary) would lead to an increase in lateral movement (and hence systematic change in scratch orientation) distally along the length of the tooth row. Disarticulation of the facial bones would cause multiple changes in the relative attitude of the maxillae, leading to variations in scratch orientation across the surface of a tooth and between adjacent teeth.

How does the pattern of microwear in *Edmontosaurus* fit these predictions? That scratches occur as four distinct classes with significantly different orientations suggests a more complex jaw action than was initially anticipated or has been suggested by previous authors. The 4 classes reflect 4 distinct jaw motions: 2 around 20° from the long axis of the tooth row (classes 1 and 4), 1 at 110° (class 3), and the dominant pattern 60° from the axis (class 2). On the inclined plane of the functional surface of the tooth battery (50° slope, 7.5° rake relative to sagittal plane (Ostrom 1961; Weishampel *et al.* 2004)) these orientations equate to the following 3D axes (relative to anterior direction in horizontal plane): class 1 trends 11°, and plunges 21°; class 2 trends 50°, and plunges 45°; class 3 trends 121°, and plunges 43°; class 4 trends 164°, and plunges 9° (see Fig. S2 for stereographic projection).

We interpret class 2 scratches as being formed during the power stroke, and that most food processing jaw motions were in this direction: scratches in this class outnumber all other scratches (both combined (Table 1), and in all sites except 4 of the 23 sampled (Table S1 and Table S2)) and cut across microwear fabrics in other orientations because they are more deeply incised into the tooth surface (up to 3 µm deep). This indicates more frequent movements and higher forces. The orientation of this dominant microwear indicates that jaw closure was not brought about by pure vertical adduction (which equates to a trend of 82.5 ° and plunge of 50° on the occlusal surface). This steeply oblique motion with a posterior component was, however, much

closer to the vertical adduction and/or lateral translation predicted by the pleurokinetic model than to propalinal movements (trending 30° off pure vertical adduction; Fig. S2). Other points of note are the straightness of class 2 scratches, their high degree of parallelism (high R values, increasing towards the jaw hinge), the lack of variation in mean orientation within a tooth and the lack of significant variation in orientation along the length of the jaw (Fig. 1; Table S1 and Table S2). These data provide direct evidence that the leading edges of the maxillary and dentary tooth batteries were parallel during jaw closure (i.e., motion was not scissor like)(Galton 1973; Weishampel 1983; Crompton and Attridge 1986), and that jaw articulation was very tightly constrained.

Class 3 scratches, in contrast, vary more in mean orientation, both within and between teeth (Fig. 1, Table S1 and Table S2), and have lower overall R values (Table 1), indicating that this second steeply oriented oblique motion (trending approximately 40° off pure vertical adduction/lateral translation) was under looser mechanical constraint. This suggests that these scratches were formed during jaw opening. This is consistent with models of jaw opening in herbivorous reptiles (King 1996).

Class 1 and 4 scratches are less frequent and were formed by propalinal action, but we are unable to determine whether scratches assigned to class 1 were formed during anteroposterior (palinal) or posteroanterior (proal) movement, and the same is true of class 4 scratches. That the orientation of class 1 and 4 scratches does not differ significantly between maxillary and dentary teeth, indicates that they formed while the teeth were in occlusion. This evidence of propalinal movement, albeit weaker and less frequent, is somewhat surprising given that enamel thickness (greater on the lingual margin of dentary teeth and on the labial margin of maxillary teeth) seems to be strongly adapted to the transverse power stroke, with thicker enamel on the leading

edge of the teeth (Norman and Weishampel 1985). The change in the orientation of Class 4 scratches and the increase in parallelism along the length of the jaw indicates slight rotation of the tooth row and a greater freedom of movement at the back of the jaw during formation of these scratches.

Except for class 4, the lack of significant systematic variation in scratch orientation along the tooth row indicates that there was no marked long axis rotation of the jaw element in the horizontal plane during feeding. However, the strong parallelism and straightness of the scratches, especially those in classes 1, 2 and 4, and the lack of variation, both within and between teeth, is not consistent with disarticulation of facial bones during jaw closure (Rybczynski *et al.* 2008).

All but three of our sample sites were from dentine surfaces. It has been suggested that dentine microwear may be unsuited to quantitative analysis (Lucas 2004), but our results do not support this. Quantitative analysis of scratch orientations provides direct evidence of both steeply inclined and anteroposterior relative motion of the jaws during feeding. This confirms that the predictions of both Ostrom (Ostrom 1961) and Norman & Weishampel (Norman and Weishampel 1985) were correct in part, but our data provide direct evidence of high-angle oblique adduction and an isognathous oblique transverse power stroke, which is consistent with and supports the hypothesis of flexure along a pleurokinetic hinge. If class 3 scratches were formed in the way we suggest above, this lends additional support to the hypothesis as it implies tooth on tooth contact during at least part of the jaw opening phase of feeding.

In terms of our initial hypotheses, our results clearly demonstrate that in *Edmontosaurus*, teeth exhibit microwear that, within classes, does not differ between sample sites within the occlusal surface of a tooth, and differs little between teeth along a tooth row. We also found no significant differences between individuals. Perhaps

surprisingly, our results demonstrate that the microwear in an area of 0.1 mm^2 provides a reasonably representative sample of the whole tooth, and the whole jaw, and thus provides reliable information about the diet and jaw mechanics of an individual animal. One important implication of this result is that microwear based analysis of jaw mechanics in hadrosaurs could be carried out using isolated teeth. Obviously, these are much more common as fossils than complete skulls or substantial parts of dentary and maxilla elements. Whilst relatively complete jaw elements provide a frame of reference for tooth orientation within the jaw and allow more detailed testing of mechanical hypotheses, being able to conduct microwear analysis based on isolated teeth hugely increases the potential database for such work.

In addition to providing robust tests of models of jaw mechanics, microwear is also informative with regard to diet. In herbivorous mammals, microwear textures in grazers (grass eaters) differ from those of browsers (which eat less abrasive vegetation, such as leaves, and twigs) (Solounias *et al.* 1988). If the same microwear-diet relationship holds true for herbivorous dinosaurs, the dominance of scratches and lack of pits on both the dentine and enamel of the teeth of *Edmontosaurus* indicates that they were grazers rather than browsers. Early grasses certainly existed in the Cretaceous (Prasad *et al.* 2005), but it is unlikely that they were common enough to have formed a major part of herbivore diets, and it is tempting to conclude that, if they grazed, *Edmontosaurus* fed on plant material with similar mechanical and abrasive properties to those of grass. There has been much speculation about the diet of herbivorous dinosaurs. Direct evidence from gut contents and coprolites (Molnar and Clifford 2000; Ghosh *et al.* 2003; Chin 2007; Tweet *et al.* 2008) is rare and often tenuous but indicates a range of plant food materials including hornworts, liverworts, lycopsids, ferns, horsetails, twigs, branches, needles, leaves, bark, fruit and seeds. Of these only the

horsetails would appear to be sufficiently abrasive to generate the microwear patterns of a grazer (silica concentration in horsetails >25% dry mass (Chen and Lwein 1969)).

However, we cannot assume that silica phytoliths alone are responsible for tooth microwear as there is evidence that heavily striated enamel surfaces in grazing mammals can be caused by high levels of soil ingestion (Mainland 2006). If they grazed on low-stature vegetation this could also be case with *Edmontosaurus*.

Our results demonstrate that, with appropriate statistical testing, microwear analysis of dinosaur teeth can provide robust tests of hypotheses of jaw mechanics and feeding mechanisms. More hadrosaurid specimens and specimens of other ornithopods need to be analysed to determine how microwear varies within and between species, but morphological analysis suggests that hadrosaurs were ecologically comparable to modern ungulates (Carrano *et al.* 1999). In mammals, microwear patterns can be associated with specific food plants and trophic niches (Rivals and Deniaux 2003; Merceron *et al.* 2007; Calandra *et al.* 2008): microwear has great potential for unravelling the mystery of dinosaur feeding mechanisms, diet, and trophic niche partitioning.

Materials and Methods

The teeth studied are from left and right maxillae and dentaries of the hadrosaurid ornithopod *Edmontosaurus* sp., that were collected from the Lance Formation (Upper Cretaceous, late Maastrichtian) of Niobrara County, Wyoming (right maxilla NHMUK R3638, complete, with ca. 70% of full tooth row preserved; right maxilla NHMUK R3653, complete with full but damaged tooth row; left maxilla NHMUK R3654, preservation as R3653; right dentary NHMUK R3658, fragment). For details of specimen preparation and microwear data acquisition see supporting information SI

Text. All microwear features within each sampling area were recorded. All microwear was scored by the same operator (VW) to minimise operator error (Grine *et al.* 2002; Purnell *et al.* 2006). The software used to score microwear (Ungar 2001) produces overlay files of x/y co-ordinates. It also calculates summary statistics for feature length, width and orientation, but these were not used in this study. Our analysis was based on raw microwear data extracted from Microware 4.02 output as x/y co-ordinates and processed using simple trigonometric functions in a database to derive the length, width, and long axis orientation for every feature in a sample site. Length data were not normally distributed and were therefore log transformed prior to statistical analysis. Previous microwear analyses that have used mean scratch length have not taken this into account.

Statistical testing and analyses of microwear data were conducted using JMP IN 5.1 (SAS Institute, Cary, NC) and Oriana 2.02e software (Kovach 2006). Discriminant function analysis (DFA) was performed to test the robustness of the allocation of data to orientation classes. DFA was first performed using scratch length, count, angular dispersion and orientation combined, and then using orientation alone (the latter reported here). Within tooth and between tooth variation were also tested using ANOVA and a variety of other statistical techniques. Orientation data are directional, and such data have statistical properties that differ from those upon which standard statistical tests are based. Consequently, our hypothesis testing employed a number of tests specifically formulated for data of this kind.

Acknowledgements. We thank Adrian Doyle and the Palaeontology Conservation Unit, as well as Sandra Chapman, at the Natural History Museum (London), for advice regarding cleaning consolidant from fossil teeth and access to material. Alicona are

thanked for the loan of a lens and objective head for the Alicona IFM.

Coltène/Whaledent are thanked for donating polyvinylsiloxane moulding compound.

Paul Hart and 3 reviewers provided helpful comments on the manuscript. MAP

acknowledges the funding of the Natural Environment Research Council.

Supporting information

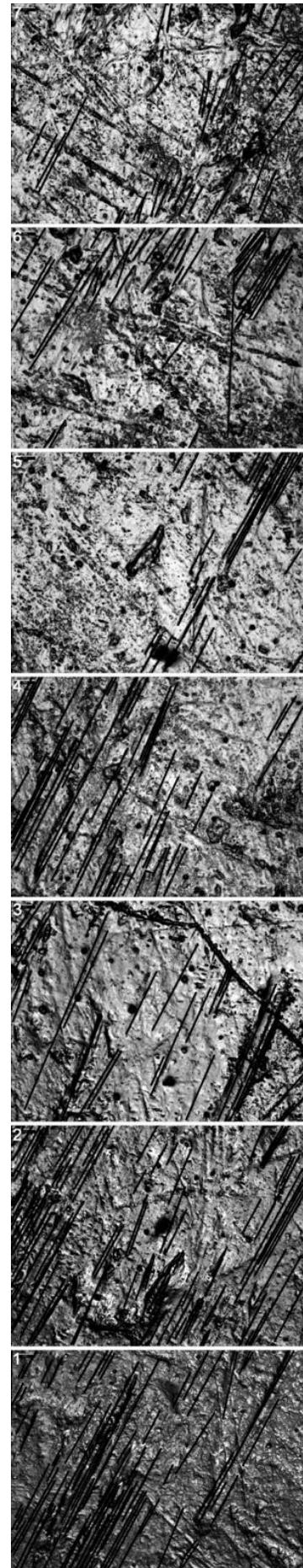
SI text

Methods of microwear sampling and imaging. To avoid coating original material or subjecting it to analysis under vacuum, high-resolution epoxy replicas were prepared for scanning electron micrography by using methods known to reproduce microwear with high fidelity (Galbany *et al.* 2006; Williams *et al.* 2006). Occlusal surfaces of teeth were cleaned nonabrasively with a combination of liquid acetone/ethanol and ethomeen-based solvent gels (Hedley 1980; Southall 1988) by using techniques developed at the Natural History Museum Palaeontology Conservation Unit for cleaning without abrasion. Moulds were prepared using polyvinylsiloxane impression medium (Coltene/Whaledent, Speedex Light). Casts were made using Araldite 20/20 epoxy resin. Replicas were coated with gold (Emitech K500X sputter coater).

Imaging for the main analyses of within-tooth and between-tooth variation used a Hitachi S-3600N SEM (SE, TSE mode) with settings standardized at: accelerating voltage 15 kV, working distance 18 mm, and automatic contrast and brightness. Standardization is important for comparability of data sets (Gordon 1988). For image capture the orientation of the occlusal surface of the teeth was standardized, with the long axis of the tooth row and the flat occlusal surfaces of the teeth perpendicular to the electron beam. SEM images were captured at a magnification of 300, providing a sampling site field of view of 417 x 312 μm , comparable with that commonly used in analysis of occlusal microwear in mammals (Grine *et al.* 2002; Scott *et al.* 2005). Microwear was sampled at 11 different sites on 1 distal tooth of *Edmontosaurus* right maxilla NHMUK R3638 (tooth 2), and at 1 central site on each of 9 further teeth from the same tooth row. Additional data were obtained from 1 central site from 1 tooth in each of the 3 additional specimens (right maxilla NHMUK R3653, left maxilla

NHMUK R3654 and right dentary NHMUK R3658). Sampling sites were selected in order to maximise the chances of obtaining *in vivo* microwear and minimise post mortem artefacts. The latter are less problematic than might be supposed, because physical and chemical post mortem processes tend to obliterate microwear features, rather than create artefacts (Teaford 1988b; King *et al.* 1999). In order to evaluate alternative statistical approaches to testing for differences in feature orientation between sites, microwear was also sampled at 7 sites along a vertical transect across *Edmontosaurus* right maxilla NHMUK R3638 (tooth 2). Images for this analysis were acquired using an Alicona IFM (Infinite Focus Microscope – an optical, focus variation based technique). Sampling site field of view was 285 x 216 μm ; illumination coaxial. The 3D surface data acquired during this sampling were also used to assessments of scratch depth. Digital scanning electron micrographs and IFM images were downsampled to 900 pixels wide by 675 pixels high using Adobe Photoshop 7. Microwear data were generated using the custom software package Microware 4.02 (Ungar 1995, 2001) running on a Dell Latitude D505 computer running Windows XP Professional with a 15 inch active matrix TFT display set at a screen resolution of 1024 x 768 pixels, resulting in an onscreen magnification of approximately x 630 for SEM and x 1000 for IFM.

Fig. S1. Transect from apex (site 1) to base (site 7) across the functional surface of second tooth from posterior, right maxilla specimen NHMUK R3638 (see Fig. 1) for locations of sample sites). Class 2 microwear features are marked. Field of view is 285 μm wide.



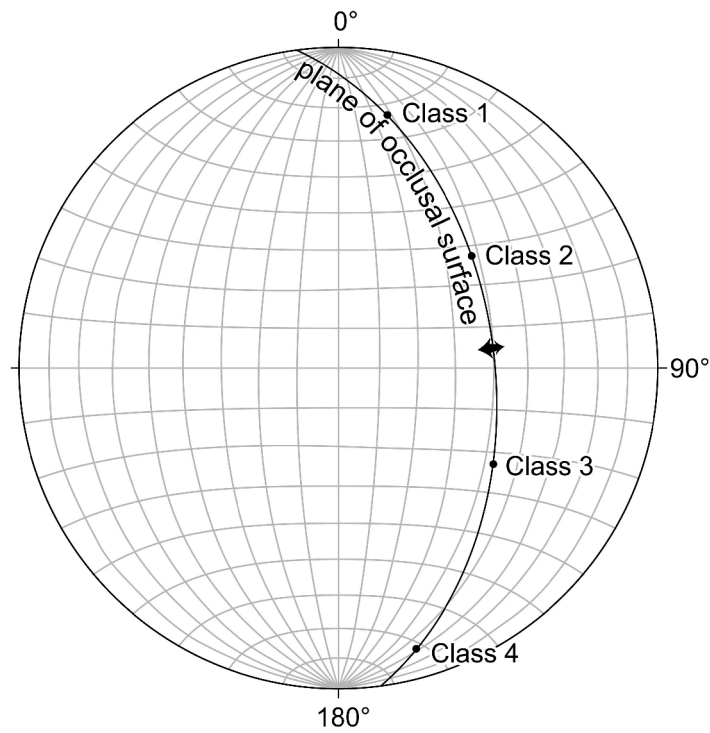


Fig. S2. Equal area stereographic projection showing tooth occlusal surface inclined at 50° from horizontal, raking 7° from anterior, and containing microwear classes 1-4 (in vivo orientations). Microwear data were scored in images acquired from horizontally oriented surfaces and they were reoriented by using standard stereographic techniques. Arrow shows trend and plunge in tooth surfaces of pure orthal movement. Pure lateral translation, relative to sagittal plane, would be along the 90° axis of stereonet.

Table S1. Analysis of variation in orientation between sites, within tooth 2 of maxilla NHMUK R3638 (8 dentine sites , 3 enamel sites)

	enamel sites			dentine sites							
Class 1	T2-1	T2-4	T2-5	T2-2	T2-3	T2-6	T2-7	T2-8	T2-9	T2-10	T2-11
N	10	14	10	0	17	13	24	2	5	4	22
Angular dispersal R	0.972	0.98	0.95		0.944	0.953	0.931	0.988	0.97	0.945	0.935
Rayleigh test (Z , p)	9.45 , << 0.001	13.45 , << 0.001	9.02 , << 0.001		15.17 , << 0.001	11.82 , << 0.001	20.81 , << 0.001	1.95 , 0.146	4.71 , 0.002	3.57 , 0.016	19.23 , << 0.001
Rao's spacing (U , p)	273.15 , < 0.01	293.66 , < 0.01	266.63 , < 0.01		283.93 , < 0.01	272.15 , < 0.01	268.91 , < 0.01		256.15 , < 0.01	218.20 , < 0.05	269.55 , < 0.01
mean orientation (μ)	13.72	13.36	20.62		26.45	15.8	19.98	33.09	29.21	22.23	21.65
Class 2											
N	32	29	25	141	154	82	120	99	64	61	55
Angular dispersal R	0.957	0.988	0.887	0.978	0.937	0.949	0.948	0.97	0.969	0.982	0.929
Rayleigh test (Z , p)	29.31 , << 0.001	28.30 , << 0.001	19.67 , << 0.001	134.78 , << 0.001	135.12 , << 0.001	73.78 , << 0.001	107.86 , << 0.001	93.22 , << 0.001	60.14 , << 0.001	58.85 , << 0.001	47.48 , << 0.001
Rao's spacing (U , p)	272.85 , < 0.01	311.75 , < 0.01	249.02 , < 0.01	293.99 , < 0.01	271.05 , < 0.01	299.01 , < 0.01	279.01 , < 0.01	291.43 , < 0.01	285.25 , < 0.01	302.85 , < 0.01	271.43 , < 0.01
mean orientation (μ)	59.45	56.05	67.67	66.53	65.98	64.71	60.94	62.24	63.14	56.39	61.26
Class 3											
N	17	14	34	74	66	12	10	40	38	15	34
Angular dispersal R	0.939	0.963	0.936	0.942	0.913	0.99	0.894	0.979	0.898	0.902	0.923
Rayleigh test (Z , p)	14.99 , << 0.001	12.99 , << 0.001	29.76 , << 0.001	65.73 , << 0.001	54.97 , << 0.001	11.76 , << 0.001	8.00 , << 0.001	38.36 , << 0.001	30.64 , << 0.001	12.22 , << 0.001	28.97 , << 0.001
Rao's spacing (U , p)	274.16 , < 0.01	274.17 , < 0.01	265.51 , < 0.01	268.96 , < 0.01	269.90 , < 0.01	305.41 , < 0.01	238.61 , < 0.01	304.43 , < 0.01	258.46 , < 0.01	258.07 , < 0.01	275.02 , < 0.01
mean orientation (μ)	122.82	116.93	116.93	108.76	112.64	114.91	128.37	107.27	122.74	110.95	122.29
Class 4											
N	6	14	8	11	9	1	17	8	16	14	9
Angular dispersal R	0.895	0.942	0.979	0.913	0.906	1	0.965	0.945	0.929	0.938	0.87
Rayleigh test (Z , p)	4.80 , 0.003	12.42 , << 0.001	7.67 , << 0.001	9.16 , << 0.001	7.39 , << 0.001	1.00 , 0.512	15.83 , << 0.001	7.15 , << 0.001	13.81 , << 0.001	12.31 , << 0.001	6.81 , << 0.001
Rao's spacing (U , p)	237.79 , < 0.01	271.09 , < 0.01	276.56 , < 0.01	251.73 , < 0.01	246.11 , < 0.01		284.47 , < 0.01	253.90 , < 0.01	267.39 , < 0.01	263.08 , < 0.01	245.17 , < 0.01
mean orientation (μ)	159.05	163.15	149.96	162.86	160.49	148.11	158.7	161.19	159.56	164.34	150.83

Mean of means (μ of μ) and confidence intervals are calculated from tooth 2 dentine sites only (8 sites: sites 2,3,7,8,9,10 and 11). Class 1: mean of means 24.14, 99% confidence interval 11.18 - 36.33,

Class 2: mean of means 62.63, 99% confidence interval 56.79 - 68.56, Class 3: mean of means 115.84, 99% confidence interval 103.16 - 129.7, Class 4: mean of means 158.23, 99% confidence interval 147.97 - 168.67.

Table S2. Analysis of variation in orientation between teeth (1 site per tooth, 10 teeth, maxilla NHMUK R3638) and between jaw elements NHMUK R3658, R3654, and R3653 (data for right dentary R3658 and left maxilla R3654 transformed to allow direct comparison with right maxillae R3638 and R3653; see Fig. 1)

	T1-1	T2-3	T3-1	T5-2	T9-1	T15-1	T17-1	T18-1	T20-1	T23-1	R3658, T1-1	R3654, T2-1	R3653, T6-1
Class 1													
N	25	17	51	13	32	40	9	13	13	24	11	22	5
Angular dispersal R	0.948	0.944	0.947	0.895	0.937	0.954	0.966	0.946	0.868	0.893	0.943	0.955	0.956
Rayleigh test (Z, p)	22.46, << 0.001	15.17, << 0.001	45.78, << 0.001	10.40, << 0.001	28.08, << 0.001	36.37, << 0.001	8.40, << 0.001	11.63, << 0.001	9.80, << 0.001	19.14, << 0.001	9.79, << 0.001	20.06, << 0.001	4.57, 0.003
Rao's spacing (U, p)	278.46, < 0.01	283.93, < 0.01	287.92, < 0.01	253.06, < 0.01	275.80, < 0.01	277.05, < 0.01	272.56, < 0.01	262.90, < 0.01	256.03, < 0.01	271.82, < 0.01	269.06, < 0.01	284.76, < 0.01	240.50, < 0.01
mean orientation (μ)	14.58	26.45	13.85	25.34	21.58	12.49	19.86	24.82	20.8	22.05	22.59	23.16	17.37
Class 2													
N	233	154	34	54	84	99	22	26	18	100	23	27	36
Angular dispersal R	0.979	0.937	0.975	0.945	0.984	0.909	0.939	0.959	0.906	0.903	0.866	0.994	0.91
Rayleigh test (Z, p)	223.25, << 0.001	1135.12, << 0.001	32.34, << 0.001	48.22, << 0.001	81.26, << 0.001	81.83, << 0.001	19.39, << 0.001	23.90, << 0.001	14.79, << 0.001	81.53, << 0.001	17.24, << 0.001	26.70, << 0.001	29.84, << 0.001
Rao's spacing (U, p)	309.04, < 0.01	271.05, < 0.01	294.57, < 0.01	269.37, < 0.01	300.75, < 0.01	313.03, < 0.01	271.33, < 0.01	290.98, < 0.01	269.57, < 0.01	278.38, < 0.01	258.67, < 0.01	316.52, < 0.01	272.13, < 0.01
mean orientation (μ)	58.89	65.98	59.98	65.94	71.6	79.37	56.97	65.28	59.07	62.96	57.85	68.46	66.36
Class 3													
N	18	66	12	3	0	4	0	4	3	4	12	8	27
Angular dispersal R	0.855	0.913	0.932	0.736		1		0.915	1	0.945	0.937	0.948	0.944
Rayleigh test (Z, p)	13.15, << 0.001	54.97, << 0.001	10.42, << 0.001	1.63, 0.21		4.00, 0.007		3.35, 0.023	3.00, 0.033	3.57, 0.016	10.55, << 0.001	7.19, << 0.001	24.05, << 0.001
Rao's spacing (U, p)	251.22, < 0.01	269.90, < 0.01	249.69, < 0.01			269.21, < 0.01		209.14, < 0.05		223.30, < 0.01	260.38, < 0.01	257.76, < 0.01	278.25, < 0.01
mean orientation (μ)	121.47	112.64	116.23	122.43		90.71		125.77	109.33	129.88	115.16	119.36	123.16
Class 4													
N	18	9	55	17	9	20	7	29	16	29	5	2	53
Angular dispersal R	0.9	0.906	0.935	0.922	0.954	0.947	0.946	0.972	0.969	0.966	0.986	0.997	0.962
Rayleigh test (Z, p)	14.57, << 0.001	7.39, << 0.001	48.04, << 0.001	14.46, << 0.001	8.19, << 0.001	17.94, << 0.001	6.27, << 0.001	27.42, << 0.001	15.02, << 0.001	27.08, << 0.001	4.86, 0.002	1.99, 0.14	49.00, << 0.001
Rao's spacing (U, p)	260.40, < 0.01	246.11, < 0.01	288.66, < 0.01	273.08, < 0.01	257.71, < 0.01	278.75, < 0.01	259.99, < 0.01	285.65, < 0.01	272.76, < 0.01	290.71, < 0.01	260.93, < 0.01		290.37, < 0.01
mean orientation (μ)	151.89	160.49	166.1	159.67	163.77	164.47	167.49	164.19	164	168.63	163.72	157.75	157.29

Mean of means (μ of μ) and confidence intervals calculated from 10 teeth on maxilla NHM R3638 only. Class 1: mean of means 20.13, 99% confidence interval 13.2 - 27.26, Class 2: mean of means 64.56, 99% confidence interval 55.4 - 74, Class 3: mean of means 115.62, 99% confidence interval 94.16 - 138.72, Class 4: mean of means 163.17, 99% confidence interval 156.44 - 169.45. Mean orientation values in bold, fall outside 99% confidence interval.

CHAPTER 10

Dental microwear analysis: the implications for pleurokinesis in ornithopods

Targeted for the journal *Paleobiology*

Introduction

Kinematic analyses of the skulls and jaws of ornithopod dinosaurs identified the pleurokinetic hinge (a series of moveable joints within the skull that allow flexion and expansion during feeding) and showed that all but the most basal ornithopod could chew by mobilizing either cranial or mandibular segments to generate a transverse grinding power stroke (Norman 1984; Weishampel 1984; Norman and Weishampel 1985) (Figure 1). A recent analysis of the evidence for cranial kinesis in dinosaurs questioned the existence of the pleurokinetic hinge and concluded that it was unlikely that anything more than very slight movements at sutural junctures would be possible (Holliday and Witmer 2009). The inference being that any cranial flexibility would be limited and would serve to dissipate mechanical stresses and strains rather than facilitate a transverse power stroke during feeding. Finite element analysis (FEA) of a hadrosaurid (Bell *et al.* 2009) and three dimensional animation modelling of the hadrosaurid *Edmontosaurus* (Rybczynski *et al.* 2008) have also questioned the Norman and Weishampel pleurokinesis model. The 3D animation modelling suggested that extensive secondary (intracranial) movements beyond the pleurokinetic hinge would be required and FEA argued that a transverse translation occurred through rotation of the mandible about its longitudinal axis rather than through lateral movement of the maxilla.

Of the ornithopod dinosaurs, hadrosaurids have the most advanced jaw mechanisms (Weishampel 1984); this includes a homodont dentition of lanceolate teeth, taller than they are wide with a near circular cross section, packed together in batteries that contain both replacement and functional teeth (Figure 2). Tooth eruption was continual and replacement teeth pushed up as functional teeth wore down (Figure 2.1).

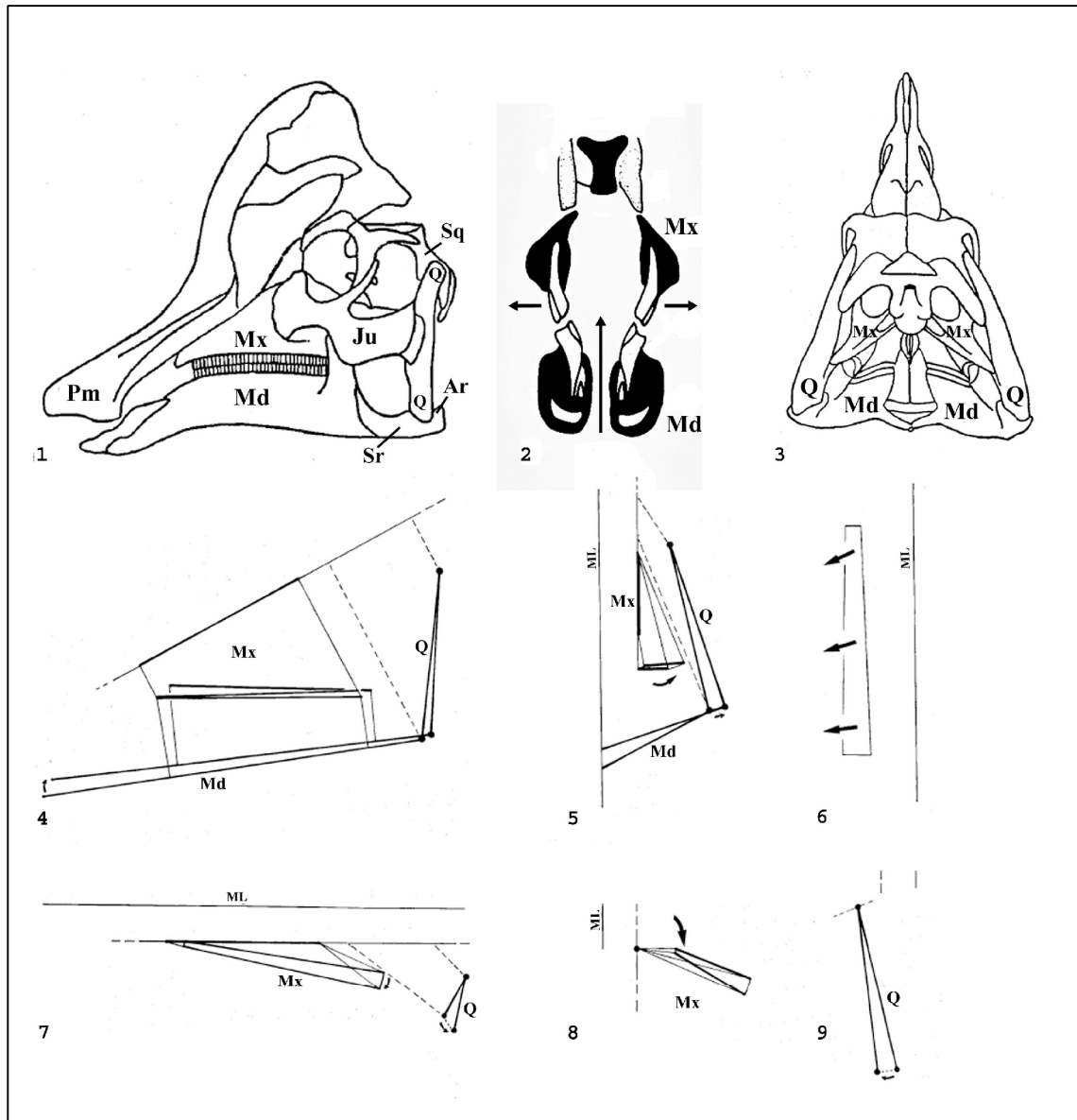


Figure 1. Skull and partial kinematic diagram of the ornithopod dinosaur *Corythosaurus casuarius* illustrating the predicted movements of the mandible, maxilla and quadrate, after Weisampel (1984). 1.1 Skull in left lateral view showing the articulation points of the quadrate bone (with the squamosal in the cranium and the articular/surangular of the mandible) that could allow a propalinal translation of the lower jaw (fore-aft movement of the mandible against the maxilla). 1.2 Transverse section through skull showing the displacement, of the maxilla about the pleurokinetic hinge, that takes place during jaw closure; arrows show the upward movement of the lower jaws and the lateral displacement of the upper jaws. 1.3 Skull in caudal view. 1.4 Left lateral view. 1.5 Anterior view. 1.6 Occlusal view of the left dentary teeth; arrows indicate direction of relative motion of the maxillary teeth against the dentary teeth. 1.7 Dorsal view. 1.8 View along the pre-maxilla/maxilla joint. 1.9 View of the left quadrate along its plane of motion. Abbr: Ar – articular; Ju – jugal; Md – mandible; ML – midline; Mx – maxilla; Pm – pre-maxilla; Q – quadrate; Sq – squamosal; Sr – surangular.

In occlusion the dentary teeth which curve outward and the maxillary teeth which curve inward, relative to the long axis of the tooth row, cut across each other laterally producing an occlusal plane. The interlocking nature, both vertical and lateral, of the lanceolate teeth within the battery provide a near continuous grinding surface (the occlusal plane) within which teeth at various stages of wear can be seen (Figure 2.2). One tooth of the maxilla can cut across several teeth of the dentary and individual scratches moving from tooth to adjacent tooth reflect this.

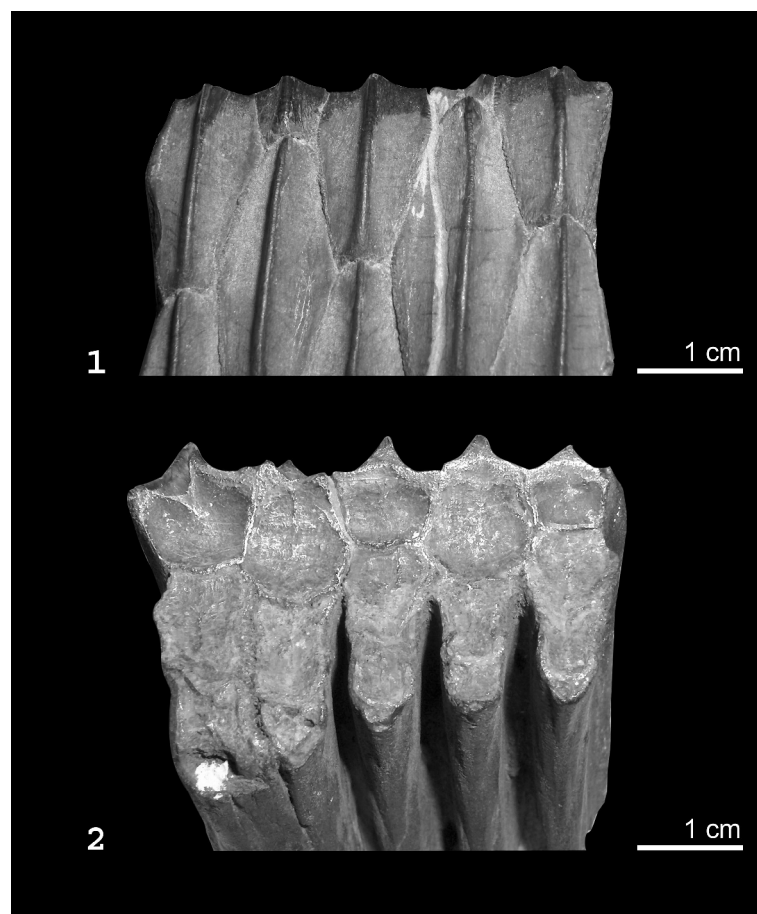


Figure 2. Teeth from a left dentary fragment of a hadrosaurid (AMNH 1181). 2.1 Labial view of the tooth battery showing the functional teeth at various stages of wear and the replacement teeth below them. The lanceolate profile of the replacement teeth, wider in the centre and tapering toward both base and crown, gives the interlocking teeth a staggered arrangement through the battery. 2.2 Occlusal view of the tooth battery showing the wear surface of the functional teeth. The different sizes of adjacent teeth relate to their staggered arrangement in the tooth battery. As a new tooth emerges and is worn down it will increase in size until the widest point of the tooth is reached and then decrease again. Individual scratches can be seen to extend from tooth to tooth.

With enamel on only one side of the tooth crown, lingual for dentary teeth and labial for maxillary teeth, the bulk of the occlusal surface consists of dentine. Only the most medial of the dentary tooth rows have enamel on their lingual face; the teeth of subsequent more lateral rows consist entirely of dentine. The same distribution is not

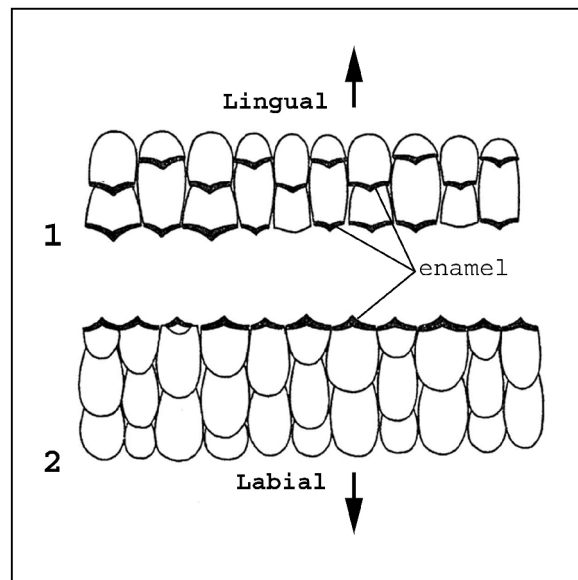


Figure 3. Diagram of portions of the occlusal surface of hadrosaurid tooth batteries. 3.1 Right maxilla. 3.2 Right dentary. The black bands indicate the position of the enamel crowns of individual teeth. Notice that the enamel is restricted to the lingual margin in the lower battery but is distributed discontinuously over the grinding surface of the upper battery. After Ostrom (1961).

repeated on the maxilla. Here thick enamel coats the labial face of each maxillary tooth. Since different teeth are at varying stages of wear in the occlusal surface of the maxilla, enamel is distributed discontinuously (Figure 3). If the tooth rows (left and right) were parallel, this arrangement would not make a particularly good grinding surface for a propalinal (anteroposterior) translation as longitudinal grooves would be cut into the predominantly dentine dentary surface by the enamel distributed over the maxillary surface. Grooves of this nature are not seen in fossil hadrosaurid dentaries and it was for this reason that Norman discounted Ostrom's (1961) suggestion of a propalinal power stroke for hadrosaurids.

In a preliminary study of the hadrosaurid *Edmontosaurus* (Williams *et al.* 2009), quantitative microwear analysis (an examination of the microscopic scratches on teeth

generated during feeding) demonstrated that the teeth of *Edmontosaurus* bear evidence of a transverse power stroke in the form of distinct sets of scratches in different orientations that relate to relative jaw motion. These results support the pleurokinesis model for feeding in *Edmontosaurus* above any other model. Results of later research into the jaw mechanics of the more basal ornithopod *Hypsilophodon foxii* showed evidence of a propalinal power stroke but were inconclusive with regard to cranial kinesis (see Chapter 8). Dental microwear analysis is now widely used to reveal evidence of dietary habit and the mastication process. Relative jaw motion can be deduced from the microscopic scratches and pits on the surface of teeth (e.g., Walker *et al.* 1978; Teaford and Byrd 1989; Semprebon *et al.* 2004; Ungar *et al.* 2007) and the orientation of these scratches reflect the dominant direction of jaw movements (Butler 1952; Mills 1967; Teaford and Byrd 1989). In this study I expand on the work of Williams *et al.* (2009) and test the following hypotheses: that microwear varies between jaw elements in an individual hadrosaur; that microwear varies between hadrosaur species and that microwear in an iguanodontid differs from that in hadrosaurs. A broader analysis of orientation of microwear features in a range of taxa provides a robust test of the pleurokinesis model in advanced ornithopods.

Materials and Methods

The teeth studied are from left and right maxillae and dentaries of the hadrosaurids *Bactrosaurus johnsoni* (2 individuals), *Edmontosaurus regalis* (2 individuals), *Edmontosaurus* sp. (9 individuals), *Corythosaurus casuarius* (5 individuals), *Lambeosaurus lambei* (1 individual), *Hypacrosaurus altispinus* (1 individual), *Kritosaurus navajovius* (1 individual), material labelled hadrosaur or trachodon (17 individuals) and the basal iguanodontian *Camptosaurus dispar* (2

individuals); (see Table 1). 44 jaw elements from 40 individuals in total. *Corythosaurus casuarius* was chosen for detailed analyses due the availability of complete, undamaged jaw elements from multiple specimens, including opposing elements from the same individual.

To avoid coating original material or subjecting it to analysis under vacuum, high-resolution epoxy replicas were prepared for scanning electron micrography by using methods know to reproduce microwear with high fidelity (Galbany *et al.* 2006; Williams *et al.* 2006). Occlusal surfaces of teeth were cleaned non-abrasively with a combination of acetone/ethanol and ethomeen-based solvent gels (Hedley 1980; Southall 1988); see Chapter 2. It was not practical or acceptable to the museum conservators to remove consolidant from the entire occlusal surface of all specimens, particularly the larger jaw elements. Small sections of each tooth row, containing several teeth, were cleaned prior to moulding. This allowed a number of moulds, at various points along the tooth row anterior to posterior, to be made. Moulds were prepared using polyvinylsiloxane impression medium (Speedex Light; Coltene Whaledent). Casts were made using Araldite 20/20 epoxy resin. Replicas were coated with gold (Emitech K500X sputter coater). Imaging for the microwear analysis was performed using a Scanning Electron Microscope (Hitachi S-3600N SEM), operated in full vacuum SE mode; SEM settings were standardized at: accelerating voltage, 15kV; working distance, 18 mm; and automatic contrast and brightness. Standardisation is important for comparability of datasets (Gordon 1988).

Table 1. Specimen list

Species	Jaw element	Specimen number	Age
<i>Bactrosaurus johnsoni</i>	L. maxilla	AMNH 6514	U. Cretaceous, Mongolia
	Dent. frag.	AMNH 6553	U. Cretaceous, Mongolia
	L. dentary	AMNH 6553	U. Cretaceous, Mongolia
<i>Corythosaurus casuarius</i>	L. dentary	AMNH 3971 LD	U. Cretaceous, Montana
	Max. frag.	CM 1074	U. Cretaceous, Montana
	Max. frag.	CM 1077	U. Cretaceous, Montana
	L. dentary	CM 11376	U. Cretaceous, Alberta
	R. dentary	CM 11376	U. Cretaceous, Alberta
	R. maxilla	CM 11376	U. Cretaceous, Alberta
	R. dentary	SM 11893	U. Cretaceous, Montana
<i>Edmontosaurus regalis</i>	R. maxilla	CM 1202	U. Cretaceous, Montana
	L. maxilla	SM 12711	Cretaceous, no data
<i>Edmontosaurus</i> sp.	Dent. frag.	AMNH 2342	Cretaceous, no data
	Max. frag.	AMNH 2342	Cretaceous no data
	L. dentary	AMNH 8145	U. Cretaceous, Montana
	R. maxilla	NHMUK R3638	U. Cretaceous, Wyoming
	R. maxilla	NHMUK R3653	U. Cretaceous, Wyoming
	L. maxilla	NHMUK R3654	U. Cretaceous, Wyoming
	Dent. frag.	NHMUK R3658	U. Cretaceous, Wyoming
	Max. frag.	NHMUK R4292	U. Cretaceous, Alberta
	L. dentary	SM 4807	U. Cretaceous, Wyoming
	L. dentary	SM 4808	U. Cretaceous, Wyoming
	L. dentary	SM 11950	U. Cretaceous, Montana
<i>Hypacrosaurus altispinus</i>	L. dentary	SM 8629	U. Cretaceous, Mexico
<i>Kritosaurus navajovius</i>	L. dentary	SM 8629	U. Cretaceous, Mexico
<i>Lambeosaurus lambei</i>	I. tooth	YPM 21849	U. Cretaceous, Montana
Hadrosaurid	Dent. frag.	AMNH 1181	Cretaceous no data
	L. dentary	AMNH 21523	U. Cretaceous, Alberta
	L. dentary	AMNH 21524	U. Cretaceous, Montana
	Max. frag.	AMNH 21525	U. Cretaceous, Montana
	I. tooth	AMNH 21700	U. Cretaceous, Montana
	L. dentary	AMNH 5465	U. Cretaceous, Montana
	Max. frag.	AMNH 5896	U. Cretaceous, Montana
	R. dentary	AMNH 6375	U. Cretaceous, Mongolia
	L. dentary	AMNH 6380	U. Cretaceous, Mongolia
	R. maxilla	AMNH 6388	U. Cretaceous, Mongolia
	R. dentary	AMNH 6529	U. Cretaceous, Mongolia
	R. dentary	AMNH 6530	U. Cretaceous, Mongolia
	L. dentary	AMNH 6547	U. Cretaceous, Mongolia
	L. dentary	AMNH 6549	U. Cretaceous, Mongolia
	L. dentary	AMNH 6550	U. Cretaceous, Mongolia
	R. dentary	AMNH 6581	U. Cretaceous, Mongolia
	Max. frag.	AMNH 107	U. Cretaceous, Wyoming
	Max. frag.	YPM 1886	Jurassic, Wyoming
	R. maxilla	YPM 7416	Jurassic, Wyoming

Institutional abbreviations:

AMNH - The American Museum of Natural History, New York

CM - The Carnegie Museum of Natural History, Pittsburgh

SM - The Smithsonian Institution National Museum of Natural History, Washington, D.C.

NHMUK - The Natural History Museum, London

YPM - The Peabody Museum of Natural History at Yale University

The specimens were inserted into the SEM chamber and oriented with the long axis of the tooth row as a reference frame (using the labial edge of the tooth battery as a datum) and then rotated about the long axis of the tooth row such that the flat occlusal surface being imaged was perpendicular to the electron beam. Photomicrographs (micrographs) were taken at a magnification of x300 providing a field of view of 417 x 312 μm . In mammals, microwear patterns develop on wear facets and at specific points that relate to the places where teeth are abraded by food or occlusion with other teeth (Teaford 1988b) making sampling strategies relatively simple to formulate. In dinosaurs, there have been too few microwear studies to establish which sites should be used for microwear acquisition or at what magnification. As the whole of the occlusal surface is functional in food processing in hadrosaurids and iguanodontids, and it is predominantly made from dentine, most of the sample sites were from dentine surfaces. Enamel accounts for a very small proportion of the occlusal surface, and only the outer edge of the dentary. It has been suggested that dentine microwear may be unsuited to quantitative analysis (Lucas 2004), but my results do not support this (Williams *et al.* 2009). For diet related quantitative microwear research in mammals a magnification of x500 is the standard choice (e.g., Teaford 1988a). As this study relates to jaw motion, magnification was not as important as surface area and a magnification of x300 was chosen to maximize the field of view without compromising detail. Previous work on hadrosaur teeth (Williams *et al.* 2009) found microwear to occur consistently across the whole occlusal surface of teeth, and sauropod studies (Fiorillo 1991, 1998) found the length, width and frequency of microwear features to be consistent within the occlusal surface. Exploratory micrographs taken across the surface of a single tooth, examined qualitatively, suggested that a central site was representative of the occlusal surface; so central sites were sampled as standard. Where this portion of the tooth surface was

damaged, a slightly more anterior or posterior site was selected. For the within tooth analysis of CM 11376 a selection of sites were chosen to span the entire occlusal surface of the tooth, including two sites immediately adjacent to each other. Teeth from each available jaw element were imaged. Damaged teeth (those with unusually large gouges, cracks or pieces broken off that were suspected to be the result of post-mortem activity) were excluded, as were part erupted teeth which were found to have zero microwear features. A total of 50171 microwear features were captured and analysed for this study. The digital SEM micrographs were downsampled to 900 pixels wide by 675 pixels high using Adobe Photoshop 7. As pits (features of roughly equal length and width) were rare to absent and this study is concerned particularly with relative jaw motion and therefore microwear orientation, only scratches (elongate features) were considered. All microwear scratches within each photomicrograph were measured and recorded using the custom software package Microware 4.02 (Ungar 2001). This produces overlay files of x,y co-ordinates; these were processed in a database using simple trigonometric functions to calculate the length, width and long axis orientation of each feature/scratch. Where the number of scratches per image exceeded 1000, more than one overlay file was used to cover the entire image (Microware 4.02 has a limitation of 1000 features per overlay file). The grid lines option in Microware 4.02 was used to ensure the same feature was not measured twice. Scratch orientation data were suitably transformed for comparison to the labial face of left dentary teeth; e.g. when looking at the labial face of a left dentary tooth, anterior will be to the left but on a right dentary tooth anterior will be to the right, in order to compare microwear patterns one set of data will need to be transformed – to achieve the equivalent of flipping the photomicrograph image horizontally before measuring the scratches. Measurement and recording took place on a Dell Latitude D505 computer running

Windows XP Professional (Microsoft), with a 15-inch active matrix TFT display set at a screen resolution of 1024 x 768 pixels, resulting in an onscreen magnification of approximately x630 for SEM micrographs taken at x300.

Analyses of variance (ANOVA) for linear data and mean of mean angle confidence interval (CI) tests for circular data were conducted on scratch count (N), orientation, angular dispersion (i.e. the degree of parallelism as measured by R), length and width to determine if significant differences occur between sites within a tooth, between teeth within a jaw element and between teeth of different jaw elements.

Scratch length data were not normally distributed (Shapiro-Wilk W; $P < 0.01$) and were therefore log-transformed before statistical analysis. Fiorillo (1998) assessed dominant directions of wear via rose diagram plots, and interpreted these as reflecting directions of jaw movements. This approach was used here to identify dominant modes that could be used to infer relative jaw motion and to assess the distribution of dominant scratch orientations among taxa. Boundaries for these modes (classes of orientation) were identified visually (via 1° resolution rose diagram if necessary) and tested by discriminant function analysis (DFA) for an acceptable error rate (typically < 2%).

Statistical analyses were carried out using the dedicated software packages Oriana 3.31 (Kovach Computing Services) for orientation data and JMP 8.0.2 (SAS Institute Inc) for both linear data and DFA. DFA was first performed using scratch length and width as covariates with orientation and then by using orientation alone (the latter being reported here). Orientation data are directional, and such data have statistical properties that differ from those upon which standard statistical tests are based. My previous analysis (Williams *et al.* 2009) does not support the view advocated in previous analyses of microwear orientation data (Gordon 1984a; Teaford and Byrd 1989; Charles *et al.* 2007) that axial data can be subjected to linear statistical tests. This approach can

wrongly indicate highly significant differences. Consequently hypothesis testing used a number of tests specifically formulated for data of this kind.

Results

Corythosaurus casuarius CM 11376

The dentary and maxillary teeth of *C. casuarius* show dominant oblique and near vertical microwear patterns on the occlusal surface. Scratches dominate and pitting is rare (with pits being defined as features with length-width ratio of 2:1 or less). Pits were therefore excluded from the analyses. Figure 4 shows an example of the microwear, captured from tooth eight of the right maxilla, which is typical of the coarse to fine scratches found on the teeth of this specimen. Scratches that are longer than 417 μm will extend beyond the field of view of the x300 micrographs and therefore their true length will not be represented in the microwear data. There are high-angle oblique, low angle oblique and near vertical scratches that do extend beyond the field of view of the x300 micrographs. A better idea of their full extent can be seen in the low magnification image (Figure 4.1) where scratches exceed 3.5 mm and still continue beyond the limits of the image. A dominant high angle oblique scratch pattern (top right to bottom left) can be seen in all of the images. Arrows indicate the differing orientations of the scratches: low angle oblique scratches slope in both directions about the horizontal (Figure 4.2), vertical scratches also occur (Figure 4.3) and high angle oblique scratches slope in the opposite direction, about the vertical, to the dominant pattern (Figure 4.4).

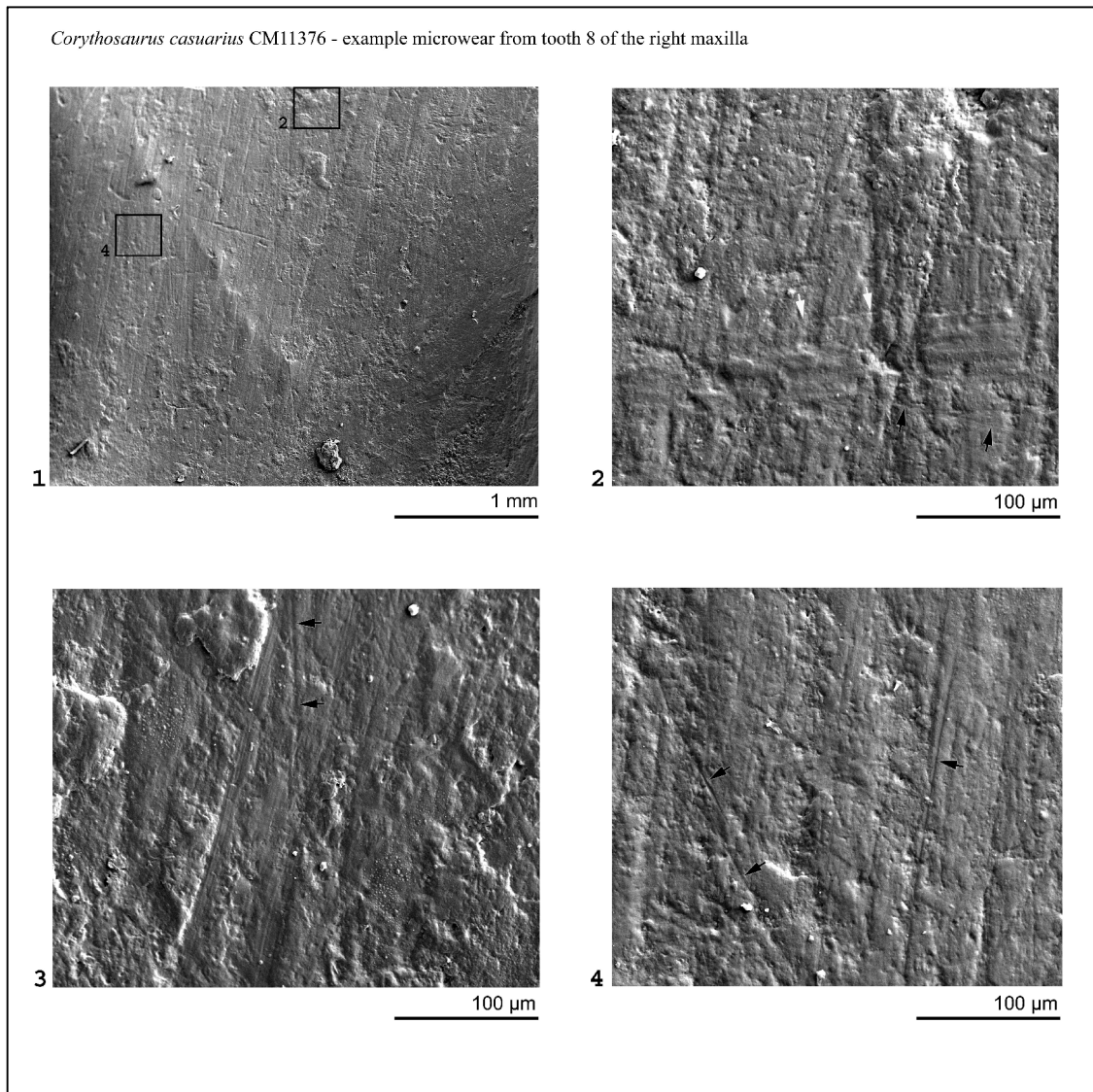


Figure 4. Microwear distribution on a tooth surface of *Corythosaurus casuarius* CM 11376. 4.1 Occlusal view of tooth 8 of the right maxilla, with inset boxes showing location for (4.2) and (4.4), the location for 4.3 is not within this image; anterior is to the right, crown ward is up. 4.2 Occlusal surface microwear showing scratches in various orientations. White and black arrows indicate low angle scratches sloping in opposite directions indicative of some propalinal (anteroposterior) motion. Notice the cross cutting nature of these low angle scratches, removing existing microwear which can be seen to continue above and below them. 4.3 Occlusal surface microwear, arrows indicate vertical scratches. This site was above and to the right of inset box 2 (shown on 4.1). 4.4 Occlusal surface microwear, arrows indicate near symmetrical high-angle oblique scratches.

Scratches are not random in orientation, appearing to fall into a small number of classes, within which scratches are predominantly straight and subparallel, but with an orientation that differs from that of other classes. Not all sample sites showed all orientation classes as is evident in Figure 5. Combining all of the data from the 56 sites on the 36 teeth examined, it is clear that there are at least two classes of scratches but

the precise boundaries between classes are difficult to establish visually. With the data partitioned by jaw element (left dentary 8394 scratches from 32 sites on 15 teeth, right dentary 1929 scratches from 11 sites on nine teeth and right maxilla 3464 scratches from 13 sites on 12 teeth) the right dentary dataset displays the boundaries more clearly, identifying multiple dominant modes (Figure 5).

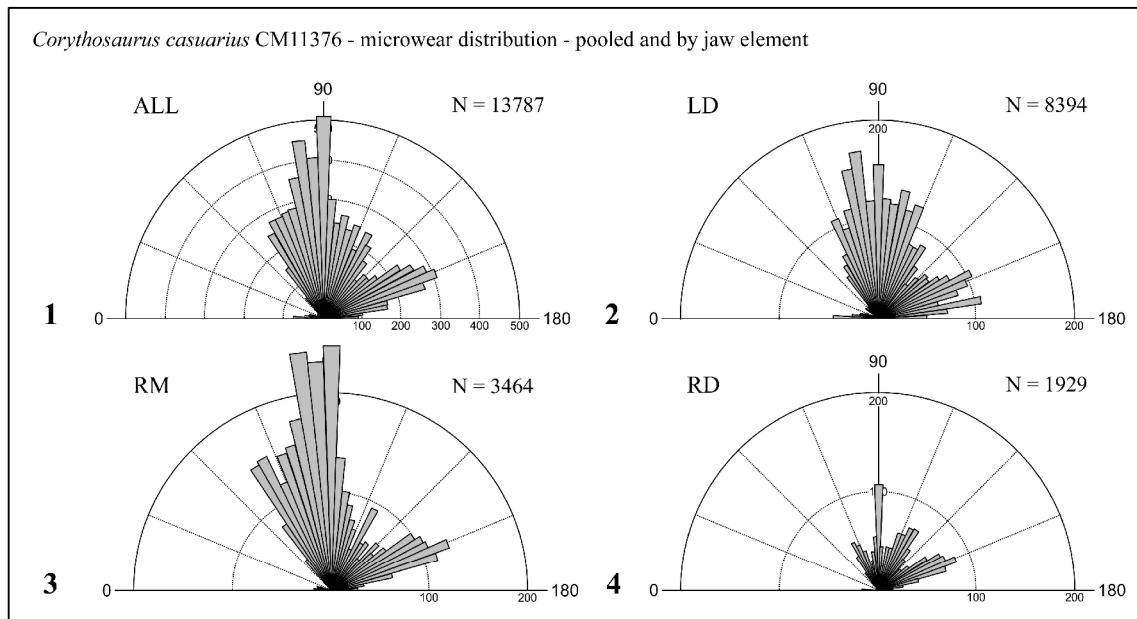


Figure 5. Rose diagrams of microwear scratch orientations on the teeth of *Corythosaurus casuarius* CM 11376, pooled and by jaw element. Data have been transformed for comparison to the left dentary labial face (see Material and Methods for details on transforming data). Frequency is shown by the radius of the wedge, inner circles measure hundreds, bin size = 4°. 5.1 All data (13787 scratches from 56 sites on 36 teeth), scale N=500. 5.2 Left dentary (LD) data (8394 scratches from 32 sites on 15 teeth), scale N=200. 5.3 Right maxilla (RM) data (3464 scratches from 13 sites on 12 teeth), scale N=200. 5.4 Right dentary (RD) data (1929 scratches from 11 sites on 9 teeth), scale N=200. Boundaries between modes are more clearly defined in the right dentary.

To test the hypothesis that discrete classes of scratches exist, the occlusal microwear data from the right dentary were partitioned into five subsets (classes 1-5), based on visual assessment of scratch orientation from detailed rose diagrams. Discriminant function analysis (DFA) provides strong confirmation that the microwear data falls into five distinct classes – 98.7% of scratches classified by visual inspection were correctly assigned by DFA. Rather than conduct subsequent statistical testing on these imperfectly classified data, the DFA results were used to reassign the incorrectly

assigned scratches to their correct class (leading to 100% correct discrimination; see Table 2 for summary). The established class boundaries (from the right dentary dataset) were used as the starting point for the right maxilla and left dentary.

Table 2. *Corythosaurus casuarius* – summary statistics from the right dentary of CM 11376 (11 sites on 9 teeth) unclassified and partitioned into five classes based on scratch orientation.

Subgroup	Right Dentary					
	Unclassified	Class 1	Class 2	Class 3	Class 4	Class 5
No. Of observations	1929	27	346	466	474	616
Angular dispersion, R	0.369	0.976	0.962	0.970	0.959	0.947
Mean orientation (mean vector, μ)	114.35°	5.37°	60.03°	89.65°	118.56°	154.68°
95% confidence interval for μ	$\pm 2.36^\circ$	$\pm 2.36^\circ$	$\pm 0.84^\circ$	$\pm 0.64^\circ$	$\pm 0.74^\circ$	$\pm 0.74^\circ$
99% confidence interval for μ	$\pm 3.10^\circ$	$\pm 3.10^\circ$	$\pm 1.11^\circ$	$\pm 0.84^\circ$	$\pm 0.97^\circ$	$\pm 0.98^\circ$
Mean scratch length, μm	77.71	63.16	69.41	79.13	79.86	80.29
Mean log scratch length, μm	4.35	4.15	4.24	4.37	4.38	4.39
Mean scratch width, μm	1.49	1.17	1.20	1.35	1.86	1.50

Microwear data from the left dentary (8394 scratches from 32 sites on 15 teeth) and the right maxilla (3464 scratches from 13 sites on 12 teeth) were partitioned into five subsets (classes 1-5), based on the class boundaries from the right dentary dataset. DFA on the right maxilla dataset identified 19 (0.5%) incorrectly assigned scratches. DFA on the left dentary dataset identified 161 (<2%) incorrectly assigned scratches. This equated to a difference of one degree or less in class boundaries between the jaw elements (right maxilla: class 2 to class 3 boundary differed by $+0.75^\circ$ and class 4 to class 5 boundary by $+0.95^\circ$, left dentary: class 2 to class 3 boundary differed by -1° and class 4 to class 5 boundary by $+1^\circ$). The DFA results were used to reassign the incorrectly assigned scratches to their correct class (leading to 100% correct discrimination; see Table 3 for summary). Analysis of the recombined dataset revealed significant differences ($P < 0.05$) in scratch count (N), angular dispersion (i.e., the degree of parallelism of scratches as measured by R, mean vector length), length and width between classes (Table 4). Differences in N, R, length and width are illustrated in Table 5. In this combined dataset (all jaw elements), the class 3 (near-vertical) scratches dominate.

Table 3. *Corythosaurus casuarius* - summary statistics for all microwear data from CM 11376 (56 sites on 36 teeth) unclassified and partitioned into five classes based on scratch orientation.

Subgroup	All Elements					
	Unclassified	Class 1	Class 2	Class 3	Class 4	Class 5
No. Of observations	13787	521	2743	4386	2788	3349
Angular dispersion, R	0.344	0.916	0.951	0.965	0.945	0.943
Mean orientation (mean vector, μ)	102.191°	15.831°	60.505°	88.86°	120.289°	156.401°
95% confidence interval for μ	$\pm 0.95^\circ$	$\pm 1.02^\circ$	$\pm 0.34^\circ$	$\pm 0.22^\circ$	$\pm 0.74^\circ$	$\pm 0.33^\circ$
99% confidence interval for μ	$\pm 1.25^\circ$	$\pm 1.35^\circ$	$\pm 0.44^\circ$	$\pm 0.29^\circ$	$\pm 0.97^\circ$	$\pm 0.43^\circ$
Mean scratch length, μm	70.33	69.35	63.95	73.34	69.52	72.45
Mean log scratch length, μm	4.25	4.23	4.15	4.29	4.24	4.28
Mean scratch width, μm	1.19	0.94	1.08	1.30	1.27	1.12

Table 4. *Corythosaurus casuarius* - results of null hypothesis testing for differences in microwear between classes in CM 11376.

Unclassified	d.f.	F	P
Length does not differ between classes (one way ANOVA; log data)	4,13782	31.62	< 0.0001
Width does not differ between classes (one way ANOVA)	4,13782	29.32	< 0.0001
R does not differ between classes (one way ANOVA)	4,260	19.72	< 0.0001
N does not differ between classes (one way ANOVA)	4,260	33.95	< 0.0001

Table 5. *Corythosaurus casuarius* – significant differences in microwear data between classes, CM 11376 unclassified data (13787 scratches). Classes not connected by the same letter, differ significantly.

N			R		
Class		Mean	Class		Mean
3	A	78.321	1	A	0.981
5	B	59.804	2	B	0.969
2	B	49.873	3	B	0.967
4	B	49.786	5	C	0.957
1	C	12.405	4	C	0.951

Length			Width		
Class		(Log) Mean	Class		Mean
1	A	4.409	4	A	1.770
3	B	4.307	3	A	1.751
5	B	4.304	5	B	1.636
4	C	4.234	2	B	1.624
2	D	4.175	1	A B	1.583

Analysis of the combined dataset (all jaw elements) reveals that overall, the hypothesis that data for each site are uniformly distributed can be rejected (i.e. they show a preferred orientation; Rayleigh uniformity test and Rao spacing test, $P < 0.05$; Table S1). For the unclassified data, mean orientation for each site does not differ significantly from the pooled mean (V test expected mean 92.99° , $P < 0.05$). Of the 56 sites tests there was only one exception to this result. Analysis of the five subsets of data (classes 1-5) provides confirmation of this result and the hypothesis that data within classes for each site are uniformly distributed can be rejected (i.e., they show a preferred orientation; Rayleigh uniformity test and Rao spacing test, $P < 0.05$; Tables S2 to S6). Mean orientation for each class for each site does not differ significantly from the overall class mean (all sites, all teeth; V test expected means: class 1 = 15.83° , class 2 = 60.50° , class 3 = 88.86° , class 4 = 120.28° , class 5 = 156.40° , $P < 0.05$; Table 3 and Tables S2 to S6). Of the 265 samples tested (five classes, 56 sites, 15 sites with $n = 0$), there were only 11 exceptions to this result; eight class 1, two class 2 and one class 5 site failed the Rayleigh uniformity test, but in all 11 cases the number of scratches assigned to the sample that failed the test was 3 or lower.

Subdividing a distribution of circular (orientation) data into classes will invariably lead to an increase in parallelism (R) within each class. Even with a random or uniform distribution, as the number of classes increase or the width of a specific class decreases R will approach 1. To test the hypotheses that the distribution of scratches does not differ from a random distribution, results from the analysis of a random distribution of 13787 orientations unclassified and partitioned into the five classes (1-5) were compared with those of the real data. The random dataset produced R values of 0.01 for the pooled unclassified data (a uniform distribution), and 0.94, 0.91, 0.95, 0.94 and 0.90 respectively for the pooled classes (1-5), and by site the R values ranges were:

unclassified 0.01 to 0.1, and 0.92 to 0.96, 0.87 to 0.94, 0.95 to 0.97, 0.94 to 0.95 and 0.89 to 0.92 respectively for the classes (1-5). The real data, unclassified and by class (1-5), both pooled and by site show a greater degree of parallelism than would be expected from a random distribution. This analysis reveals that overall we can reject the hypothesis that the distribution of scratches does not differ from a random distribution. To test for variation within a tooth, data from seven sites on tooth three of the left dentary were analysed (Figure 6). Within tooth analyses (testing unclassified data from seven sites, class 1 data from seven sites, and so on for each of the five classes) reveal that microwear orientation does not differ significantly between samples sites within the tooth. No site to site differences were significant (99% CI test; Table 6). Whilst the hypothesis that orientation differs between sites within a tooth can be rejected, the hypothesis that other aspects of microwear differ between sites within a tooth cannot be rejected. Significant differences ($P < 0.5$) exist in both scratch length and width, for the unclassified data and by class (1-5). These are illustrated in Table 7 for scratch length and Table 8 for width, where the results of pairwise comparisons (Tukey-Kramer honestly significant difference) show sites that differ significantly from each other for the unclassified data and by class (1-5). The differences in N between sites are illustrated in Figure 6 (rose diagrams show frequency within 4° bins, scale: $N = 25$). The differences between sites appear random and include sites 4 and 5, which differ in length (unclassified data and classes 3, 4 & 5) and width (unclassified data and class 3) and yet are located immediately adjacent to each other.

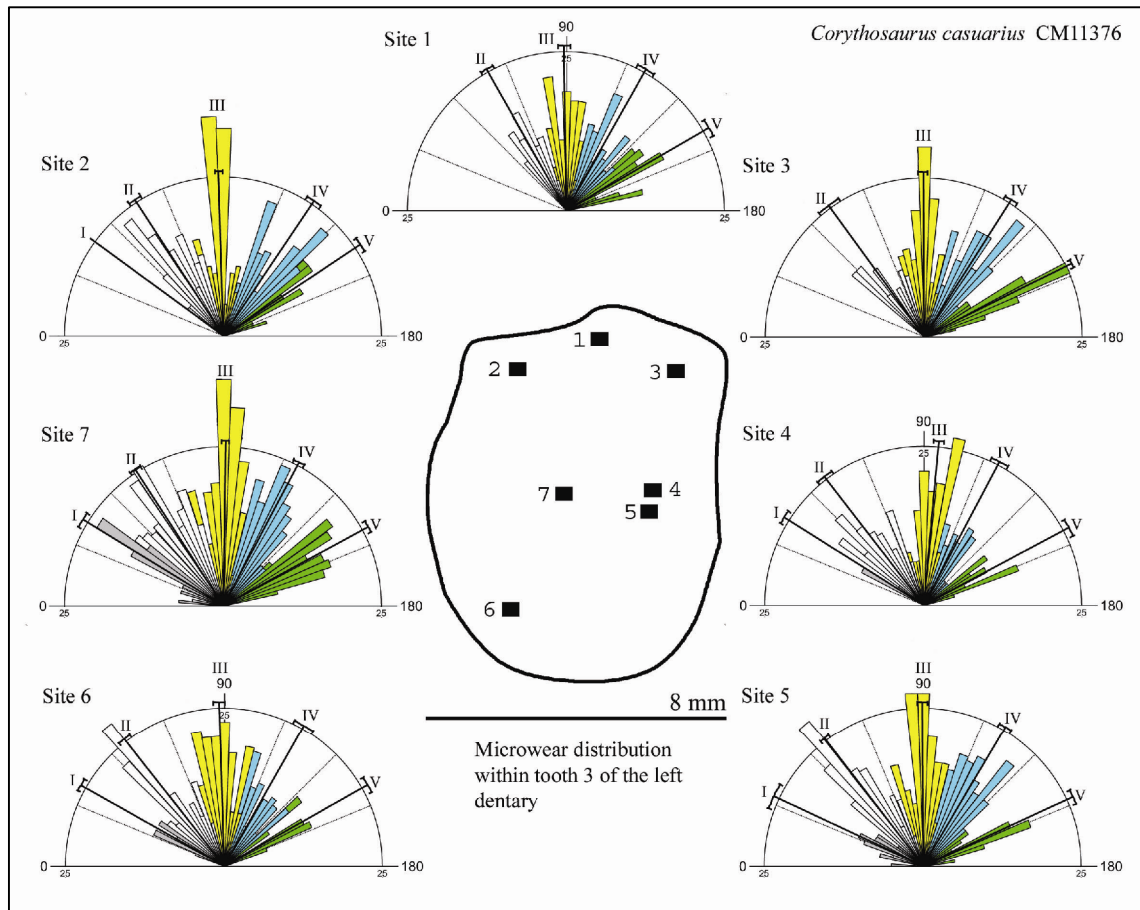


Figure 6. *Corythosaurus casuarius* CM 11376 - diagram of the occlusal surface of left dentary tooth 3 showing the physical positions of the 7 within tooth analysis sites and rose diagrams of microwear scratch orientations, partitioned into orientation classes for each site. Black lines running from the centre of the rose diagram to the outer edge, with arcs extending to either side show the mean orientation and 99% confidence interval for each of the five classes (I to V), class I does not exist for all sites. Frequency is shown by the area of the wedge, bin size = 4°, scale: N=25.

Further analyses of scratch length and width show significant differences ($P < 0.05$) between teeth, for the combined dataset and by jaw element dataset (for the unclassified data, and by class (1-5)). There is no significant variation in scratch length or width with distance from the posterior of the jaw; (no linear-linear correlation for the unclassified data or by class (1-5)). Figure 7 shows scratch length and width for the tooth to tooth sample sites along the length of the left dentary tooth row (one way ANOVA; d.f. 31,8362; $P < 0.05$) and illustrates the lack of any systematic variation.

Table 6. *Corythosaurus casuarius* – analysis of variation in orientation between sites, within tooth 3 of the left dentary of CM 11376.

Left dentary tooth 3: Site	1	2	3	4	5	6	7
Unclassified angular dispersal, R	0.507	0.518	0.480	0.458	0.409	0.466	0.378
Mean vector, μ	101.635	94.267	108.883	88.663	88.608	82.743	91.363
Class 1 angular dispersal, R		1	0.997		0.961	0.992	0.966
Mean vector, μ		36.304	32.341		25.057	29.618	31.394
Class 2 angular dispersal, R	0.975	0.952	0.928	0.935	0.967	0.953	0.948
Mean vector, μ	60.643	56.952	53.948	52.365	52.432	51.875	57.020
Class 3 angular dispersal, R	0.966	0.982	0.974	0.973	0.966	0.957	0.975
Mean vector, μ	89.251	88.375	89.566	95.303	89.654	88.156	90.853
Class 4 angular dispersal, R	0.943	0.936	0.954	0.965	0.948	0.929	0.959
Mean vector, μ	119.446	124.012	122.462	117.976	120.483	119.483	117.808
Class 5 angular dispersal, R	0.959	0.979	0.988	0.974	0.979	0.979	0.965
Mean vector, μ	149.939	146.430	153.657	151.945	155.192	150.356	151.379

Unclassified mean of means 94.06, 99% confidence interval 73.23 – 111.95
Class 1 mean of means 30.98, 99% confidence interval 13.90 – 46.30
Class 2 mean of means 55.05, 99% confidence interval 47.90 – 61.98
Class 3 mean of means 90.16, 99% confidence interval 84.97.30 – 95.35
Class 4 mean of means 120.22, 99% confidence interval 115.41 – 125.17
Class 5 mean of means 151.27, 99% confidence interval 145.21 – 157.26

Table 7. *Corythosaurus casuarius* - significant differences in scratch length between sites, within tooth 3 of the left dentary of CM 11376; for the unclassified data and by class (1-5). Sites not connected by the same letter differ significantly.

	Unclassified	Class 1	Class 2	Class 3	Class 4	Class 5
Site	Mean	Mean	Mean	Mean	Mean	Mean
1	A 4.21		A 4.18	B 4.25	A B 4.25	A 4.13
2	B 4.12	A 3.34	A B 4.07	B C 4.16	A B 4.16	A B 4.00
3	B C 4.05		A B C 3.91	B C 4.09	B C 4.10	A 4.02
4	A 4.26	A 4.01	A B C 4.01	A 4.52	A 4.35	A B 4.01
5	D 3.96	A 3.77	B C 3.95	B C 4.06	C D 3.96	B 3.76
6	E 3.87	A 3.73	C 3.82	C 4.02	D 3.76	B 3.74
7	C 4.04	A 3.87	A B 4.00	B C 4.09	B C 4.10	A 4.01

Table 8. *Corythosaurus casuarius* - significant differences in scratch width between sites, within tooth 3 of the left dentary of CM 11376; for the unclassified data and by class (1-5). Sites not connected by the same letter differ significantly.

	Unclassified	Class 1	Class 2	Class 3	Class 4	Class 5
Site	Mean	Mean	Mean	Mean	Mean	Mean
1	B 1.02		A 1.09	B 1.16	A B C 1.13	A 0.55
2	A B 1.07	A 0.23	A B 0.80	A B 1.55	B C 0.90	A 0.50
3	B 0.96		B 0.42	A B 1.33	A B C 1.05	A 0.57
4	A 1.29	A 0.73	A 1.11	A 1.66	A B 1.36	A 0.57
5	B 1.01	A 0.74	A 0.95	B 1.17	A B C 1.07	A 0.56
6	B 0.95	A 0.26	A B 0.83	A B 1.32	C 0.65	A 0.78
7	B 1.05	A 0.64	A B 0.83	A B 1.35	A 1.45	A 0.52

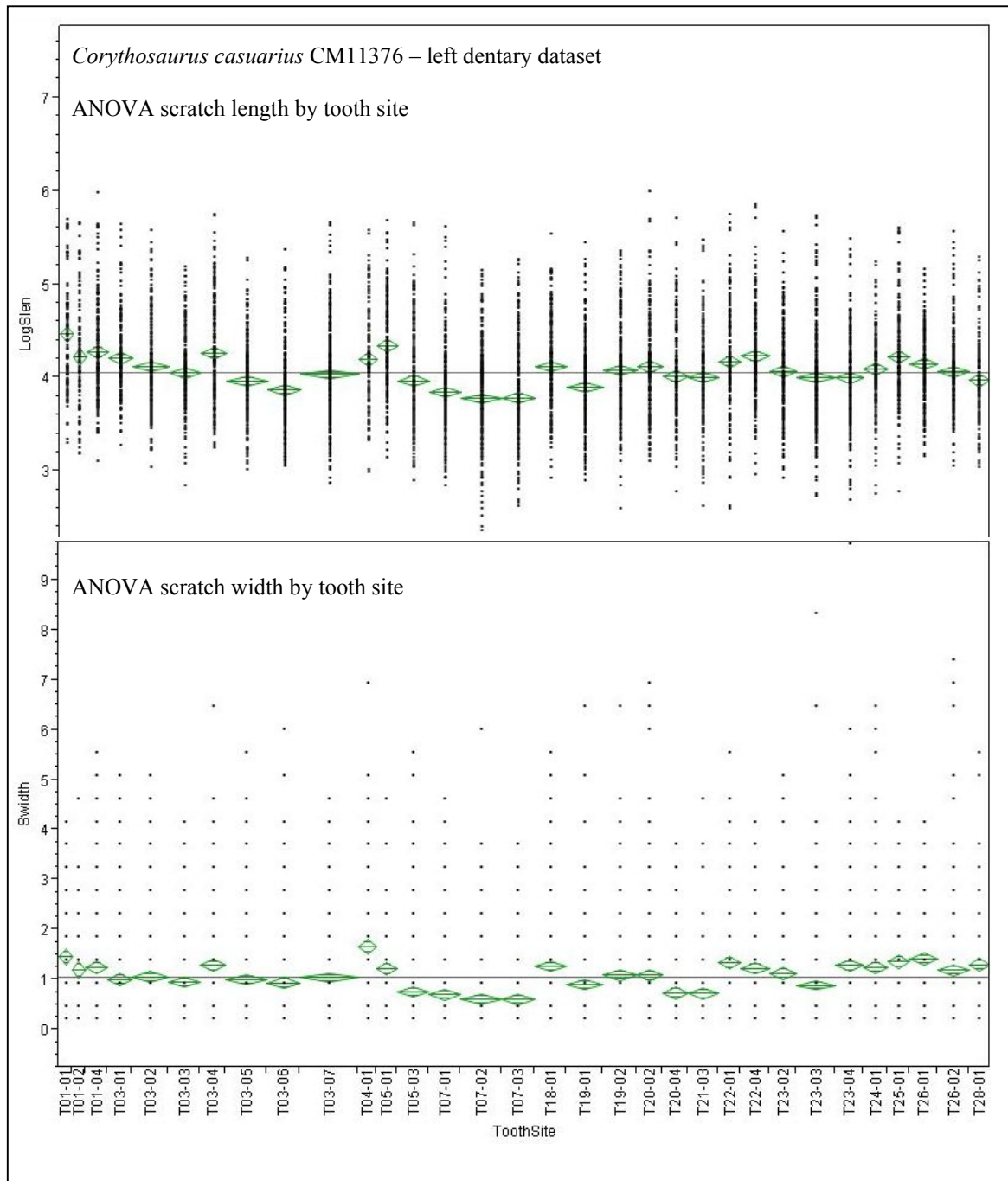


Figure 7. Results of between tooth analyses of scratch length and width for the left dentary of *Corythosaurus casuarius* CM 11376. One way ANOVA for scratch length (log data) by tooth site and one way ANOVA for scratch width by tooth site, showing significant differences between teeth but no systematic variation along the tooth row. The X axis shows tooth site, the order of these data (tooth site) reflects position along the tooth row, anterior is to the left.

Significant differences also exist between jaw elements (pooled data) for scratch length (one way ANOVA; d.f. 2,13784; $F = 182.62$; $P < 0.05$; means: LD 4.05, RD 4.23, RM 4.21) and width (one way ANOVA; d.f. 2,13784; $F = 171.78$; $P < 0.05$; means: LD 1.05, RD 1.49, RM 1.35). The results of pairwise comparisons (Tukey-Kramer honestly

significant difference) show that the left dentary (LD) differs from both the right dentary (RD) and right maxilla (RM), but the RD does not differ from the RM.

To test the null hypothesis that microwear orientation does not differ between teeth within a jaw element, subsets of data were generated for the left dentary, right dentary and right maxilla. Mean of mean angles and their 99% confidence intervals (Zar 1999) were calculated for each within jaw dataset (for the unclassified microwear data and by class (1-5); one site per tooth, 11 left dentary teeth, nine right dentary). Analysis of these datasets reveal that tooth to tooth variation in class mean orientation is significant in only 30 of the 321 samples (99% CI test; Table S7 and Table S8). For the left dentary, 22 of the 187 samples fall outside the 99% confidence interval of the mean of mean angles; two unclassified, three class 1, eight class 3, three class 4 and six class 5. For the right dentary only three of the 61 samples fail the 99% CI test; one unclassified, one class 3 and one class 4, and for the right maxilla five of the 73 fail; one class 1, one class, two class 4 and one class 5.

To test for variation between jaw elements a 99% CI test based on a mean of means calculated from the combined dataset (five teeth selected from each jaw element) resulted in significant differences in mean orientation in 89 of the 321 samples (27%). Applying the 99% CI test to the left dentary and using the mean of means calculated from the right dentary, resulted in significant differences in mean orientation in 37 of the 187 samples (20%). For the right dentary and right maxilla (using the left dentary mean of means), eight of the 61 right dentary samples differ significantly (13%) and nine of the 73 right maxilla samples differ significantly (12%). In none of the jaws does orientation vary significantly with distance from the posterior of the jaw (there is no circular linear correlation for the unclassified data or by class (1-5)).

To assess variation between individuals of *Corythosaurus casuarius*, teeth selected from the right maxillae of CM 1077 (2791 scratches from 7 sites on 5 teeth) and CM 1074 (1328 scratches from 2 sites on 2 teeth), the right dentary of SM 11893 (973 scratches from 2 sites on 2 teeth) and the left dentary of AMNH 3971 (944 scratches from 5 sites on 5 teeth) were analyzed. Scratches dominate the teeth of all the *C. casuarius* specimens with the same dominant oblique and near vertical microwear patterns on the occlusal surface that were observed in CM 11376. Rose diagrams of scratch orientations suggest that the same five orientation classes that were identified in CM 11376, exist in all of the *C. casuarius* specimens. DFA was applied independently to the dataset of each specimen using class boundaries located via detailed rose diagrams for that specimen. In each case the number of incorrectly classified scratches reported by DFA was less than 2%. When DFA is applied to datasets of random orientations, of equal size to each of the *C. casuarius* specimen datasets, which have been partitioned into the five orientation classes, the result is a consistent 4.6% of incorrectly classified scratches.

Analyses of the unclassified datasets and the datasets partitioned by class (1-5) for each specimen produced comparable results to those obtained from CM 11376 (Table S9); scratches within classes have preferred orientations and the mean orientations for each class for the pooled data fall within the 99% confidence interval of the mean of means calculated from the CM 11376 datasets with only one exception (the class 4 mean for AMNH 3971). Of the 73 samples tested (16 sites, five classes, seven sites with N = 0), variation is significant in only 16; one class 1, two class 3, six class 4, and six class 5 (See Table S10 for summary). Of the 16 samples that failed the 99% CI test, eight relate to AMNH 3971 which appears to differ from the other specimens in its class 4 and class 5 orientations. The class 4/5 boundary for AMNH 3971 was

established at approximately 130° whilst that of CM 11376 and the other specimens is in excess of 138°.

Edmontosaurus sp. NHMUK R3638

Previous research on *Edmontosaurus* sp. NHMUK R3638 (Williams *et al.* 2009) determined that scratches occur as 4 distinct classes with significantly different orientations. These orientation classes reflect 4 distinct jaw motions with the dominant pattern, 60° from the long axis of the tooth row, relating to the power stroke. The class boundaries were similar to those in *C. casuarius* CM 11376, but with the vertical mode (class 3 in *C. casuarius*) absent; i.e. *C. casuarius* has an additional mode at 90° inserted between the 60° and 120° modes identified in *Edmontosaurus*.

In my previous study, in histograms of the between-tooth dataset for NHMUK R3638 (1384 scratches from 10 sites on 10 teeth), a vertical mode was not obvious visually due to the dominance of the 60° mode. In this study, detailed rose diagrams (using 2° bins) identified a potential class boundary for an additional mode with a mean orientation of 90°. Two types of rose diagram were used, one showing frequency (N) as the radius of the wedge and one showing it as the area of the wedge (where frequency is shown as the radius of the wedge, a dominant mode can obscure minor modes). In Figure 8.3, a detailed rose diagram (showing frequency as the radius of the wedge, rescaled to a maximum N of 50 and with 2° bins) suggests position A for the boundary to a near vertical mode, with the next clear space between modes at B. DFA does not support either position, reporting 182 (13%) incorrectly classified scratches for a boundary at position A, and 41 (2.9%) incorrectly classified scratches for a boundary

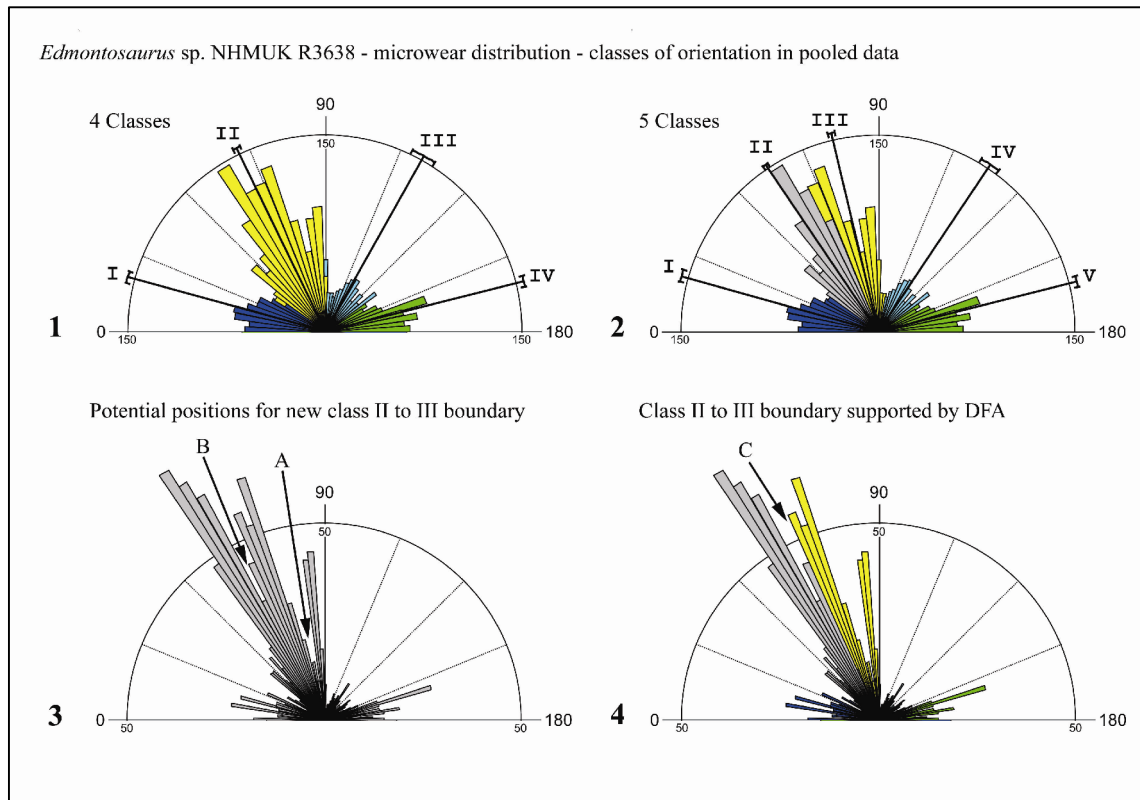


Figure 8. Rose diagrams of microwear scratch orientations on the teeth of *Edmontosaurus* sp. NHMUK R3638, from the between-tooth dataset (1384 scratches from 10 sites on 10 teeth), unclassified and partitioned into orientation classes. 8.1 and 8.2 Show data partitioned into 4 and 5 classes respectively. Black lines running from the centre of the rose diagram to the outer edge, with arcs extending to either side show the mean orientation and 99% confidence interval for each class. Frequency is shown by the area of the wedge, bin size = 4°, scale N=150. 8.3 and 8.4 show the data unclassified and partitioned into 5 classes. Frequency is shown by the radius of the wedge, bin size = 2°, scale N=50. A & B mark potential boundary positions for class II to III. C marks the DFA supported boundary.

at position B. Correcting the classifications to those predicted by DFA for either A or B results in a boundary at position C (Figure 8.4). Accepting position C as a class boundary would result in a new class 3 (vertical mode) with class boundaries between approximately 66° and 100°. When the data are reassigned and the new class 3 is inserted between the original class 2 and 3, the result is a 26° incursion across the boundary of the original class 2, and a 10° incursion across the boundary of the original class 3. Class 1 is unchanged as is the original class 4, which becomes the new class 5. The four class and five class models are illustrated in Figure 8.1 and 8.2. Boundaries from both models (four and five classes) achieve 100% correct discrimination through DFA. However, it was only by looking at other taxa that a vertical mode was suspected

and whilst a vertical mode can be seen on the detailed rose diagrams, statistically DFA cannot distinguish it from noise around the dominant mode. This suggests that NHMUK R3638 does not have a vertical class and the four class model is a better fit.

To determine if discrete classes of scratches exist in other individuals of *Edmontosaurus* sp., occlusal microwear data from eight additional specimens were analysed and partitioned into subsets based on visual assessment of scratch orientation via detailed rose diagrams. DFA was used to test potential class boundaries resulting in five orientation classes for each specimen (with less than 2% of scratches incorrectly assigned in each case) with the exception of AMNH 8145 where no class 1 was found. Incorrectly assigned scratches were re-assigned based on the DFA results. Table 9 shows the established class boundaries for each jaw element of each specimen and supports the existence of five distinct orientation classes, with similar boundaries in *Edmontosaurus* sp.

Table 9. Comparison of class boundaries in specimens of *Edmontosaurus* sp. Figures shown either side of hyphens relate to the first and last scratch orientations either side of a boundary, where a precise figure cannot be given.

Specimen	Element	N	Class boundaries			
			1 to 2	2 to 3	3 to 4	4 to 5
AMNH 2342	dentary	838	12.6 - 55.3	81.7	105.8	135
AMNH 2342	maxilla	473	3.8 - 56.1	81.9	105.8	135
AMNH 8145	L. dentary	558	-36.7	76	108.3	139.9
NHMUK R3638*	R. maxilla	1284	36	66.3	101.3	136.2
NHMUK R3653	R. maxilla	2788	42	76.5	103.5	143.9
NHMUK R3654	L. maxilla	1307	35.8	69.6	104.4	137.6
NHMUK R3658	dentary	625	23.5 - 47.6	78.3	106.4	141.8
NHMUK R4939	L. dentary	774	35.2 - 57.3	78.4	107.9	137.3
SM 4807	L. dentary	547	33.4 - 39.6	75.9	107.8	141.1
SM 4808	L. dentary	470	14.2 - 50.7	76.5	102.1	133.6 - 136.2

* Boundaries from 5 class model shown for NHMUK R3638

Between teeth analyses of variance, to test the five class model in NHMUK R3638, (testing unclassified data from ten sites, class 1 data from ten sites, and so on

for each of the 5 classes) reveal that microwear orientation does not differ significantly between samples sites from tooth-to-tooth, confirming the results of the previous study. Variation is significant in only five of the 57 samples tested (99% CI test; Table S11); mean orientations from two unclassified samples and one sample each from classes 1, 3 and 5 fall outside the 99% confidence interval of the mean of means. In the previous study (four classes) tooth-to-tooth variation in orientation was significant in only four of the 38 samples.

Results of an analysis of variance between individuals of *Edmontosaurus* sp. reveal no significant difference in microwear orientation between individuals. Testing unclassified data from each individual, class 1 data from each individual, and so on for each of the 5 classes) variation is significant in only five of the 59 samples tested (99% CI test; table S12); mean orientations from one unclassified sample and one each from classes 2 to 5 fall outside the 99% confidence interval of the mean of means.

Camptosaurus dispar YPM 7416 and YPM 1886

Microwear on the occlusal tooth surfaces of *C. dispar* is dominated by scratches and pits are rare. Unlike the occlusal surfaces of hadrosaurid teeth, which although heavily scratched are relatively smooth, those of *C. dispar* have an underlying texture of raised circular features with an approximate diameter of 6 μm . Figure 9 shows samples of the microwear, captured from tooth 1 of the right maxilla of YPM 1886. The abundant raised circular features can be seen on all micrographs and evidence that these have not been introduced by the moulding and casting process can be seen in Figure 9.3; where a preparation artefact (a mark cutting across the tooth surface) has removed them. Arrows indicate the patterns of near vertical, high-angle oblique and sub

horizontal scratches with similar orientations to those on hadrosaurid teeth. Sub-horizontal scratches, symmetrical about the horizontal, that extend beyond the limits of the high magnification images are common to all sites on all teeth.

Visual assessment of the scratch orientations via detailed rose diagrams suggest that the microwear distribution is multimodal and the five discrete classes of scratches found in the hadrosaurids *Edmontosaurus* sp. and *Corythosaurus casuarius* are common to *Camptosaurus dispar* (a iguanodontid). DFA of the pooled data (3929 scratches from 5 sites on 4 teeth) confirmed the visual assessment (with only 1.1% of the scratches incorrectly assigned). DFA of the individual datasets YMP 7416 (1430 scratches from 2 sites on 2 teeth) and YPM 1886 (2498 scratches from 3 sites on 2 teeth), in each case, reported less than 1% of scratches incorrectly assigned. These data were then correctly assigned.

Figure 9. Microwear distribution on a tooth surface of *Camptosaurus dispar* YPM 1886. 9.1 Occlusal view of tooth 1 of the right maxilla, with inset boxes showing location for (9.2) and (9.3); anterior is to the right, crown ward is up. 9.2 Occlusal surface microwear showing scratches in various orientations. White arrows indicate high angle oblique scratches sloping in opposite directions (symmetrical about the vertical), black arrows indicate low angle scratches exceeding the dimensions of the image and the grey arrow shows near-vertical scratches. 9.3 Occlusal surface microwear, white arrows indicate sub-horizontal scratches sloping in opposite directions symmetrical about the horizontal, black arrows indicate a preparation artefact (a mark on the tooth surface) that has removed the surface pitting, and the grey arrows shows near-vertical scratches that have been overprinted.

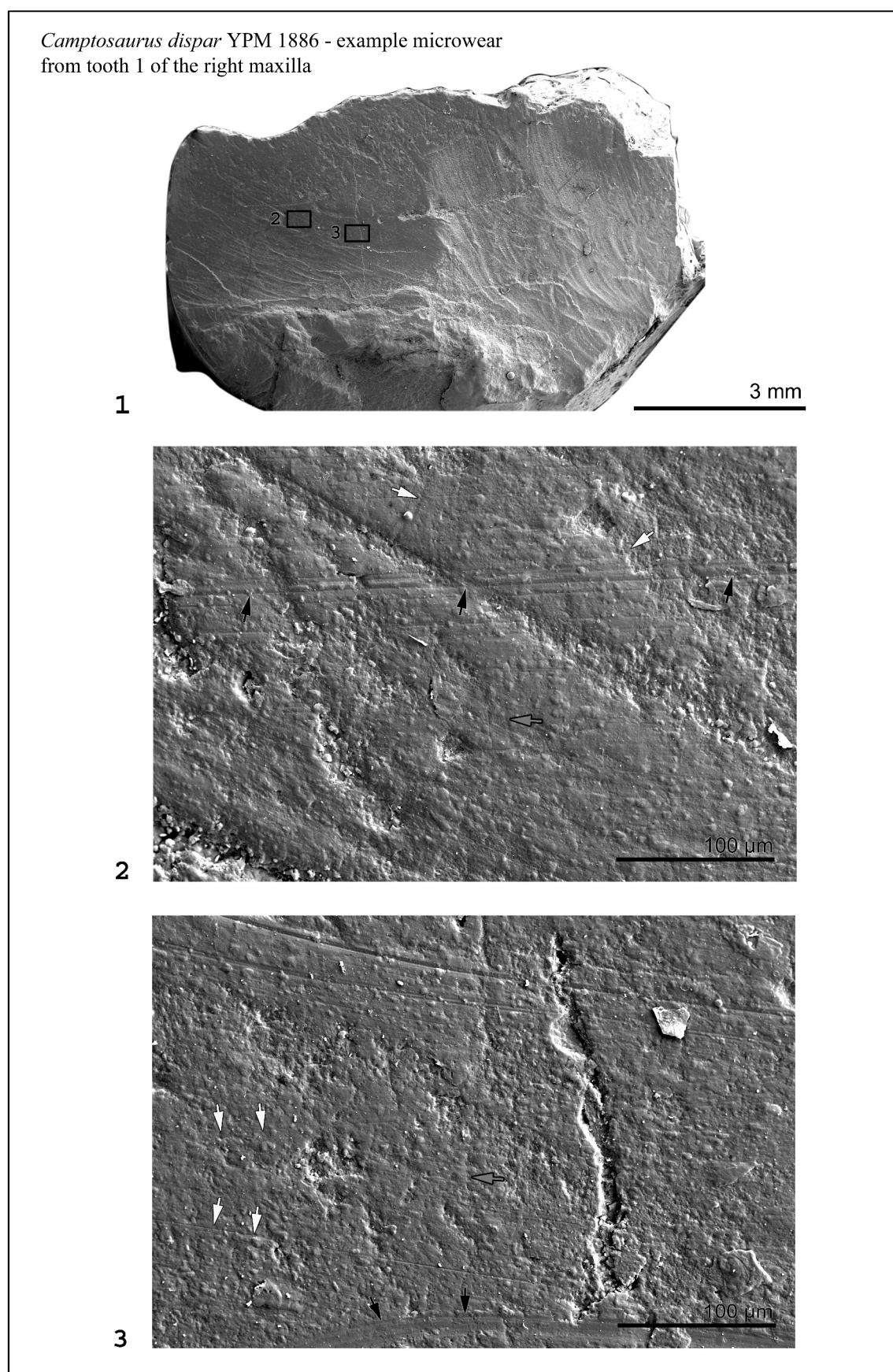


Figure 9.

In *Camptosaurus dispar*, unlike in hadrosaurids, scratch length and width cannot be used to distinguish between classes of scratches reliably. Scratch length differs significantly ($P < 0.05$) between classes in YPM 1886 but not in YPM 7416, and scratch width does not differ significantly between classes in either individual. Scratch length also differs significantly between all sites for the unclassified data and when partitioned by class (1-5).

The results of pairwise comparisons (Watson-Williams F test) reveal significant differences in orientation ($P < 0.05$) between all sites for the unclassified data and when partitioned by class (1-5), with the exception of two sites from the same tooth (YPM 1886 tooth 1, sites 1 and 2) which do not differ significantly for classes 2,3,4 and 5.

Hadrosaurid and Iguanodontid Microwear

To determine if microwear varies between species, occlusal microwear from 24 additional hadrosaurid specimens (25 jaw elements) was analysed. The results of these analyses confirm that the five discrete classes of scratches, found in *Edmontosaurus* sp. and *Corythosaurus casuarius* are common to hadrosaurids. Data from each jaw element were partitioned into subsets based on visual assessment of scratch orientation from detailed rose diagrams. Potential class boundaries, identified by rose diagram, were tested and confirmed by DFA ($< 2\%$ of scratches incorrectly assigned in each case). Incorrectly assigned scratches were re-assigned based on the DFA results. Table 10 shows the established class boundaries for each jaw element of each specimen. Data for *C. casuarius*, *Edmontosaurus* sp. and *C. dispar* is included for completeness. Although class boundaries are generally comparable within and between hadrosaurid and

Chapter 10: Dental microwear analysis: the implications for pleurokinesis in ornithopods

Table 10. Comparison of class boundaries in all hadrosaurid specimens; established by DFA. Figures shown either side of hyphens relate to the first and last scratch orientations either side of a boundary, where a precise figure cannot be given.

Species	Specimen	Element	N	Class boundaries			
				1 to 2	2 to 3	3 to 4	4 to 5
<i>Bactrosaurus johnsoni</i>	AMNH 6514	L. maxilla	1217	18.6 - 55.9	79.3	109.6 - 110.7	142
	AMNH 6553	R. dentary	596	9 - 46.7	75.5 - 76.3	108 - 114.6	144.9 - 145.6
	AMNH 6553	L. dentary	323	7.1 - 46.7	68.3 - 73.5	104.5 - 114.6	143.5 - 147.2
<i>Edmontosaurus regalis</i>	CM 1202	R. maxilla	848	2.66 - 38.4	74.3 - 75.9	106.09	138.9
	SM 12711	L. maxilla	702	1.3 - 40.9	69.8 - 74.6	105	139.7
<i>Corythosaurus casuarius</i>	AMNH 3971	L. dentary	944	24.9 - 45.4	74.6 - 75.1	101.7	130.6
	CM 1074	R. maxilla	1328	34.5	78.8	111.9	146.2
	CM 1077	R. maxilla	2791	37.8	73.3	102.6	137.4
	CM 11376	L. dentary	8394	37.9 - 38.3	74	105	138
	CM 11376	R. dentary	1929	36.6	75	104	137
	CM 11376	R. maxilla	3464	30.2 - 39.9	75.7	104	137.9
	SM 11893	R. maxilla	973	6.7 - 50.1	75.7	105.3	138.1
<i>Edmontosaurus</i> sp.	AMNH 2342	dentary	838	12.6 - 55.3	81.7	105.8	135
	AMNH 2342	maxilla	473	3.8 - 56.1	81.9	105.8	135
	AMNH 8145	L. dentary	558	-36.7	76	108.3	139.9
	NHMUK R3638	R. maxilla	1284	36	66.3	101.3	136.2
	NHMUK R3653	R. maxilla	2788	42	76.5	103.5	143.9
	NHMUK R3654	L. maxilla	1307	35.8	69.6	104.4	137.6
	NHMUK R3658	dentary	625	23.5 - 47.6	78.3	106.4	141.8
	NHMUK R4939	L. dentary	774	35.2 - 57.3	78.4	107.9	137.3
	SM 4807	L. dentary	547	33.4 - 39.6	75.9	107.8	141.1
	SM 4808	L. dentary	470	14.2 - 50.7	76.5	102.1	133.6 - 136.2
Hadrosaurids	AMNH 1181	dentary	671	37 - 42.2	74	100.4 - 106.2	136.7 - 137.8
	AMNH 21523	L. dentary	639	41.8 - 42.1	69.6 - 70.8	102.7	132
	AMNH 21524	L. dentary	614	11.4 - 37.5	70.6 - 73.3	106.7 - 107.4	137.6
	AMNH 21525	maxilla	1234	-30.34	72	104.6 - 104.9	138.2
	AMNH 21700	i. tooth	670	2.5 - 47.8	74.6 - 75.2	106.5	140.9
	AMNH 5465	L. dentary	752	37.9 - 62.1	82.1 - 82.7	106.8 - 107.1	140.7 - 141
	AMNH 5896	maxilla	545	4.1 - 34.4	76	109.7	140.6
	AMNH 6375	R. dentary	839	20 - 38.4	77.3	105.5	138
	AMNH 6380	L. dentary	538	36	76.2	105	138
	AMNH 6388	R. maxilla	1453	13.7 - 45.3	74	105.5	140.1
	AMNH 6529	R. dentary	777	2.1 - 41.9	76.5	107.5	141.9
	AMNH 6530	R. dentary	627	2 - 36.8	64.7 - 79.9	108.8	143.1
	AMNH 6547	L. dentary	289	9.4 - 39.9	75.5	103.6	140.6
	AMNH 6549	L. dentary	225	43.2	73.2	104.4 - 106.1	133.8 - 135.8
	AMNH 6550	L. dentary	270	-50.19	76.5	101.2 - 109.4	136.6 - 138
	AMNH 6581	R. dentary	702	4.8 - 46.5	73.7	103.8	138.3
<i>Hypacrosaurus altispinus</i>	SM 11950	L. dentary	596	36.2	74.4 - 74.8	106.6 - 107.1	140.1 - 141.5
<i>Kritosaurus navajovius</i>	SM 8629	L. dentary	416	35.7 - 37.3	75	104.2 - 113	142.5 - 143.5
<i>Lambeosaurus lambei</i>	YPM 21849	i. tooth	538	12.3 - 44.4	75.5	108.8 - 110.3	143.5
<i>Trachodon</i>	AMNH 107	maxilla	575	2.8 - 38.8	79.4	106.7	136.8
<i>Camptosaurus dispar</i>	YPM 7416	R. Maxilla	1430	30.8 - 32.3	69.8 - 70	106.3 - 107.1	139.8 - 140.1
	YPM 1886	maxilla	2498	29.1 - 31.8	74.1 - 74.5	109.6 - 109.9	145.2

iguanodontid species, there is variation in mean orientation for the unclassified data and for each orientation class (1-5), see Table S13 for summary data. Introduced bias (e.g., due to imperfect alignment of casts in the SEM) is possible, but this would result in a consistent shift in all class boundaries and hence all class mean orientations. There does not appear to be a pattern to the variation. In all cases the data show multiple dominant orientation modes.

Figures 10 to 13 display the scratch orientations for all of the hadrosaurid specimens in rose diagrams, with data suitably transformed for comparison (i.e. for the labial face of a left dentary tooth, anterior will be to the left but for the labial face of a right dentary tooth anterior will be to the right; in order to compare microwear patterns one set of data will need to be transformed and in this study all data requiring transformation has been transformed for comparison to the left dentary labial face). The relative frequency of the classes is shown by the area of the wedge and the diagrams have been automatically scaled for clarity (as the number of sites sampled varies by specimen). The black lines running from the centre of the rose to the outer edge, with arcs extending to either side show the mean orientation and 99% confidence interval for each class. The variation in microwear distribution between individuals in *Edmontosaurus* sp. (Figure 10) is evident, with the dominance of individual classes and the order of dominance changing from specimen to specimen. In contrast the consistency in scratch orientation and distribution between individuals in *Corythosaurus casuarius* (Figure 11) is equally evident. A comparison of different hadrosaurid species (Figure 12), non-specific hadrosaur specimens (Figure 11 and Figure 13) and iguanodontid (Figure 14) illustrates the similarities in microwear distribution and orientation between these taxa. The same number of orientation classes, with similar boundaries and mean orientations, can be seen in all of the taxa. The data

shows that scratches in the class 1 orientation are highly variable and not always present, and scratches in the class 5 orientation dominate more consistently than any other class (in terms of N - which is represented by frequency in the rose diagrams). The relative jaw motions that generate these classes of scratches, and the complexity of the jaw mechanics that can produce more than one dominant class, also appears common to all of the taxa in this study.

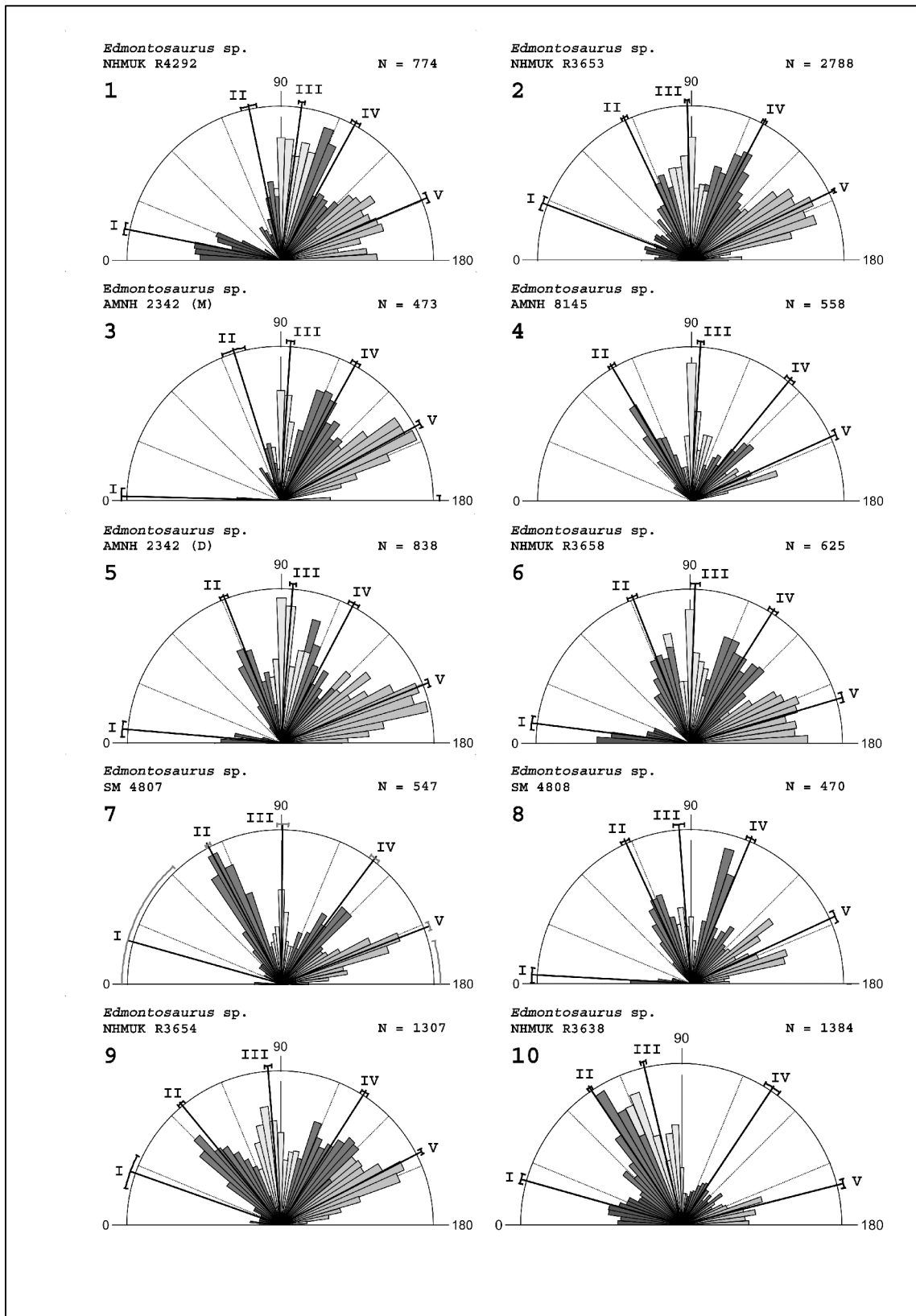


Figure 10. Rose diagrams of microwear scratch orientations on the teeth of specimens of *Edmontosaurus* sp. showing variation between individuals. Shading indicates individual classes. Black lines running from the centre of the rose diagram to the outer edge, with arcs extending to either side show the mean orientation and 99% confidence interval for each class (I to V). Frequency is shown by the area of the wedge. Bin size = 4°.

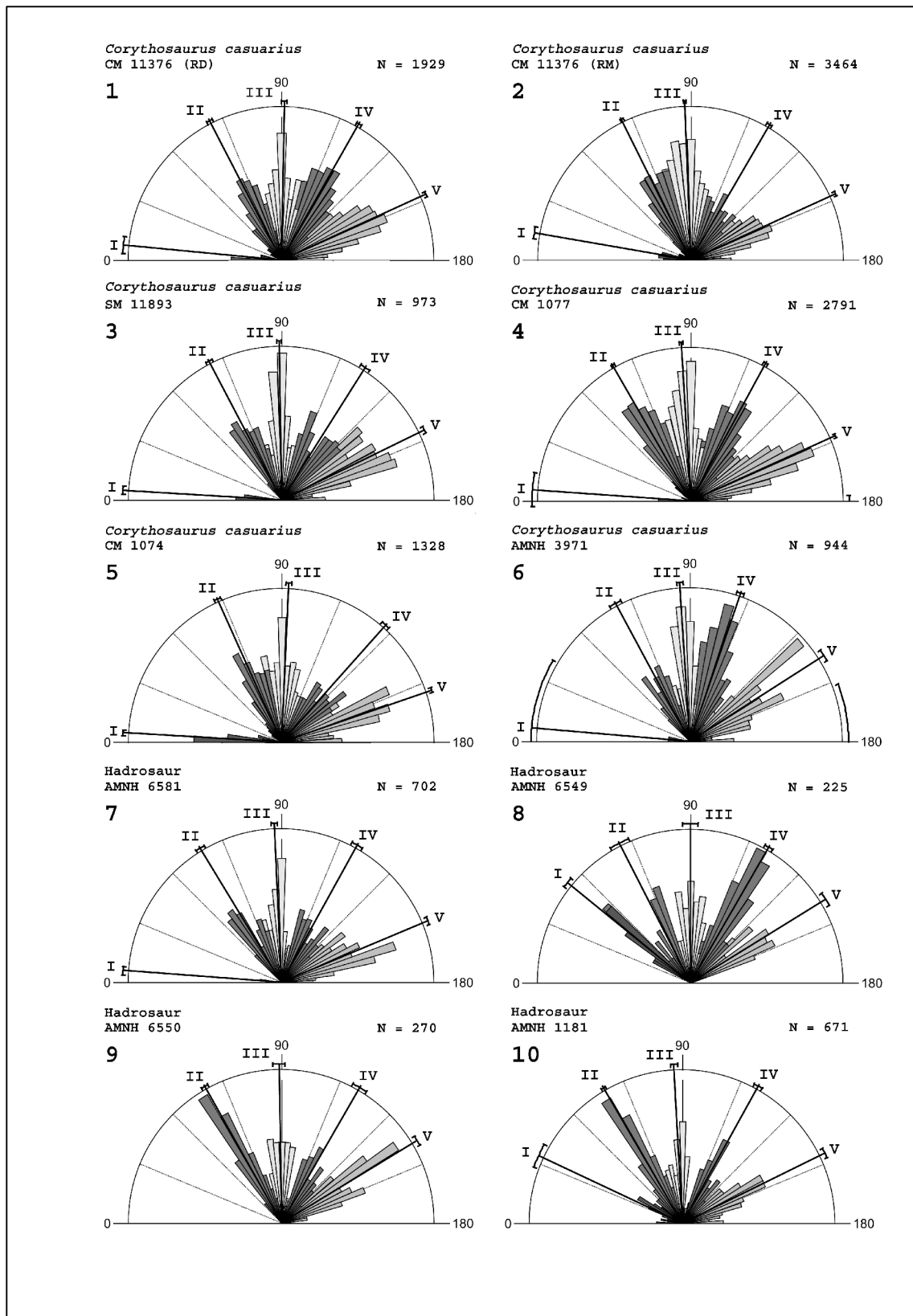


Figure 11. Rose diagrams of microwear scratch orientations on the teeth of 5 specimens (6 jaw elements) of *Corythosaurus casuarius* and 4 specimens of non-specific hadrosaurids (*Hadrosaur*?) showing consistent distributions between individuals. Shading indicates individual classes. Black lines running from the centre of the rose diagram to the outer edge, with arcs extending to either side show the mean orientation and 99% confidence interval for each class (I to V). Frequency is shown by the area of the wedge. Bin size = 4°.

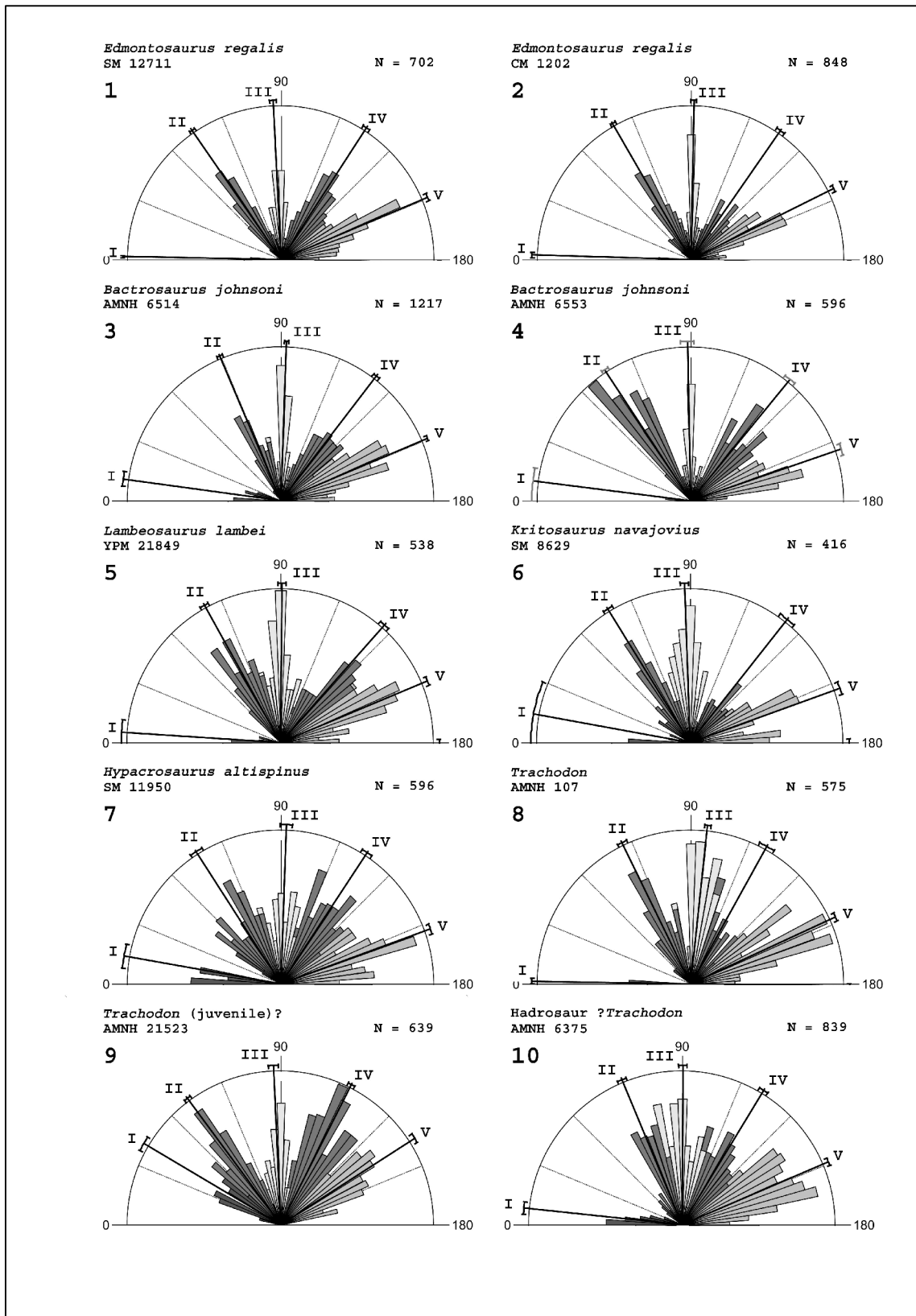


Figure 12. Rose diagrams of microwear scratch orientations on the teeth of specimens of various species of hadrosaurid showing consistent distributions between species. Shading indicates individual classes. Black lines running from the centre of the rose diagram to the outer edge, with arcs extending to either side show the mean orientation and 99% confidence interval for each class (I to V). Frequency is shown by the area of the wedge. Bin size = 4°.

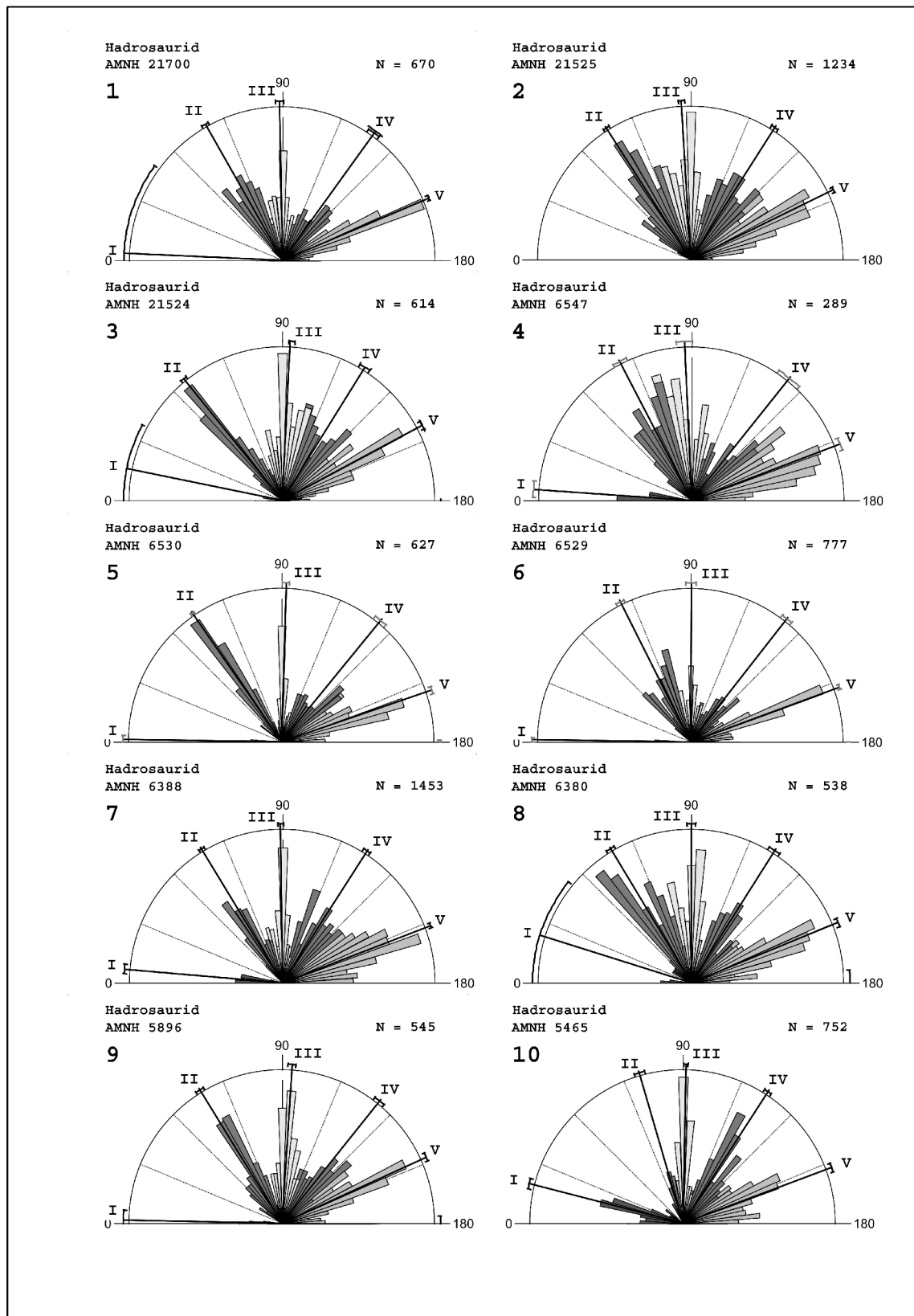


Figure 13. Rose diagrams of microwear scratch orientations on the teeth of specimens of non-specific hadrosaurids (*Hadrosaurus*?) showing consistent distributions between individuals/species. Shading indicates individual classes. Black lines running from the centre of the rose diagram to the outer edge, with arcs extending to either side show the mean orientation and 99% confidence interval for each class (I to V). Frequency is shown by the area of the wedge. Bin size = 4°.

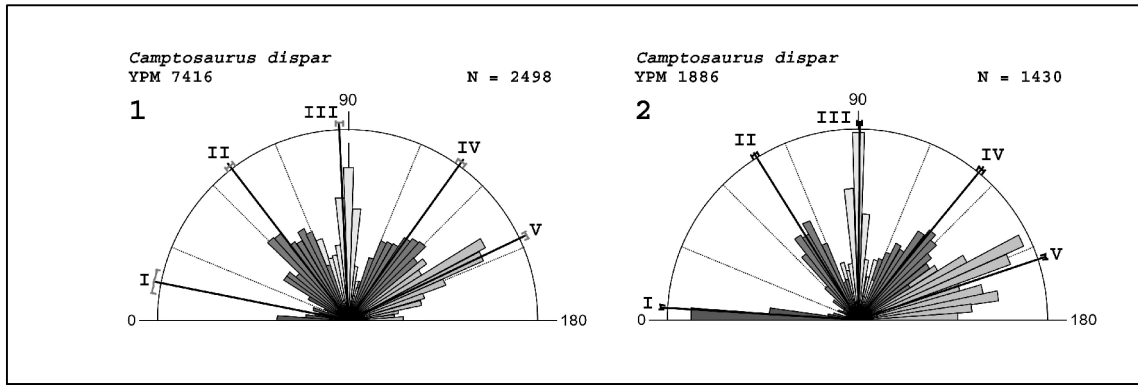


Figure 14. Rose diagrams of microwear scratch orientations on the teeth of specimens of the basal iguanodontian *Camptosaurus dispar* showing consistent distributions between two individuals. Shading indicates individual classes. Black lines running from the centre of the rose diagram to the outer edge, with arcs extending to either side show the mean orientation and 99% confidence interval for each class (I to V). Frequency is shown by the area of the wedge. Bin size = 4°.

At high magnification (x300), continuous scratches are rare due to cross cutting by scratches in other orientations. At lower magnifications the cross cutting does not prevent the true extent of the scratch being observed. The recorded scratch lengths, from analyses of x300 magnification micrographs in this study, do not reflect the degree of translation of maxillary teeth across dentary teeth. Figure 15 shows the microwear distribution of a hadrosaurid tooth (AMNH 1181) at low magnification. Arrows highlight examples of continuous scratches that cross the entire tooth surface travelling in excess of 15mm and the low angle scratch suggests propalinal (anteroposterior) motion of at least this distance.

Even with these limitations, a plot of mean scratch length by width (Figure 16) for individual teeth from each of the hadrosaurid specimens identifies some separation of species. There is a concentration of samples with a scratch length between 40 and 70 μm and a width of around 1 μm however the wider and shorter scratches of the *Bactrosaurus johnsoni* microwear separate it from the other hadrosaurids and, *C. casuarius* also appears to form a group with slightly wider scratches than the most of the other species.

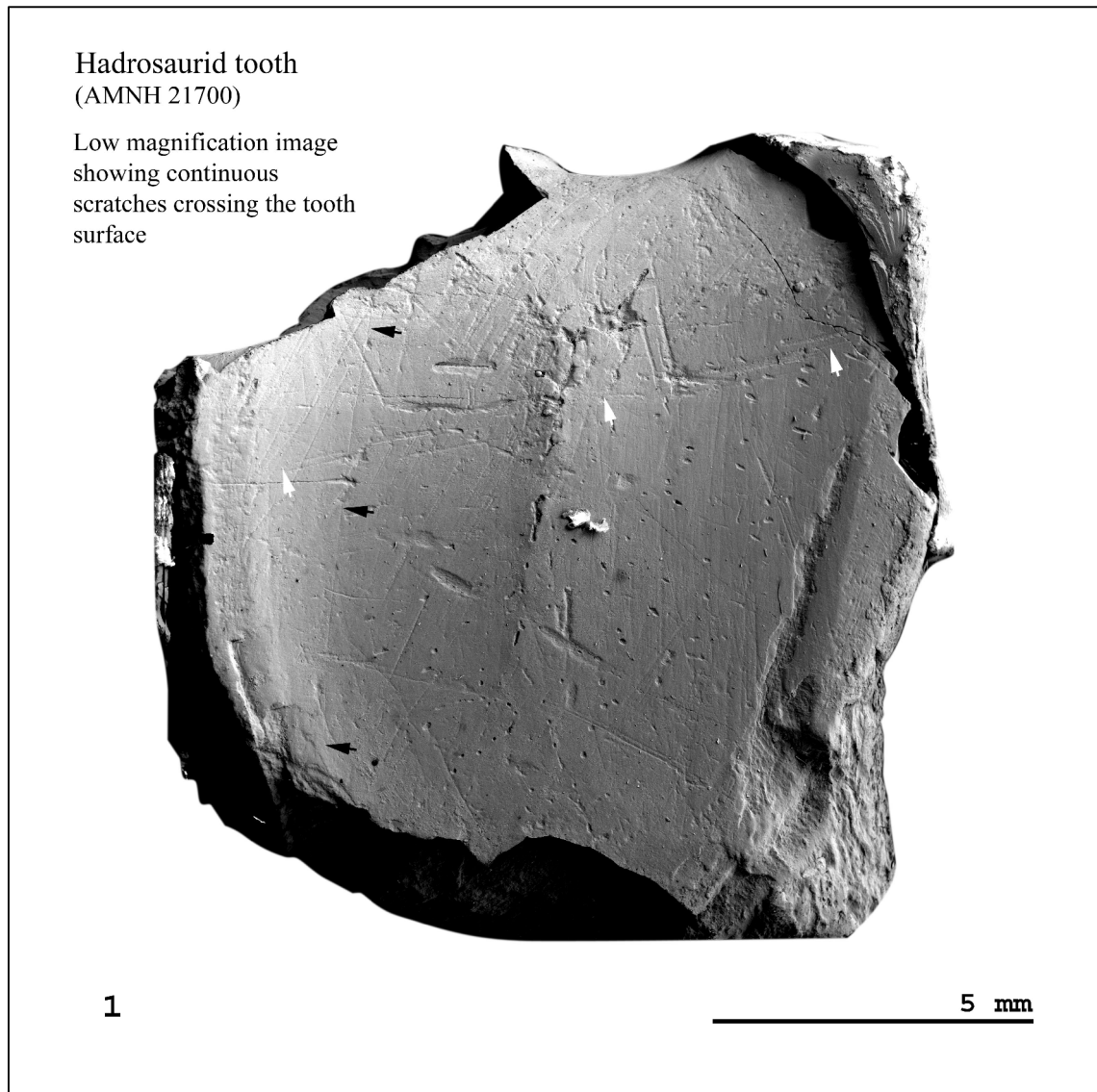


Figure 15. Microwear distribution on a tooth surface of *Hadrosaurus* ? AMNH 21700. 15.1 Occlusal view of an isolate dentary tooth with scratches extending beyond the limits of the tooth face. Arrows indicate two separate continuous scratches that traverse the entire tooth surface extending in both directions towards teeth that would have been adjacent in the tooth battery. The low angle scratch suggests propalinal (anteroposterior) motion in excess of 15mm.

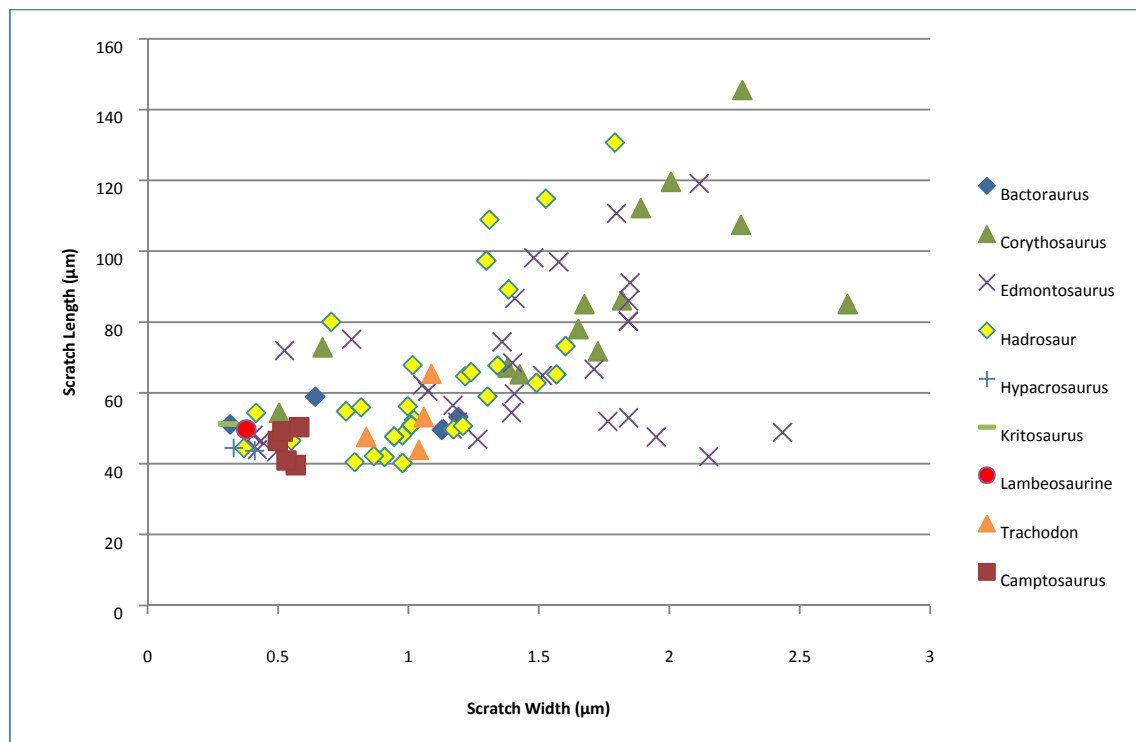


Figure 16. Mean scratch length (log) by width plot of microwear from equal area samples of individual teeth from all hadrosaurid and iguanodontid specimens, showing distribution/separation of species.

Discussion

To grind food effectively, teeth need to do more than simply shear past each other. Given the nature of hadrosaurid/iguanodontid skull morphology and jaw mechanics, something more complicated than this occurred. Dental microwear is the result of a combination of mechanical processes and the material properties of both the food being masticated and the teeth. In mammal studies scratch length and width are generally informative about diet and the food processing action (e.g. shearing/crushing) and the compressive forces involved. Teaford and Walker (1984) demonstrated that the ratio of pits to scratches (short wide scratches to longer narrower ones) can be used to distinguish between harder and softer diets. They also determined that longer scratch lengths result from a shearing rather than a crushing motion of the jaws and relate to a softer diet. For scratch width (and depth) a key influencing factor is the compressive forces applied during mastication (Gordon 1984a). Feature density (N) from equal area

sites is also considered a useful measure for testing variance (Gordon 1988). Previous microwear research has generally used these four variables (length, width, N and orientation consistency) to assess microwear patterns. In mammals, these patterns will change in terms of scratch and pit dimension and orientation, as the relative motion of the upper and lower jaws change or as the compression/shear force between them changes.

However, there are significant differences between dinosaur and mammal feeding mechanisms that make microwear analysis and interpretation more difficult. In mammals, microwear is accumulated on the permanent dentition throughout life. Their teeth can retain informative microwear, which may have been formed over a relatively short period. By contrast, dinosaurs shed and replaced their teeth continually. The nature of the occlusal surface of a hadrosaurid tooth row is such that the enamel outer edge of a maxillary tooth effectively ‘planes’ the dentine surface of one or more dentary teeth, repeatedly. Simultaneously the enamel inner edge of the most medial dentary tooth ‘planes’ the dentine surface of that maxillary tooth as part of the same action. As teeth are worn down microwear is repeatedly overprinted. Due to changes in relative jaw motion during hadrosaurid mastication, multiple patterns of parallel scratches in different orientations are produced. The results suggest that pre-existing patterns of scratches are being partially removed and overprinted by subsequent patterns making statistical analysis problematic, particularly analyses of variability of orientation. One of the effects of overprinting is that N cannot be relied upon as a measure of variability in diet (e.g. abrasiveness). The existence of multiple dominant modes in the orientation data, within which scratches have a consistently high degree of parallelism (R), results in R being largely uninformative in hadrosaurid studies other than as an indicator of orientation class. Pitting is rare to absent on hadrosaurid teeth and this combined with a

high R value would, if the teeth belonged to a mammal, be interpreted as reflecting a diet that does not contain hard objects. A soft diet does not seem parsimonious.

However, the lack of pitting on the teeth of hadrosaurids and iguanodontids may be a function of the softer dentine occlusal surface, rather than an indicator of a softer diet.

The scratches on the teeth of hadrosaurid and iguanodontid dinosaurs occur as five distinct classes with significantly differing orientations. The five classes are common to all of the specimens tested and reflect relative jaw motion. No single mode is consistently dominant and the dominant mode can vary between sample sites within an individual, and between individuals and species. My initial findings that a single tooth could be representative of an animal need some revision, or at least a qualification. If microwear in all orientations can be found then the original hypothesis holds true, and isolated teeth can make a contribution to the study of jaw mechanics and diet. However, if the microwear has been overprinted by a dominant mode to the exclusion of one or more of the others then sampling from multiple sites and/or teeth will be necessary; and potentially multiple individuals. An example of the problem can be seen in the data from *Edmontosaurus* sp. NHMUK R3638. All five orientations can be determined and are consistent between teeth, however all five are not present on all teeth. Because of the overlap between adjacent classes, removal of one can affect the mean orientation of another. Within all hadrosaurid specimens, the switching of highest frequency (N) between the dominant modes (classes 2, 3, 4 and 5) can be seen both between jaw elements and within a jaw element. For studies of this kind, that attempt the reconstruction of relative jaw motion, researchers will need to develop a sampling strategy that will allow sufficient data to be captured to ensure that all orientation classes are represented.

Some of the observed variation in microwear distribution and the relative motion of the jaws could relate to changes in food processing. Scratches are produced when hard particles are dragged or sheared between tooth surfaces and the physical properties of the plant can influence how this occurs. Tough plant material can affect the applied compressive forces, and therefore the resultant microwear pattern, generating scratches in a non-preferred orientation (e.g., Gügel *et al.* 2001). An animal can also modify its mastication, changing the relative motion of its jaws, to reflect the physical properties of the plant being processed. The consistency in class boundaries and class mean orientation within hadrosaurids and iguanodontids suggests that they had the same or similar jaw movements and certain of those movements were more frequent than others. The nature of the occlusal surface, a single flattened obliquely sloping ($\sim 40^\circ$ to 55°) grinding platform consisting of multiple rows of teeth that curves and widens slightly along its length, means that the shear and compression forces cannot be uniform. This could account for some of the observed variation in microwear orientation between teeth, within an individual. Bite force could also be expected to change, reducing with distance from the jaw hinge however no evidence of systematic variation was found. Another potential source of variation is the inclination of the occlusal surface which varies in hadrosaurids (between individuals and species), and can vary between the left and right hand jaw elements within an individual. Mastication in hadrosaurids occurred in 3D, on tooth rows that were not necessarily parallel and may not have been oriented as mirror images in life. This could account for the significant differences between the left and right jaw elements of *Corythosaurus casuarius* CM 11376. The methodology used for micrograph imaging by rotating the flat occlusal plane such that it is perpendicular to the SEM beam may also introduce variation. This will not cause a problem for jaw elements that occluded with each other

but could introduce a variation if the attitude of the occlusal planes of the jaw elements being compared were different in life. Finally, when dealing with fragments of dentaries and maxillae it is not always clear if they are from the right or left jaw; they are often simply labelled as dentary or maxilla without any further qualification. It is not always clear from the microwear patterns either. In other ornithopods such as *Hypsilophodon* there is a clear asymmetry to the microwear but this is not always true for hadrosaurids or iguanodontids. The class 1 and class 5, and the class 2 and class 4 are largely symmetrical about the near vertical class 3. An assessment can be made using frequency (N) of class 1 as this is typically low, much lower than that of class 5 but not in all cases. One example of this is the microwear patterns from R3638, which is labelled as a right maxilla. These show little difference in frequency between class 1 and class 5 and were it an unlabelled specimen could have caused it to be incorrectly classified as a left maxilla (see Figure 10.10).

How then do the actual microwear patterns relate to those predicted by the various models for feeding in hadrosaurids? Simple vertical adduction, which can be seen in extant reptiles, produces unidirectional shearing or crushing. The resultant microwear pattern from a simple rotation at the hinge would show a single dominant mode with scratch orientations near 90° to the tooth row long axis (allowing for some retraction of the lower jaw during closure). A propalinal (anteroposterior) translational movement of the jaws would produce dominant near horizontal microwear orientations if the tooth rows are parallel, or highly oblique orientations if the tooth rows converge anteriorly (the tooth rows of both *Edmontosaurus* sp. and *Corythosaurus casuarius* converge anteriorly). The pleurokinesis model combines vertical adduction with a lateral translation and allows for some streptostylic movement. As teeth of the dentaries and maxillae come together, the vertical moment of the dentaries carry them upward

driving the maxillae outward and forcing a lateral power stroke. Simultaneously some movement of the quadrate against the squamosal (part of the brain case) allows a propalinal (anteroposterior) translation. This could produce dominant near vertical and minor sub horizontal scratch orientations, or if the motions were combined it could produce dominant oblique scratch orientations. Disarticulation of the facial bones during the power stroke (Rybczynski *et al.* 2008; Williams *et al.* 2009) would affect the attitude of the maxillae, generating multiple changes in scratch orientation and leading to variations both within the surface of a tooth and between teeth. Similarly rotation of the dentaries about their long axis (Bell *et al.* 2009) would lead to a systematic variation in scratch length and orientation along the tooth row, with longer and more oblique scratches at back of the jaw.

The actual microwear orientations contain multiple dominant modes and whilst frequency coupled with differences in scratch width could be expected to identify the power stroke, they do not in hadrosaurids or iguanodontids. In hadrosaurids there are statistically significant differences in scratch width between the classes but they do not differ sufficiently to be useful in identifying a power stroke. Coarse scratches can be found in all 4 dominant orientation classes. In *Corythosaurus casuarius* CM 11376 the 4 dominant modes have class means of 60°, 88°, 120° and 156°. In the pooled data (all jaw elements) the highest frequency is in the near vertical (88°) mode, but the right dentary data show the highest frequency in the sub-horizontal (156°) mode. Similarly, whilst most of the *Edmontosaurs* sp. specimens show multiple dominant modes with the highest frequency in the sub-horizontal mode (156°), NHMUK R3638 upon which my preliminary research was performed, shows a single dominant mode at 60°. These data indicate that jaw closure was not brought about by simple vertical adduction and support my preliminary findings for a pleurokinetic hinge. I interpret class 3 scratches

as simple vertical adduction followed by transverse translation of the maxillae over the dentaries (pleurokinesis (Weishampel 1984; Norman and Weishampel 1985)). Class 2 and class 4 scratches relate to a combination of transverse and propalinal translation (and are also supportive of the pleurokinesis model with streptostyly), whilst class 5 scratches reflect pure propalinal translation. Contrary to my previous findings, the dominance (N) of the class 5 scratches suggest that a propalinal action was significant in food processing within hadrosaurids, rather than a minor component related to the kinetic activity of the cranium about the pleurokinetic hinge. The data (for class 5) support the mastication model predicted by Ostrom (1961), that movement at the articular/surangular/quadrangle joint (protraction and retraction of the lower jaws) and potentially streptostylic movement (of the quadrangle against the squamosal) allowed a propalinal translation of the lower jaw.

The sequence of jaw movements is then closure bringing the teeth of the upper and lower jaws into contact, followed by a continued upward movement of the dentaries forcing a transverse translation of the maxillae (a power stroke). There are two different methods by which this transverse translation can occur. The first is with no protraction or retraction of the dentaries, which will produce class 3 scratches and the second is with either a protraction or retraction of the dentaries, which will produce class 2 or class 4 scratches. A repeated sequence of jaw opening and closing will generate mastication. Continuous high angle oblique scratches crossing tooth rows (labial to lingual) show that the teeth remained in contact during the opening and closing stage. The third option for a food processing movement is a propalinal translation of the dentaries, with the teeth fully occluded (i.e. this movement needs to follow both jaw closure, and a transverse translation of the maxillae over the dentaries). A repeated sequence of protraction and retraction of the dentaries will produce class 5 scratches.

With parallel tooth rows, these will be near horizontal and with tooth rows that converge anteriorly, the scratches will be oblique. Continuous low angle oblique and near horizontal scratches from tooth to tooth along the tooth row and on each tooth row (labial to lingual) show that the teeth remained in occlusion during the propalinal power stroke.

That hadrosaurids and iguanodontids could switch between these three sets of relative jaw motions is an important finding. It may be that the choice of relative jaw motion (mastication method) was governed by the physical properties of the plants being masticated and dental microwear analysis targeted at determining diet may resolve this. It is not clear if the two high-angle oblique microwear patterns (class 2 and class 4) involve both an opening and closing stroke or if one is related to opening and one to closing, (only class 2 can be seen in AMNH R3638). Gordon (1984b) described a method that can indicate the direction an abrasive particle took from the shape of fracture cones formed at the margin of the scratch. However scratches showing these characteristics are rare and to date have proven inconclusive.

The evolutionary implications of this microwear study are that the complex jaw mechanics necessary to generate these three sets of relative jaw motions, and enable true mastication in ornithopods, were sufficiently advanced in the basal iguanodontian *Camptosaurus dispar* that there are no significant differences between it and the hadrosaurids studied.

For future microwear analyses in ornithopod dinosaurs, one potential solution to the problem of overprinting of the occlusal surface microwear would be to use the off occlusal labial surface of the maxillary teeth. The labial surface of maxillary teeth is composed of enamel rather than dentine and will have a functional life (and hence a recording time) that greatly exceeds that of the occlusal surface. My research on

Hypsilophodon foxii has shown that the off-occlusal surface (with some blurring of the class boundaries) preserves the same microwear orientations as the occlusal surface.

Dental microwear analysis is a powerful tool for palaeontological and biomechanical research and has the potential to unravel the mysteries of diet and feeding in diverse taxa including those with no modern functional analogues.

Supplementary information

Table S1. Microwear summary statistics for *Corythosaurus casuarius* CM 11376, unclassified data

Pooled Element	Tooth	Site	Angular disp. n	r	Rayleigh Z	p	Rao U	p	Orientation μ	(μ m) length	(μ m) width
L. dentary	1	1	121	0.531	34.116	<< 0.001	192.484	< 0.01	74.754	103.1	1.5
	1	2	117	0.571	38.145	<< 0.001	209.907	< 0.01	104.529	82.1	1.2
	1	4	203	0.369	27.658	<< 0.001	217.008	< 0.01	99.878	84.4	1.3
	3	1	220	0.507	56.484	<< 0.001	188.036	< 0.01	101.635	74.4	1.0
	3	2	322	0.518	86.364	<< 0.001	208.159	< 0.01	94.267	68.2	1.1
	3	3	288	0.480	66.439	<< 0.001	198.776	< 0.01	108.883	62.1	1.0
	3	4	236	0.458	49.587	<< 0.001	195.427	< 0.01	88.663	82.9	1.3
	3	5	372	0.409	62.194	<< 0.001	179.332	< 0.01	88.608	57.6	1.2
	3	6	296	0.466	64.316	<< 0.001	197.062	< 0.01	82.743	53.7	0.9
	3	7	528	0.378	75.444	<< 0.001	172.596	< 0.01	91.363	62.7	1.0
	4	1	158	0.464	33.963	<< 0.001	201.042	< 0.01	103.847	77.7	1.7
	5	1	192	0.349	23.378	<< 0.001	192.156	< 0.01	115.334	87.4	1.2
	5	3	280	0.428	51.240	<< 0.001	175.847	< 0.01	97.026	63.1	0.8
	7	1	283	0.397	44.549	<< 0.001	182.552	< 0.01	107.608	54.3	0.7
	7	2	376	0.320	38.584	<< 0.001	165.723	< 0.01	101.968	50.0	0.6
	7	3	295	0.332	32.458	<< 0.001	169.771	< 0.01	97.138	51.3	0.6
	18	1	286	0.311	27.671	<< 0.001	190.466	< 0.01	124.464	68.8	1.3
	19	1	329	0.289	27.412	<< 0.001	188.028	< 0.01	129.783	55.5	0.9
	19	2	307	0.329	33.189	<< 0.001	175.344	< 0.01	115.477	67.5	1.1
	20	2	234	0.225	11.820	<< 0.001	182.360	< 0.01	116.606	72.0	1.1
	20	4	231	0.212	10.406	<< 0.001	187.511	< 0.01	124.692	64.5	0.7
	21	3	271	0.486	63.894	<< 0.001	196.066	< 0.01	99.227	62.3	0.7
	22	1	198	0.530	55.608	<< 0.001	212.588	< 0.01	147.517	76.5	1.4
	22	4	266	0.242	15.573	<< 0.001	191.194	< 0.01	133.975	77.9	1.2
	23	2	244	0.367	32.807	<< 0.001	170.205	< 0.01	115.094	65.9	1.1
	23	3	346	0.205	14.528	<< 0.001	174.442	< 0.01	103.745	62.4	0.9
	23	4	257	0.287	21.229	<< 0.001	180.623	< 0.01	105.468	61.3	1.3
	24	1	221	0.243	13.102	<< 0.001	203.551	< 0.01	103.118	65.2	1.3
	25	1	192	0.344	22.663	<< 0.001	215.095	< 0.01	88.496	77.2	1.4
	26	1	257	0.382	37.526	<< 0.001	191.576	< 0.01	99.108	68.5	1.4
	26	2	277	0.367	37.237	<< 0.001	177.410	< 0.01	108.980	64.2	1.2
	28	1	191	0.360	24.726	<< 0.001	184.571	< 0.01	88.542	59.5	1.3

Table S1. continued

Pooled Element	Tooth	Site	Angular disp. n	r	Rayleigh Z	p	Rao U	p	Orientation μ	(μm) length	(μm) width
R. dentary	3	2	57	0.771	33.905	<< 0.001	211.329	< 0.01	134.775	91.8	2.7
	3	3	336	0.465	72.659	<< 0.001	196.616	< 0.01	116.415	73.2	1.3
	4	1	210	0.383	30.751	<< 0.001	192.302	< 0.01	120.496	88.2	2.0
	4	3	110	0.434	20.680	<< 0.001	214.425	< 0.01	124.030	87.5	3.4
	7	2	100	0.531	28.157	<< 0.001	194.703	< 0.01	135.627	69.6	1.4
	8	1	212	0.369	28.921	<< 0.001	208.672	< 0.01	111.563	92.1	1.2
	10	1	200	0.216	9.308	<< 0.001	175.089	< 0.01	101.527	78.7	1.2
	11	1	178	0.402	28.820	<< 0.001	199.502	< 0.01	115.937	91.8	1.5
	24	1	182	0.376	25.689	<< 0.001	186.445	< 0.01	104.256	69.4	1.1
	25	1	158	0.331	17.275	<< 0.001	193.031	< 0.01	93.459	55.4	0.8
	32	1	186	0.398	29.415	<< 0.001	180.136	< 0.01	103.186	64.5	1.5
R. maxilla	1	1	171	0.406	28.155	<< 0.001	183.091	< 0.01	92.235	88.3	1.0
	2	1	186	0.427	33.967	<< 0.001	200.927	< 0.01	101.635	96.5	1.5
	2	2	195	0.389	29.541	<< 0.001	186.462	< 0.01	115.319	78.0	1.4
	5	1	176	0.272	12.984	<< 0.001	198.597	< 0.01	107.048	71.7	1.5
	7	1	244	0.313	23.966	<< 0.001	175.796	< 0.01	93.939	86.2	1.6
	8	3	449	0.401	72.166	<< 0.001	198.722	< 0.01	103.979	85.1	1.4
	9	3	460	0.401	74.087	<< 0.001	189.260	< 0.01	93.479	65.3	1.2
	20	2	338	0.386	50.417	<< 0.001	185.427	< 0.01	84.596	67.2	1.2
	22	2	278	0.469	61.185	<< 0.001	195.339	< 0.01	89.415	67.1	1.5
	23	1	205	0.514	54.131	<< 0.001	196.997	< 0.01	96.839	75.7	1.5
	24	1	199	0.486	46.931	<< 0.001	210.433	< 0.01	94.236	86.4	1.4
	25	1	190	0.482	44.217	<< 0.001	198.474	< 0.01	87.597	76.9	1.2
	29	3	373	0.517	99.717	<< 0.001	196.707	< 0.01	88.620	72.4	1.2

Table S2. Microwear summary statistics for *Corythosaurus casuarius* CM 11376, class 1 data

Class 1				Angular disp.	Rayleigh				Rao	Rayleigh (expected mean 15.83°)			Orientation	(μm)	(μm)	
Element	Tooth	Site	n	r	Z	p		U	p	V	u	p	μ	length	w idth	
L. dentary	1	1	14	0.960	12.910	<< 0.001		285.980	< 0.01	0.937	4.958	<< 0.001	28.501	85.1	1.4	
	1	2	2	0.998	1.992	0.139				0.947	1.893	0.026	34.320	42.6	0.6	
	1	4	0													
	3	1	0													
	3	2	1	1.000	1.000	0.512				0.937	1.325	0.120	36.304	28.3	0.2	
	3	3	7	0.997	6.965	<< 0.001		294.951	< 0.01	0.956	3.578	<< 0.001	32.341	59.0	0.7	
	3	4	0													
	3	5	20	0.961	18.484	<< 0.001		278.804	< 0.01	0.949	6.001	<< 0.001	25.057	48.1	0.7	
	3	6	16	0.992	15.754	<< 0.001		312.986	< 0.01	0.964	5.451	<< 0.001	29.618	44.7	0.3	
	3	7	49	0.966	45.706	<< 0.001		306.612	< 0.01	0.930	9.210	<< 0.001	31.394	56.2	0.6	
	4	1	0													
	5	1	3	0.998	2.990	0.034				0.943	2.309	0.007	35.035	89.1	0.3	
	5	3	9	0.989	8.810	<< 0.001		292.742	< 0.01	0.967	4.101	<< 0.001	28.161	41.0	0.3	
	7	1	4	0.983	3.863	0.009		242.938	< 0.01	0.959	2.713	0.001	28.383	38.1	0.3	
	7	2	15	0.984	14.520	<< 0.001		293.070	< 0.01	0.979	5.364	<< 0.001	21.368	30.8	0.4	
	7	3	16	0.929	13.809	<< 0.001		266.922	< 0.01	0.921	5.209	<< 0.001	23.461	34.7	0.3	
	18	1	24	0.983	23.193	<< 0.001		299.736	< 0.01	0.970	6.720	<< 0.001	6.489	93.4	1.3	
	19	1	29	0.970	27.283	<< 0.001		299.294	< 0.01	0.963	7.337	<< 0.001	9.135	43.6	0.9	
	19	2	29	0.944	25.817	<< 0.001		280.206	< 0.01	0.943	7.183	<< 0.001	14.360	82.7	1.2	
	20	2	18	0.985	17.455	<< 0.001		298.322	< 0.01	0.979	5.871	0.000	9.369	84.9	1.4	
	20	4	37	0.989	36.182	<< 0.001		320.478	< 0.01	0.977	8.404	<< 0.001	6.916	114.8	1.1	
	21	3	13	0.968	12.193	<< 0.001		276.748	< 0.01	0.968	4.938	<< 0.001	15.958	89.6	0.8	
	22	1	36	0.972	34.025	<< 0.001		305.568	< 0.01	0.968	8.213	<< 0.001	10.455	87.9	1.2	
	22	4	19	0.989	18.585	<< 0.001		308.309	< 0.01	0.972	5.992	<< 0.001	5.215	83.3	1.3	
	23	2	6	0.954	5.458	<< 0.001		245.342	< 0.01	0.947	3.280	<< 0.001	22.679	36.4	0.5	
	23	3	15	0.972	14.175	<< 0.001		289.484	< 0.01	0.960	5.258	<< 0.001	24.879	37.5	0.6	
	23	4	0													
	24	1	13	0.996	12.888	<< 0.001		315.576	< 0.01	0.979	4.993	<< 0.001	5.378	56.2	1.2	
	25	1	1	1.000	1.000	0.512					0.967	1.368	0.110	1.181	44.9	4.2
	26	1	6	0.991	5.897	<< 0.001		280.806	< 0.01	0.972	3.367	<< 0.001	4.507	88.8	2.1	
	26	2	8	0.994	7.910	<< 0.001		296.740	< 0.01	0.979	3.917	<< 0.001	5.799	84.4	1.1	
	28	1	15	0.986	14.573	<< 0.001		303.022	< 0.01	0.944	5.169	<< 0.001	32.587	45.7	0.4	

Table S2. continued.

Class 1	Element	Tooth	Site	Angular disp. n	r	Rayleigh Z	p	Rao U	p	Rayleigh (expected mean 15.83°) V	u	p	Orientation μ	(μm) length	(μm) width
R. Dentary		3	2	0											
		3	3	4	0.995	3.959	0.008	255.326	< 0.01	0.984	2.784	<< 0.001	7.494	72.2	1.4
		4	1	1	1.000	1.000	0.512			0.966	1.366	0.111	0.754	70.4	2.3
		4	3	0											
		7	2	8	0.999	7.982	<< 0.001	306.482	< 0.01	0.974	3.897	<< 0.001	3.099	47.9	1.0
		8	1	0											
		10	1	1	1.000	1.000	0.512			0.966	1.367	0.111	0.939	28.3	1.4
		11	1	3	0.904	2.450	0.076			0.903	2.212	0.010	13.736	48.5	0.9
		24	1	0											
		25	1	4	0.991	3.929	0.008	251.878	< 0.01	0.986	2.789	<< 0.001	10.090	59.6	0.7
		32	1	6	0.999	5.992	<< 0.001	293.576	< 0.01	0.969	3.356	<< 0.001	1.652	91.8	1.5
	R. maxilla	1	1	6	0.995	5.940	<< 0.001	282.158	< 0.01	0.989	3.427	<< 0.001	9.615	133.2	0.8
		2	1	2	0.973	1.895	0.158			0.973	1.947	0.022	16.796	50.3	0.9
		2	2	4	0.999	3.992	0.007	262.784	< 0.01	0.985	2.786	<< 0.001	6.214	65.4	1.7
		5	1	0											
		7	1	23	0.986	22.361	<< 0.001	313.122	< 0.01	0.981	6.655	<< 0.001	10.178	79.7	1.1
		8	3	14	0.935	12.248	<< 0.001	273.354	< 0.01	0.935	4.949	<< 0.001	15.850	88.1	1.5
		9	3	15	0.990	14.714	<< 0.001	304.282	< 0.01	0.975	5.342	<< 0.001	5.787	55.8	0.8
		20	2	0											
		22	2	0											
		23	1	0											
		24	1	0											
		25	1	1	1.000	1.000	0.512			0.964	1.363	0.112	0.317	83.9	1.9
		29	3	4	0.991	3.926	0.008	247.928	< 0.01	0.977	2.764	<< 0.001	6.341	71.7	0.8

Table S3. Microwear summary statistics for *Corythosaurus casuarius* CM 11376, class 2 data.

Class 2			Angular disp.		Rayleigh	Rao			Rayleigh (expected mean 60.50°)			Orientation	(μm)	(μm)	
Element	Tooth	Site	n	r	Z	p	U	p	V	u	p	μ	length	width	
L. dentary	1	1	40	0.943	35.536	<< 0.001	282.618	< 0.01	0.939	8.399	<< 0.001	55.539	85.9	1.2	
	1	2	19	0.965	17.711	<< 0.001	291.975	< 0.01	0.964	5.939	<< 0.001	64.166	48.0	0.8	
	1	4	59	0.988	57.580	<< 0.001	315.550	< 0.01	0.987	10.725	<< 0.001	62.509	77.8	1.4	
	3	1	44	0.975	41.835	<< 0.001	304.880	< 0.01	0.975	9.147	<< 0.001	60.643	73.9	1.1	
	3	2	85	0.952	77.023	<< 0.001	287.189	< 0.01	0.950	12.388	<< 0.001	56.952	65.5	0.8	
	3	3	41	0.928	35.308	<< 0.001	288.471	< 0.01	0.922	8.348	<< 0.001	53.948	51.6	0.4	
	3	4	73	0.935	63.793	<< 0.001	291.947	< 0.01	0.925	11.182	<< 0.001	52.365	61.9	1.1	
	3	5	103	0.967	96.342	<< 0.001	293.554	< 0.01	0.958	13.744	<< 0.001	52.432	58.2	0.9	
	3	6	86	0.953	78.051	<< 0.001	301.612	< 0.01	0.942	12.353	<< 0.001	51.875	48.6	0.8	
	3	7	125	0.948	112.344	<< 0.001	286.578	< 0.01	0.946	14.962	<< 0.001	57.020	57.4	0.8	
	4	1	18	0.884	14.052	<< 0.001	274.656	< 0.01	0.879	5.271	<< 0.001	54.407	64.2	2.0	
	5	1	48	0.956	43.874	<< 0.001	294.248	< 0.01	0.955	9.361	<< 0.001	62.650	78.3	1.2	
	5	3	69	0.968	64.671	<< 0.001	298.545	< 0.01	0.968	11.368	<< 0.001	58.812	41.5	0.6	
	7	1	37	0.952	33.529	<< 0.001	287.070	< 0.01	0.947	8.148	<< 0.001	54.758	47.8	0.7	
	7	2	77	0.963	71.368	<< 0.001	295.959	< 0.01	0.961	11.926	<< 0.001	57.051	45.3	0.6	
	7	3	58	0.920	49.098	<< 0.001	288.246	< 0.01	0.918	9.889	<< 0.001	56.783	49.2	0.6	
	18	1	14	0.999	13.964	<< 0.001	324.652	< 0.01	0.981	5.192	<< 0.001	71.229	71.1	1.5	
	19	1	21	0.997	20.874	<< 0.001	328.299	< 0.01	0.981	6.359	<< 0.001	70.681	67.4	1.2	
	19	2	15	0.974	14.243	<< 0.001	298.088	< 0.01	0.972	5.326	<< 0.001	64.155	56.0	0.9	
	20	2	12	0.970	11.298	<< 0.001	289.820	< 0.01	0.967	4.739	<< 0.001	65.011	46.8	0.6	
	20	4	27	0.983	26.103	<< 0.001	308.665	< 0.01	0.981	7.209	<< 0.001	64.318	54.9	0.5	
	21	3	27	0.978	25.819	<< 0.001	293.607	< 0.01	0.977	7.179	<< 0.001	62.954	45.1	0.4	
	22	1	1	1.000	1.000		0.512			0.943	1.333	0.118	41.028	47.3	1.9
	22	4	10	0.974		9.489	<< 0.001	286.672	< 0.01	0.967	4.323	<< 0.001	67.589	68.7	0.8
	23	2	40	0.958		36.737	<< 0.001	288.946	< 0.01	0.956	8.554	<< 0.001	56.826	59.8	1.0
	23	3	88	0.974		83.463	<< 0.001	295.727	< 0.01	0.972	12.900	<< 0.001	57.311	58.0	0.9
	23	4	60	0.965		55.855	<< 0.001	298.532	< 0.01	0.961	10.522	<< 0.001	55.080	52.6	0.9
	24	1	51	0.984		49.419	<< 0.001	323.002	< 0.01	0.975	9.850	<< 0.001	68.308	77.0	1.7
	25	1	82	0.994		80.998	<< 0.001	320.956	< 0.01	0.988	12.653	<< 0.001	66.732	87.1	1.3
	26	1	47	0.984		45.526	<< 0.001	315.490	< 0.01	0.977	9.475	<< 0.001	67.281	66.9	1.2
	26	2	30	0.984		29.048	<< 0.001	315.016	< 0.01	0.982	7.610	<< 0.001	63.685	61.7	0.7
	28	1	43	0.916		36.057	<< 0.001	281.088	< 0.01	0.916	8.491	<< 0.001	61.229	54.1	1.0

Table S3. continued.

Class 2			Angular disp.		Rayleigh	Rao			Rayleigh (expected mean 60.50°)			Orientation	(μ m)	(μ m)
Element	Tooth	Site	n	r	Z	p	U	p	V	u	p	μ	length	width
R. Dentary	3	2	0											
	3	3	41	0.992	40.349	<< 0.001	325.332	< 0.01	0.986	8.932	<< 0.001	66.614	72.8	1.1
	4	1	32	0.989	31.322	<< 0.001	317.864	< 0.01	0.986	7.892	<< 0.001	64.852	76.8	1.5
	4	3	19	0.953	17.249	<< 0.001	283.517	< 0.01	0.953	5.873	<< 0.001	61.259	59.8	3.1
	7	2	1	1.000	1.000	0.512			0.999	1.412	0.101	63.613	133.4	1.9
	8	1	40	0.988	39.039	<< 0.001	312.800	< 0.01	0.986	8.818	<< 0.001	56.792	86.2	1.0
	10	1	64	0.967	59.873	<< 0.001	289.824	< 0.01	0.967	10.941	<< 0.001	59.497	68.3	1.0
	11	1	25	0.993	24.636	<< 0.001	318.630	< 0.01	0.991	7.006	<< 0.001	56.968	91.2	1.3
	24	1	42	0.943	37.337	<< 0.001	278.129	< 0.01	0.938	8.601	<< 0.001	54.949	56.7	0.9
	25	1	38	0.971	35.799	<< 0.001	299.789	< 0.01	0.962	8.386	<< 0.001	52.844	58.5	0.7
R. maxilla	32	1	44	0.982	42.401	<< 0.001	307.052	< 0.01	0.977	9.166	<< 0.001	66.034	59.0	1.4
	1	1	49	0.964	45.510	<< 0.001	298.389	< 0.01	0.963	9.538	<< 0.001	61.848	74.3	1.1
	2	1	33	0.990	32.344	<< 0.001	313.211	< 0.01	0.972	7.898	<< 0.001	71.382	83.3	1.5
	2	2	27	0.987	26.310	<< 0.001	312.601	< 0.01	0.986	7.249	<< 0.001	62.699	96.0	1.4
	5	1	47	0.965	43.803	<< 0.001	285.792	< 0.01	0.964	9.351	<< 0.001	58.019	77.7	1.6
	7	1	59	0.988	57.544	<< 0.001	321.420	< 0.01	0.980	10.643	<< 0.001	67.697	96.2	1.7
	8	3	41	0.979	39.289	<< 0.001	303.507	< 0.01	0.970	8.780	<< 0.001	68.405	59.6	2.1
	9	3	98	0.976	93.424	<< 0.001	307.385	< 0.01	0.973	13.625	<< 0.001	65.112	53.1	1.2
	20	2	121	0.969	113.566	<< 0.001	294.137	< 0.01	0.968	15.054	<< 0.001	57.799	55.8	1.0
	22	2	91	0.977	86.805	<< 0.001	305.226	< 0.01	0.971	13.100	<< 0.001	66.673	57.9	1.2
	23	1	47	0.983	45.397	<< 0.001	310.168	< 0.01	0.980	9.497	<< 0.001	65.177	55.5	1.0
	24	1	69	0.970	64.953	<< 0.001	307.761	< 0.01	0.970	11.393	<< 0.001	62.207	78.5	1.4
	25	1	76	0.964	70.620	<< 0.001	295.797	< 0.01	0.959	11.829	<< 0.001	66.059	75.3	1.2
	29	3	89	0.968	83.332	<< 0.001	293.921	< 0.01	0.967	12.904	<< 0.001	62.213	64.5	1.4

Table S4. Microwear summary statistics for *Corythosaurus casuarius* CM 11376, class 3 data.

Class 3			Angular disp.		Rayleigh	Rao			Rayleigh (expected mean 88.86°)			Orientation	(μm)	(μm)
Element	Tooth	Site	n	r	Z	p	U	p	V	u	p	μ	length	width
L. dentary	1	1	47	0.978	44.968	<< 0.001	305.116	< 0.01	0.978	9.479	<< 0.001	87.019	123.1	1.8
	1	2	27	0.944	24.058	<< 0.001	288.715	< 0.01	0.943	6.930	<< 0.001	91.422	101.4	1.3
	1	4	66	0.978	63.173	<< 0.001	301.261	< 0.01	0.976	11.211	<< 0.001	93.019	100.1	1.6
	3	1	75	0.966	69.915	<< 0.001	297.360	< 0.01	0.965	11.825	<< 0.001	89.251	79.0	1.2
	3	2	115	0.982	110.791	<< 0.001	314.732	< 0.01	0.981	14.885	<< 0.001	88.375	72.6	1.6
	3	3	100	0.974	94.920	<< 0.001	296.878	< 0.01	0.974	13.777	<< 0.001	89.566	65.3	1.3
	3	4	93	0.973	87.973	<< 0.001	301.774	< 0.01	0.966	13.181	<< 0.001	95.303	103.6	1.7
	3	5	119	0.966	111.147	<< 0.001	297.062	< 0.01	0.966	14.908	<< 0.001	89.654	63.5	1.2
	3	6	113	0.957	103.492	<< 0.001	297.752	< 0.01	0.957	14.386	<< 0.001	88.156	65.1	1.3
	3	7	160	0.975	152.150	<< 0.001	299.292	< 0.01	0.975	17.434	<< 0.001	90.853	66.0	1.3
	4	1	71	0.959	65.265	<< 0.001	295.545	< 0.01	0.959	11.424	<< 0.001	88.091	89.0	2.0
	5	1	32	0.968	29.969	<< 0.001	293.336	< 0.01	0.965	7.721	<< 0.001	93.046	92.1	1.2
	5	3	89	0.955	81.137	<< 0.001	295.633	< 0.01	0.953	12.720	<< 0.001	91.968	66.8	0.8
	7	1	102	0.973	96.590	<< 0.001	297.913	< 0.01	0.973	13.892	<< 0.001	87.040	55.5	0.8
	7	2	119	0.958	109.196	<< 0.001	296.414	< 0.01	0.958	14.773	<< 0.001	90.420	55.3	0.8
	7	3	102	0.968	95.638	<< 0.001	300.088	< 0.01	0.968	13.827	<< 0.001	87.555	56.8	0.7
	18	1	88	0.940	77.799	<< 0.001	294.189	< 0.01	0.940	12.474	<< 0.001	88.540	71.8	1.3
	19	1	91	0.972	86.053	<< 0.001	294.764	< 0.01	0.972	13.119	<< 0.001	89.322	48.5	0.8
	19	2	116	0.974	110.012	<< 0.001	298.630	< 0.01	0.973	14.827	<< 0.001	90.546	71.2	1.3
	20	2	87	0.960	80.189	<< 0.001	295.184	< 0.01	0.959	12.647	<< 0.001	85.925	70.0	0.9
	20	4	63	0.978	60.208	<< 0.001	302.809	< 0.01	0.977	10.968	<< 0.001	90.681	52.4	0.6
	21	3	131	0.978	125.220	<< 0.001	304.496	< 0.01	0.977	15.822	<< 0.001	87.625	66.1	0.8
	22	1	5	0.959	4.599	0.003	243.020	< 0.01	0.959	3.033	<< 0.001	89.005	67.5	1.4
	22	4	84	0.959	77.204	<< 0.001	304.175	< 0.01	0.956	12.390	<< 0.001	84.490	63.0	1.2
	23	2	73	0.977	69.693	<< 0.001	299.847	< 0.01	0.975	11.776	<< 0.001	92.980	64.1	1.4
	23	3	83	0.959	76.392	<< 0.001	295.617	< 0.01	0.959	12.361	<< 0.001	88.771	58.4	0.9
	23	4	79	0.970	74.309	<< 0.001	296.248	< 0.01	0.969	12.186	<< 0.001	90.551	64.9	1.4
	24	1	60	0.961	55.374	<< 0.001	298.762	< 0.01	0.960	10.518	<< 0.001	86.952	60.7	1.3
	25	1	36	0.938	31.691	<< 0.001	289.638	< 0.01	0.938	7.961	<< 0.001	89.369	68.2	1.5
	26	1	85	0.964	79.060	<< 0.001	296.661	< 0.01	0.961	12.530	<< 0.001	84.045	73.6	1.5
	26	2	107	0.961	98.885	<< 0.001	298.172	< 0.01	0.961	14.059	<< 0.001	90.323	57.6	1.1
	28	1	69	0.935	60.287	<< 0.001	297.767	< 0.01	0.934	10.969	<< 0.001	86.235	72.4	1.8

Table S4. continued.

Class 3			Angular disp.		Rayleigh	Rao			Rayleigh (expected mean 88.86°)			Orientation	(μm)	(μm)
Element	Tooth	Site	n	r	Z	p	U	p	V	u	p	μ	length	width
R. dentary	3	2	5	0.995	4.954	0.001	272.860	< 0.01	0.985	3.115	<< 0.001	97.146	138.2	5.0
	3	3	86	0.980	82.528	<< 0.001	306.984	< 0.01	0.980	12.847	<< 0.001	89.508	76.2	1.1
	4	1	51	0.979	48.903	<< 0.001	302.157	< 0.01	0.979	9.888	<< 0.001	87.841	87.9	1.8
	4	3	15	0.953	13.624	<< 0.001	279.676	< 0.01	0.953	5.220	<< 0.001	89.180	89.7	3.2
	7	2	12	0.972	11.346	<< 0.001	283.134	< 0.01	0.972	4.763	<< 0.001	87.888	61.9	1.2
	8	1	61	0.982	58.806	<< 0.001	306.075	< 0.01	0.982	10.845	<< 0.001	89.079	79.2	1.0
	10	1	32	0.964	29.712	<< 0.001	296.462	< 0.01	0.963	7.707	<< 0.001	87.650	93.6	1.4
	11	1	48	0.984	46.493	<< 0.001	306.222	< 0.01	0.984	9.641	<< 0.001	87.861	106.2	1.9
	24	1	45	0.962	41.604	<< 0.001	294.936	< 0.01	0.960	9.109	<< 0.001	91.843	70.6	0.9
	25	1	60	0.951	54.230	<< 0.001	300.470	< 0.01	0.950	10.405	<< 0.001	91.349	58.6	0.8
	32	1	51	0.970	47.945	<< 0.001	296.647	< 0.01	0.969	9.783	<< 0.001	91.336	67.5	1.4
R. maxilla	1	1	56	0.953	50.831	<< 0.001	301.191	< 0.01	0.951	10.067	<< 0.001	92.069	93.3	1.1
	2	1	67	0.969	62.872	<< 0.001	302.351	< 0.01	0.967	11.194	<< 0.001	85.441	108.7	1.7
	2	2	65	0.964	60.461	<< 0.001	300.460	< 0.01	0.964	10.996	<< 0.001	89.395	85.3	1.4
	5	1	46	0.977	43.932	<< 0.001	300.754	< 0.01	0.977	9.373	<< 0.001	88.574	76.0	1.7
	7	1	74	0.974	70.200	<< 0.001	300.637	< 0.01	0.974	11.849	<< 0.001	88.866	82.8	1.8
	8	3	200	0.977	190.872	<< 0.001	306.012	< 0.01	0.977	19.530	<< 0.001	87.206	89.4	1.5
	9	3	188	0.975	178.793	<< 0.001	304.894	< 0.01	0.975	18.904	<< 0.001	87.417	66.9	1.3
	20	2	93	0.980	89.288	<< 0.001	307.836	< 0.01	0.978	13.344	<< 0.001	85.809	83.6	1.5
	22	2	95	0.962	87.862	<< 0.001	300.067	< 0.01	0.961	13.249	<< 0.001	90.724	71.0	1.9
	23	1	82	0.963	76.046	<< 0.001	300.044	< 0.01	0.963	12.332	<< 0.001	89.112	83.0	2.0
	24	1	48	0.961	44.331	<< 0.001	299.548	< 0.01	0.961	9.413	<< 0.001	90.302	74.9	1.2
	25	1	50	0.969	46.991	<< 0.001	305.440	< 0.01	0.969	9.694	<< 0.001	88.445	75.5	1.2
	29	3	169	0.977	161.449	<< 0.001	307.387	< 0.01	0.976	17.936	<< 0.001	85.345	76.1	1.3

Table S5. Microwear summary statistics for *Corythosaurus casuarius* CM 11376, class 4 data.

Class 4			Angular disp.		Rayleigh	Rao		Rayleigh (expected mean 120.28°)				Orientation	(μm)	(μm)
Element	Tooth	Site	n	r	Z	p	U	p	V	u	p	μ	length	w idth
L. dentary	1	1	19	0.970	17.883	<< 0.001	285.855	< 0.01	0.960	5.919	<< 0.001	128.500	96.6	1.1
	1	2	50	0.970	47.009	<< 0.001	304.210	< 0.01	0.960	9.596	<< 0.001	112.046	98.2	1.6
	1	4	15	0.925	12.826	<< 0.001	269.456	< 0.01	0.918	5.029	<< 0.001	127.060	60.6	0.8
	3	1	58	0.943	51.630	<< 0.001	287.712	< 0.01	0.943	10.161	<< 0.001	119.446	76.4	1.1
	3	2	90	0.936	78.834	<< 0.001	296.542	< 0.01	0.934	12.530	<< 0.001	124.012	69.6	0.9
	3	3	88	0.954	80.083	<< 0.001	290.286	< 0.01	0.953	12.646	<< 0.001	122.462	65.4	1.1
	3	4	36	0.965	33.532	<< 0.001	292.670	< 0.01	0.964	8.183	<< 0.001	117.976	92.6	1.4
	3	5	97	0.948	87.218	<< 0.001	289.074	< 0.01	0.948	13.207	<< 0.001	120.483	56.1	1.7
	3	6	56	0.929	48.279	<< 0.001	287.093	< 0.01	0.928	9.825	<< 0.001	119.483	45.6	0.6
	3	7	111	0.959	102.015	<< 0.001	291.684	< 0.01	0.958	14.271	<< 0.001	117.808	67.0	1.4
	4	1	31	0.945	27.677	<< 0.001	285.243	< 0.01	0.945	7.439	<< 0.001	119.357	67.9	1.2
	5	1	39	0.938	34.316	<< 0.001	284.513	< 0.01	0.937	8.274	<< 0.001	117.391	85.0	1.2
	5	3	66	0.909	54.540	<< 0.001	290.665	< 0.01	0.909	10.444	<< 0.001	120.487	73.4	0.9
	7	1	68	0.943	60.461	<< 0.001	288.404	< 0.01	0.942	10.991	<< 0.001	122.058	59.0	0.8
	7	2	77	0.941	68.229	<< 0.001	288.019	< 0.01	0.941	11.681	<< 0.001	120.874	52.6	0.7
	7	3	59	0.921	50.032	<< 0.001	287.614	< 0.01	0.920	9.999	<< 0.001	121.914	59.7	0.7
	18	1	64	0.948	57.561	<< 0.001	289.878	< 0.01	0.947	10.716	<< 0.001	117.396	56.5	0.9
	19	1	63	0.962	58.260	<< 0.001	293.001	< 0.01	0.960	10.780	<< 0.001	117.319	56.7	1.0
	19	2	68	0.946	60.816	<< 0.001	287.892	< 0.01	0.945	11.018	<< 0.001	122.837	57.9	1.0
	20	2	41	0.955	37.385	<< 0.001	297.574	< 0.01	0.955	8.643	<< 0.001	118.628	62.6	1.1
	20	4	53	0.973	50.201	<< 0.001	297.507	< 0.01	0.969	9.973	<< 0.001	125.809	54.1	0.7
	21	3	57	0.937	50.016	<< 0.001	294.178	< 0.01	0.935	9.979	<< 0.001	124.159	53.3	0.7
	22	1	88	0.982	84.817	<< 0.001	302.436	< 0.01	0.981	13.020	<< 0.001	121.696	69.4	1.3
	22	4	46	0.931	39.840	<< 0.001	287.134	< 0.01	0.931	8.926	<< 0.001	120.785	67.7	1.1
	23	2	48	0.956	43.884	<< 0.001	288.496	< 0.01	0.955	9.357	<< 0.001	123.065	64.7	1.2
	23	3	56	0.947	50.261	<< 0.001	289.819	< 0.01	0.946	10.014	<< 0.001	123.053	70.5	0.8
	23	4	47	0.950	42.435	<< 0.001	291.541	< 0.01	0.946	9.170	<< 0.001	125.807	61.8	1.4
	24	1	29	0.928	24.988	<< 0.001	290.798	< 0.01	0.928	7.066	<< 0.001	118.406	69.1	1.0
	25	1	20	0.938	17.593	<< 0.001	280.814	< 0.01	0.938	5.932	<< 0.001	120.658	60.4	1.4
	26	1	55	0.959	50.544	<< 0.001	292.900	< 0.01	0.956	10.031	<< 0.001	116.389	65.7	1.5
	26	2	52	0.942	46.132	<< 0.001	285.181	< 0.01	0.942	9.604	<< 0.001	119.280	65.2	1.4
	28	1	34	0.964	31.576	<< 0.001	293.564	< 0.01	0.960	7.914	<< 0.001	125.489	50.3	1.3

Table S5. continued.

Class 4			Angular disp.		Rayleigh	p	Rao	p	Rayleigh (expected mean 120.28°)			Orientation	(μm)	(μm)
Element	Tooth	Site	n	r	Z		U		V	u	p	μ	length	width
R. dentary	3	2	22	0.941	19.479	<< 0.001	280.158	< 0.01	0.941	6.241	<< 0.001	120.866	86.3	2.8
	3	3	94	0.956	85.976	<< 0.001	292.881	< 0.01	0.955	13.097	<< 0.001	117.458	63.6	1.3
	4	1	46	0.968	43.102	<< 0.001	296.664	< 0.01	0.967	9.278	<< 0.001	122.372	98.1	2.6
	4	3	36	0.988	35.119	<< 0.001	309.796	< 0.01	0.987	8.377	<< 0.001	118.602	97.6	4.9
	7	2	37	0.973	35.031	<< 0.001	289.934	< 0.01	0.969	8.338	<< 0.001	115.261	66.8	1.4
	8	1	39	0.971	36.763	<< 0.001	293.145	< 0.01	0.971	8.575	<< 0.001	120.649	87.7	1.7
	10	1	42	0.977	40.056	<< 0.001	290.729	< 0.01	0.976	8.948	<< 0.001	118.975	89.6	1.3
	11	1	48	0.947	43.032	<< 0.001	291.602	< 0.01	0.946	9.271	<< 0.001	122.383	98.3	1.4
	24	1	47	0.970	44.229	<< 0.001	297.931	< 0.01	0.960	9.312	<< 0.001	112.194	77.2	1.8
	25	1	17	0.967	15.906	<< 0.001	296.494	< 0.01	0.960	5.598	<< 0.001	113.279	55.1	0.8
R. maxilla	32	1	46	0.968	43.100	<< 0.001	291.464	< 0.01	0.968	9.284	<< 0.001	120.974	65.3	1.3
	1	1	26	0.949	23.437	<< 0.001	286.704	< 0.01	0.945	6.816	<< 0.001	114.843	83.7	0.8
	2	1	33	0.950	29.802	<< 0.001	287.224	< 0.01	0.950	7.716	<< 0.001	118.248	83.3	1.6
	2	2	36	0.958	33.073	<< 0.001	288.282	< 0.01	0.951	8.071	<< 0.001	127.355	66.0	1.4
	5	1	18	0.934	15.702	<< 0.001	275.582	< 0.01	0.931	5.584	<< 0.001	125.062	55.6	2.2
	7	1	36	0.947	32.286	<< 0.001	290.554	< 0.01	0.947	8.032	<< 0.001	118.624	83.8	1.7
	8	3	70	0.946	62.627	<< 0.001	292.043	< 0.01	0.946	11.192	<< 0.001	119.966	86.3	1.3
	9	3	57	0.934	49.697	<< 0.001	288.400	< 0.01	0.933	9.966	<< 0.001	121.900	74.4	1.3
	20	2	58	0.934	50.645	<< 0.001	287.887	< 0.01	0.934	10.064	<< 0.001	119.604	61.7	1.1
	22	2	34	0.934	29.689	<< 0.001	282.954	< 0.01	0.931	7.676	<< 0.001	115.218	76.2	1.5
	23	1	33	0.948	29.655	<< 0.001	288.106	< 0.01	0.948	7.701	<< 0.001	120.248	75.2	1.2
	24	1	53	0.982	51.060	<< 0.001	299.929	< 0.01	0.981	10.105	<< 0.001	119.824	91.9	1.6
	25	1	30	0.957	27.496	<< 0.001	286.166	< 0.01	0.957	7.414	<< 0.001	119.136	71.3	1.5
	29	3	49	0.938	43.088	<< 0.001	289.385	< 0.01	0.937	9.278	<< 0.001	122.232	67.1	1.0

Table S6. Microwear summary statistics for *Corythosaurus casuarius* CM 11376, class 5 data.

Class 5			Angular disp.		Rayleigh	Rao			Rayleigh (expected mean 156.40°)			Orientation	(μm)	(μm)
Element	Tooth	Site	n	r	Z	p	U	p	V	u	p	μ	length	width
L. dentary	1	1	1	1.000	1.000	0.512			0.999	1.413	0.101	159.014	223.8	1.1
	1	2	19	0.977	18.138	<< 0.001	287.437	< 0.01	0.977	6.023	<< 0.001	156.224	50.5	1.6
	1	4	63	0.973	59.657	<< 0.001	300.779	< 0.01	0.967	10.858	<< 0.001	150.152	79.7	0.8
	3	1	43	0.959	39.518	<< 0.001	297.304	< 0.01	0.953	8.834	<< 0.001	149.939	63.9	1.1
	3	2	31	0.979	29.706	<< 0.001	307.503	< 0.01	0.964	7.592	<< 0.001	146.430	56.7	0.9
	3	3	59	0.988	57.597	<< 0.001	310.023	< 0.01	0.987	10.721	<< 0.001	153.657	58.9	1.1
	3	4	27	0.974	25.611	<< 0.001	307.897	< 0.01	0.971	7.135	<< 0.001	151.945	61.3	1.4
	3	5	33	0.979	31.642	<< 0.001	295.384	< 0.01	0.979	7.953	<< 0.001	155.192	45.1	1.7
	3	6	25	0.979	23.974	<< 0.001	306.322	< 0.01	0.974	6.886	<< 0.001	150.356	43.9	0.6
	3	7	83	0.965	77.247	<< 0.001	301.793	< 0.01	0.961	12.382	<< 0.001	151.379	62.4	1.4
	4	1	38	0.972	35.931	<< 0.001	293.763	< 0.01	0.972	8.473	<< 0.001	154.644	71.2	1.2
	5	1	70	0.978	67.011	<< 0.001	307.447	< 0.01	0.973	11.512	<< 0.001	150.329	92.8	1.2
	5	3	47	0.942	41.710	<< 0.001	292.013	< 0.01	0.938	9.096	<< 0.001	151.201	77.3	0.9
	7	1	72	0.970	67.807	<< 0.001	301.090	< 0.01	0.970	11.641	<< 0.001	154.832	52.4	0.8
	7	2	88	0.954	80.078	<< 0.001	290.785	< 0.01	0.954	12.655	<< 0.001	156.680	48.1	0.7
	7	3	60	0.971	56.616	<< 0.001	292.894	< 0.01	0.971	10.640	<< 0.001	155.819	40.4	0.7
	18	1	96	0.937	84.216	<< 0.001	283.302	< 0.01	0.931	12.904	<< 0.001	162.547	67.8	0.9
	19	1	125	0.941	110.653	<< 0.001	284.804	< 0.01	0.936	14.796	<< 0.001	162.346	60.6	1.0
	19	2	79	0.938	69.575	<< 0.001	284.524	< 0.01	0.933	11.727	<< 0.001	162.624	67.0	1.0
	20	2	76	0.953	69.041	<< 0.001	294.347	< 0.01	0.942	11.611	<< 0.001	165.265	80.3	1.1
	20	4	51	0.952	46.183	<< 0.001	284.112	< 0.01	0.942	9.514	<< 0.001	164.526	58.7	0.7
	21	3	43	0.956	39.277	<< 0.001	280.918	< 0.01	0.956	8.863	<< 0.001	155.852	65.1	0.7
	22	1	68	0.933	59.150	<< 0.001	282.752	< 0.01	0.922	10.751	<< 0.001	165.121	80.9	1.3
	22	4	107	0.937	94.002	<< 0.001	278.562	< 0.01	0.928	13.582	<< 0.001	164.272	93.9	1.1
	23	2	77	0.948	69.172	<< 0.001	291.355	< 0.01	0.946	11.745	<< 0.001	153.336	73.8	1.2
	23	3	104	0.963	96.451	<< 0.001	293.122	< 0.01	0.963	13.885	<< 0.001	155.021	68.6	0.8
	23	4	71	0.954	64.570	<< 0.001	286.907	< 0.01	0.954	11.363	<< 0.001	157.148	64.3	1.4
	24	1	68	0.956	62.087	<< 0.001	277.268	< 0.01	0.955	11.136	<< 0.001	158.521	60.3	1.0
	25	1	53	0.966	49.489	<< 0.001	289.835	< 0.01	0.966	9.942	<< 0.001	154.306	75.0	1.4
	26	1	64	0.941	56.620	<< 0.001	278.971	< 0.01	0.939	10.626	<< 0.001	159.481	63.2	1.5
	26	2	80	0.919	67.559	<< 0.001	282.572	< 0.01	0.916	11.581	<< 0.001	161.333	71.3	1.4
	28	1	30	0.979	28.753	<< 0.001	305.684	< 0.01	0.979	7.581	<< 0.001	157.700	54.9	1.3

Table S6. continued.

Class 5			Angular disp.		Rayleigh	Rao			Rayleigh (expected mean 156.40°)			Orientation	(μm)	(μm)
Element	Tooth	Site	n	r	Z	p	U	p	V	u	p	μ	length	width
R. dentary	3	2	30	0.945	26.807	<< 0.001	286.778	< 0.01	0.940	7.278	<< 0.001	150.121	88.1	2.8
	3	3	111	0.953	100.808	<< 0.001	284.890	< 0.01	0.952	14.188	<< 0.001	154.134	79.1	1.3
	4	1	80	0.951	72.348	<< 0.001	287.242	< 0.01	0.951	12.026	<< 0.001	155.075	87.5	2.6
	4	3	40	0.984	38.746	<< 0.001	307.994	< 0.01	0.984	8.801	<< 0.001	155.148	90.6	4.9
	7	2	42	0.945	37.507	<< 0.001	276.317	< 0.01	0.945	8.659	<< 0.001	157.790	76.9	1.4
	8	1	72	0.959	66.173	<< 0.001	288.196	< 0.01	0.955	11.454	<< 0.001	151.063	108.7	1.7
	10	1	61	0.935	53.369	<< 0.001	273.415	< 0.01	0.935	10.324	<< 0.001	158.554	75.1	1.3
	11	1	54	0.965	50.334	<< 0.001	283.793	< 0.01	0.963	10.010	<< 0.001	152.516	75.9	1.4
	24	1	48	0.952	43.521	<< 0.001	281.564	< 0.01	0.952	9.326	<< 0.001	154.817	71.5	1.8
	25	1	39	0.935	34.076	<< 0.001	284.081	< 0.01	0.934	8.250	<< 0.001	154.231	47.1	0.8
	32	1	39	0.921	33.078	<< 0.001	277.798	< 0.01	0.920	8.123	<< 0.001	159.392	61.7	1.3
	1	1	34	0.929	29.373	<< 0.001	270.898	< 0.01	0.929	7.663	<< 0.001	155.304	95.7	0.8
R. maxilla	2	1	51	0.960	47.001	<< 0.001	298.169	< 0.01	0.960	9.695	<< 0.001	156.002	99.3	1.6
	2	2	63	0.961	58.226	<< 0.001	287.355	< 0.01	0.959	10.769	<< 0.001	152.752	70.5	1.4
	5	1	65	0.957	59.581	<< 0.001	286.916	< 0.01	0.951	10.846	<< 0.001	149.909	68.9	2.2
	7	1	52	0.930	45.013	<< 0.001	277.950	< 0.01	0.930	9.484	<< 0.001	158.114	84.0	1.7
	8	3	124	0.954	112.904	<< 0.001	285.622	< 0.01	0.954	15.016	<< 0.001	158.576	85.4	1.3
	9	3	102	0.952	92.369	<< 0.001	281.901	< 0.01	0.951	13.586	<< 0.001	158.110	70.2	1.3
	20	2	66	0.949	59.488	<< 0.001	281.821	< 0.01	0.949	10.904	<< 0.001	155.025	69.7	1.1
	22	2	58	0.947	52.003	<< 0.001	283.178	< 0.01	0.945	10.177	<< 0.001	160.090	69.8	1.5
	23	1	43	0.967	40.172	<< 0.001	298.308	< 0.01	0.962	8.922	<< 0.001	150.890	84.5	1.2
	24	1	29	0.972	27.427	<< 0.001	288.657	< 0.01	0.968	7.369	<< 0.001	150.665	114.4	1.6
	25	1	33	0.973	31.241	<< 0.001	309.475	< 0.01	0.973	7.901	<< 0.001	154.608	87.5	1.5
	29	3	62	0.957	56.738	<< 0.001	281.954	< 0.01	0.955	10.635	<< 0.001	153.083	77.8	1.0

Table S7. *Corythosaurus casuarius* - analysis of variation in orientation between teeth, within the left dentary CM 11376. Figures in bold fall outside the 99% confidence interval.

Left dentary: Tooth-site	1-1	1-2	1-4	3-1	3-2	3-3	3-4	3-5	3-6	3-7	4-1	5-1	5-3	7-1	7-2	7-3
Mean vector, μ : Unclassified	74.754	104.529	99.878	101.635	94.267	108.883	88.663	88.608	82.743	91.363	103.847	115.334	97.026	107.608	101.968	97.138
Class 1	28.501	34.320			36.304	32.341		25.057	29.618	31.394		35.035	28.161	28.383	21.368	23.461
Class 2	55.539	64.166	62.509	60.643	56.952	53.948	52.365	52.432	51.875	57.020	54.407	62.650	58.812	54.758	57.051	56.783
Class 3	87.019	91.422	93.019	89.251	88.375	89.566	95.303	89.654	88.156	90.853	88.091	93.046	91.968	87.040	90.420	87.555
Class 4	128.500	112.046	127.060	119.446	124.012	122.462	117.976	120.483	119.483	117.808	119.357	117.391	120.487	122.058	120.874	121.914
Class 5	159.014	156.224	150.152	149.939	146.430	153.657	151.945	155.192	150.356	151.379	154.644	150.329	151.201	154.832	156.680	155.819
Tooth-site	18-1	19-1	19-2	20-2	20-4	21-3	22-1	22-4	23-2	23-3	23-4	24-1	25-1	26-1	26-2	28-1
Mean vector, μ : Unclassified	124.464	129.783	115.477	116.606	124.692	99.227	147.517	133.975	115.094	103.745	105.468	103.118	88.496	99.108	108.980	88.542
Class 1	6.489	9.135	14.360	9.369	6.916	15.958	10.455	5.215	22.679	24.879		5.378	1.181	4.507	5.799	32.587
Class 2	71.229	70.681	64.155	65.011	64.318	62.954	41.028	67.589	56.826	57.311	55.080	68.308	66.732	67.281	63.685	61.229
Class 3	88.540	89.322	90.546	85.925	90.681	87.625	89.005	84.490	92.980	88.771	90.551	86.952	89.369	84.045	90.323	86.235
Class 4	117.396	117.319	122.837	118.628	125.809	124.159	121.696	120.785	123.065	123.053	125.807	118.406	120.658	116.389	119.280	125.489
Class 5	162.547	162.346	162.624	165.265	164.526	155.852	165.121	164.272	153.336	155.021	157.148	158.521	154.306	159.481	161.333	157.700
Unclassified mean of means 107.31, 99% confidence interval 79.18 – 139.08																
Class 1 mean of means 19.05, 99% confidence interval 0.87 - 37.51																
Class 2 mean of means 60.06, 99% confidence interval 49.32 - 70.34																
Class 3 mean of means 88.79, 99% confidence interval 86.25 - 91.31																
Class 4 mean of means 121.37, 99% confidence interval 116.50 – 126.11																
Class 5 mean of means 157.73, 99% confidence interval 150.51 - 165.19																

Table S8. *Corythosaurus casuarus* - analysis of variation in orientation between teeth, within the right dentary and maxilla CM 11376. Figures in bold fall outside the 99% confidence interval.

Right dentary: Tooth-site	3-2	3-3	4-1	4-3	7-2	8-1	10-1	11-1	24-1	25-1	32-1		
Mean vector, μ : Unclassified	134.775	116.415	120.496	124.030	135.627	111.563	101.527	115.937	104.256	93.459	103.186		
Class 1		7.494	0.754		3.099		0.939	13.736		10.090	1.652		
Class 2		66.614	64.852	61.259	63.613	56.792	59.497	56.968	54.949	52.844	66.034		
Class 3	97.146	89.508	87.841	89.180	87.888	89.079	87.650	87.861	91.843	91.349	91.336		
Class 4	120.866	117.458	122.372	118.602	115.261	120.649	118.975	122.383	112.194	113.279	120.974		
Class 5	150.121	154.134	155.075	155.148	157.790	151.063	158.554	152.516	154.817	154.231	159.392		
Right maxilla: Tooth-site	1-1	2-1	2-2	5-1	7-1	8-3	9-3	20-2	22-2	23-1	24-1	25-1	29-1
Mean vector, μ : Unclassified	92.235	101.635	115.319	107.048	93.939	103.979	93.479	84.596	89.415	96.839	94.236	87.597	88.620
Class 1	9.615	16.796	6.214		10.178	15.850	5.787					0.317	6.341
Class 2	61.848	71.382	62.699	58.019	67.697	68.405	65.112	57.799	66.673	65.177	62.207	66.059	62.213
Class 3	92.069	85.441	89.395	88.574	88.866	87.206	87.417	85.809	90.724	89.112	90.302	88.445	85.345
Class 4	114.843	118.248	127.355	125.062	118.624	119.966	121.900	119.604	115.218	120.248	119.824	119.136	122.232
Class 5	155.304	156.002	152.752	149.909	158.114	158.576	158.110	155.025	160.090	150.890	150.665	154.608	153.083
Unclassified mean of means 117.28, 99% confidence interval 72.36 – 135.42													
Class 1 mean of means 5.26, 99% confidence interval 355.36 - 16.46													
Class 2 mean of means 60.28, 99% confidence interval 52.18 - 68.14													
Class 3 mean of means 90.22, 99% confidence interval 85.230 - 95.12													
Class 4 mean of means 118.53, 99% confidence interval 112.44 – 124.69													
Class 5 mean of means 154.81, 99% confidence interval 149.82 - 159.82													

Table S9. Comparison of pooled mean orientations (unclassified and by class 1-5) for jaw elements from five individual specimens of *Corythosaurus casuarius*.

		L. dentary AMNH 3971	L. dentary CM 11376	R. maxilla CM 1074	R. maxilla CM 1077	R. maxilla CM 11376	R. dentary SM 11893	R. dentary CM 11376
Unclassified	N	944	8394	1328	2791	3464	973	1929
	R	0.481	0.325	0.236	0.335	0.407	0.368	0.369
	Mean μ	105.89°	102.89°	119.41°	106.80°	94.80°	117.40°	114.35°
Class 1	N	3	425	77	12	69	15	27
	R	0.937	0.913	0.993	0.970	0.969	0.997	0.976
	Mean μ	11.41°	17.55°	3.35°	4.14°	9.84°	3.43°	5.37°
Class 2	N	177	1550	282	593	847	156	346
	R	0.974	0.945	0.962	0.973	0.965	0.974	0.962
	Mean μ	60.99°	58.82°	65.76°	60.08°	63.73°	62.35°	60.04°
Class 3	N	266	2687	347	723	1233	257	466
	R	0.974	0.963	0.962	0.974	0.969	0.981	0.970
	Mean μ	88.94°	89.20°	92.69°	86.51°	87.83°	89.14°	89.66°
Class 4	N	223	1781	229	632	533	204	474
	R	0.956	0.942	0.943	0.960	0.942	0.932	0.959
	Mean μ	114.24°	120.78°	131.68°	118.54°	120.22°	122.32°	118.57°
Class 5	N	275	1951	393	831	782	341	616
	R	0.938	0.929	0.966	0.957	0.948	0.949	0.947
	Mean μ	146.74°	157.33°	161.00°	155.80°	155.46°	153.93°	154.68°

Table S10. Microwear summary statistics for *Corythosaurus casuarius* - AMNH3971, CM1077, CM1074 and SM11893, by tooth site and orientation class. Figures in bold show mean orientations that fall outside the 99% confidence interval of the mean of means calculated from the CM11376 datasets.

Specimen	Tooth	Site	Class 1			Class 2			Class 3			Class 4			Class 5		
			n	μ	r	n	μ	r	n	μ	r	n	μ	r	n	μ	r
AMNH3971	1	1	1	24.974	1	44	66.977	0.99	83	88.171	0.972	18	118.305	0.956	52	150.635	0.92
L. dentary	1	2	2	4.732	0.988	14	64.361	0.977	6	87.99	0.967	85	112.074	0.978	34	153.824	0.96
	1	3				49	59.198	0.984	67	85.976	0.991	38	121.845	0.968	56	148.772	0.958
	3	1				64	58.231	0.983	105	91.25	0.971	60	114.501	0.947	75	146.326	0.935
	5	1				6	53.038	0.943	5	94.781	0.982	22	105.862	0.996	58	138.07	0.997
CM1077	4	2				33	63.333	0.99	30	86.129	0.954	14	120.08	0.92	23	148.853	0.98
R. maxilla	5	1				109	59.29	0.971	133	85.947	0.975	80	120.191	0.95	69	154.668	0.966
	8	2				95	62.112	0.976	57	84.842	0.958	57	113.035	0.958	101	154.987	0.965
	8	3	2	19.917	0.998	79	62.867	0.992	81	88.819	0.981	53	115.22	0.969	79	154.462	0.962
	11	1	7	1.352	0.999	84	58.954	0.963	95	86.972	0.984	192	119.78	0.985	218	160.08	0.961
	11	4	3	0.637	1	89	58.883	0.981	189	86.394	0.977	134	120.107	0.949	169	154.042	0.963
	12	1				104	57.781	0.969	138	86.282	0.969	102	117.391	0.959	172	154.606	0.954
CM1074	6	1	72	3.36	0.993	98	66.837	0.946	154	89.068	0.969	105	128.098	0.949	207	162.955	0.966
R. maxilla	23	1	5	3.19	0.998	184	65.203	0.97	193	95.586	0.968	124	134.707	0.949	186	158.836	0.972
SM11893	4	1	9	3.746	0.998	92	61.033	0.973	174	89.007	0.988	118	127.563	0.956	246	153.94	0.947
R. dentary	7	2	6	2.95	0.997	64	64.219	0.98	83	89.412	0.968	86	115.035	0.95	95	153.921	0.955

CM11376 L. dentary

Class 1 mean of means 19.05, 99% confidence interval 0.87 - 37.51

Class 2 mean of means 60.06, 99% confidence interval 49.32 - 70.34

Class 3 mean of means 88.79, 99% confidence interval 86.25 - 91.31

Class 4 mean of means 121.37, 99% confidence interval 116.50 – 126.11

Class 5 mean of means 157.73, 99% confidence interval 150.51 - 165.19

CM11376 R.dentary & R. Maxilla

Class 1 mean of means 5.26, 99% confidence interval 355.36 - 16.46

Class 2 mean of means 60.28, 99% confidence interval 52.18 - 68.14

Class 3 mean of means 90.22, 99% confidence interval 85.230 - 95.12

Class 4 mean of means 118.53, 99% confidence interval 112.44 – 124.69

Class 5 mean of means 154.81, 99% confidence interval 149.82 - 159.82

Table S11. *Edmontosaurus* sp. Analysis of variation in orientation between teeth within the right maxilla of NHMUK R3638. Figures in bold fall outside the 99% confidence interval.

NHMUK R3638	1-1	2-3	3-1	5-2	9-1	15-1	17-1	18-1	20-1	23-1
Mean vector, μ : Unclassified	57.085	74.786	7.895	57.177	59.763	66.817	39.369	17.266	22.8	49.794
Class 1	13.668	25.801	11.999	16.06	21.093	11.867	19.858	22.393	12.611	16.063
Class 2	57.817	57.211	55.216	55.852	58.702	50.56	55.201	56.761	50.634	50.536
Class 3	81.375	76.262	71.714	75.095	72.317	84.574	75.66	69.768	78.92	72.785
Class 4	133.612	117.936	125.689	135.890				128.872	116.944	129.884
Class 5	163.106	162.738	168.295	159.669	163.772	164.474	167.494	164.959	165.302	168.632

Unclassified mean of means 48.58, 99% confidence interval 11.03 – 72.03

Class 1 mean of means 17.12, 99% confidence interval 10.38 - 23.95

Class 2 mean of means 54.84, 99% confidence interval 50.45 - 59.24

Class 3 mean of means 75.82, 99% confidence interval 69.38 - 82.38

Class 4 mean of means 127.15, 99% confidence interval 110.71 - 141.64

Class 5 mean of means 164.88, 99% confidence interval 160.98 - 168.82

Table S12. Comparison of mean orientations (unclassified and by class 1-5) for nine individual specimens of *Edmontosaurus* sp. (AMNH 2342 jaw elements, listed separately). Figures in bold fall outside the 99% confidence interval for the mean of means.

		dentary	maxilla	L. dentary	R. maxilla	R. maxilla	L. maxilla	dentary	L. dentary	L. dentary	L. dentary
		AMNH 2342	AMNH 2342	AMNH 8145	NHMK R3638	NHMK R3653	NHMK R3654	NHMK R3658	NHMK R4292	SM 4807	SM 4808
Unclassified	N	838	473	558	1384	2788	1307	625	774	547	470
	R	0.372	0.644	0.401	0.415	0.377	0.272	0.301	0.402	0.192	0.36
	Mean μ	128.25	130.31	99.94	55.91	123.98	113	129.12	128.98	104.29	113.46
Class 1	N	18	4		212	155	23	45	97	4	14
	R	0.987	0.999		0.944	0.916	0.921	0.975	0.961	0.866	0.993
	Mean μ	4.91	1.38		15.88	20.73	19.52	7.25	11.34	15.75	3.01
Class 2	N	109	22	150	490	323	282	97	54	197	103
	R	0.977	0.963	0.974	0.969	0.96	0.962	0.967	0.958	0.979	0.975
	Mean μ	68.54	72.48	59.4	56.01	64.65	50.57	68.54	78.2	62.1	65.2
Class 3	N	199	72	192	383	559	296	107	187	72	52
	R	0.977	0.988	0.974	0.961	0.97	0.953	0.973	0.979	0.971	0.981
	Mean μ	94.28	93.62	93.45	76.69	88.52	85.52	92.07	97.64	90.68	85.71
Class 4	N	135	156	111	107	710	340	171	177	114	153
	R	0.952	0.96	0.962	0.914	0.958	0.947	0.947	0.953	0.964	0.955
	Mean μ	117.74	118.91	129.34	123.69	117.97	122.54	122.29	118.69	126.84	112.6
Class 5	N	377	219	105	192	1041	366	205	259	160	148
	R	0.931	0.962	0.97	0.955	0.951	0.961	0.94	0.914	0.967	0.933
	Mean μ	158.01	151.39	155.48	165.78	154.32	152.61	163.38	156.91	158.77	155.09

Unclassified mean of means 114.49, 99% confidence interval 70.94 - 140.36

Class 1 mean of means 10.83, 99% confidence interval 0.22 - 22.76

Class 2 mean of means 64.55, 99% confidence interval 53.53 - 75.61

Class 3 mean of means 89.86, 99% confidence interval 81.46 - 98.00

Class 4 mean of means 121.05, 99% confidence interval 114.23 - 127.90

Class 5 mean of means 157.15, 99% confidence interval 150.85 - 163.55

Table S13. Microwear mean orientation statistics for all hadrosaurid and iguanodontid specimens, pooled data and by class.

			Unclassified			Class 1			Class 2			Class 3			Class 4			Class 5		
Species	Specimen	Element	N	Mean μ	R	N	Mean μ	R	N	Mean μ	R	N	Mean μ	R	N	Mean μ	R	N	Mean μ	R
<i>Bactrosaurus</i>	AMNH 6514	L. maxilla	1217	128.937	0.383	34	7.901	0.976	190	66.950	0.978	246	92.034	0.987	279	127.518	0.960	468	156.955	0.957
<i>johnsoni</i>	AMNH 6553	R. dentary	596	115.963	0.166	12	3.481	0.996	191	60.407	0.968	87	90.872	0.979	136	131.285	0.952	170	159.536	0.963
	AMNH 6553	L. dentary	323	104.131	0.126	1	7.125	1.000	117	56.711	0.979	40	88.787	0.978	82	129.280	0.960	83	161.105	0.965
<i>Edmontosaurus</i>	CM 1202	R. maxilla	848	111.282	0.279	7	1.580	1.000	224	60.152	0.974	195	91.064	0.984	136	124.881	0.963	286	153.612	0.959
<i>regalis</i>	SM 12711	L. maxilla	702	124.941	0.311	4	1.010	1.000	142	55.415	0.984	110	87.048	0.985	206	122.996	0.962	240	156.935	0.956
<i>Corythosaurus</i>	AMNH 3971	L. dentary	944	105.894	0.481	3	11.406	0.937	177	60.994	0.974	266	88.939	0.974	223	114.241	0.956	275	146.743	0.938
<i>casuarius</i>	CM 1074	R. maxilla	1328	119.406	0.236	77	3.349	0.993	282	65.762	0.962	347	92.693	0.962	229	131.678	0.943	393	160.999	0.966
	CM 1077	R. maxilla	2791	106.803	0.335	12	4.137	0.970	593	60.083	0.973	723	86.509	0.974	632	118.536	0.960	831	155.800	0.957
	CM 11376	L. dentary	8394	102.890	0.325	425	17.552	0.913	1550	58.817	0.945	2687	89.200	0.963	1781	120.776	0.942	1951	157.326	0.929
	CM 11376	R. dentary	1929	114.350	0.369	27	5.372	0.976	346	60.035	0.962	466	89.655	0.970	474	118.567	0.959	616	154.684	0.947
	CM 11376	R. maxilla	3464	94.795	0.407	69	9.843	0.969	847	63.728	0.965	1233	87.825	0.969	533	120.218	0.942	782	155.462	0.948
	SM 11893	R. maxilla	973	117.404	0.368	15	3.428	0.997	156	62.345	0.974	257	89.136	0.981	204	122.317	0.932	341	153.934	0.949
<i>Edmontosaurus</i>	AMNH 2342	dentary	838	128.247	0.372	18	4.905	0.987	109	68.538	0.977	199	94.284	0.977	135	117.737	0.952	377	158.005	0.931
sp.	AMNH 2342	maxilla	473	130.307	0.644	4	1.380	0.999	22	72.478	0.963	72	93.615	0.988	156	118.905	0.960	219	151.388	0.962
	AMNH 8145	L. dentary	558	99.943	0.401				150	59.400	0.974	192	93.449	0.974	111	129.339	0.962	105	155.482	0.970
	NHMMUK R3638	R. maxilla	1384	55.911	0.415	212	15.878	0.944	490	56.006	0.969	383	76.694	0.961	107	123.694	0.914	192	165.783	0.955
	NHMMUK R3653	R. maxilla	2788	123.982	0.377	155	20.726	0.916	323	64.653	0.960	559	88.517	0.970	710	117.965	0.958	1041	154.324	0.951
	NHMMUK R3654	L. maxilla	1307	113.003	0.272	23	19.523	0.921	282	50.565	0.962	296	85.521	0.953	340	122.543	0.947	366	152.612	0.961
	NHMMUK R3658	dentary	625	129.124	0.301	45	7.246	0.975	97	68.543	0.967	107	92.070	0.973	171	122.293	0.947	205	163.383	0.940
	NHMMUK R4939	L. dentary	774	128.980	0.402	97	11.343	0.961	54	78.199	0.958	187	97.638	0.979	177	118.685	0.953	259	156.905	0.914
	SM 4807	L. dentary	547	104.290	0.192	4	15.750	0.866	197	62.099	0.979	72	90.680	0.971	114	126.836	0.964	160	158.773	0.967
	SM 4808	L. dentary	470	113.456	0.360	14	3.011	0.993	103	65.201	0.975	52	85.709	0.981	153	112.595	0.955	148	155.094	0.933

Table S13. continued.

Species	Specimen	Element	Unclassified			Class 1			Class 2			Class 3			Class 4			Class 5		
			N	Mean μ	R	N	Mean μ	R	N	Mean μ	R	N	Mean μ	R	N	Mean μ	R	N	Mean μ	R
Hadrosaurids	AMNH 1181	dentary	671	86.914	0.260	35	25.133	0.936	231	59.696	0.980	127	86.966	0.979	110	119.012	0.972	168	153.788	0.948
	AMNH 21523	L. dentary	639	108.432	0.337	46	30.582	0.967	131	53.459	0.979	95	87.367	0.971	217	116.843	0.962	150	147.187	0.958
	AMNH 21524	L. dentary	614	108.552	0.333	1	11.416	1.000	138	50.814	0.981	186	92.984	0.958	120	122.002	0.950	169	151.840	0.963
	AMNH 21525	maxilla	1234	104.146	0.286				334	57.322	0.953	292	86.662	0.963	261	122.528	0.948	347	153.946	0.967
	AMNH 21700	i. tooth	670	110.946	0.217	1	2.564	1.000	190	60.240	0.971	140	88.917	0.972	112	125.736	0.944	227	156.895	0.981
	AMNH 5465	L. dentary	752	129.177	0.385	84	14.380	0.973	34	73.806	0.987	185	91.109	0.990	216	122.879	0.962	233	159.569	0.945
	AMNH 5896	maxilla	545	111.638	0.308	4	1.045	0.998	129	58.231	0.967	155	93.634	0.970	99	128.709	0.956	158	155.345	0.963
	AMNH 6375	R. dentary	839	124.548	0.327	35	5.932	0.984	131	67.306	0.964	194	90.259	0.959	153	121.238	0.953	326	156.740	0.939
	AMNH 6380	L. dentary	538	99.584	0.222	6	17.428	0.860	163	58.851	0.958	125	89.990	0.971	82	122.199	0.961	162	157.744	0.962
	AMNH 6388	R. maxilla	1453	134.665	0.318	36	5.010	0.990	225	58.693	0.976	250	89.206	0.977	326	122.624	0.936	616	158.869	0.948
	AMNH 6529	R. dentary	777	117.270	0.147	9	0.854	1.000	254	63.203	0.941	119	90.222	0.962	116	128.109	0.951	279	159.696	0.979
	AMNH 6530	R. dentary	627	130.499	0.102	4	0.891	1.000	192	55.144	0.991	95	91.596	0.985	118	129.372	0.931	218	161.134	0.967
	AMNH 6547	L. dentary	289	122.961	0.139	10	4.037	0.994	76	62.469	0.948	57	87.326	0.954	38	128.693	0.924	108	159.220	0.950
	AMNH 6549	L. dentary	225	107.539	0.441	24	39.060	0.992	30	62.954	0.961	50	89.889	0.963	80	120.094	0.981	41	148.329	0.976
	AMNH 6550	L. dentary	270	104.203	0.324				83	60.551	0.986	54	89.031	0.977	45	120.151	0.967	88	148.819	0.970
	AMNH 6581	R. dentary	702	113.132	0.268	3	4.160	1.000	147	58.651	0.960	168	87.471	0.980	138	119.108	0.939	246	157.276	0.949
<i>Hypacrosaurus</i>	SM 11950	L. dentary	596	127.367	0.201	45	10.038	0.924	135	57.357	0.925	90	91.895	0.960	153	123.311	0.943	173	159.928	0.945
<i>altispinus</i>																				
<i>Kritosaurus</i>	SM 8629	L. dentary	416	95.540	0.228	13	10.503	0.877	92	58.265	0.968	147	87.914	0.971	42	128.234	0.959	122	160.115	0.938
<i>navajovius</i>																				
<i>Lambeosaurus</i>	YPM 21849	i. tooth	538	116.629	0.281	7	3.596	0.991	121	60.843	0.965	135	90.575	0.972	114	131.543	0.960	161	157.280	0.960
<i>lambei</i>																				
<i>Trachodon</i>	AMNH 107	maxilla	575	117.215	0.338	8	0.963	0.999	116	64.003	0.965	165	96.166	0.979	63	119.076	0.949	223	155.189	0.950
<i>Camptosaurus</i>	YPM 7416	R. maxilla	1430	112.365	0.192	59	11.318	0.935	353	52.436	0.939	324	87.446	0.967	294	125.622	0.956	400	154.539	0.957
<i>dispar</i>	YPM 1886	maxilla	2498	143.515	0.283	239	3.588	0.989	334	57.957	0.968	511	90.482	0.974	489	129.422	0.951	925	161.391	0.953

SUMMARY

Dinosaur teeth preserve microwear and the microwear patterns are dominated by scratches. Pitting is rare to absent on all of the ornithopod specimens examined. If the teeth belonged to mammals, the lack of pitting would be a dietary indicator, however it is more likely to be a function of the mechanical properties of dentine.

The scratches are not random in orientation and fall into a small number of orientation classes within which scratches are sub-parallel. The hypothesis that scratch orientation relates to relative jaw motion was tested with the extant squamate *Iguana iguana*. Here microwear orientations were predicted based upon the known jaw mechanics of *I. guana* and the observed feeding behaviour. Actual microwear orientation matched those predicted and reflected the dominant dorsoventral cropping action used by the animal.

The nature of iguana teeth is such that an outward facing portion (the labial surface) of each tooth does not interact with any other tooth. It slices through food, so there is tooth-food contact but the absence of cheeks means that there is no tooth-food-cheek contact; plant material simply falls from the outside of the tooth row when an iguana closes its jaws. Microwear scratch density on these non-interactive labial tooth surfaces is very low relative to the interactive tooth faces which shear past each other. This makes *I. iguana* a good extant model for feeding in early ornithischians and basal ornithopods and provides a test for the presence or absence of muscular cheeks.

Results of microware analyses comparing *I. iguana* to the basal ornithischian *Lesothosaurus diagnosticus* indicate that both processed food using simple vertical adduction, and so *L. diagnosticus* lacked the adaptations to herbivory (the mobile quadrate and cranial kinesis) seen in ornithopods. The presence of muscular cheeks in *L. diagnosticus* could not be supported by microwear analyses either. Muscular cheeks

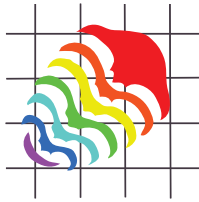
would act to trap food and hold it against the non-interactive labial tooth surfaces, concentrating microwear. Whilst the dentary tooth rows of *L. diagnosticus* are partially inset, creating cheek space that is suggestive of muscular cheeks, scratch density on the non-interactive labial tooth surfaces was low relative to that on the active surfaces (comparable to that of *I. iguana*) causing a rejection of the hypothesis that *L. diagnosticus* had muscular cheeks. By contrast microwear analyses of the ornithopod *Hypsilophodon foxii* does support muscular cheeks. Scratch density of the off-occlusal labial tooth surface (the equivalent of *I. iguana*'s non-interactive labial tooth surface) was almost twice that of the occlusal surface. Microwear data also indicated a propalinal (fore-aft) movement of the lower jaw in *H. foxii*; evidence of a mobile quadrate. However, no evidence was found for a transverse movement of the maxillae over the dentaries (pleurokinesis) in *H. foxii*.

Using quantitative microwear analyses to test hypotheses of jaw mechanics in the advanced ornithopods resulted in the discovery of a number of complex relative jaw motions that are shared by both iguanodontids and hadrosaurids. The microwear data support the pleurokinesis hypothesis of a transverse movement of the maxillae over the dentaries, and also indicate that a propalinal (fore-aft) movement was a significant food processing action. A comparison of the microwear data of multiple individuals and species shows little variation in the orientation of the complex relative jaw motions, between individuals or between species. The success of the ornithopods has been attributed to their advanced jaw mechanics and it is significant in evolutionary terms that the jaw mechanics in the basal iguanodontian *Camptosaurus dispar* were sufficiently advanced that its relative jaw motions do not differ significantly from that of the hadrosaurids.

In hadrosaurids and basal iguanodontians, repetitive jaw movements in one orientation appear to erase and overprint existing occlusal surface microwear orientations, leading to a loss of data. A robust sampling strategy will mitigate this, however an alternative worth investigation is the use of off-occlusal microwear. This has been shown to capture the the same orientation classes as occlusal microwear in *Hypsilophodon foxii*.

Microwear orientation can provide direct evidence for the relative motion of jaws and can be used to provide a robust test of hypothesis of jaw mechanics that have been based on bio-mechanical analyses, finite element analyses or 3D animation modelling.

APPENDICES



CLEANING FOSSIL TOOTH SURFACES FOR MICROWEAR ANALYSIS: USE OF SOLVENT GELS TO REMOVE RESISTANT CONSOLIDANT

Vincent S. Williams and Adrian M. Doyle

ABSTRACT

Fine-scale surface texture analysis of teeth has become increasingly useful for anthropologists and palaeontologists to infer diet and jaw mechanics in fossil animals. We describe a fast, non-abrasive and residue free method for the removal of resistant consolidant from fossil teeth. The method utilises solvent gels, and its use is a significant improvement over previous techniques, particularly where microwear analysis is to be performed. The method adapts techniques originally developed by art conservators for the removal of varnish from oil paintings without damaging the oil paint beneath. A combination of Carbopol (a water soluble acrylic polymer) and Ethomeen (a polyoxyethylene cocoamine detergent) allows solvents such as acetone and ethanol to be suspended in a gel for application to consolidant coated tooth surfaces. Key advantages are that dissolved consolidant is lifted away from the tooth surface into the solvent gel and a high degree of control is possible such that small discrete areas can be cleaned of consolidant. Because the solvents are held within a gel, cleaning of the tooth surface can be performed without the need for a fume hood.

Vincent S. Williams. Department of Geology, University of Leicester, University Road, Leicester, LE1 7RH, UK. vw13@le.ac.uk

Adrian M. Doyle. Conservation Department, Museum of London, 150 London Wall, London, EC2Y 5HN, UK. adoyle@museumoflondon.org.uk

KEY WORDS: solvent gel; microwear; consolidant removal

INTRODUCTION

Microwear analysis requires images or 3D data to be acquired from tooth surfaces at relatively high magnification, sampling data from very small areas, typically only a few hundred micrometres across. In order for the microwear features and textures to be accurately detected or replicated it is imperative that the tooth surface be thoroughly

cleaned prior to imaging or moulding. Any surface contaminant or coating that could potentially mask microwear must be removed. The cleaning process must not abrade or etch the tooth surface or leave residue that might obscure the original microwear.

Quantitative analysis of tooth microwear has been applied extensively to mammals (Walker et al. 1978; Gordon 1984; Teaford 1988; Organ et al.

PE Article Number: 13.3.23A

Copyright: Palaeontological Association November 2010

Submission: 9 July 2010. Acceptance: 10 September 2010

Williams, Vincent S, Doyle, Adrian M., 2010. Cleaning Fossil Tooth Surfaces for Microwear Analysis: Use of Solvent Gels to Remove Resistant Consolidant. *Palaeontologia Electronica* Vol. 13, Issue 3; 2T:12p;
http://palaeo-electronica.org/2010_3/247/index.html

2005; Ungar et al. 2007) and is starting to be applied to dinosaurs (Williams et al. 2009); prior studies of dinosaur tooth microwear have been qualitative (e.g., Fiorillo 1991, 1998; Upchurch and Barrett 2000; Schubert and Ungar 2005). The cleaning methods employed by most of these researchers involve soft brushing or gentle swabbing (using cotton swabs) with either distilled water or a solvent such as acetone or ethanol. Whilst these methods work well on material that has been treated with modern consolidants such as the methacrylate co-polymer Paraloid, they have proven time consuming and laborious where more traditional consolidants such as shellac or glyptal have been used and totally ineffective where the shellac has aged.

Material from the older museum collections (19th and early 20th century), particularly dinosaur material, has often been treated with one or both of two consolidants: shellac and animal resin. As shellac ages it darkens and becomes cross-linked (bonds develop that link one polymer chain to another) making it extremely resistant to solvents. As microwear analysis is increasingly applied to dinosaurs, more researchers are likely to discover this problem.

Problems with Brush-Based Cleaning:

When attempting to remove consolidant from the occlusal surface of a tooth by the brushing on of a solvent and continual cleaning of the brush, or by the use of disposable swabs, the whole tooth and surrounding area tends to become soaked in a combination of the solvent and dissolved consolidant. Given that consolidants like shellac typically form a coating rather than penetrate a surface when they are originally applied, this is a backward step. The brushing process also tends to move consolidant around, smearing it over microwear and making it difficult to determine when all vestiges have been removed. This technique is especially problematic if SEM analysis is to be performed on moulds and casts rather than the original specimens (brush marks in remaining consolidant are a particular hazard). Use of this technique also results in a high rate of solvent evaporation requiring the use of a fume cupboard. It has also been suggested that repeated applications of solvents such as alcohol and acetone can dehydrate enamel and dentine leading to surface damage (Fernandez-Jalvo and Monfort 2008) although this damage is questioned by dental researchers who claim dentine in particular becomes more resistant (e.g., Nalla et al. 2005).

The possibility of acetone-caused cracking is of particular concern as the process can be time consuming and requires repeated application of brushed-on solvent where the consolidant is shellac, as the older shellac is, the more resistant it tends to become.

Figure 1 shows a tooth surface after each of two consecutive attempts to remove the consolidant coating via the brushing on of ethanol. Figure 1.1, 1.3 and 1.5 show the first attempt. Brush strokes are clearly visible in the higher magnification images Figure 1.3 and 1.5. Figure 1.2, 1.4 and 1.6 show the second attempt. Whilst an underlying pervasive and dominant near vertical microwear pattern is emerging, sufficient varnish remains to in-fill and partially obscure this pattern. Figure 2 shows a tooth surface that was cleaned whilst being viewed under a stereo microscope (at x40 magnification giving a 5 mm field-of-view) by brushing on ethanol until it appeared to be clear of consolidant. The higher magnification SEM images (Figure 2.2 and 2.3) clearly show that the tooth surface is still coated in consolidant.

It is both time consuming and frustrating to complete a sequence of brush cleaning, moulding, casting and SEM imaging only to discover that a tooth surface is not clean, especially if the original tooth is in a remote museum collection and a return visit must be arranged. A more reliable cleaning method is needed.

Solvent Gels

Art conservators wanting to clean varnish from paintings without damaging the oil paint beneath discovered that by suspending the solvent in a gel, they could limit evaporation and control both contact time and the pH. The addition of soaps and detergents to the gel allowed the dissolved varnish to be sequestered by the gel and thus easily removed from the painting (Southall 1988). They found that overpainted areas could be dealt with by the addition of xylene to the gel, causing partial dissolution and swelling of the paint layer (Wolbers et al. 1990). It is this solvent gel formulation, used for varnish on paintings, which we have adapted for the removal of various consolidants from dinosaur teeth, including aged shellac.

This paper describes the cleaning method used by the authors, developed from a technique pioneered by museum conservators. This technique, for the removal of varnish from oil paintings via the application of solvent gels, is not widely known, and papers describing its use (Hedley 1980; Burnstock and White 1990; Eastaugh 1990;

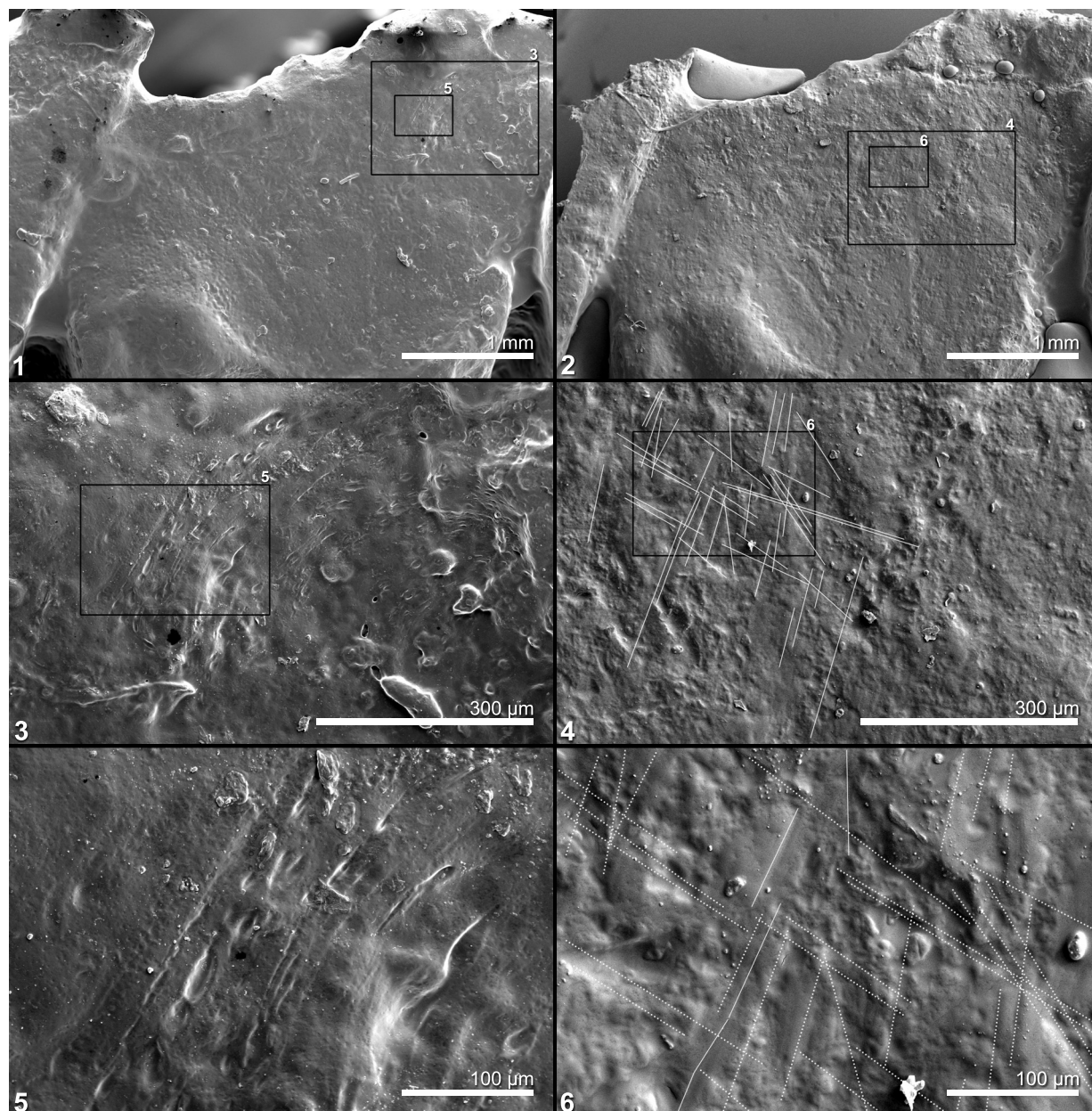


FIGURE 1. Occlusal surface of tooth of a *Heterodontosaurus* (SEM images of casts of SAM PK-1332 right dentary tooth, 3rd from posterior) illustrating the difficulties of cleaning by brush and solvent (ethanol). **1.1** Cast 1 made after first attempt to remove varnish from tooth surface; boxes show areas illustrated in 1.3 and 1.5. **1.2** Cast 2 made after second attempt to remove varnish from tooth surface, at low magnification the tooth appears to be clean; boxes show areas illustrated in 1.4 and 1.6. Microwear patterns can be identified at this magnification. **1.3** Enlargement of area in box 3 of 1.1; varnish has been smeared across the tooth surface and brush marks can be seen clearly in it. **1.4** Enlargement of area in box 4 of 1.2; a dominant near vertical microwear pattern (part highlighted with solid white lines) is discernable but varnish still remains infilling and obscuring the pattern. **1.5** Enlargement of area in box 5 of 1.1 and 1.3; at higher magnification there is still no visible microwear beneath the brush marks in the varnish. **1.6** Enlargement of area in box 6 of 1.2 and 1.4; at higher magnification several different orientations of microwear (part highlighted with solid white lines (visible microwear) and dashed white lines (obscured microwear)) are just discernable through the obscuring varnish, highlighting the amount of varnish still remaining on the surface of a tooth that had been cleaned twice and appeared to be free of varnish at low magnification.

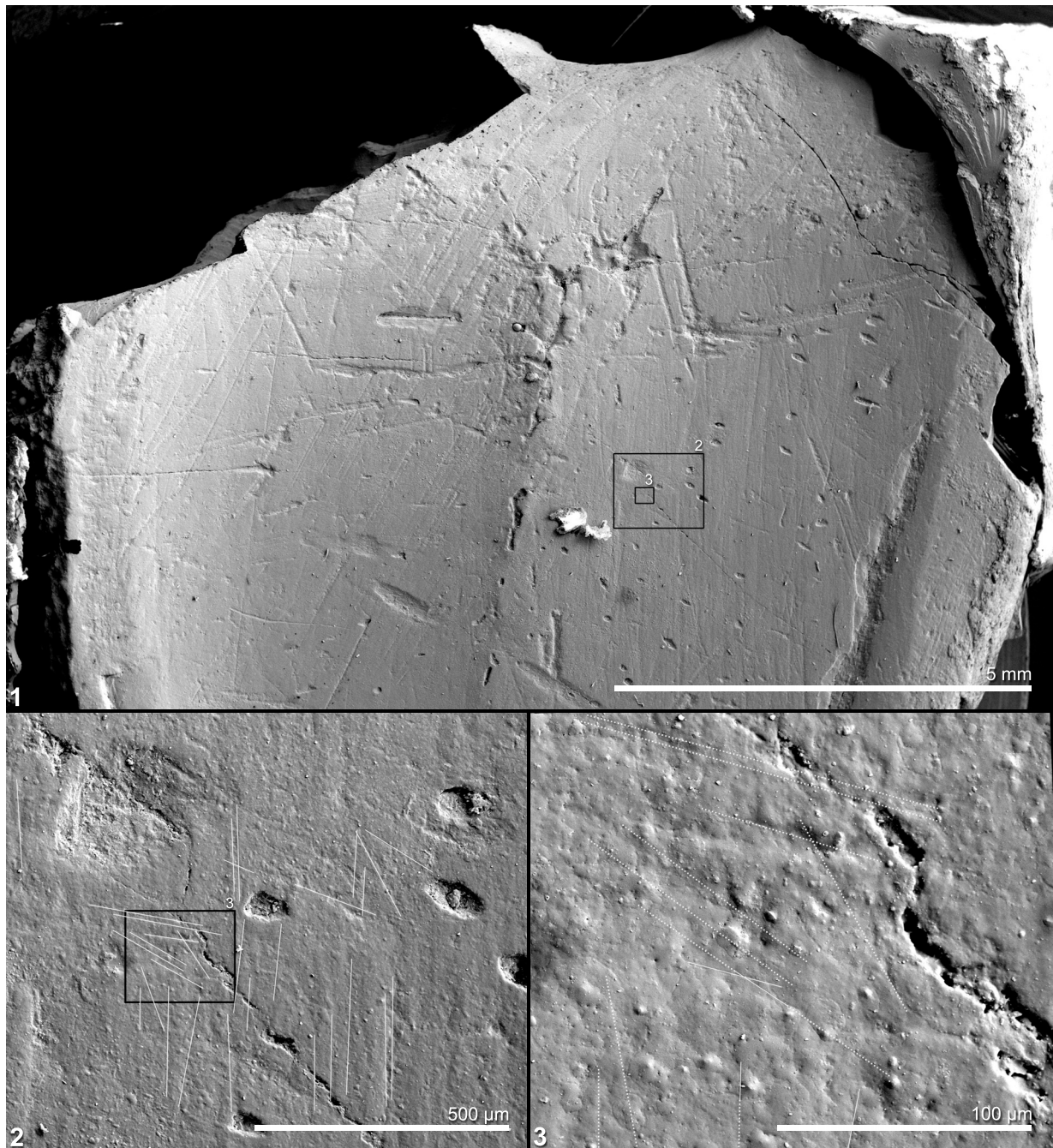


FIGURE 2. Occlusal surface of an isolated tooth of hadrosaurid (SEM images of cast of AMNH 21700) illustrating the difficulties of cleaning with brush and solvent (ethanol). **2.1** Low magnification image showing full width of tooth, at this magnification the tooth appears to be clean; boxes show areas illustrated in 2.2 and 2.3. Microwear patterns can be identified at this magnification. **2.2** Enlargement of area in box 2 of 2.1; at higher magnification it can be seen that the microwear (part highlighted with solid white lines) is largely obscured. **2.3** Enlargement of area in box 3 of 2.1 and 2.2; at higher magnification it is clear the surface is still coated in consolidants and the microwear patterns (part highlighted with solid white lines (visible microwear) and dashed white lines (obscured microwear)) are largely obscured.

Wolbers et al. 1990; Wolbers 1992) are not widely available.

MATERIAL AND METHODS

Ornithopod dinosaur specimens to which the cleaning methods described herein have been applied include teeth and jaw elements from the collections of the Natural History Museum, London, the American Museum of Natural History, New York (AMNH), the Peabody Museum of Natural History, Yale University, the Smithsonian Institution National Museum of Natural History, Washington DC (SM), the Carnegie Museum of Natural History, the Iziko South African Museum (SAM), the Dinosaur Isle Museum, Isle of Wight and the Oxford University Museum of Natural History, Oxford. All were cleaned using solvent gels and then moulded with a vinyl polysiloxane impression medium. Epoxy resin casts were taken from the vinyl polysiloxane moulds, sputter coated with gold and imaged in a Hitachi S-3600N Scanning Electron Microscope (SEM).

Shellac, glyptal and shellac/animal resin combinations were removed by the application of solvent gels from the occlusal surfaces of hundreds of teeth from 143 specimens, which consisted of individual teeth, teeth within jaw fragments and teeth within complete jaw elements.

Fossil teeth that were cleaned by the traditional brushing on of ethanol method were also moulded, cast and imaged.

Creating the Solvent Gel

Components:

- 200 ml ethanol (IMS)
- 200 ml acetone
- 50 ml xylene
- 20 ml Ethomeen C/25 (a polyoxyethylene cocoamine detergent; Akzo / Linden Chemicals)
- 6g Carbopol EZ2 (a water soluble acrylic acid polymer; Noveon / Linden Chemicals)
- 50 ml pure water (distilled or deionised)

Care should be taken to follow the manufacturer's instructions regarding safe use and storage of all of these products. Material Safety Data Sheets (MSDS) are available via the manufacturer's and distributor's web sites. Both Ethomeen and Carbopol can be obtained from Linden Chemicals (www.lindenchemicals.com), Ethomeen is a product of Akzo (www.akzonobel.com), and Car-

bopol is a product of Noveon (www.lubrizol.com). Ethanol, iso-propanol, acetone and xylene can be obtained from standard suppliers of laboratory chemicals.

The solvent gel should be prepared and stored in polyethylene or polypropylene bottles to prevent reaction between container and gel. Bottles with transparent sides allow progress to be monitored during preparation of the gel. Bottles with wide openings and tightly sealing lids are preferable.

The quantities listed above will produce approximately 500 ml of solvent gel; for smaller volumes reduce the component quantities on a pro-rata basis. The solvent gel can be created quickly for immediate use via a one stage method, but a two stage method (see below) produces a more consistent gel, allows the pH of the gel to be controlled and gives flexibility in the combination of solvents used. Standard laboratory procedures should be followed with reference to all relevant health and safety legislation. We recommend that the addition of ethanol, acetone and/or xylene to the solvent gel should be performed in a fume cupboard. However, once the solvents have been added to the gel, a fume cupboard is no longer required. The solvent gel can be used with standard air extraction systems or in a well ventilated area.

For the one stage method of gel preparation, sprinkle the Carbopol EZ2 powder onto the Ethomeen C/25 whilst stirring continuously until a uniform paste is produced. Stir in the required combination of solvents ethanol/acetone/xylene, and then add the pure water gradually whilst stirring continuously. Apply a tight fitting lid to the bottle, and shake the bottle vigorously.

For the two stage method, first prepare a Carbopol gel as follows: Sprinkle the Carbopol EZ2 powder onto pure water whilst stirring continuously, until a smooth, stiff 'wallpaper paste'-like mixture forms. This Carbopol gel can be used within a few minutes if necessary (as soon as it settles and takes on a uniform consistency) but will benefit from being left to stand overnight in a sealed bottle to allow the Carbopol to fully disperse. Next, pour the Ethomeen EZ2 into the Carbopol gel and stir until a smooth, colourless and transparent Carbopol/Ethomeen gel forms. The bottle lid can be screwed tight and the bottle shaken vigorously to aid mixing at this stage. The introduction of Ethomeen should neutralize the acidity of the Carbopol. Testing with pH paper strips should show a pH between 7 and 8. If these numbers do not

result, adding more Ethomeen will increase the pH and adding more Carbopol gel will reduce the pH.

Next, mix the required combination of solvents ethanol/acetone/xylene in a second bottle, and then cut in the Carbopol/Ethomeen gel gradually. If the gel becomes cloudy or if a sticky white residue begins to form, water must be added to the gel to allow the solvents to be fully absorbed. Adding the above solvents should result in Solvent gel with a pH of around 8.5.

The advantage of using the two stage method of production is that stock Carbopol/Ethomeen gel can be made up as a first stage. Later, small samples of this gel can be cut into various combinations of solvents for testing on unknown consolidants.

Variations in Composition

Various formulations of the gel can be made by substituting one solvent for another. The above formula, which adds a small quantity of xylene to a 50:50 solution of acetone and ethanol, acts to break the cross-links in aged shellac and enables it to be dissolved. It is effective on glyptal as it takes the guess work out of which solvent was used in the formulation of the glyptal, and it will also work on young shellac (although not as effectively as ethanol alone) and so can be used as a universal formula. An alternative formulation substituting additional ethanol for the acetone and xylene (i.e., 450 ml of ethanol) is more effective on shellac that has not developed cross-links. Typically this is shellac that is less than two years old. However, depending upon the additives used in the shellac, it may still dissolve readily in ethanol after many years. It is worth testing a small area to assess how first to treat shellac.

When solvents are added to the Carbopol/Ethomeen gel, the pH can be tested. If it is too acidic, Ethomeen can be added to reduce the acidity. Whilst slight acidity of the solvent gel is not critical for use on the highly resistant enamel and dentine surfaces of teeth, this ability to control pH has great importance for the wider application of solvent gels to less resistant surfaces such as bone.

It is worth noting that linseed oil may be a component in shellac. Whilst we did not encounter a consolidant of this composition, in such instances the acetone/ethanol combination would not be as effective. Tests carried out on oleo-resinous varnish by Burnstock and White (1990) had greater success with iso-propanol.

Application of the Solvent Gel

Loose dirt should be brushed from the surface being cleaned and a thick layer (>8 mm) of solvent gel applied. A layer of stretch plastic wrap should be wrapped over the solvent gel and the teeth/jaw to hold the gel in place. This has a number of positive effects. The plastic wrap provides gentle pressure, keeping the gel in contact with the consolidant surface, it prevents the gel from spreading to adjacent surfaces, and it reduces the amount of solvent evaporation from the gel. We found that a 17 µm thick, commercial, food quality, polyethylene stretch film plastic wrap, with cling/tack on one side, worked well for our purposes, but thicker versions of the domestic 'cling film' (UK) or Saran™ Wrap (US) should be equally suitable.

Over a period of 15 to 20 minutes the consolidant will soften, dissolve and be drawn into the gel. Typically, the dissolved consolidant (particularly shellac) discolours the gel, and, as both plastic wrap and gel are transparent, the process can be monitored. One application of gel is usually enough. If the consolidant has been applied in multiple layers it may be necessary to repeat the process. The plastic wrap can be used to scoop the gel from the tooth surface, and both plastic wrap and gel can be discarded (subject to the relevant local regulations on the disposal of hazardous waste). With shellac, a very thin blistered film typically remains that should be 'teased' away from the tooth surface. A wooden spatula, wooden dental stick or latex block (to avoid introducing scratches) will work well for this purpose. Any remaining solvent gel can be brushed from the tooth surface with a little ethanol or water and a fine soft brush.

The Carbopol EZ2 gel allows a solvent or combination of solvents to be held in suspension, preventing immediate evaporation and allowing their action to be concentrated at a specific point and over a significant period of time. Being an amine with detergent properties Ethomeen C/25 serves two purposes when mixed with a Carbopol EZ2 gel. The slight alkalinity of the amine neutralizes the acidity of the gel and the detergent properties enable the gel to sequester material dissolved by the suspended solvents. This latter quality is of key importance in that the dissolved consolidant is taken away from the tooth surface and locked into the gel. As a layer of shellac dissolves into the gel it thins and eventually reaches the point where it will distort and blister, lifting away from the tooth surface cleanly. The clean separation virtually eliminates instances of remaining consolidant and the consequent need to re-clean and re-mould/cast.

Solvent gels need to be stored, handled and disposed of as hazardous chemicals, but no more so than their solvent components. The lower rate of evaporation from gels makes them considerably more pleasant to work with. Carbopol/Ethomeen gel is not hazardous until solvents are added, so it can be made up in bulk and stored for extended periods of time. Small volumes for immediate use can be measured out as needed and the solvents added moments before use. Alternatively, solvent gel can be made up from scratch within an hour and potentially within a few minutes.

RESULTS AND DISCUSSION

Figures 1 and 2 show casts taken from teeth that were cleaned by the traditional brushing on of ethanol method. These casts appear to be free of consolidant at low magnification (Figures 1.1 and 2.1), but at higher magnifications (Figures 1.2, 1.3, 2.2, 2.3) the microwear is clearly being obscured by smeared consolidant.

Figures 3 and 4 compare the quality of microwear obtained from tooth surfaces that have been cleaned via the application of solvent gel to that from adjacent uncleaned areas. It can be seen from these images that the use of solvent gel leaves little or no remaining consolidant. The ability of solvent gels to lift consolidant cleanly rather than dissolve it and allow it to in-fill microwear can be seen in Figure 5. Here we show a selection of teeth that were marginal to areas cleaned with solvent gel, such that only part of the tooth surface has been cleaned. In each case there is no smearing or blurring, the edge of the consolidant coating is sharp and well defined. All of these casts showed large areas of tooth surface that were either completely free of consolidant or that had only small, discrete patches of consolidant within them.

A combination of acetone, ethanol and xylene makes a good universal solvent gel, and holding the pH down to a value around 8.5 slows the action of the solvent gel, causing the shellac to swell and blister. This amount has proven more effective at removing thick coatings of shellac than using more alkaline solvent gels. These tend to act more rapidly, penetrate the shellac and remove it unevenly.

A note of caution on the removal of shellac: Conservators are aware that removing any consolidant from a fossil may cause damage. In the case of aged shellac that damage can be significant. This is due to the tendency of shellac to shrink over time, exerting pressure on the fossil. In some cases, if this pressure is removed the fossil can fracture and disintegrate (Davidson and Alderson

2009). For microwear analysis there is no alternative to removing the consolidant, but by using solvent gels the area of removal can be restricted to very small parts of the tooth, minimizing the risk. None of the hundreds of teeth to which our solvent gel cleaning method has been applied showed any evidence of resulting damage.

Solvent gels concentrate the action of the solvent on the specific part of the surface being cleaned and in doing so reduce the diffusion of the solvent into the surrounding area. Where a tooth or jaw has been reconstructed by gluing several parts together, use of a solvent gel will enable cleaning of a portion of the tooth without compromising the reconstruction.

By retaining the solvent within the gel, the volume of evaporate is greatly reduced, conserving the solvent and allowing cleaning to be performed with simple air extraction rather than a fume cupboard (subject to all relevant health and safety legislation, especially where xylene is used within a solvent gel). A more comfortable working environment is the result.

SUMMARY

Solvent gels remove consolidant more cleanly, more reliably, in considerably less time and in a more comfortable working environment than the brushing on of solvent method. Specific areas of interest can be cleaned without any adverse effects on adjacent areas and the flexibility in formulation allows various consolidants to be tackled. These advantages, coupled with the ability to control pH (and thus the level of aggression) allows the possibility of its wider application to less resistant consolidant coated surfaces.

ACKNOWLEDGMENTS

This paper has benefited from discussions with M. Purnell of The University of Leicester, N. Eastaugh of The Pigmentum Project and the comments of the anonymous reviewers. We are grateful to P. Barrett and S. Chapman, Natural History Museum, C. Norris, C. Mehling and J. Kelly, American Museum of Natural History, W. Joyce and M. Fox, Yale Peabody Museum, M. Lamanna and A. Henrici, Carnegie Museum, M. Carrano, Smithsonian Institution, D. Siveter and P. Jeffery, Oxford University Museum of Natural History and M. Munt and L. Steel, Dinosaur Isle Museum, for granting access to and permission to clean the dinosaur teeth. J. Larkham of Coltène Whaledent is thanked for donating polyvinylsiloxane molding compound.

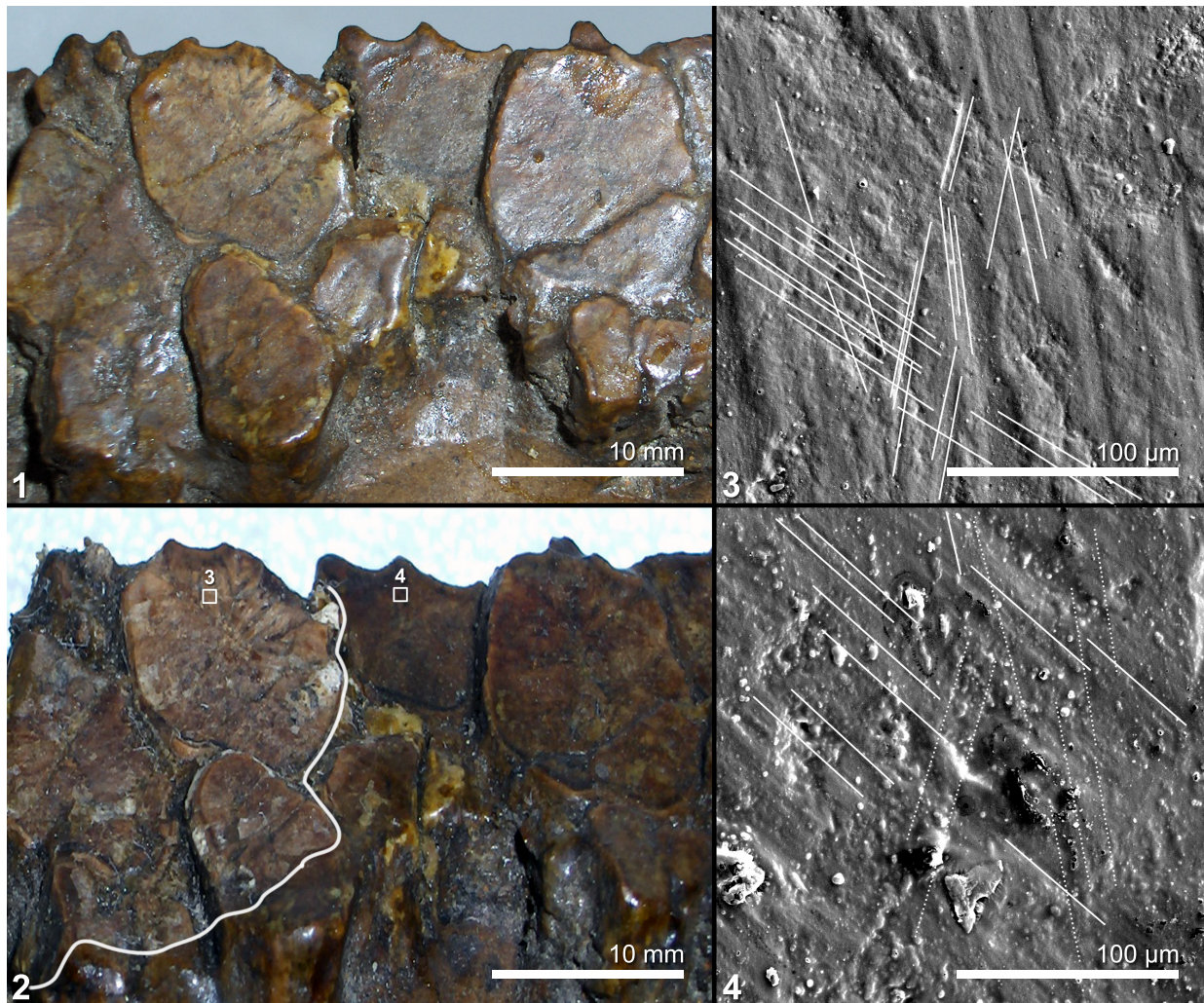


FIGURE 3. Occlusal surface of left dentary teeth of *Corythosaurus casuarius* (AMNH 3971), illustrating the results of cleaning with solvent gel. **3.1** Photograph of mesial fragment of left dentary prior to cleaning. **3.2** Post cleaning, shellac removed from teeth on the left by application of solvent gel; boxes show areas illustrated in 3.3 and 3.4. Broad white line drawn on to highlight the sharp boundary of the area from which shellac has been removed. **3.3** SEM micrograph of cast of central portion of a cleaned tooth (area in box 3 of 3.2); multiple microwear orientations (part highlighted with solid white lines) are visible with no remnant of varnish. **3.4** SEM micrograph of cast of central portion of an uncleaned tooth (area in box 4 of 3.2); microwear (part highlighted with solid white lines) is discernable but is largely obscured by varnish; in particular the near vertical microwear (part highlighted with dashed white lines), which is visible in 3.3, is barely noticeable here.

REFERENCES

- Burnstock, A., and White, R. 1990. The effects of selected solvents and soaps on a simulated canvas painting, p. 111-118. In Mills, J.S., and Smith, P. (eds.), *Cleaning, retouching and coatings: Contributions to the 1990 IIC Congress, Brussels*. International Institute for Conservation of Historic and Artistic Work, London.
- Davidson, A., and Alderson, S. 2009. An introduction to solution and reaction adhesives for fossil preparation, p. 53-62. In Brown, M.A., Kane, J.F., and Parker, W.G. (eds.), *Methods in Paleontology: Proceedings of the First Annual Fossil Preparation and Collections Symposium*.
- Eastaugh, N. 1990. The visual effects of dirt on paintings, p. 19-23. In Hackney, S., Townsend, J., and Eastaugh, N. (eds.), *Dirt and Pictures Separated*. United Kingdom Institute for Conservation, London.

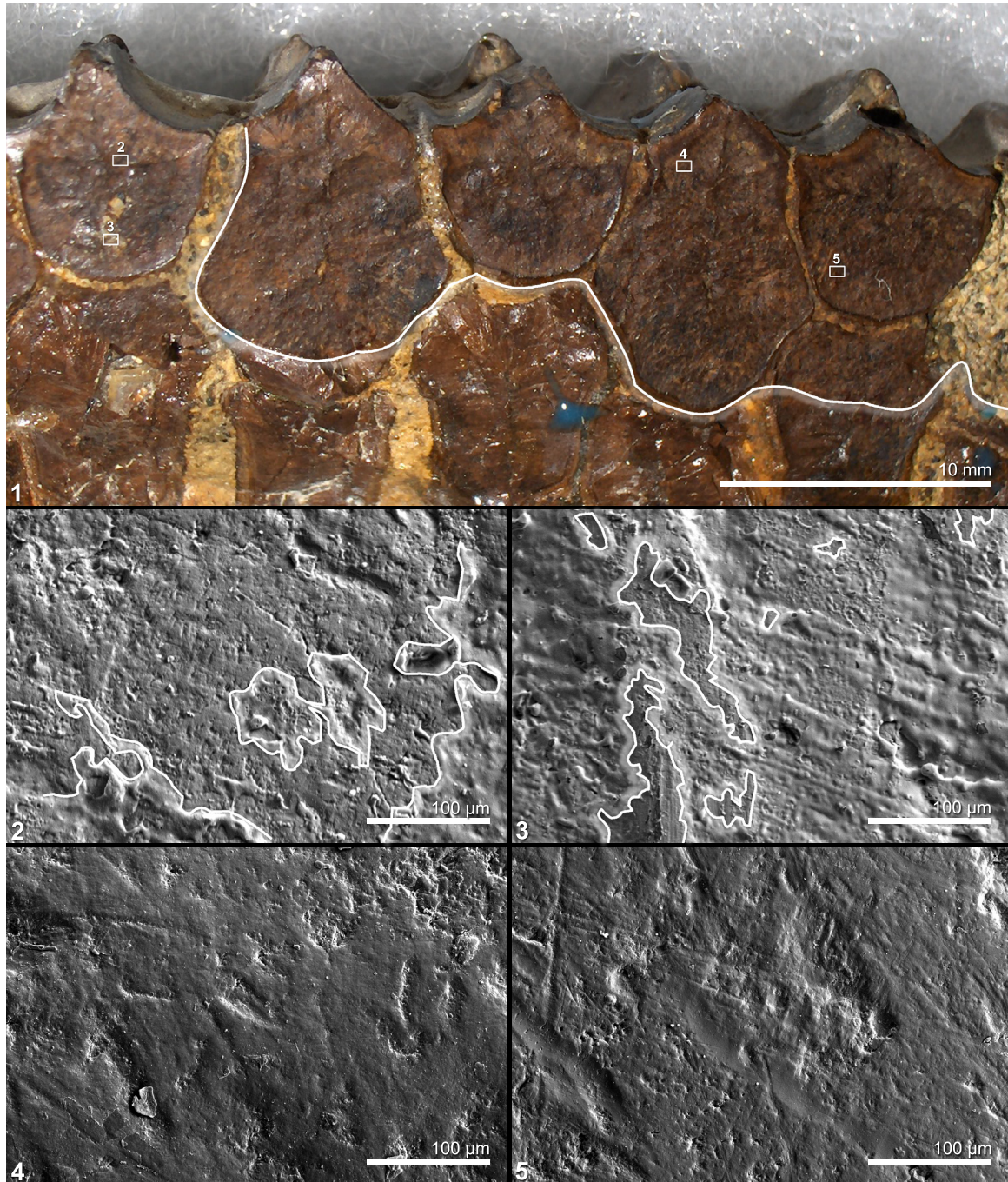


FIGURE 4. Occlusal surface of left dentary teeth of *Edmontosaurus* (SM 22102), illustrating the results of cleaning with solvent gel. **4.1** Photograph of distal section of a left dentary. White line drawn on to highlight the sharp boundary of the area from which shellac has been removed. The teeth on the top row and to the right have been cleaned by application of solvent gel. The teeth on the left and along the bottom row were not cleaned and remain coated in shellac. Boxes show areas of tooth illustrated in 4.2 to 4.5. **4.2** SEM micrograph of cast of site on uncleaned tooth (area in box 2 of 4.1); microwear is obscured by shellac. White lines drawn around areas of shellac, with shading in the shellac. **4.3** SEM micrograph of cast of site on uncleaned tooth (area in box 3 of 4.1); microwear is obscured by shellac. White lines drawn around areas of shellac, with shading in the shellac. **4.4** SEM micrograph of cast of site on cleaned tooth (area in box 4 of 4.1); showing microwear with no remnant of shellac. **4.5** SEM micrograph of cast of site on cleaned tooth (area in box 5 of 4.1); showing microwear with no remnant of shellac. (Note: the broad shallow grooves are typical of tool marks left by a vibro-tool during preparation of a fossil.)

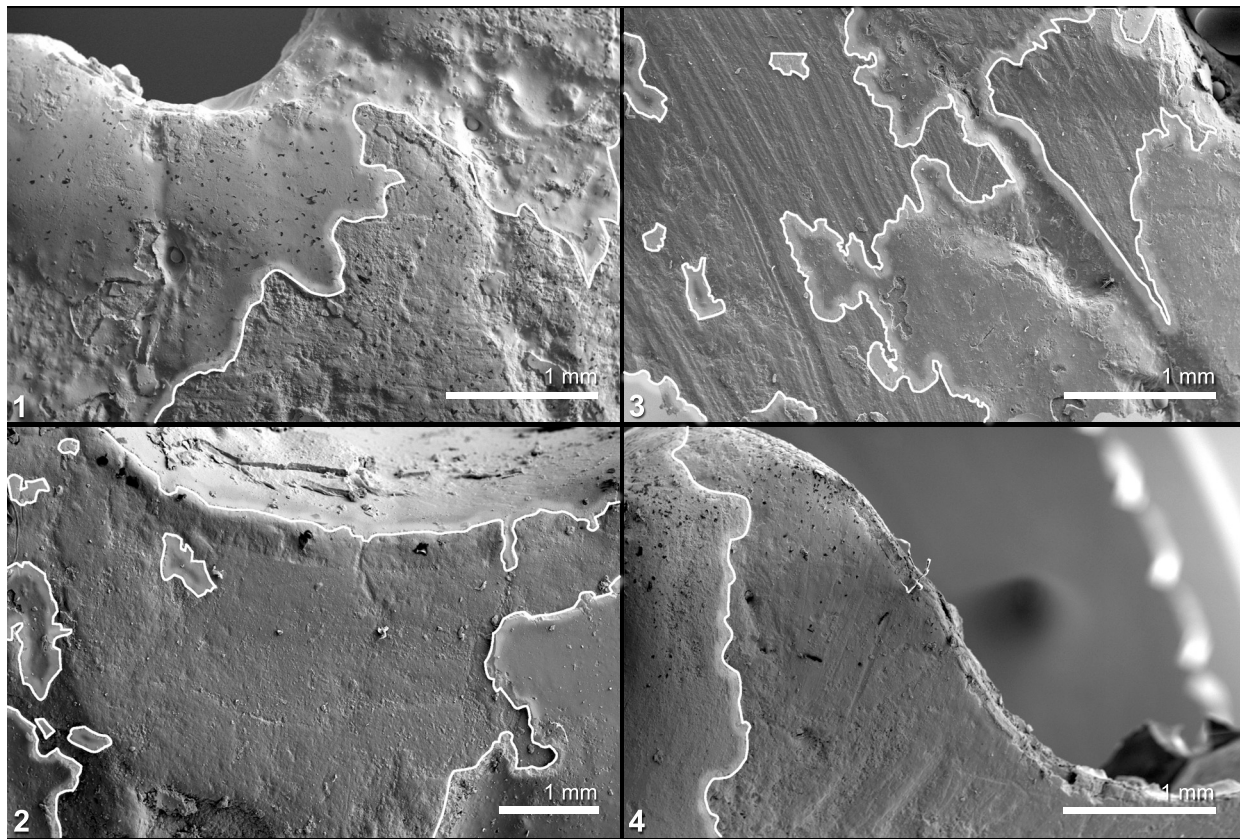


FIGURE 5. Occlusal surfaces of hadrosaurid teeth (SEM images of casts) illustrating the results of cleaning with solvent gel. These teeth were marginal to areas that were cleaned by the application of solvent gel prior to moulding and casting and show the clear boundary between the consolidant layer and clean tooth surface. White lines are drawn around areas of shellac, with shading in the shellac. **5.1** *Edmontosaurus* AMNH 5879 right maxilla tooth, right hand side of tooth has been cleaned. **5.2** Hadrosaurid AMNH 5896 maxilla tooth, left hand side of tooth has been cleaned; vestiges of consolidant remain on the left hand side in depressions. **5.3** *Hadrosaurus notabilis* SM 5465 left dentary tooth, left hand side of tooth has been cleaned. **5.4** Hadrosaurid AMNH 6387 right maxilla tooth, right hand side of tooth has been cleaned.

- Fernandez-Jalvo, Y., and Monfort, M.D.M. 2008. Experimental taphonomy in museums: Preparation protocols for skeletons and fossil vertebrates under the scanning electron microscopy. *Geobios*, 41:157-181.
- Fiorillo, A.R. 1991. Dental microwear on the teeth of *Camarasaurus* and *Diplodocus*; implications for sauropod paleoecology, p. 23-24. In Kielan-Jaworowska, Z., Heintz, N., and Nakrem, H.A. (eds.), *Fifth symposium on Mesozoic terrestrial ecosystems and biota*. Paleontologisk Museum, University of Oslo
- Fiorillo, A.R. 1998. Dental microwear patterns of the sauropod dinosaurs *Camarasaurus* and *Diplodocus*: Evidence for resource partitioning in the Late Jurassic of North America. *Historical Biology*, 13:1-16.
- Gordon, K.D. 1984. The assessment of jaw movement direction from dental microwear. *American Journal of Physical Anthropology*, 63:77-84.
- Hedley, G. 1980. Solubility parameters and varnish removal: a survey. *The Conservator*, 4:12-18.
- Nalla, R.K., Balooch, M., Ager lli, J.W., Kruzic, J.J., Kinney, J.H., and Ritchie, R.O. 2005. Effects of polar solvents on the fracture resistance of dentin: role of water hydration. *Acta Biomaterialia*, 1:31-43.
- Organ, J.M., Teaford, M.F., and Larsen, C.S. 2005. Dietary inferences from dental occlusal microwear at Mission San Luis de Apalachee. *American Journal of Physical Anthropology*, 128(4):801-811.
- Schubert, B.W., and Ungar, P.S. 2005. Wear facets and enamel spalling in tyrannosaurid dinosaurs. *Acta Palaeontologica Polonica*, 50:93-99.
- Southall, A. 1988. New approach to cleaning painted surfaces. *Conservation News*, 37:43-44.
- Teaford, M.F. 1988. A review of dental microwear and diet in modern mammals. *Scanning Microscopy*, 2:1149-1166.

- Ungar, P.S., Merceron, G., and Scott, R.S. 2007. Dental microwear texture analysis of Varswater bovids and early Pliocene paleoenvironments of Langebaanweg, Western Cape Province, South Africa. *Journal of Mammalian Evolution*, 14(3):163-181.
- Upchurch, P., and Barrett, P.M. 2000. The evolution of sauropod feeding mechanisms, p. 79-122. In Sues, H.-D. (ed.), *Evolution of Herbivory in Terrestrial Vertebrates: perspectives from the fossil record*. Cambridge University Press, Cambridge
- Walker, A., Hoeck, H.N., and Perez, L. 1978. Microwear of mammalian teeth as an indicator of diet. *Science*, 201:908-910.
- Williams, V.S., Barrett, P.M., and Purnell, M.A. 2009. Quantitative analysis of dental microwear in hadrosaurid dinosaurs, and the implications for hypotheses of jaw mechanics and feeding. *Proceedings of the National Academy of Sciences*, 106(27):11194-11199.
- Wolbers, R. 1992. Recent development in the use of gel formulations for the cleaning of paintings, p. 74-75. In *Restoration 1992 Conference Preprint*. UKIC.
- Wolbers, R., Sterman, N., and Stavroudis, C. 1990. *Notes for the workshop on new methods in the cleaning of paintings*, The Getty Conservation Institute, Marina del Ray, California.

APPENDIX

Components and Suppliers:

Carbopol was originally manufactured by B.F. Goodrich (now Noveon). It was available in several formulations (e.g., 934, 940, 950 and 954), and it is these that are discussed by painting conservators (Southall 1988; Wolbers et al. 1990). EZ2 is a newer but comparable formulation of Carbopol and is more readily available today than the older versions. It is supplied as a white powder. When mixed with pure water it forms a clear, slightly acidic, viscous gel. The water must be pure, otherwise any minerals present (particularly calcium) will react with the Carbopol and precipitate out. The manufacturers claim that the EZ formulations disperse more quickly, which certainly appears to be

the case (EZ2 can be used within minutes of mixing whereas 954 took over an hour to achieve a uniform consistency). Carbopol 954 based solvent gels were used within the Palaeontology Conservation Unit at the Natural History Museum, London, and Carbopol EZ2 based solvent gels were used on specimens at all other sites.

Ethomeen is manufactured by Akzo. There are two forms suitable for use in solvent gels (C/12 and C/25), with C/25 being recommended for use with the more polar solvents (Wolbers et al. 1990). Ethomeen is an ochre coloured viscous liquid and is slightly alkaline. Both forms are available from Linden Chemicals.

Dental microwear in dinosaurs: a comparative analysis of polysiloxane replication

Vince Williams, Mark Purnell and Sarah Gabbott
Department of Geology, University of Leicester

EVERY time a tooth comes into contact with food or with another tooth, it is damaged. Abrasive particles cause microscopic scratching and pitting, and while this may seem undesirable from the point of view of the tooth's owner, it is good news for palaeontologists because the "microwear" that accumulates on the tooth surface provides a record of what has been eaten and the range of tooth movements involved.

This is true of humans and any other animals with teeth, both extant and fossil, and studies of living mammals with controlled or known diets have established the relationship between feeding and microwear sufficiently well for the microwear footprint on fossil teeth to be used to interpret diet.

This is an extremely powerful tool with which to analyse feeding in extinct animals and has been applied extensively to fossil hominoids in order to evaluate the role of dietary changes in human evolution (Teaford and Ungar, 2000).

It has also been applied to extinct mammals and has revealed in surprising detail how feeding in mammals has tracked past environmental change (Semperebon *et al* 2004; Solounias and Hayek, 1993). But can the same technique be applied to dinosaurs?

We are attempting to find out by conducting the first systematic study of dinosaur microwear. Our main aims are to understand how diet and feeding changed

during the evolution of a major group of herbivorous dinosaurs, and assess whether dietary changes were related to known changes in the environment and vegetation.

For example, we know from the fossil record that between 150 and 60 million years ago, the gymnosperm conifer forests – which had dominated the global flora for more than 100 million years – were replaced by angiosperm flowering plants. It seems quite likely that such a major change in food supply would have had a significant effect on herbivorous dinosaurs and their evolution.

More surprisingly, it has also been suggested that the grazing activities of dinosaurs may have been an important factor in causing this change in vegetation.

Before we can evaluate what the microwear footprint of dinosaurs can tell us, however, we need to understand two things. Firstly, we need to see what microwear in dinosaur teeth looks like, because dinosaur teeth are very different to those of mammals.

Mammals replace their teeth just once, so adult teeth are retained in the mouth for a long time over which microwear can accumulate. Dinosaurs, on the other hand, shed worn teeth and continued to grow replacements throughout their life.

To further complicate matters, dinosaur jaw articulation is very different to that of mammals and they did not bite or chew their food in the same way. In fact the jaws of most dinosaurs, including all of the earliest forms, could only move up and down, meaning that their tooth surfaces could not slide across each other like those of mammals do, making chewing impossible.

Secondly, we cannot conduct the experiments required to establish the relationship between food type and microwear in dinosaurs because most of them are extinct and those that survive (birds) have no teeth. The nearest extant relatives with teeth are reptiles, so we need to investigate microwear and feeding in living reptiles.

Our dinosaur study will focus on ornithomorphs, a large group of herbivorous dinosaurs including well-known characters like *Iguanodon*. They make an ideal group to

investigate because they are known from strata of earliest Jurassic through to latest Cretaceous age, an interval of 140 million years, with their continuous evolutionary history spanning most of the time that dinosaurs existed.

The earliest ornithomorphs had no ability to masticate food as their jaws occluded in the vertical plane only, slicing and shredding vegetation in a manner similar to that of living iguanas. Later ornithomorphs, however, evolved two different but highly successful mechanisms for masticating food. The most advanced forms evolved a hinge in the top of their skulls that allowed the upper jaws to slide laterally over the lower jaws and grind plant material between them, in essence allowing them to chew.

To carry out our research we need to examine teeth under high magnifications in a scanning electron microscope (SEM), but ornithomorph specimens are distributed in various museums and private collections around the world, and most are either too large to fit in a SEM or unavailable for loan.

Consequently we need to obtain casts of teeth, and this requires a moulding material that will replicate tooth microwear with high fidelity and, crucially, leave fragile dinosaur material undamaged.

This is a tough challenge because after millions of years dinosaur teeth tend to be rather brittle and cracked, and are usually held together with a cross between glue and varnish known as a consolidant. The varnish-like sheen can be seen in **Fig 1a**, a *Lambeosaurus lambei* skull that is coated in consolidant.

Obviously this has to be removed from the tooth surface to get at the microwear, so what starts out as an already fragile fossil suddenly becomes very fragile indeed. Similar studies on fossil mammal teeth have used room temperature vulcanising (RTV) silicone rubbers, but these are unsuitable for a number of reasons.

The silicon fluid they contain tends to penetrate and stain the surface of fossils, and many have a high tear strength, meaning that unless a release agent is used, parts of the fossil can be pulled away as the mould is removed – and this is not good. In addition most RTV silicone rubbers have long cure times, and while this may be acceptable for use on fossils, it is unworkable where live reptiles, an important part of our study, are concerned.



FIG 1a – *Lambeosaurus lambei* skull, from the Upper Cretaceous Oldman Formation of Alberta, Canada. YPM 3222



FIG 1b – Speedex Light moulds of *Hypsilophodon foxii* isolated teeth, from the Wessex Formation, Isle of Wight. MIWG.6362



FIG 1c – Araldite 20/20 cast of *Hypsilophodon foxii* tooth, made from Speedex Light mould, mounted on SEM stub and sputter-coated with gold



Above: FIG 2a – SEM image of microwear on a fossil hyena canine tooth

Below: FIG 2b – SEM image of microwear on a cast made from a GC Exafast mould



FIG 2c – SEM image of microwear on a cast made from a Speedex Light mould

Polysiloxane impression mediums have none of these drawbacks and look to be ideal for our purposes. Their low tear strength in particular means that they are likely to give way before a fossil tooth gets pulled apart.

The only aspect of using polysiloxanes about which we were uncertain was the fidelity with which they can replicate microwear.

The scratches and pits we are interested in are measured in microns (thousandths of a millimetre), and the replicated surface must pick up every feature or the statistical analysis of the microwear patterns will be fatally flawed.

In order to evaluate whether polysiloxanes were up to the job, we performed a comparative test of a number of polysiloxane dental impression mediums, including Aquasil, Reprosil, GC Examix, GC Exafast, Coltène President Jet and Coltène Speedex.

After removal of any consolidant, tooth

surfaces were cleaned with a fine, soft brush. Impression medium was mixed according to the manufacturer's instructions; small quantities (less than 30ml) were generally used, but this varied according to the size of the specimen being moulded.

After surface moulding (**Fig 1b**), casts were prepared using low viscosity Araldite 20/20 epoxy resin. These were then mounted for SEM and splutter-coated with gold (**Fig 1c**).

Due to the fragile nature of dinosaur teeth, the initial testing was performed on hyena teeth, progressing to dinosaur teeth only when the moulding process was proven safe.

Results

The results of comparative testing showed that the condensation polymerising polysiloxanes gave the best performance, and out of these the best was Coltène Whaledent's Speedex Light, which produced near perfect replication of the dental

microwear once the casts were splutter-coated in gold.

Fig 2 compares microwear on a fossil hyena tooth (**Fig 2a**) to that replicated on casts made from a GC Exafast mould (**Fig 2b**) and a Speedex Light mould (**Fig 2c**). (GC Exafast was the next best performing medium after Speedex Light).

Fig 3 compares microwear, at a much higher magnification, on a dinosaur (*Hypsilophodont foxii*) tooth (**Fig 3a**) to that replicated on a cast made from Speedex Light (**Fig 3b**); the microwear in which we are interested is highlighted in **Fig 3c**.

Here the cast gives better definition than the original tooth; this is typical and relates to the coating in gold which cannot be applied to the original tooth.

Multiple casts were taken from the same Speedex Light mould with no appreciable difference in the quality of the casts and there was no significant shrinkage of the

moulds over three months.

Summary

Care needs to be taken when de-moulding as the polysiloxanes, while reasonably elastic, will tear if more than gentle "teasing" is attempted. Immediately after de-moulding, the polysiloxanes are susceptible to condensation and the moulds must be dried thoroughly before casting. Many of the polysiloxanes require mixing guns and while these were very easy to use, the ability to be hand-mixed proved to be a great advantage as it allowed the working time to be varied.

Due to the low viscosity of the polysiloxanes, it was necessary to create a "dam" around some specimens to prevent overflow from the area to be moulded. No damage was caused to any of our specimens by Speedex Light or GC Exafast.

Our results demonstrate that Speedex

Light can replicate tooth microwear at magnifications in excess of 300 times and this is more than sufficient for our research needs. Using this medium, our research will progress to form a systematic investigation of tooth microwear in ornithomimid dinosaurs, building on previous microwear work. Our studies will have clear implications for understanding the diet and the evolution of feeding mechanisms in dinosaurs and present day reptiles.

Acknowledgements

We thank Martin Munt and Lorna Steel (Dinosaur Isle Museum, Isle of Wight) for loan of the *Hypsilophodont foxii* specimens, and Walter Joyce (Yale Peabody Museum) for access to the *Lambeosaurus lambei* specimen. We also thank Coltène Whaledent and GC for supplying samples of their polysiloxane impression mediums for inclusion in our comparative testing.

References

- Semprebon G, Janis C and Solounias N. The diets of the dromomerycidae (Mammalia: Artiodactyla) and their response to miocene vegetational change. *Journal Of Vertebrate Paleontology* 2004; **24**: 427-444.
- Solounias N and Hayek L A C. New methods of tooth microwear analysis and application to dietary determination of two extinct antelopes. *Journal of Zoology* 1993; **229**: 421-445.
- Teaford M F and Ungar P S. Diet and the evolution of the earliest human ancestors. *Proceedings of the National Academy of Sciences of the United States of America* (2000); **97**: 13,506-13,511.

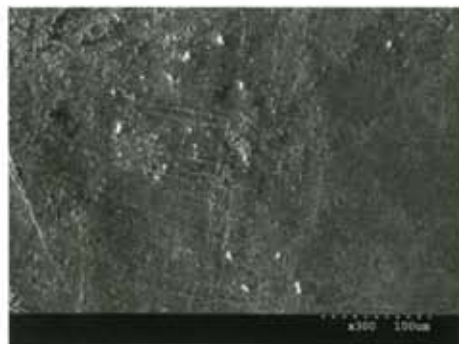


FIG 3a – SEM image of microwear on a *Hypsilophodont foxii* tooth. MIWG.6362

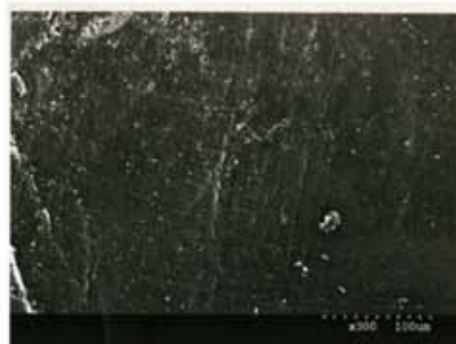


FIG 3b – SEM image of microwear on a cast made from a Speedex Light mould



FIG 3b – SEM image of microwear on a cast made from a Speedex Light mould

Quantitative analysis of dental microwear in hadrosaurid dinosaurs, and the implications for hypotheses of jaw mechanics and feeding

Vincent S. Williams^a, Paul M. Barrett^b, and Mark A. Purnell^{a,1}

^aDepartment of Geology, University of Leicester, Leicester LE1 7RH, United Kingdom; and ^bDepartment of Palaeontology, Natural History Museum, Cromwell Road, London SW7 5BD, United Kingdom

Edited by Peter R. Crane, University of Chicago, Chicago, IL, and approved May 5, 2009 (received for review December 11, 2008)

Understanding the feeding mechanisms and diet of nonavian dinosaurs is fundamental to understanding the paleobiology of these taxa and their role in Mesozoic terrestrial ecosystems. Various methods, including biomechanical analysis and 3D computer modeling, have been used to generate detailed functional hypotheses, but in the absence of either direct observations of dinosaur feeding behavior, or close living functional analogues, testing these hypotheses is problematic. Microscopic scratches that form on teeth in vivo during feeding are known to record the relative motion of the tooth rows to each other during feeding and to capture evidence of tooth–food interactions. Analysis of this dental microwear provides a powerful tool for testing hypotheses of jaw mechanics, diet, and trophic niche; yet, quantitative analysis of microwear in dinosaurs has not been attempted. Here, we show that analysis of tooth microwear orientation provides direct evidence for the relative motions of jaws during feeding in hadrosaurid ornithopods, the dominant terrestrial herbivores of the Late Cretaceous. Statistical testing demonstrates that *Edmontosaurus* teeth preserve 4 distinct sets of scratches in different orientations. In terms of jaw mechanics, these data indicate an isognathic, near-vertical posterodorsal power stroke during feeding; near-vertical jaw opening; and propalinal movements in near anterior and near posterior directions. Our analysis supports the presence of a pleurokinetic hinge, and the straightness and parallelism of scratches indicate a tightly controlled occlusion. The dominance of scratched microwear fabrics suggests that *Edmontosaurus* was a grazer rather than a browser.

Cretaceous | Ornithopoda | tooth | trophic ecology | Vertebrata

Reconstructing the feeding mechanisms and details of trophic ecology of extinct animals based on functional morphology is fraught with difficulty (1). In vertebrates, tooth form provides only a general guide to diet: the same tooth form can serve more than one function, and that function can vary with specific feeding behavior. Further complications arise because functional optimization of tooth form can be constrained by the need to process fallback foods during times of resource scarcity (2), and animals with an apparently specialized feeding apparatus can have generalist diets (3). These problems are especially acute in groups like herbivorous, nonavian dinosaurs, where most species have generalized homodont dentitions and lack close living analogues.

Among herbivorous dinosaurs, feeding of hadrosaurids has attracted particular attention. They were the dominant herbivorous vertebrates in many Late Cretaceous ecosystems, in terms of both species richness and abundance, and they achieved a near-global distribution (4, 5). This success is frequently attributed to the complex jaw mechanisms possessed by these taxa, which would have given them a level of masticatory prowess equal to that of many extant mammals (6). Current models of feeding mechanisms in hadrosaurid dinosaurs are based on analyses of functional morphology and rely on interpretations of musculature rather than direct evidence. No extant species has a sufficiently similar skull morphology to act as a convincing

functional analogue, and no fossil evidence exists to show the size and shape of the interarticular fibrocartilages and the limitations these would have placed on jaw motions. Here, we present the results of quantitative tooth microwear analysis of a hadrosaurian dinosaur, and we demonstrate how these provide a robust test of functional hypotheses.

Previous research into hadrosaurid feeding mechanisms reached contradictory conclusions. The extensive early work of Ostrom (7) suggested propalinal translation of the mandibles (an anteroposterior movement of the lower jaw during the power stroke). This was later questioned (8), and tooth wear was used to infer side-to-side (transverse) movements of the mandibles relative to the maxilla. Norman and Weishampel (6, 9–11) conducted kinematic and detailed functional anatomical analyses of all available hypotheses of hadrosaurid jaw mechanics and postulated a novel jaw mechanism, termed pleurokinesis. In this model, isognathic vertical adduction of the lower jaws generated a transverse power stroke. This was brought about by lateral rotation of the maxillae and suspensorium relative to the skull roof and driven by contact between the dentary and maxillary teeth during occlusion. Lateral rotation of the maxillae was accommodated by a pleurokinetic hinge (between the maxilla/jugal/quadrate and the akinetic skull) and was associated with slight propalinal movements caused by abduction and retraction of the quadrate (streptostylysm). However, recent work involving 3D modeling of feeding kinematics in *Edmontosaurus* has suggested that pleurokinesis would generate extensive secondary (intracranial) movements beyond the pleurokinetic hinge (12). Testing of these functional models has been difficult because of the absence of direct evidence for the mastication process in hadrosaurids.

Quantitative analysis of tooth microwear offers a hitherto unexplored route to testing feeding mechanisms in nonavian dinosaurs. Microwear refers to the microscopic polished, scratched, or pitted textures produced in vivo by the actions of abrasives in food and by the compressive and shearing forces that act on teeth during feeding (13, 14). Quantitative analysis of tooth microwear is an extremely powerful tool and has been applied extensively to fossil primates and hominins to evaluate the role of dietary changes in human evolution (15, 16). Applied to extinct nonprimate mammals, quantitative tooth microwear analysis has also provided direct evidence of tooth use, diet, and feeding (13, 17, 18) and has revealed how feeding in ungulates has tracked past environmental change (19).

Author contributions: V.S.W. and M.A.P. designed research; V.S.W. and M.A.P. performed research; V.S.W. and M.A.P. analyzed data; and V.S.W., P.M.B., and M.A.P. wrote the paper.

The authors declare no conflict of interest.

This article is a PNAS Direct Submission.

¹To whom correspondence should be addressed. E-mail: mark.purnell@le.ac.uk.

This article contains supporting information online at www.pnas.org/cgi/content/full/0812631106/DCSupplemental.

Table 1. Summary statistics from pooled raw microwear data (20 sites on 10 teeth on maxilla NHM R3638) partitioned into 4 classes based on feature orientation

Subgroup	Class 1	Class 2	Class 3	Class 4
No. of observations	300	1581	424	283
Angular dispersion, R	0.95	0.93	0.89	0.95
Mean orientation (mean vector, μ)	15.91°	63.29°	117.30°	164.57°
95% confidence interval for μ	$\pm 1.02^\circ$	$\pm 0.55^\circ$	$\pm 1.31^\circ$	$\pm 1.08^\circ$
99% confidence interval for μ	$\pm 1.35^\circ$	$\pm 0.72^\circ$	$\pm 1.72^\circ$	$\pm 1.42^\circ$
Mean scratch length, μm	72.33	52.85	54.75	70.85
Mean log scratch length, μm	4.04	3.74	3.74	4.02
Mean scratch width (microns), μm	1.59	1.68	1.54	1.42

analysis (DFA) provides strong confirmation that the microwear data fall into 4 distinct classes—98.3% of scratches classified by visual inspection were correctly assigned by DFA. Rather than conduct subsequent statistical testing on these imperfectly classified data, the DFA results were used to reassign the few incorrectly assigned scratches to their correct class (leading to 100% correct discrimination; see Table 1 for summary). Analysis of this dataset revealed significant differences in scratch count, orientation, length, and width between classes (Table 2). A test based on the mean of means (see below) also rejects the null hypothesis that scratch orientation does not differ between classes (99% and 95% confidence intervals; Table 1). We were unable to reject the null hypothesis that angular dispersal (i.e., the degree of parallelism of scratches as measured by R , mean vector length) does not vary between classes.

Pairwise comparisons (Tukey–Kramer honestly significant difference for linear variables, Watson–Williams F for axial variables) indicate that for the within-tooth data, orientation differs significantly between all classes, and that for length, all classes except 2 and 3 differ significantly ($P < 0.05$). For the between-tooth data, orientation differs significantly between all classes; length differs significantly except between classes 1 and 4, and between classes 2 and 3 ($P < 0.05$). Variation within class for both within- and between- tooth datasets is illustrated in Fig. 1 C and F .

Analysis of Microwear Orientation. Despite the increasing use of microwear analysis, there has been little discussion of analysis of

feature orientations and statistical hypothesis testing. A few authors have acknowledged that, strictly speaking, standard tests based on properties of linear distributions are not applicable to directional data (16, 17), but we are unaware of any analysis that has applied directional statistical tests to microwear data. Rather, nonparametric linear statistical tests have been applied, either with or without explicit justification (16, 17, 27). To determine how best to test our null hypotheses, we applied 3 different tests (1 based on linear distributions; 2 specific to axial data) to a set of class 2 scratch orientation data sampled from 7 sites along a straight line transect from tip to base of tooth 2 (Fig. 1 and Fig. S1).

Scratches are straight, and the data exhibit a consistently high degree of parallelism (i.e., angular dispersion as measured by mean vector length, $R > 0.97$; ref. 28), and the Rayleigh uniformity test along with the V test show the pooled data for the 7 sites to be nonuniformly distributed, with a significant mean orientation ($V > 0.96$; $P < 0.001$). Two alternative interpretations of these data are possible: either the samples are drawn from a single population of scratches that are straight, strongly parallel, and occur over the whole length of the transect (i.e., orientation is the same across the surface of the tooth), or the samples are drawn from multiple populations of scratches that differ slightly in orientation, but within which scratches are straight and parallel. For the purposes of this study, with controlled sampling across the transect, it is quite clear that the first of these hypotheses is the correct one; yet, two of the tests reject it (type 1 error): a nonparametric Wilcoxon test shows significant differences between the 7 samples ($P < 0.05$), as does the Watson–Williams F test (29), with pairwise testing indicating significant differences ($P < 0.05$) in mean feature angle in 10 of the 21 comparisons. Even when sites 1 to 4, which are close together and clearly the most similar, are compared, the Wilcoxon test finds significant differences between all of the sites except 1 and 2, and the Watson–Williams F test finds that site 4 differs significantly from sites 1 and 2. The results of this analysis indicate that when testing for differences in microwear scratch orientation between sample sites, the Wilcoxon and Watson–Williams F tests are susceptible to type 1 errors. Taken at face value, the results of these tests would lead us to reject the hypothesis that scratch orientations for the 7 sites are drawn from the same population (i.e., the tests wrongly indicate that their means differ), when in fact they are drawn from the same population and, in the context of this analysis, the means are not

Table 2. Results of null hypothesis testing for differences in microwear collected from 11 sites on 1 tooth (within-tooth; 8 dentine, 3 enamel sites, tooth 2) and from single sites on each of 9 teeth (between-tooth; all dentine) on maxilla NHM R3638

	Within-tooth			Between-tooth			Within-tooth, enamel			Within-tooth, dentine		
Null hypothesis	df	<i>F</i>	<i>P</i>	df	<i>F</i>	<i>P</i>	df	<i>F</i>	<i>P</i>	df	<i>F</i>	<i>P</i>
Orientation does not differ between classes (Watson–Williams <i>F</i> ; W, B, WE, WD)	3,1446	3794.49	0.0001	3,1380	3119.81	0.0001	3,209	937.85	0.0001	3,1233	2918.10	0.0001
Log length does not differ between classes (1-way ANOVA; W, B, WE, WD)	3,1446	30.49	0.001	3,1380	12.11	0.0001	3,209	30.89	0.0001	3,1233	15.02	0.0001
<i>R</i> does not differ between classes (1-way ANOVA)	3,39	1.644	0.194	3,34	0.83	0.485	3,8	0.39	0.76	3,27	1.56	0.22
<i>N</i> does not differ between classes (1-way ANOVA; W, B, WE, WD)	3,39	16.48	0.0001	3,34	6.69	0.0011	3,8	6.52	0.01	3,27	23.28	0.0001
Width does not differ between classes (Kruskal–Wallis 1-way; W, B, WD)	3,1446	χ^2 19.27	0.0002	3,1380	χ^2 19.54	0.0002	3,209	χ^2 7.18	0.07	3,1233	χ^2 17.93	0.0005

W, B, WE, WD in parentheses indicate for which dataset the null hypothesis is rejected ($P < 0.05$). W, within-tooth; B, between teeth; WE, within-tooth, enamel sites; and WD, within-tooth, dentine sites.

Class 3 scratches, in contrast, vary more in mean orientation, both within and between teeth (Fig. 1, Table S1, and Table S2), and have lower overall *R* values (Table 1), indicating that this second steeply oriented oblique motion (trending $\approx 40^\circ$ off pure vertical adduction/lateral translation) was under looser mechanical constraint. This suggests that these scratches were formed during jaw opening. This is consistent with models of jaw opening in herbivorous reptiles (36).

Class 1 and 4 scratches are less frequent and were formed by propalinal action, but we are unable to determine whether scratches assigned to class 1 were formed during anteroposterior (palinal) or posteroanterior (proal) movement, and the same is true of class 4 scratches. That the orientation of class 1 and 4 scratches does not differ significantly between maxillary and dentary teeth indicates that they formed while the teeth were in occlusion. This evidence of propalinal movement, albeit weaker and less frequent, is somewhat surprising, given that enamel thickness (greater on the lingual margin of dentary teeth and on the labial margin of maxillary teeth) seems to be strongly adapted to the transverse power stroke, with thicker enamel on the leading edge of the teeth (11). The change in the orientation of class 4 scratches and the increase in parallelism along the length of the jaw indicate slight rotation of the tooth row and a greater freedom of movement at the back of the jaw during formation of these scratches.

Except for class 4, the lack of significant systematic variation in scratch orientation along the tooth row indicates that there was no marked long-axis rotation of the jaw element in the horizontal plane during feeding. However, the strong parallelism and straightness of the scratches, especially those in classes 1, 2, and 4, and the lack of variation, both within and between teeth, are not consistent with disarticulation of facial bones during jaw closure (12).

All but 3 of our sample sites were from dentine surfaces. It has been suggested that dentine microwear may be unsuited to quantitative analysis (37), but our results do not support this. Quantitative analysis of scratch orientations provides direct evidence of both steeply inclined and anteroposterior relative motion of the jaws during feeding. This confirms that the predictions of both Ostrom (7) and Norman and Weishampel (11) were correct in part, but our data provide direct evidence of high-angle oblique adduction and an isognathous oblique transverse power stroke, which is consistent with and supports the hypothesis of flexure along a pleurokinetic hinge. If class 3 scratches were formed in the way we suggest above, this lends additional support to the hypothesis, because it implies tooth-on-tooth contact during at least part of the jaw-opening phase of feeding.

In terms of our initial hypotheses, our results clearly demonstrate that in *Edmontosaurus*, teeth exhibit microwear that within classes does not differ between sample sites within the occlusal surface of a tooth, and differs little between teeth along a tooth row. We also found no significant differences between individuals. Perhaps surprisingly, our results indicate that the microwear in an area of 0.1 mm² provides a reasonably representative sample of the whole tooth as well as the whole jaw, and thus provides reliable information about the diet and jaw mechanics of an individual animal. One important implication of this result is that microwear-based analysis of jaw mechanics in hadrosaurs could be carried out by using isolated teeth. Obviously, these are much more common as fossils than complete skulls or substantial parts of dentary and maxilla elements. Although relatively complete jaw elements provide a frame of reference for tooth orientation within the jaw and allow more detailed testing of mechanical hypotheses, being able to conduct microwear analysis based on isolated teeth hugely increases the potential database for such work.

In addition to providing robust tests of models of jaw mechanics, microwear is also informative with regard to diet. In herbivorous mammals, microwear textures in grazers (grass eaters) differ from

those of browsers (which eat less abrasive vegetation, such as leaves, as well as twigs) (38). If the same microwear–diet relationship holds true for herbivorous dinosaurs, the dominance of scratches and lack of pits on both the dentine and enamel of the teeth of *Edmontosaurus* indicate that they were grazers rather than browsers. Early grasses certainly existed in the Cretaceous (39), but it is unlikely that they were common enough to have formed a major part of herbivore diets, and it is tempting to conclude that if they grazed, *Edmontosaurus* fed on plant material with mechanical and abrasive properties similar to those of grass. There has been much speculation about the diet of herbivorous dinosaurs. Direct evidence from gut contents and coprolites (40–43) is rare and often tenuous but indicates a range of plant food materials, including hornworts, liverworts, lycopsids, ferns, horsetails, twigs, branches, needles, leaves, bark, fruit, and seeds. Of these, only the horsetails would appear to be sufficiently abrasive to generate the microwear patterns of a grazer (silica concentration in horsetails >25% dry mass; ref. 44). However, we cannot assume that silica phytoliths alone are responsible for tooth microwear, because there is evidence that heavily striated enamel surfaces in grazing mammals can be caused by high levels of soil ingestion (45). If they grazed on low-stature vegetation, this could also be case with *Edmontosaurus*.

Our results demonstrate that with appropriate statistical testing, microwear analysis of dinosaur teeth can provide robust tests of hypotheses of jaw mechanics and feeding mechanisms. More hadrosaurid specimens and specimens of other ornithomimids need to be analyzed to determine how microwear varies within and between species, but morphological analysis suggests that hadrosaurs were ecologically comparable to modern ungulates (46). In mammals, microwear patterns can be associated with specific food plants and trophic niches (47–49): microwear has great potential for unraveling the mystery of dinosaur feeding mechanisms, diet, and trophic niche partitioning.

Materials and Methods

The teeth studied are from left and right maxillae and dentaries of the hadrosaurid ornithomimid *Edmontosaurus* sp. that were collected from the Lance Formation (Upper Cretaceous, late Maastrichtian) of Niobrara County, Wyoming (right maxilla NHM R3638, complete, with $\approx 70\%$ of full tooth row preserved; right maxilla NHM R3653, complete with full but damaged tooth row; left maxilla NHM R3654, preservation as R3653; right dentary NHM R3658, fragment). For details of specimen preparation and microwear data acquisition, see *SI Text*. All microwear features within each sampling area were recorded. All microwear was scored by the same operator (V.S.W.) to minimize operator error (25, 50). The software used to score microwear (51) produces overlay files of *x/y* coordinates. It also calculates summary statistics for feature length, width, and orientation, but these were not used in this study. Our analysis was based on raw microwear data extracted from Microware 4.02 (51) output as *x/y* coordinates and processed by using simple trigonometric functions in a database to derive the length, width, and long-axis orientation for every feature in a sample site. Length data were not normally distributed, and were therefore log-transformed before statistical analysis. Previous microwear analyses that have used mean scratch length have not taken this into account.

Statistical testing and analyses of microwear data were conducted by using JMP IN 5.1 (SAS Institute) and Oriana 2.02e software (52). DFA was performed to test the robustness of the allocation of data to orientation classes. DFA was first performed by using scratch length, count, angular dispersion, and orientation combined, and then by using orientation alone (the latter reported here). Within-tooth and between-tooth variation were also tested by using ANOVA and a variety of other statistical techniques. Orientation data are directional, and such data have statistical properties that differ from those upon which standard statistical tests are based. Consequently, our hypothesis testing used a number of tests specifically formulated for data of this kind.

ACKNOWLEDGMENTS. We thank Adrian Doyle and the Palaeontology Conservation Unit, as well as Sandra Chapman, at the Natural History Museum (London) for advice regarding cleaning consolidant from fossil teeth and access to material. Alicona is thanked for the loan of a lens and objective head for the Alicona IFM. Coltène Whaledent is thanked for donating polyvinylsiloxane molding compound. Paul Hart and 3 reviewers provided helpful comments on the manuscript. M.A.P. acknowledges the funding of the Natural Environment Research Council.

1. Lauder GV (1995) On the inference of function from structure. *Functional Morphology in Vertebrate Paleontology*, ed Thomason JJ (Cambridge Univ Press, Cambridge, UK), pp 1–18.
2. Ungar P (2004) Dental topography and diets of *Australopithecus afarensis* and early *Homo*. *J Hum Evol* 46:605–622.
3. Ferry-Graham LA, Bolnick DI, Wainwright PC (2002) Using functional morphology to examine the ecology and evolution of specialization. *Integr Comp Biol* 42:265–277.
4. Horner JR, Weishampel DB, Forster CA (2004) Hadrosauridae. *The Dinosauria*, eds Weishampel DB, Dodson P, Osmólska H (Univ of California Press, Berkeley, CA), 2nd Ed, pp 438–463.
5. Weishampel DB, et al. (2004) Dinosaur distribution. *The Dinosauria*, eds Weishampel DB, Dodson P, Osmólska H (Univ of California Press, Berkeley, CA), 2nd Ed, pp 517–606.
6. Weishampel DB, Norman DB (1989) Vertebrate herbivory in the Mesozoic; Jaws, plants, and evolutionary metrics. *Paleobiology of the Dinosaurs*, ed Farlow JO (Geological Society of America, Boulder, CO), Special Paper 238, pp 87–100.
7. Ostrom JH (1961) Cranial morphology of the hadrosaurian dinosaurs of North America. *Bull Am Mus Nat Hist* 122:37–186.
8. Hopson JA (1980) Tooth function and replacement in early Mesozoic ornithischian dinosaurs: Implications for aestivation. *Lethaia* 13:93–105.
9. Norman DB (1984) On the cranial morphology and evolution of ornithomimid dinosaurs. *Symp Zool Soc Lond* 52:521–547.
10. Weishampel DB (1984) Evolution of jaw mechanisms in ornithomimid dinosaurs. *Adv Anat Embryol Cell Biol* 87:1–109.
11. Norman DB, Weishampel DB (1985) Ornithomimid feeding mechanisms - their bearing on the evolution of herbivory. *Am Nat* 126:151–164.
12. Rybczynski N, Tirabasso A, Bloskie P, Cuthbertson R, Holliday C (2008) A three-dimensional animation model of *Edmontosaurus* (Hadrosauridae) for testing chewing hypotheses. *Palaeontol Electronica* 11(9A).
13. Walker A, Hoeck HN, Perez L (1978) Microwear of mammalian teeth as an indicator of diet. *Science* 201:908–910.
14. Teaford MF (1988) A review of dental microwear and diet in modern mammals. *Scanning Microsc* 2:1149–1166.
15. Teaford MF, Ungar PS (2000) Diet and the evolution of the earliest human ancestors. *Proc Natl Acad Sci USA* 97:13506–13511.
16. Gordon KD (1984) The assessment of jaw movement direction from dental microwear. *Am J Phys Anthropol* 63:77–84.
17. Teaford MF, Byrd KE (1989) Differences in tooth wear as an indicator of changes in jaw movement in the guinea pig *Cavia porcellus*. *Arch Oral Biol* 34:929–936.
18. Ungar PS, Merceron G, Scott RS (2007) Dental microwear texture analysis of Varswater bovids and early Pliocene paleoenvironments of Langebaanweg, Western Cape Province, South Africa. *J Mamm Evol* 14:163–181.
19. Semperebon G, Janis C, Solounias N (2004) The diets of the dromomerycidae (Mammalia: Artiodactyla) and their response to miocene vegetational change. *J Vertebr Paleontol* 24:427–444.
20. Fiorillo AR (1991) Dental microwear on the teeth of *Camarasaurus* and *Diplodocus*; implications for sauropod paleoecology. *Fifth Symposium on Mesozoic Terrestrial Ecosystems and Biota*, eds Kielan-Jaworowska Z, Heintz N, Nakrem HA (Paleontologisk Museum, Univ of Oslo, Oslo), pp 23–24.
21. Fiorillo AR (1998) Dental microwear patterns of the sauropod dinosaurs *Camarasaurus* and *Diplodocus*: Evidence for resource partitioning in the Late Jurassic of North America. *Hist Biol* 13:1–16.
22. Upchurch P, Barrett PM (2000) The evolution of sauropod feeding mechanisms. *Evolution of Herbivory in Terrestrial Vertebrates: Perspectives from the Fossil Record*, ed Sues HD (Cambridge Univ Press, Cambridge, UK), pp 79–122.
23. Schubert BW, Ungar PS (2005) Wear facets and enamel spalling in tyrannosaurid dinosaurs. *Acta Palaeontol Pol* 50:93–99.
24. Purnell MA, Bell MA, Baines DC, Hart PJB, Travis MP (2007) Correlated evolution and dietary change in fossil stickleback. *Science* 317:1887.
25. Purnell MA, Hart PJB, Baines DC, Bell MA (2006) Quantitative analysis of dental microwear in threespine stickleback: A new approach to the analysis of trophic ecology in aquatic vertebrates. *J Anim Ecol* 75:967–977.
26. Erickson GM (1996) Incremental lines of von Ebner in dinosaurs and the assessment of tooth replacement rates using growth line counts. *Proc Natl Acad Sci USA* 93:14623–14627.
27. Charles C, Jaeger JJ, Michaux J, Viriot L (2007) Dental microwear in relation to changes in the direction of mastication during the evolution of Myodonta (Rodentia, Mammalia). *Naturwissenschaften* 94:71–75.
28. Zar JH (1999) *Biostatistical Analysis* (Prentice Hall, Upper Saddle River, NJ), 4th Ed.
29. Fisher N (1993) *Statistical Analysis of Circular Data* (Cambridge Univ Press, Cambridge, UK).
30. Grigg GC, Underwood AJ (1977) An analysis of the orientation of 'magnetic' termite mounds. *Aust J Zool* 25:87–94.
31. Batschelet E (1978) Second-order statistical analysis of directions. *Animal Orientation, Navigation and Homing*, eds Schmidt-Koenig K, Keeton WT (Springer, Berlin), pp 194–198.
32. Mardia KV, Jupp PE (2000) *Directional Statistics* (Wiley, Chichester, UK).
33. Crompton AW, Attridge J (1986) Masticatory apparatus of the larger herbivores during Late Triassic and Early Jurassic times. *The Beginning of the Age of Dinosaurs. Faunal Change Across the Triassic-Jurassic Boundary*, ed Padian K (Cambridge Univ Press, Cambridge, UK), pp 223–236.
34. Galton PM (1973) The cheeks of ornithischian dinosaurs. *Lethaia* 6:67–89.
35. Weishampel DB (1983) Hadrosaurid jaw mechanics. *Acta Palaeontol Pol* 28:271–280.
36. King G (1996) *Reptiles and Herbivory* (Chapman and Hall, London).
37. Lucas PW (2004) *Dental Functional Morphology: How Teeth Work* (Cambridge Univ Press, Cambridge, UK), p 355.
38. Solounias N, Teaford M, Walker A (1988) Interpreting the diet of extinct ruminants-the case of a non-browsing giraffid. *Paleobiology* 14:287–300.
39. Prasad V, Stromberg CAE, Alimohammadian H, Sahni A (2005) Dinosaur coprolites and the early evolution of grasses and grazers. *Science* 310:1177–1180.
40. Molnar RE, Clifford HT (2000) Gut contents of a small ankylosaur. *J Vertebr Paleontol* 20:194–196.
41. Ghosh P, et al. (2003) Dinosaur coprolites from the Late Cretaceous (Maastrichtian) Lameta Formation of India: Isotopic and other markers suggesting a C-3 plant diet. *Cretaceous Res* 24:743–750.
42. Chin K (2007) The paleobiological implications of herbivorous dinosaur coprolites from the Upper Cretaceous Two Medicine formation of Montana; Why eat wood? *Palaios* 22:554–566.
43. Tweet JS, Chin K, Braman DR, Murphy NL (2008) Probable gut contents within a specimen of *Brachylophosaurus canadensis* (Dinosauria: Hadrosauridae) from the Upper Cretaceous Judith River Formation of Montana. *Palaios* 23:624–635.
44. Chen CH, Lewin J (1969) Silicon as a nutrient element for *Equisetum arvense*. *Can J Bot* 47:125–131.
45. Mainland I (2006) Pastures lost? A dental microwear study of ovicaprine diet and management in Norse Greenland. *J Archaeol Sci* 33:238–252.
46. Carrano MT, Janis CM, Sepkoski JJ (1999) Hadrosaurs as ungulate parallels: Lost lifestyles and deficient data. *Acta Palaeontol Pol* 44:237–261.
47. Rivals F, Deniaux B (2003) Dental microwear analysis for investigating the diet of an argali population (*Ovis ammon antiqua*) of mid-Pleistocene age, Caune de l'Arago cave, eastern Pyrenees, France. *Palaeogeogr Palaeoclimatol Palaeoecol* 193:443–455.
48. Merceron G, Schulz E, Kordos L, Kaiser TM (2007) Paleoenvironment of *Dryopithecus brancoi* at Rudabánya, Hungary: Evidence from dental meso- and micro-wear analyses of large vegetarian mammals. *J Hum Evol* 53:331–349.
49. Calandra I, Gohlich U, Merceron G (2008) How could sympatric megaherbivores coexist? Example of niche partitioning within a proboscidean community from the Miocene of Europe. *Naturwissenschaften* 95:831–838.
50. Grine FE, Ungar PS, Teaford MF (2002) Error rates in dental microwear quantification using scanning electron microscopy. *Scanning* 24:144–153.
51. Ungar PS (2002) Microware software, version 4.0.2. A semi-automated image analysis system for the quantification of dental microwear. (Fayetteville, AR).
52. Kovach W (2006) Oriana version 2.02e (Kovach Computing Services, Anglesey, Wales).

Supporting Information

Williams et al. 10.1073/pnas.0812631106

SI Text

Methods of Microwear Sampling and Imaging. To avoid coating original material or subjecting it to analysis under vacuum, high-resolution epoxy replicas were prepared for scanning electron micrography by using methods known to reproduce microwear with high fidelity (1, 2). Occlusal surfaces of teeth were cleaned nonabradively with a combination of liquid acetone/ethanol and ethomeen-based solvent gels (3, 4) by using techniques developed at the Natural History Museum Palaeontology Conservation Unit for cleaning without abrasion. Molds were prepared by using polyvinylsiloxane impression medium (Specdex Light; Coltene Whaledent). Casts were made by using Araldite 20/20 epoxy resin. Replicas were coated with gold (Emitech K500X sputter coater).

Imaging for the main analyses of within- and between-tooth variation used a Hitachi S-3600N scanning electron microscope (SEM; secondary electron, topographic mode) with settings standardized at: accelerating voltage, 15 kV; working distance, 18 mm; and automatic contrast and brightness. Standardization is important for comparability of datasets (5). For image capture, the orientation of the occlusal surface of the teeth was standardized, with the long axis of the tooth row and the flat occlusal surfaces of the teeth perpendicular to the electron beam. SEM images were captured at a magnification of 300, providing a sampling site field of view of $417 \times 312 \mu\text{m}$, comparable with that commonly used in analysis of occlusal microwear in mammals (6, 7). Microwear was sampled at 11 different sites on 1

distal tooth of *Edmontosaurus* right maxilla NHM R3638 (tooth 2) and at 1 central site on each of 9 further teeth from the same tooth row. Additional data were obtained from 1 central site from 1 tooth in each of the 3 additional specimens (right maxilla NHM R3653, left maxilla NHM R3654, and right dentary NHM R3658). Sampling sites were selected to maximize the chances of obtaining in vivo microwear and to minimize postmortem artefacts. The latter are less problematic than might be supposed, because physical and chemical postmortem processes tend to obliterate microwear features rather than create artefacts (8, 9). To evaluate alternative statistical approaches to testing for differences in feature orientation between sites, microwear was also sampled at 7 sites along a vertical transect across *Edmontosaurus* right maxilla NHM R3638 (tooth 2). Images for this analysis were acquired by using an Alicona IFM (infinite focus microscope; an optical, focus variation-based technique). Sampling site field of view was $285 \times 216 \mu\text{m}$; illumination coaxial. The 3D surface data acquired during this sampling were also used for assessments of scratch depth. Digital scanning electron micrographs and IFM images were downsampled to 900 pixels wide by 675 pixels high by using Adobe Photoshop 7. Microwear data were generated by using the custom software package Microware 4.02 (10), running on a Dell Latitude D505 computer running Windows XP Professional (Microsoft), with a 15-inch active matrix TFT display set at a screen resolution of 1024×768 pixels, resulting in an onscreen magnification of approximately $630\times$ for SEM and $1000\times$ for IFM.

1. Galbany J, et al. (2006) Comparative analysis of dental enamel polyvinylsiloxane impression and polyurethane casting methods for SEM research. *Microsc Res Tech* 69:246–252.
2. Williams V, Purnell M, Gabbott S (2006) Dental microwear in dinosaurs: A comparative analysis of polysiloxane replication. *Dent Pract* 44:22–23.
3. Hedley G (1980) Solubility parameters and varnish removal: A survey. *Conservator* 4:12–18.
4. Southall A (1988) New approach to cleaning painted surfaces. *Conserv News* 37:43–44.
5. Gordon KD (1988) A review of methodology and quantification in dental microwear analyses. *Scanning Microsc* 2:1139–1147.
6. Grine FE, Ungar PS, Teaford MF (2002) Error rates in dental microwear quantification using scanning electron microscopy. *Scanning* 24:144–153.
7. Scott RS, et al. (2005) Dental microwear texture analysis shows within-species diet variability in fossil hominins. *Nature* 436:693–695.
8. King T, Andrews P, Boz B (1999) Effect of taphonomic processes on dental microwear. *Am J Phys Anthropol* 108:359–373.
9. Teaford MF (1988) Scanning electron microscope diagnosis of wear patterns versus artifacts on fossil teeth. *Scanning Microsc* 2:1167–1175.
10. Ungar PS (1995) A semiautomated image analysis procedure for the quantification of dental microwear II. *Scanning* 17:57–59.

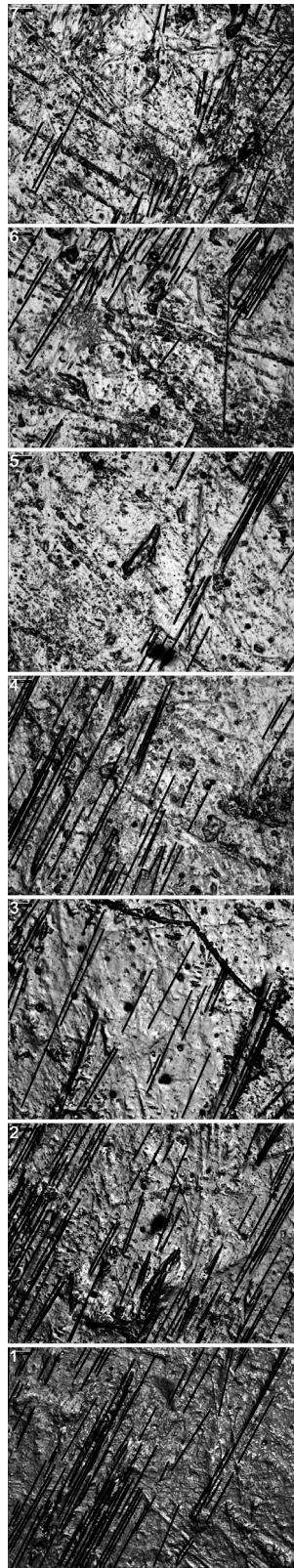


Fig. S1. Transect from apex (site 1) to base (site 7) across the functional surface of second tooth from posterior, right maxilla specimen NHM R3638 (see Fig. 1 for locations of sample sites). Class 2 microwear features are marked. Field of view is 285 μm wide.

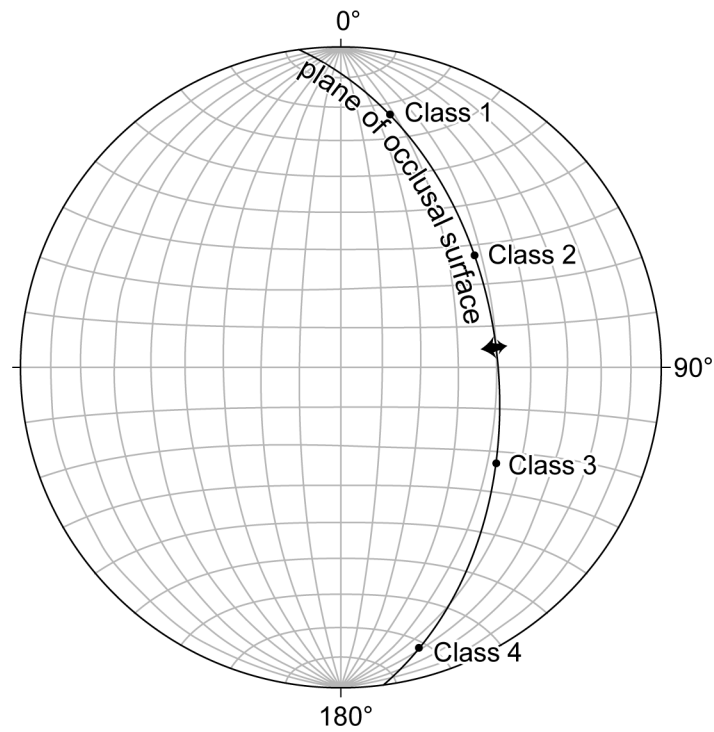


Fig. S2. Equal area stereographic projection showing tooth occlusal surface inclined at 50° from horizontal, raking 7.5° from anterior, and containing microwear classes 1–4 (in vivo orientations). Microwear data were scored in images acquired from horizontally oriented surfaces, and they were reoriented by using standard stereographic techniques. Arrow shows trend and plunge in tooth surface of pure orthal movement. Pure lateral translation, relative to sagittal plane, would be along the 90° axis of stereonet.

Table S1. Analysis of variation in orientation between sites, within tooth 2 of maxilla NHM R3638 (8 dentine sites, 3 enamel sites)

Enamel sites					Dentine sites						
Class 1	T2-1	T2-4	T2-5	T2-2	T2-3	T2-6	T2-7	T2-8	T2-9	T2-10	T2-11
<i>n</i>	10	14	10	0	17	13	24	2	5	4	22
Angular dispersal, <i>R</i>	0.972	0.980	0.950		0.944	0.953	0.931	0.988	0.970	0.945	0.935
Rayleigh test (<i>Z</i> , <i>P</i>)	9.45, <<0.001	13.45, <<0.001	9.02, <<0.001		15.17, <<0.001	11.82, <<0.001	20.81, <<0.001	1.95, 0.146	4.71, 0.002	3.57, 0.016	19.23, <<0.001
Rao spacing (<i>U</i> , <i>P</i>)	273.15, <0.01	293.66, <0.01	266.63, <0.01		283.93, <0.01	272.15, <0.01	268.91, <0.01		256.15, <0.01	218.20, <0.05	269.55, <0.01
Mean orientation (mean vector, μ)	13.72	13.36	20.62		26.45	15.80	19.98	33.09	29.21	22.23	21.65
Class 2											
<i>n</i>	32	29	25	141	154	82	120	99	64	61	55
Angular dispersal, <i>R</i>	0.957	0.988	0.887	0.978	0.937	0.949	0.948	0.970	0.969	0.982	0.929
Rayleigh test (<i>Z</i> , <i>P</i>)	29.31, <<0.001	28.30, <<0.001	19.67, <<0.001	134.78, <<0.001	135.12, <<0.001	73.78, <<0.001	107.86, <<0.001	93.22, <<0.001	60.14, <<0.001	58.85, <<0.001	47.48, <<0.001
Rao spacing (<i>U</i> , <i>P</i>)	272.85, <0.01	311.75, <0.01	249.02, <0.01	293.99, <0.01	271.05, <0.01	299.01, <0.01	279.01, <0.01	291.43, <0.01	285.25, <0.01	302.85, <0.01	271.43, <0.01
Mean orientation (mean vector, μ)	59.45	56.05*	67.67	66.53	65.98	64.71	60.94	62.24	63.14	56.39*	61.26
Class 3											
<i>n</i>	17	14	34	74	66	12	10	40	38	15	34
Angular dispersal, <i>R</i>	0.939	0.963	0.936	0.942	0.913	0.990	0.894	0.979	0.898	0.902	0.923
Rayleigh test (<i>Z</i> , <i>P</i>)	14.99, <<0.001	12.99, <<0.001	29.76, <<0.001	65.73, <<0.001	54.97, <<0.001	11.76, <<0.001	8.00, <<0.001	38.36, <<0.001	30.64, <<0.001	12.22, <<0.001	28.97, <<0.001
Rao spacing (<i>U</i> , <i>P</i>)	274.16, <0.01	274.17, <0.01	265.51, <0.01	268.96, <0.01	269.90, <0.01	305.41, <0.01	238.61, <0.01	304.43, <0.01	258.46, <0.01	258.07, <0.01	275.02, <0.01
Mean orientation (mean vector, μ)	122.82	116.93	116.93	108.76	112.64	114.91	128.37	107.27	122.74	110.95	122.29
Class 4											
<i>n</i>	6	14	8	11	9	1	17	8	16	14	9
Angular dispersal, <i>R</i>	0.895	0.942	0.979	0.913	0.906	1.000	0.965	0.945	0.929	0.938	0.870
Rayleigh test (<i>Z</i> , <i>P</i>)	4.80, 0.003	12.42, <<0.001	7.67, <<0.001	9.16, <<0.001	7.39, <<0.001	1.00, 0.512	15.83, <<0.001	7.15, <<0.001	13.81, <<0.001	12.31, <<0.001	6.81, <<0.001
Rao spacing (<i>U</i> , <i>P</i>)	237.79, <0.01	271.09, <0.01	276.56, <0.01	251.73, <0.01	246.11, <0.01		284.47, <0.01	253.90, <0.01	267.39, <0.01	263.08, <0.01	245.17, <0.01
Mean orientation (mean vector, μ)	159.05	163.15	149.96	162.86	160.49	148.11	158.70	161.19	159.56	164.34	150.83

Mean of means (μ of μ) and confidence intervals are calculated from tooth 2 dentine sites only (8 sites: sites 2, 3, 6, 7, 8, 9, 10, and 11). Class 1: mean of means, 24.14; 99% confidence interval, 11.18–36.33. Class 2: mean of means, 62.63; 99% confidence interval, 56.79–68.56. Class 3: mean of means, 115.84; 99% confidence interval, 103.16–129.7. Class 4: Mean of means, 158.23; 99% confidence interval 147.97–168.67. *Mean orientation values fall outside 99% confidence intervals.

Class 1													Class 2					Class 3					Class 4												
<i>n</i>	T1-1	T2-3	T3-1	T5-2	T7-1	T8-1	T20-1	T23-1	<i>n</i>	T1-1	T2-3	T3-1	T5-2	T7-1	T8-1	T20-1	T23-1	<i>n</i>	T1-1	T2-3	T3-1	T5-2	T7-1	T8-1	T20-1	T23-1	<i>n</i>	T1-1	T2-3	T3-1	T5-2	T7-1	T8-1	T20-1	T23-1
25	17	51	13	84	99	40	9	13	24	11	22	26	18	100	23	27	36	23	27	36	23	27	36	23	27	36	23	27	36	23	27	36	23	27	36
Angular dispersal, <i>R</i>	0.948	0.944	0.947	0.937	0.954	0.966	0.946	0.868	0.893	0.943	0.955	0.956	0.946	0.868	0.893	0.943	0.955	0.943	0.955	0.956	0.943	0.955	0.956	0.943	0.955	0.956	0.943	0.955	0.956	0.943	0.955	0.956	0.943	0.955	0.956
Rayleigh test (<i>Z</i> , <i>P</i>)	22.46, <0.001	15.17, <0.001	45.78, <0.001	10.40, <0.001	36.37, <0.001	8.40, <0.001	11.63, <0.001	9.80, <0.001	19.14, <0.001	9.79, <0.001	20.06, <0.001	4.57, 0.003	9.79, <0.001	9.80, <0.001	19.14, <0.001	9.79, <0.001	20.06, <0.001	9.79, <0.001	20.06, <0.001	4.57, 0.003	9.79, <0.001	20.06, <0.001	4.57, 0.003	9.79, <0.001	9.80, <0.001	19.14, <0.001	9.79, <0.001	20.06, <0.001	4.57, 0.003	9.79, <0.001	20.06, <0.001	4.57, 0.003	9.79, <0.001	20.06, <0.001	4.57, 0.003
Rao spacing (<i>U</i> , <i>P</i>)	278.46, <0.01	283.93, <0.01	287.92, <0.01	253.06, <0.01	277.05, <0.01	272.56, <0.01	262.90, <0.01	256.03, <0.01	271.82, <0.01	269.06, <0.01	284.76, <0.01	240.50, <0.01	269.06, <0.01	256.03, <0.01	271.82, <0.01	269.06, <0.01	284.76, <0.01	269.06, <0.01	284.76, <0.01	240.50, <0.01	269.06, <0.01	284.76, <0.01	240.50, <0.01	269.06, <0.01	256.03, <0.01	271.82, <0.01	269.06, <0.01	284.76, <0.01	240.50, <0.01	269.06, <0.01	284.76, <0.01	240.50, <0.01	269.06, <0.01	284.76, <0.01	240.50, <0.01
Mean orientation (mean vector, μ)	14.58	26.45	13.85	25.34	12.49*	19.86	24.82	20.80	22.05	22.59	23.16	17.37	22.59	20.80	22.05	22.59	23.16	22.59	23.16	17.37	22.59	23.16	17.37	22.59	20.80	22.05	22.59	23.16	17.37	22.59	23.16	17.37	22.59	23.16	17.37
233	154	34	54	84	99	40	9	13	24	23	27	36	23	27	36	23	27	23	27	36	23	27	36	23	27	36	23	27	36	23	27	36	23	27	36
Angular dispersal, <i>R</i>	0.979	0.937	0.975	0.945	0.909	0.939	0.959	0.906	0.903	0.866	0.994	0.910	0.866	0.906	0.903	0.866	0.994	0.866	0.994	0.910	0.866	0.994	0.910	0.866	0.906	0.903	0.866	0.994	0.910	0.866	0.994	0.910	0.866	0.994	0.910
Rayleigh test (<i>Z</i> , <i>P</i>)	223.25, <0.001	135.12, <0.001	32.34, <0.001	48.22, <0.001	81.83, <0.001	19.39, <0.001	23.90, <0.001	14.79, <0.001	81.53, <0.001	17.24, <0.001	26.70, <0.001	29.84, <0.001	17.24, <0.001	14.79, <0.001	81.53, <0.001	17.24, <0.001	26.70, <0.001	17.24, <0.001	26.70, <0.001	29.84, <0.001	17.24, <0.001	26.													

Mean of means (μ) and confidence intervals calculated from 10 teeth on maxilla NHM R3638 only. Class 1: mean of means, 20.13; 99% confidence interval, 13.2–27.26. Class 2: mean of means, 64.56; 99% confidence interval, 55.4–74. Class 3: mean of means, 115.62; 99% confidence interval, 94.16–138.72. Class 4: mean of means, 163.17; 99% confidence interval, 156.44–169.45.

*Mean orientation values fall outside 99% confidence intervals.

BIBLIOGRAPHY

- Baker, G., Jones, L.H.P., and Wardrop, I.D. 1959. Cause of wear in sheeps' teeth. *Nature*, 184:1583-1584.
- Barrett, P.M. 2000. Prosauropod dinosaurs and iguanas: speculations on the diets of extinct reptiles, 42-78. In Sues, H.-D. (ed.), *Evolution of Herbivory in Terrestrial Vertebrates: perspectives from the fossil record*. Cambridge University Press, Cambridge.
- Batschelet, E. 1978. Second-order Statistical Analysis of Directions, 194-198. In Schmidt-Koenig, K., and Keeton, W.T. (eds.), *Animal Orientation, Navigation and Homing*. Springer, Berlin.
- Batschelet, E. 1981. *Circular Statistics in Biology*. Academic Press, New York, 371.
- Bell, P.R., Snively, E., and Shychoski, L. 2009. A Comparison of the Jaw Mechanics in Hadrosaurid and Ceratopsid Dinosaurs Using Finite Element Analysis. *The Anatomical Record: Advances in Integrative Anatomy and Evolutionary Biology*, 292:1338-1351.
- Burda, H., Begall, S., Cervený, J., Neef, J., and Nemec, P. 2009. Extremely low-frequency electromagnetic fields disrupt magnetic alignment of ruminants. *Proceedings of the National Academy of Sciences*, 106:5708-5713.
- Burnstock, A., and White, R. 1990. The effects of selected solvents and soaps on a simulated canvas painting. In Mills, J.S., and Smith, P. (eds.), *Cleaning, retouching and coatings: Contributions to the 1990 IIC Congress, Brussels*. International Institute for Conservation of Historic and Artistic Work, London, 111-118.
- Butler, P.M. 1952. The milk molars of Perissodactyla with remarks on molar occlusion. *Proceedings of the Zoological Society of London*, 121:777-817.
- Butler, R.J., Upchurch, P., and Norman, D.B. 2008. The phylogeny of the ornithischian dinosaurs. *Journal of Systematic Palaeontology*, 6:1-40.
- Calandra, I., Hlich, U., and Merceron, G. 2008. How could sympatric megaherbivores coexist? Example of niche partitioning within a proboscidean community from the Miocene of Europe. *Naturwissenschaften*, 95:831-838.
- Carrano, M.T., Janis, C.M., and Sepkoski, J.J. 1999. Hadrosaurs as ungulate parallels: lost lifestyles and deficient data. *Acta Palaeontologica Polonica*, 44:237-261.
- Chaney, D.S. 1989. Mold making with room temperature vulcanizing silicone rubber, 284-304. In Feldman, R.M., Chapman, R.E., and Hannibal, J.T. (eds.), *Paleotechniques, Paleontological Society Special Publication no. 4*, Knoxville, Tennessee.
- Chaney, D.S., and Goodwin, M.B. 1989. R.T.V. silicone rubber compounds used for moulding fossil vertebrate specimens: a comparison. *Journal of Vertebrate Paleontology*, 9:471-473.

- Charles, C., Jaeger, J.J., Michaux, J., and Viriot, L. 2007. Dental microwear in relation to changes in the direction of mastication during the evolution of Myodonta (Rodentia, Mammalia). *Naturwissenschaften*, 94:71-75.
- Chen, C.-h., and Lwein, J. 1969. Silicon as a nutrient element for *Equisetum arvense*. *Canadian Journal of Botany*, 47:125-131.
- Chin, K. 2007. The paleobiological implications of herbivorous dinosaur coprolites from the Upper Cretaceous Two Medicine formation of Montana; Why eat wood? *Palaaios*, 22:554-566.
- Crompton, A.W., and Attridge, J. 1986. Masticatory apparatus of the larger herbivores during Late Triassic and Early Jurassic times, 223-236. In Padian, K. (ed.), *The Beginning of the Age of Dinosaurs. Faunal Change across the Triassic-Jurassic Boundary*. Cambridge University Press, Cambridge.
- Davidson, A., and Alderson, S. 2009. An introduction to solution and reaction adhesives for fossil preparation, 53-62. In Brown, M.A., Kane, J.F., and Parker, W.G. (eds.), *Methods in Paleontology: Proceedings of the First Annual Fossil Preparation and Collections Symposium*. FossilPrep.org
- Davis, J.C. 2002. *Statistics and Data Analysis in Geology*. Wiley, 656.
- Eastaugh, N. 1990. The visual effects of dirt on paintings, 19-23. In Hackney, S., Townsend, J., and Eastaugh, N. (eds.), *Dirt and Pictures Separated*. United Kingdom Institute for Conservation, London.
- Erickson, G.M. 1996. Incremental lines of von Ebner in dinosaurs and the assessment of tooth replacement rates using growth line counts. *Proceedings of the National Academy of Sciences of the United States of America*, 93:14623-14627.
- Fernandez-Jalvo, Y., and Monfort, M.D.M. 2008. Experimental taphonomy in museums: Preparation protocols for skeletons and fossil vertebrates under the scanning electron microscopy. *Geobios*, 41:157-181.
- Ferry-Graham, L.A., Bolnick, D.I., and Wainwright, P.C. 2002. Using functional morphology to examine the ecology and evolution of specialization. *Integrative and Comparative Biology*, 42:265-277.
- Fiorillo, A.R. 1991. Dental microwear on the teeth of *Camarasaurus* and *Diplodocus*; implications for sauropod paleoecology, 23-24. In Kielan-Jaworowska, Z., Heintz, N., and Nakrem, H.A. (eds.), *Fifth symposium on Mesozoic terrestrial ecosystems and biota* Paleontologisk Museum, University of Oslo.
- Fiorillo, A.R. 1998. Dental microwear patterns of the sauropod dinosaurs *Camarasaurus* and *Diplodocus*: Evidence for resource partitioning in the Late Jurassic of North America. *Historical Biology*, 13:1-16.
- Fisher, N. 1993. *Statistical Analysis of Circular Data*. Cambridge University Press, Cambridge, UK, 277.

- Galbany, J., Estebanaranz, F., Martínez, L.M., Romero, A., De Juan, J., Turbón, D., and Pérez-Pérez, A. 2006. Comparative analysis of dental enamel polyvinylsiloxane impression and polyurethane casting methods for SEM research. *Microscopy Research and Technique*, 69:246-252.
- Galbany, J., Martínez, L.M., and Pérez-Pérez, A. 2004. Tooth Replication Techniques, SEM Imaging and Microwear Analysis in Primates: Methodological Obstacles. *Anthropologie*, 42:5-12.
- Galton, P.M. 1972. Classification and Evolution of Ornithomimid Dinosaurs. *Nature*, 239:464-466.
- Galton, P.M. 1973. The cheeks of ornithomimid dinosaurs. *Lethaia*, 6:67-89.
- Galton, P.M. 1978. Fabrosauridae, the basal family of ornithomimid dinosaurs (Reptilia; Ornithomimidae). *Palaeontologische Zeitschrift*, 52:138-159.
- Gauthier, J. 1986. Saurian monophyly and the origin of birds. *Memoirs of the California Academy of Sciences*, 8:1-56.
- Ghosh, P., Bhattacharya, S.K., Sahni, A., Kar, R.K., Mohabey, D.M., and Ambwani, K. 2003. Dinosaur coprolites from the Late Cretaceous (Maastrichtian) Lameta Formation of India: isotopic and other markers suggesting a C-3 plant diet. *Cretaceous Research*, 24:743-750.
- Gordon, K.D. 1984a. The assessment of jaw movement direction from dental microwear. *American Journal of Physical Anthropology*, 63:77-84.
- Gordon, K.D. 1984b. Microfracture patterns of abrasive wear striations on teeth indicate directionality. *American Journal of Physical Anthropology*, 63:315-322.
- Gordon, K.D. 1988. A review of methodology and quantification in dental microwear analyses. *Scanning microscopy*, 2:1139-1147.
- Goswami, A., Flynn, J.J., Raviharimanana, L., and Wyss, A.R. 2005. Dental microwear in triassic amniotes: implications for paleoecology and masticatory mechanics. *Journal of Vertebrate Paleontology*, 25:320-329.
- Grigg, G.C., and Underwood, A.J. 1977. An analysis of the orientation of 'magnetic' termite mounds. *Australian Journal of Zoology*, 25:87-94.
- Grine, F.E. 1986. Dental evidence for dietary differences in *Australopithecus* and *Paranthropus*. *Journal of Human Evolution*, 15:783-822.
- Grine, F.E., Ungar, P.S., and Teaford, M.F. 2002. Error rates in dental microwear quantification using scanning electron microscopy. *Scanning*, 24:144-153.
- Gügel, I.L., Grupe, G., and Kunzelmann, K.-H. 2001. Simulation of dental microwear: Characteristic traces by opal phytoliths give clues to ancient human dietary behavior. *American Journal of Physical Anthropology*, 114:124-138.

- Hedley, G. 1980. Solubility parameters and varnish removal: a survey. *The Conservator*, 4:12-18.
- Herring, S.W. 1993. Functional Morphology of Mammalian Mastication. *American Zoologist*, 33:289-299.
- Holliday, C.M., and Witmer, L.M. 2009. Cranial Kinesis in Dinosaurs: Intracranial Joints, Protractor Muscles, and Their Significance for Cranial Evolution and Function in Diapsids. *Journal of Vertebrate Paleontology*, 28:1073-1088.
- Hopson, J.A. 1980. Tooth function and replacement in early Mesozoic ornithischian dinosaurs: implications for aestivation. *Lethaia*, 13:93-105.
- Horner, J.R., Weishampel, D.B., and Forster, C.A. 2004. Hadrosauridae, 438-463. In Weishampel, D.B., Dodson, P., and Osmólska, H. (eds.), *The Dinosauria*. University of California Press, Berkeley.
- Hotelling, H. 1931. The Generalization of Student's Ratio. *The Annals of Mathematical Statistics*, 2:360-378.
- Hsiung, T.-H., Olejnik, S., and Huberty, C.J. 1994. Comment on a Wilcox Test Statistic for Comparing Means When Variances Are Unequal. *Journal of Educational and Behavioral Statistics*, 19:111-118.
- King, G. 1996. *Reptiles and Herbivory*. Chapman and Hall, London, 160.
- King, T., Andrews, P., and Boz, B. 1999. Effect of taphonomic processes on dental microwear. *American Journal of Physical Anthropology*, 108:359-373.
- Koch, P.L. 1998. Isotopic reconstruction of past continental environments. *Annual Review of Earth and Planetary Sciences*, 26:573-613.
- Kovach, W. 2006. Oriana Version 2.02e. Kovach Computing Services, Anglesey, Wales.
- Lauder, G.V. 1995. On the inference of function from structure, 1-18. In Thomason, J.J. (ed.), *Functional morphology in vertebrate paleontology*. Cambridge University Press, Cambridge
- Lucas, P.W. 2004. *Dental Functional Morphology: How Teeth Work*. Cambridge University Press, Cambridge, 355.
- Mainland, I. 2006. Pastures lost? A dental microwear study of ovicaprine diet and management in Norse Greenland. *Journal of Archaeological Science*, 33:238-252.
- Mardia, K.V., and Jupp, P.E. 2000. *Directional statistics*. Wiley, Chichester, 429.
- Maryanska, T., and Osmolska, H. 1985. On ornithischian phylogeny. *Acta Palaeontologica Polonica*, 30:137-150.

- Merceron, G., Schulz, E., Kordos, L., and Kaiser, T.M. 2007. Paleoenvironment of *Dryopithecus branchoi* at Rudabánya, Hungary: evidence from dental meso- and micro-wear analyses of large vegetarian mammals. *Journal of Human Evolution*, 53:331-349.
- Mills, J.R.E. 1967. A comparison of lateral jaw movement in some mammals from wear facets on the teeth. *Archives of Oral Biology*, 12:645-661.
- Molnar, R.E., and Clifford, H.T. 2000. Gut contents of a small ankylosaur *Journal of Vertebrate Paleontology*, 20:194-196.
- Nalla, R.K., Balooch, M., Ager Iii, J.W., Kruzic, J.J., Kinney, J.H., and Ritchie, R.O. 2005. Effects of polar solvents on the fracture resistance of dentin: role of water hydration. *Acta Biomaterialia*, 1:31-43.
- Norman, D.B. 1984. On the cranial morphology and evolution of ornithomimid dinosaurs. *Symposium of the Zoological Society of London*, 52:521-547.
- Norman, D.B., and Weishampel, D.B. 1985. Ornithomimid feeding mechanisms - their bearing on the evolution of herbivory. *American Naturalist*, 126:151-164.
- Norman, D.B., and Weishampel, D.B. 1991. Feeding mechanisms in some small herbivorous dinosaurs: processes and patterns, 161-181. In Rayner, J.M.V., and Wootton, R.J. (eds.), *Biomechanics in evolution*. UK: Cambridge University Press, Cambridge.
- Norman, D.B., Witmer, L.M., and Weishampel, D.B. 2004. Basal Ornithomimidae, 325–334. In Weishampel, D.B., Dodson, P., and Osmólska, H. (eds.), *The Dinosauria*. University of California Press, Berkeley
- O'Leary, M.H. 1988. Carbon isotopes in photosynthesis. *BioScience*, 38:328-336.
- Organ, J.M., Teaford, M.F., and Larsen, C.S. 2005. Dietary inferences from dental occlusal microwear at Mission San Luis de Apalachee. *American Journal of Physical Anthropology*, 128:801-811.
- Ostrom, J.H. 1961. Cranial morphology of the hadrosaurian dinosaurs of North America. *Bulletin of the American Museum of Natural History* 122, article 2:37-186.
- Paul, G.S. 1984. The Segnosaurian Dinosaurs: Relics of the Prosauropod-Ornithomimid Transition? *Journal of Vertebrate Paleontology*, 4:507-515.
- Porro, L.B. 2007. Feeding and jaw mechanism in *Heterodontosaurus tucki* using finite element analysis. *Journal of Vertebrate Paleontology*, 27:131A.
- Prasad, V., Stromberg, C.A.E., Alimohammadian, H., and Sahni, A. 2005. Dinosaur coprolites and the early evolution of grasses and grazers. *Science*, 310:1177-1180.
- Purnell, M.A. 2003. Casting, Replication, And Anaglyph Stereo Imaging Of Microscopic Detail In Fossils, With Examples From Conodonts And Other Jawless Vertebrates, *Palaeontologia Electronica*, 1-11.

- Purnell, M.A., Bell, M.A., Baines, D.C., Hart, P.J.B., and Travis, M.P. 2007. Correlated evolution and dietary change in fossil stickleback. *Science*, 317:1887.
- Purnell, M.A., Hart, P.J.B., Baines, D.C., and Bell, M.A. 2006. Quantitative analysis of dental microwear in threespine stickleback: a new approach to the analysis of trophic ecology in aquatic vertebrates. *Journal of Animal Ecology*, 75:967-977.
- Rayfield, E.J. 2004. Cranial mechanics and feeding in *Tyrannosaurus rex*. *Proceedings Biological Sciences*, 271:1451-1459.
- Rivals, F., and Deniaux, B. 2003. Dental microwear analysis for investigating the diet of an argali population (*Ovis ammon antiqua*) of mid-Pleistocene age, Caune de l'Arago cave, eastern Pyrenees, France. *Palaeogeography, Palaeoclimatology, Palaeoecology*, 193:443-455.
- Robinson, B.W., and Wilson, D.S. 1998. Optimal Foraging, Specialization, and a Solution to Liem's Paradox. *The American Naturalist*, 151:223-235.
- Rose, J.J. 1983. A replication technique for scanning electron microscopy: Applications for anthropologists. *American Journal of Physical Anthropology*, 62:255-261.
- Rybczynski, N., and Reisz, R.R. 2001. Earliest evidence for efficient oral processing in a terrestrial herbivore. *Nature*, 411:684-687.
- Rybczynski, N., Tirabasso, A., Bloskie, P., Cuthbertson, R., and Holliday, C. 2008. A three-dimensional animation model of *Edmontosaurus* (Hadrosauridae) for testing chewing hypotheses. *Palaeontologia Electronica*, 11:1-14.
- Sanson, G.D., Kerr, S.A., and Gross, K.A. 2007. Do silica phytoliths really wear mammalian teeth? *Journal of Archaeological Science*, 34:526-531.
- Schubert, B.W., and Ungar, P.S. 2005. Wear facets and enamel spalling in tyrannosaurid dinosaurs. *Acta Palaeontologica Polonica*, 50:93-99.
- Schubert, B.W., Ungar, P.S., Sponheimer, M., and Reed, K.E. 2006. Microwear evidence for Plio-Pleistocene bovid diets from Makapansgat Limeworks Cave, South Africa. *Palaeogeography, Palaeoclimatology, Palaeoecology*, 241:301-319.
- Scott, A.C. 1977. Coprolites containing plant material from the Carboniferous of Britain. *Palaeontology*, 20:59-68.
- Scott, R.S., Ungar, P.S., Bergstrom, T.S., Brown, C.A., Grine, F.E., Teaford, M.F., and Walker, A. 2005. Dental microwear texture analysis shows within-species diet variability in fossil hominins. *Nature*, 436:693-695.
- Semprebon, G., Janis, C., and Solounias, N. 2004. The diets of the dromomerycidae (Mammalia : Artiodactyla) and their response to miocene vegetational change. *Journal of Vertebrate Paleontology*, 24:427-444.
- Sereno, P.C. 1984. The phylogeny of Ornithischia: a reappraisal, 219-226. In Reif, W.E., and Westphal, F. (eds.), *Third Symposium on Mesozoic Terrestrial Ecosystems, short papers*, Attempto Verlag, Tubingen.

- Sereno, P.C. 1986. Phylogeny of the bird-hipped dinosaurs (Order Ornithischia). *National Geographic Research*, 2:234-256.
- Sereno, P.C. 1991. Lesothosaurus, "Fabrosaurids," and the early evolution of ornithischia. *Journal of Vertebrate Paleontology*, 11:168-197.
- Sereno, P.C. 1997. The origin and evolution of dinosaurs. *Annual Review of Earth and Planetary Sciences*, 25:435-489.
- Solounias, N., and Hayek, L.A.C. 1993. New methods of tooth microwear analysis and application to dietary determination of 2 extinct antelopes. *Journal of Zoology*, 229:421-445.
- Solounias, N., Teaford, M., and Walker, A. 1988. Interpreting the diet of extinct ruminants - the case of a non-browsing giraffid. *Paleobiology*, 14:287-300.
- Southall, A. 1988. New approach to cleaning painted surfaces. *Conservation News*, 37:43-44.
- Teaford, M.F. 1988a. A review of dental microwear and diet in modern mammals. *Scanning Microscopy*, 2:1149-1166.
- Teaford, M.F. 1988b. Scanning electron microscope diagnosis of wear patterns versus artifacts on fossil teeth. *Scanning Microscopy*, 2:1167-1175.
- Teaford, M.F., and Byrd, K.E. 1989. Differences in tooth wear as an indicator of changes in jaw movement in the guinea pig *Cavia porcellus*. *Archives of Oral Biology*, 34:929-936.
- Teaford, M.F., and Ungar, P.S. 2000. Diet and the evolution of the earliest human ancestors. *Proceedings of the National Academy of Sciences of the United States of America*, 97:13506-13511.
- Teaford, M.F., and Walker, A. 1984. Quantitative differences in dental microwear between primate species with different diets and a comment on the presumed diet of *Sivapithecus*. *American Journal of Physical Anthropology*, 64:191-200.
- Throckmorton, G.S. 1976. Oral food processing in two herbivorous lizards, *Iguana iguana* (Iguanidae) and *Uromastix aegyptius* (Agamidae). *Journal of Morphology*, 148:363-390.
- Thulborn, R.A. 1971a. Origins and Evolution of Ornithischian Dinosaurs. *Nature*, 234:75-78.
- Thulborn, R.A. 1971b. Tooth Wear and Jaw Action in Triassic Ornithischian Dinosaur *Fabrosaurus*. *Journal of Zoology*, 164:165-179.
- Thulborn, R.A. 1974. A new heterodontosaurid dinosaur (Reptilia-Ornithischia) from Upper Triassic Red Beds of Lesotho. *Zoological Journal of the Linnean Society*, 55:151-175.

- Tweet, J.S., Chin, K., Braman, D.R., and Murphy, N.L. 2008. Probable gut contents within a specimen of *Brachylophosaurus Canadensis* (Dinosauria: Hadrosauridae) from the Upper Cretaceous Judith River Formation of Montana. *Palaaios*, 23:624-635.
- Ungar, P. 2004. Dental topography and diets of *Australopithecus afarensis* and early *Homo*. *Journal of Human Evolution*, 46:605-622.
- Ungar, P.S. 1995. A semiautomated image analysis procedure for the quantification of dental microwear II. *Scanning*, 17:57-59.
- Ungar, P.S. 1996. Dental microwear of European Miocene catarrhines: evidence for diets and tooth use. *Journal of Human Evolution*, 31:335-366.
- Ungar, P.S. 2001. Microware software, Version 4.0. A semi-automated image analysis system for the quantification of dental microwear. Unpublished. Fayetteville, USA.
- Ungar, P.S., Grine, F.E., and Teaford, M.F. 2008. Dental Microwear and Diet of the Plio-Pleistocene Hominin *Paranthropus boisei*. *PLoS ONE*, 3:e2044.
- Ungar, P.S., Merceron, G., and Scott, R.S. 2007. Dental microwear texture analysis of Varswater bovids and early Pliocene paleoenvironments of Langebaanweg, Western Cape Province, South Africa. *Journal of Mammalian Evolution*, 14:163-181.
- Ungar, P.S., and Teaford, M.F. 1996. Preliminary examination of non-occlusal dental microwear in anthropoids: Implications for the study of fossil primates. *American Journal of Physical Anthropology*, 100:101-113.
- Upchurch, P., and Barrett, P.M. 2000. The evolution of sauropod feeding mechanisms, 79-122. In Sues, H.-D. (ed.), *Evolution of Herbivory in Terrestrial Vertebrates: perspectives from the fossil record*. Cambridge University Press, Cambridge.
- Walker, A., Hoeck, H.N., and Perez, L. 1978. Microwear of mammalian teeth as an indicator of diet. *Science*, 201:908-910.
- Waters, B.T., and Savage, D.E. 1971. Making duplicates of small vertebrate fossils for teaching and research collections. *Curator*, 14:123-132.
- Weishampel, D.B. 1983. Hadrosaurid jaw mechanics. *Acta Palaeontologica Polonica*, 28:271-280.
- Weishampel, D.B. 1984. Evolution of Jaw Mechanisms in Ornithopod Dinosaurs. *Advances in Anatomy Embryology and Cell Biology*, 87:1-109.
- Weishampel, D.B., Barrett, P.M., Coria, R.A., Le Loeuff, J., Xu, X., Zhao, X.J., Sahni, A., Gomani, E.M.P., and Noto, C.R. 2004. Dinosaur distribution, 517-606. In Weishampel, D.B., Dodson, P., and Osmólska, H. (eds.), *The Dinosauria*. University of California Press, Berkeley.
- Weishampel, D.B., and Norman, D.B. 1989. Vertebrate herbivory in the Mesozoic; jaws, plants, and evolutionary metrics, 87-100. In Farlow, J.O. (ed.), *Paleobiology of the dinosaurs*. Geological Society of America Special Paper 238., Boulder, Colorado.

Williams, V., Purnell, M., and Gabbott, S. 2006. Dental microwear in dinosaurs: a comparative analysis of polysiloxane replication. *Dental Practice*, 44:22-23.

Williams, V.S., Barrett, P.M., and Purnell, M.A. 2009. Quantitative analysis of dental microwear in hadrosaurid dinosaurs, and the implications for hypotheses of jaw mechanics and feeding. *Proceedings of the National Academy of Sciences*, 106:11194-11199.

Williams, V.S., and Doyle, A.M. 2010. Cleaning fossil tooth surfaces for microwear analysis: use of solvent gels to remove resistant consolidant. *Palaeontologia Electronica*, 13:1-12.

Wolbers, R. 1992. Recent development in the use of gel formulations for the cleaning of paintings, *Restoration 1992 Conference Preprint*. UKIC, 74-75.

Wolbers, R., Sterman, N., and Stavroudis, C. 1990. Notes for the workshop on new methods in the cleaning of paintings, *The Getty Conservation Institute*, Marina del Ray, California, 1-158.

Zar, J.H. 1999. *Biostatistical Analysis*. Prentice-Hall, New Jersey, 663.